RESULTS

Within this chapter, the collected data resulting from applying the aforementioned methods and techniques is presented. First, the results from the raw material characterisation are addressed, followed by the results from the techno-typological analysis. For the techno-typological analysis, the data from the three archaeological sites are not separated but instead, addressed sequentially within each artefact category. This allows for direct inter-comparability of the artefacts. The results from the Upper site of Buhlen are always mentioned first, then the ones from Balver Höhle and at lastly the data concerning Ramioul. Within this structure, the results concerning the two artefact categories, *Keilmesser* and *Prądnik scraper* are addressed sequentially. *Prądnik spalls* as a third artefact category, are separately treated and thus mentioned after the data regarding *Keilmesser* and *Prądnik scrapers*. After this subchapter, the results regarding the quantification of the edge design, the use-wear analysis and the controlled experiments are mentioned. Scrapers and flakes – as outgroup – are not addressed in all chapters. The results concerning the scrapers and flakes are only of relevance in the chapters Quantification of edge design and Use-wear analysis.
For the analyses, in total n = 330 *Keilmesser* were studied (**tabs 3. 5. 7**). The selected assemblage from Buhlen yielded n = 130 *Keilmesser*, Balve n = 191 and n = 9 artefacts are from Ramioul. Not all of the *Keilmesser* are complete artefacts. Some of these pieces can be described as distal *Keilmesser* tips, some as fragmented or semi-finished tools. Whenever only complete *Keilmesser* have been involved in an analysis, it is mentioned within the text. *Prądnik scrapers* were analysed identically to *Keilmesser.* For the analyses, n = 54 *Prądnik scrapers* were studied in total. This assemblage is composed of n = 24 *Prądnik scrapers* from Buhlen, n = 27 from Balver Höhle and n = 3 from Ramioul. These n = 54 *Prądnik scrapers* are without exception complete tools.

RAW MATERIAL CHARACTERISATION

The sampled *Keilmesser* from Buhlen are with a clear majority (n = 128; 98.5 %) made of black silicified schist (**tab. 2**). The silicified schist appears locally within the wider region in Pleistocene terraces and immediately next to the site in and near the small riverbed. One artefact is made of a more greenish, less dark silicified schist. The only other raw materials from the studied Buhlen assemblage are items made of Baltic flint (n = 1 piece) and reddish yellow carnelian (n = 1 piece).
A similar picture as in Buhlen is becoming evident for Balve (**tab. 2**). The significant majority with 95.3 % (n = 182) of the *Keilmesser* was produced from the local silicified schist. Analogues to Buhlen, the silicified schist can be found in the small river stream next to the site. A few pieces (n = 10) are made of Baltic flint. The nearest source for flint is approximately a distance of 20 km to the north of the cave (Andree 1928; Günther 1988). The silicified schist within the Balve assemblage is not always as dark black as in Buhlen and tends to be more often light-black, greyish or green greyish.
The distribution of the raw material in Ramioul is different though (**tab. 2**). The sampled artefacts are mainly made of a local light-coloured flint. With n = 18 pieces this counts for 90.0 % of the assemblage. The other two artefacts are made of black silicified schist. The silicified schist, too, can be found in the local surroundings of the cave site.

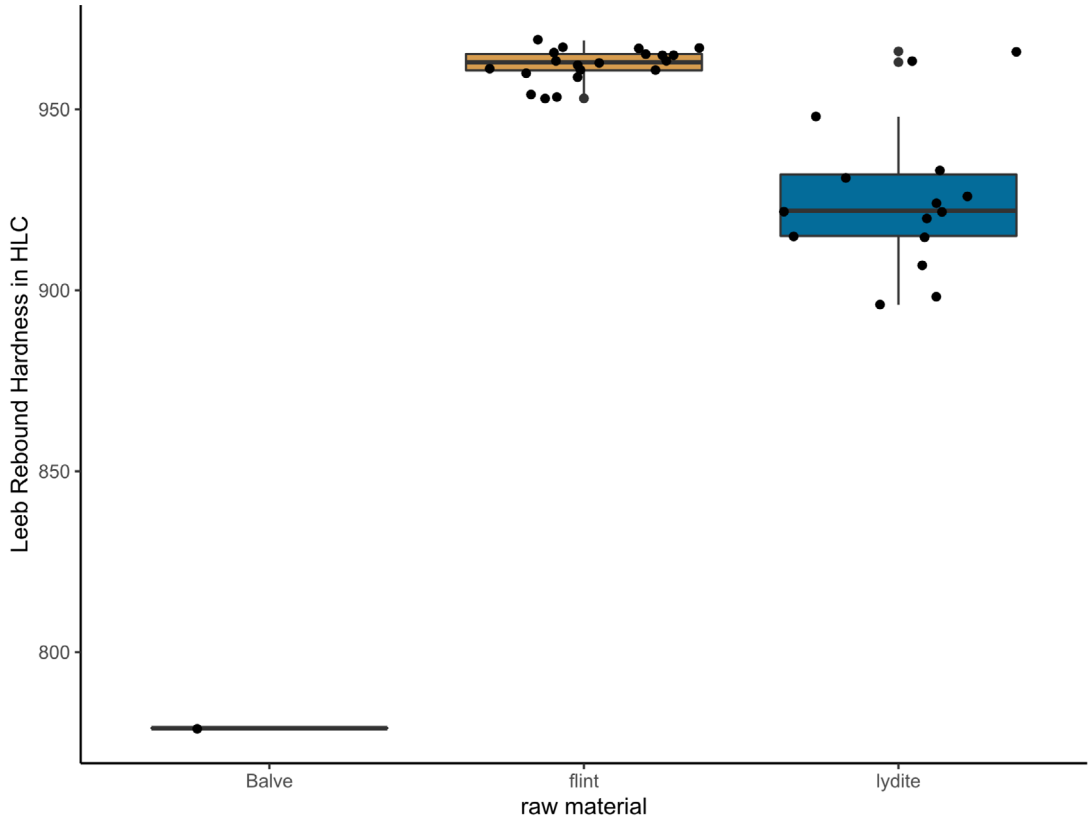

Fig. 41 Leeb Rebound Hardness in HLC measured for the two raw materials flint and lydite (samples initial experiment) and for the semi-finished tool from Balve (ID MU-278).

The *Keilmesser* from the three archaeological sites taken together result in a clear picture regarding the raw material. Nearly 94.2 % (n = 311) of the studied *Keilmesser* are silicified schist artefacts, 5.5 % (n = 18) are made of flint. The other one piece is made of carnelian.

A similar situation as described for the *Keilmesser* is documented for the *Prądnik scrapers*. The sampled *Prądnik scraper* assemblage (n = 24) from Buhlen consists without exception of tools made of black silicified schist.

In Balve, the situation is identical. All n = 27 *Prądnik scrapers* are made of silicified schist.

None of the n = 3 *Prądnik scrapers* from Ramioul is a silicified schist tool. They all are made of flint.

To summarise, 94.4 % (n = 51) of the *Prądnik scraper* assemblage from the three sites consists of tools made of silicified schist (**tab. 2**).

The properties of the two raw materials involved in the study – silicified schist (lydite) and flint – were measured. Surface roughness as well as hardness were considered for the material properties. To start, the hardness was measured with the Leeb rebound hardness tester (Proceq Equotip 550, Leeb C probe). The dataset can be found on GitHub [https://github.com/lschunk/Leeb_hardness]. As explained in the previous chapter, only one silicified schist artefact of the three assemblages fulfilled the necessary requirements to perform the hardness test. The measurements taken on this semi-finished tool from Balve (MU-278) resulted in a mean value of 779 HLC (**fig. 41**).

The same hardness test was applied for the standard samples later used in the experiments (Initial experiment and tool function experiment). Calculating properties such as the raw material hardness allows for a better understanding and also a prediction of aspects such as tool efficiency and durability (Key/Lycett 2017; Key/Fisch/Eren 2018; Key/Pargeter/Schmidt 2020; Key/Proffit/de la Torre 2020). The standard sam-

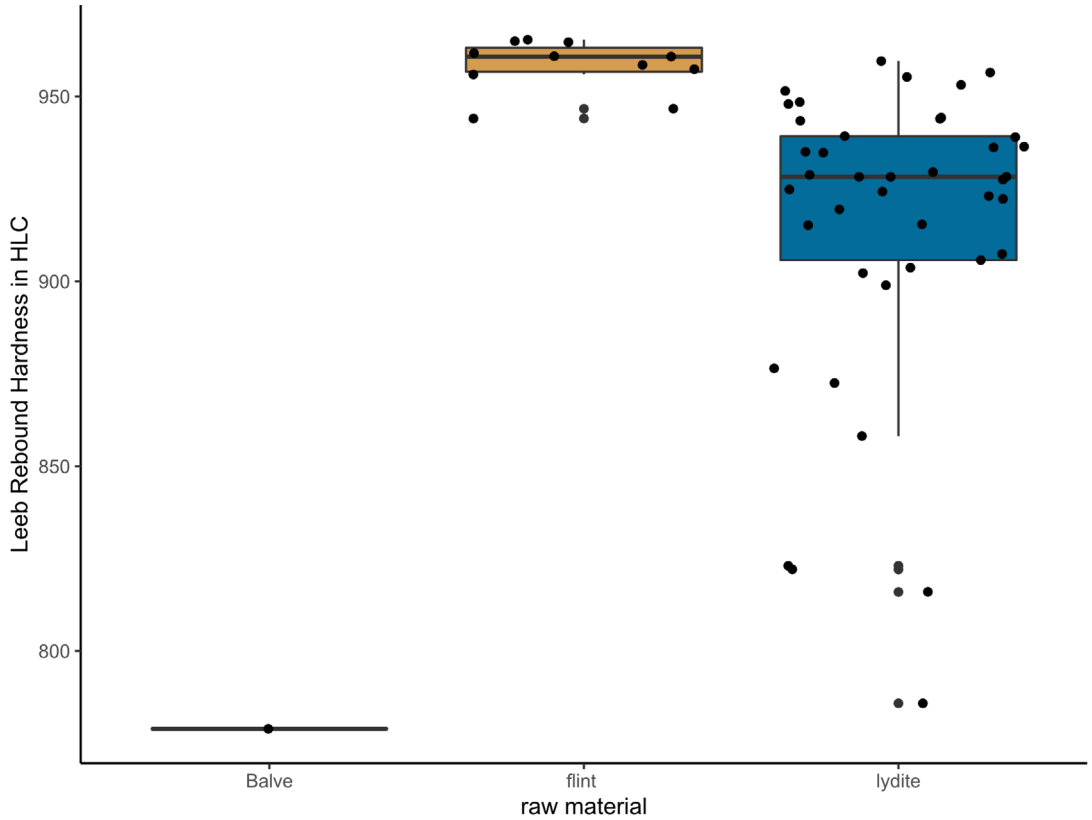

Fig. 42 Leeb Rebound Hardness in HLC measured for the two raw materials flint and lydite (samples tool function experiment) and for the semi-finished tool from Balve (ID MU-278).

ples, prepared for the experiment, are made of silicified schist and Baltic flint. The silicified schist was collected near the two sites Buhlen and Balver Höhle. These samples do have, since cut with the band saw, flat surfaces. Thus, the standard samples were perfectly suitable for the hardness measurement with the Leeb rebound tester. Neither the semi-finished *Keilmesser* from Balve nor the experimental standard samples fulfilled the size requirements. This could be compensated with some additional coupling paste, which connects the sample with the supporting base. Ten measurements per sample were taken in order to average the internal variance per sample. In total, n = 31 flint and n = 56 lydite standard samples were measured (for the experimental data lydite is here used as synonym to silicified schist). Not all of them were used in the experiments later. The measurements were mainly taken in order to get an idea, how similar or different the hardness of these two raw materials is. The Leeb rebound hardness test provides the answer for that (**fig. 42**). Based on the in total n = 87 tested samples, it is possible to say that flint has a higher HLC value than the tested silicified schist does. The arithmetic mean for the flint is 960.8 HLC while the one from silicified schist is 917.9 HLC. The hardness measurements do not only result in a value for the hardness, but they also illustrate another important aspect. The flint hardness ranges from 944.1 HLC to 969.0 HLC. However, the range for the lydite is from minimum 785.9 HLC to maximum 966.0 HLC. The variance for silicified schist is considerably higher compared to the flint. Likely, the reason for that can be seen in the schistosity planes or the banding of the lydite. Lydite is a finely layered, brittle sedimentary rock that fractures conchoidally. The raw material is also characterised by small cracks. By applying the Leeb rebound hardness test, an impact body, a small ball, is driven with a defined energy against the surface of the sample. The velocity of the impact body before and after the impact gets measured. Based on these measurements, the ratio between the impact velocity and rebound velocity defines the Leeb hardness (HL, here HLC). Whenever the

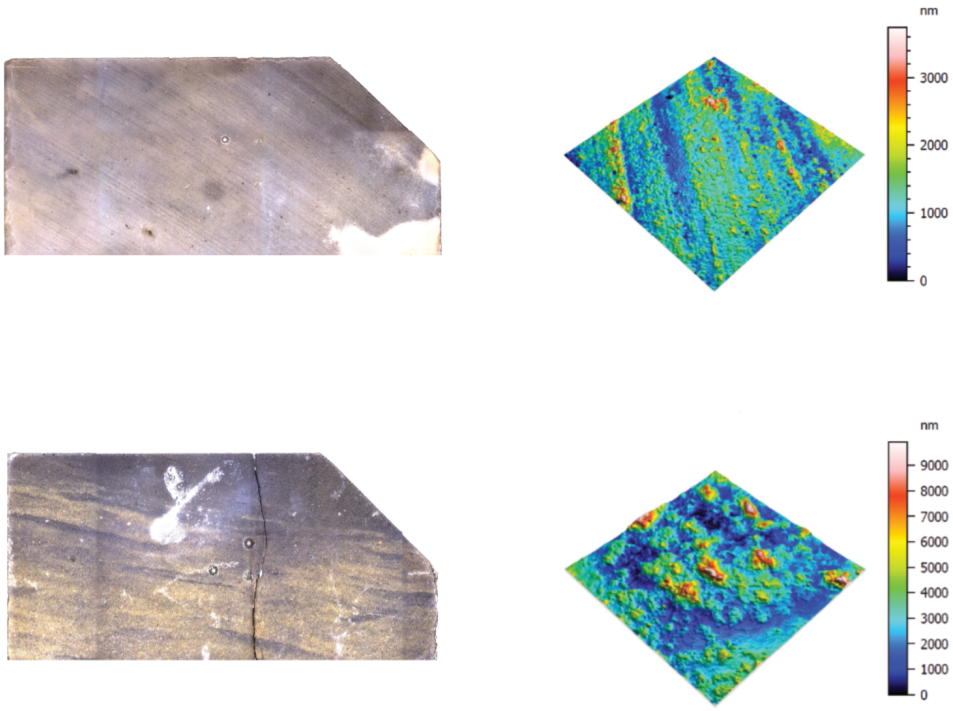

Fig. 43 Surface of unused standard samples for experimental approaches (left) and confocal micro-surface texture (right). The colour of the surfaces corresponds to the height on the z-axis. The upper row shows a flint sample, the lower row a lydite sample.

impact boy hits a less compact area of the surface (e. g. a crack underneath the surface), rebound energy gets lost and the Leeb hardness value will be smaller. This might be frequently the case for the silicified schist. Depending on the quality of the silicified schist, the Leeb hardness measurement will result in a lower or higher value per sample. When considering the range of the measured Leeb hardness of the lydite, the minimum values are comparable to the Leeb hardness of the semi-finished *Keilmesser* from Balve. The artefact has a Leeb hardness of 779 HLC and is thus similar to the lowest Leeb hardness value of 785.9 HLC from one of the standard samples.

As a second raw material property, the surface roughness was included in the raw material characterisation. Surface roughness can be measured with a confocal laser scanning microscope (for details see chapter Quantitative use-wear analysis). Unfortunately, the surface roughness of the archaeological samples were not considered during the data acquisition and thus not measured. Instead, measurements were taken on standard samples before they were used in the experiment (»artificial VS natural« experiment) (**fig. 43**). Surface roughness is a component of the surface texture and describes the unevenness of a surface height. Based on directional deviations from the surfaces, the surface roughness can be quantified. A large deviation stands therefore for rough surfaces while a small deviation is equal to smooth surfaces. In order to address the surface roughness of the measured standard sample here, *Sq*, the root mean square height, as one of the seven existing areal field parameters was chosen (for more information see Digital Surf, Besançon, France). Areal field parameters, especially *Sq*, are known to give more significant values. The results were calculated following the ISO 25178. The surface roughness was measured for n = 4 lydite as well as n = 4 flint standard samples. The arithmetic mean for the lydite samples is 22.392 µm while the one for the flint samples is 12.206 µm. Based on these values, flint surfaces are quantified as less rough than the lydite surface. It has to be pointed out that the measurements were taken on the standard samples, which are cut with a band saw (see chapter Controlled experiments). The traces from the band saw are macroscopically clearly visible on the sample surface. These traces surely affect the surface roughness. Unfortunately, there

is no reference collection or any comparable measurements taken on machine cut samples yet. Single comparable values measured on flint can be found in literature (Evans et al. 2014; Calandra et al. 2019c). These specific flint samples are knapped flakes and measured under similar (Evans et al. 2014) or even identical (Calandra et al. 2019c) settings than the standard samples within this project. The analysis for these flint samples was also done according to the ISO 25178. The measurements taken by Evans et al. lead to *Sq* values between 0.64 µm and 0.98 µm. The *Sq* values for other flint sample (Calandra et al. 2019c, supplementary table S3) ranges between 0.824 µm and 1.912 µm. Thus, these values are significantly lower than the values calculated on cut standard samples.
Additionally, the variance in the results from the standard samples has to be pointed out. While the measurements taken on the lydite samples ranging from 16.468 µm to 26.081 µm, the range is considerably bigger for the flint measurements. The minimum value for flint is 4.136 µm and the maximum is 28.733 µm. Without further measurements or a reliable reference collection, the variability within the calculated surface roughness values cannot be explained.
In general, although parameters such as the surface roughness are highly relevant, especially in the context of use-wear analysis and experimental design, they are not much explored yet in archaeology. The results presented here might indicate that lydite, even when both raw materials are cut identically with a band saw, has a higher surface roughness than flint. However, the existing information about the surface's roughness of the raw materials lydite and flint are not sufficient for further conclusions.

TECHNO-TYPOLOGICAL ANALYSIS

As mentioned above, the presentation of the results from the techno-typological analysis consider first the results from the *Keilmesser*, followed by the results from the *Prądnik scrapers*. In a later step, the focus is on the results gained from analysing the *Prądnik spalls*.

Blanks and cortex

In this part of the analysis, the distinction was made whether an artefact displays a core tool or not. This aspect is relevant to *Keilmesser* and *Prądnik scrapers*. Another interesting aspect in this context is the amount of cortex on the tool's surface, since it can provide some indications to which degree the blank was modified.
In Buhlen, 67.0 % (n = 87) of the *Keilmesser* could be defined as core tools (**fig. 44**). With 6.2 % (n = 8) only, flakes have been transformed into *Keilmesser* considerably less frequently. In 26.9 % (n = 35) of the artefacts the blank could not be determined as either core or flake. N = 55 of all *Keilmesser* are not covered with cortex at all. The remaining n = 75 artefacts have cortex. Most of them (n = 61) are core tools. Most of the time, the cortex can be found at the back of the tool (n = 38) or on the base (n = 22). Only in individual cases, the cortex is located in the proximal (n = 4) or medial (n = 9) tool area. The percentage of cortex measured on the complete tool surface is most often limited to less 25 % (n = 43). In one third (n = 25) of the tools with cortex, the percentage of cortex reaches up to 50 %.
In Balve, the majority of the tools, 71.2 %, were also manufactured as core tools with n = 136 artefacts (**fig. 45**). A comparable small number of *Keilmesser*, as in Buhlen, was produced on flakes (4.7 %, n = 9). The blank type was undeterminable in 24.1 % (n = 46) cases. The question, whether the *Keilmesser* from

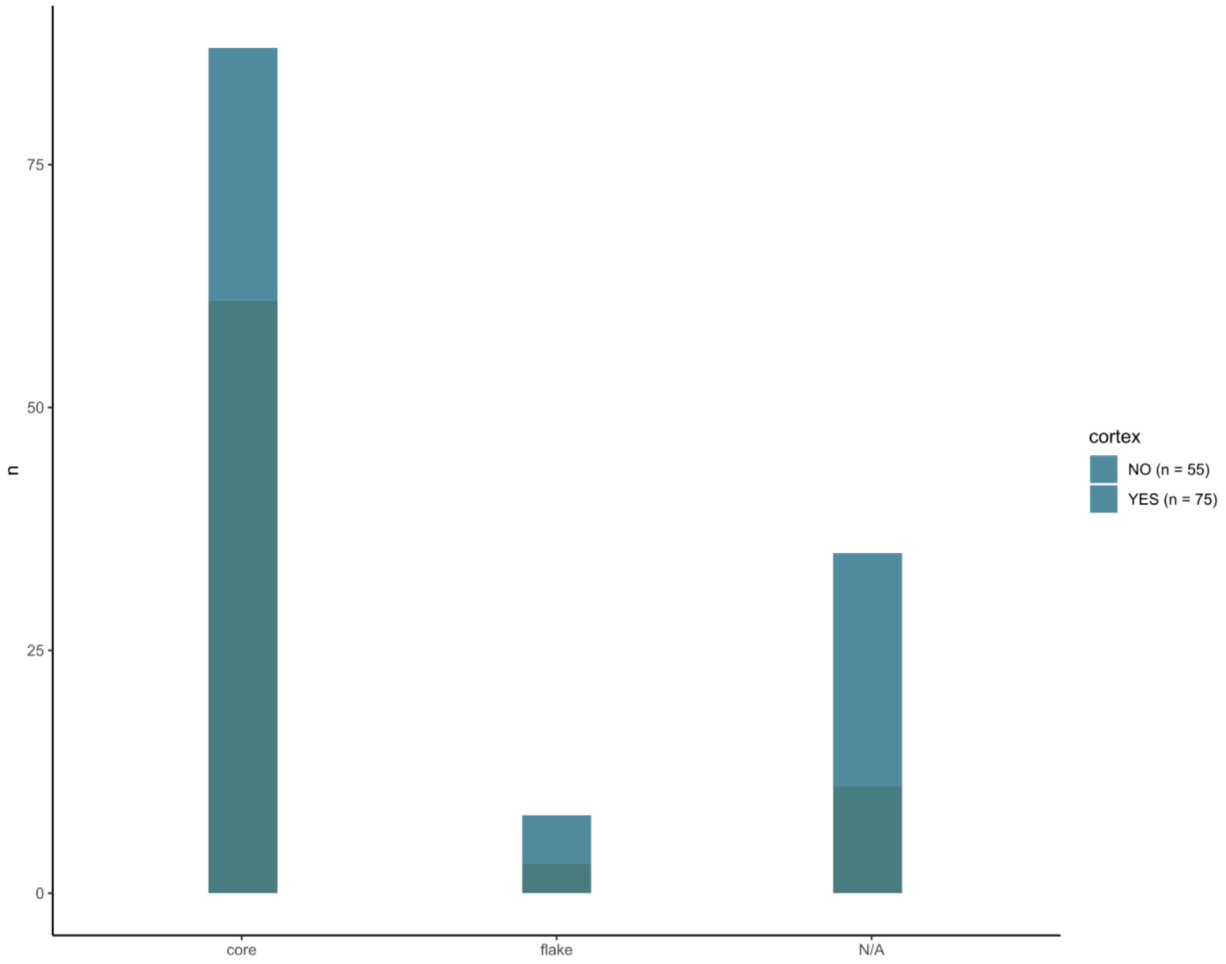

Fig. 44 Blank selection for the production of *Keilmesser* (n = 130) from Buhlen. Additionally, the figure includes the information whether an artefacts displays cortex or not.

the assemblage in Balve are covered with cortex or not, cannot be answered to full extent. One part of the assemblage was a short time loan from the LWL-Museum for Archaeology in Herne. When the material was studied a few years ago, this aspect was not part of the attribute analysis. Therefore, n = 35 *Keilmesser* need to be excluded. From the remaining n = 156 artefacts, n = 33 display no cortex. On the contrary, for n = 123 *Keilmesser*, cortex could be documented. Similar as in Buhlen, the cortex is by a majority (n = 95) located along the back of the tools. N = 6 pieces also show cortex on the tool base or in generally in the proximal area of the tool (n = 1). Cortex could be also documented in the medial (n = 14) or distal (n = 4) tool parts. N = 3 artefacts have cortex covering nearly the entire tool surface (except the active edge) with up to 75 % cortex. One of these three artefacts is a semi-finished tool. For the other tools with cortex, the same as in Buhlen counts. The percentage of cortex most commonly (n = 67) reaches up to 25 % of the surface. On n = 23 pieces, the amount of cortex is higher, but also limited to maximum 50 %.

Despite the small assemblage, the *Keilmesser* from Ramioul manufactured on cores also predominate the assemblage (**fig. 46**). 44.4 % (n = 4) are core tools, one artefact was made from a flake and again, 44.4 % (n = 4) could not be determined. All *Keilmesser*, except the one made from a flake, show cortex. The cortex is mostly located on the back (n = 7) and n = 1 artefacts has cortex on the proximal area of the dorsal tool surface. The percentage of cortex on the surface is comparable with the results from Buhlen and Balver Höhle. On only n = 2 *Keilmesser* up to 50 % of cortex could be documented. The other n = 6 artefacts display lower cortex percentages with maximum 25 %.

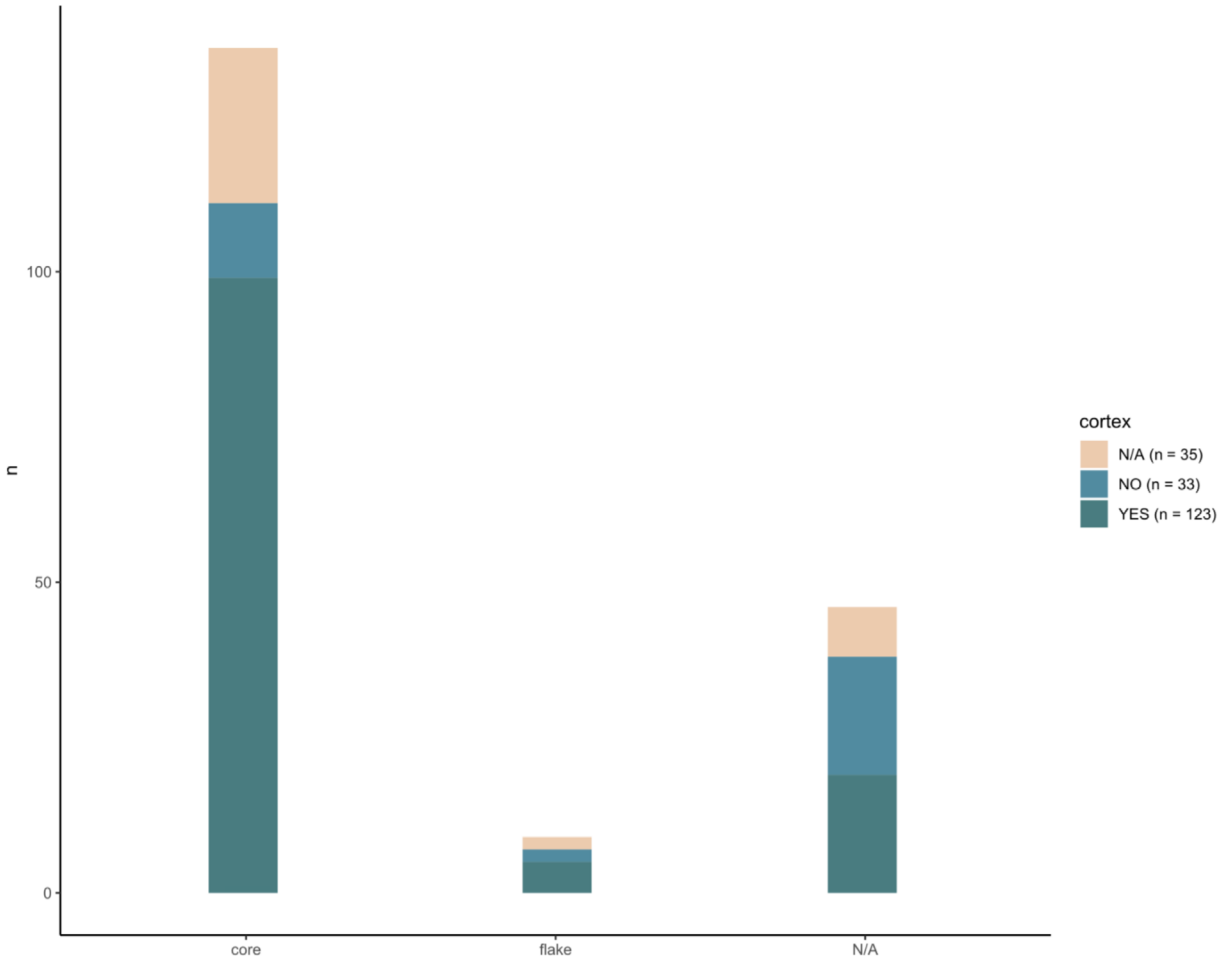

Fig. 45 Blank selection for the production of *Keilmesser* (n = 191) from Balver Höhle. Additionally, the figure includes the information whether an artefacts displays cortex or not. For some artefacts, this analysis was not done. Thus, these artefacts are labelled as N/A.

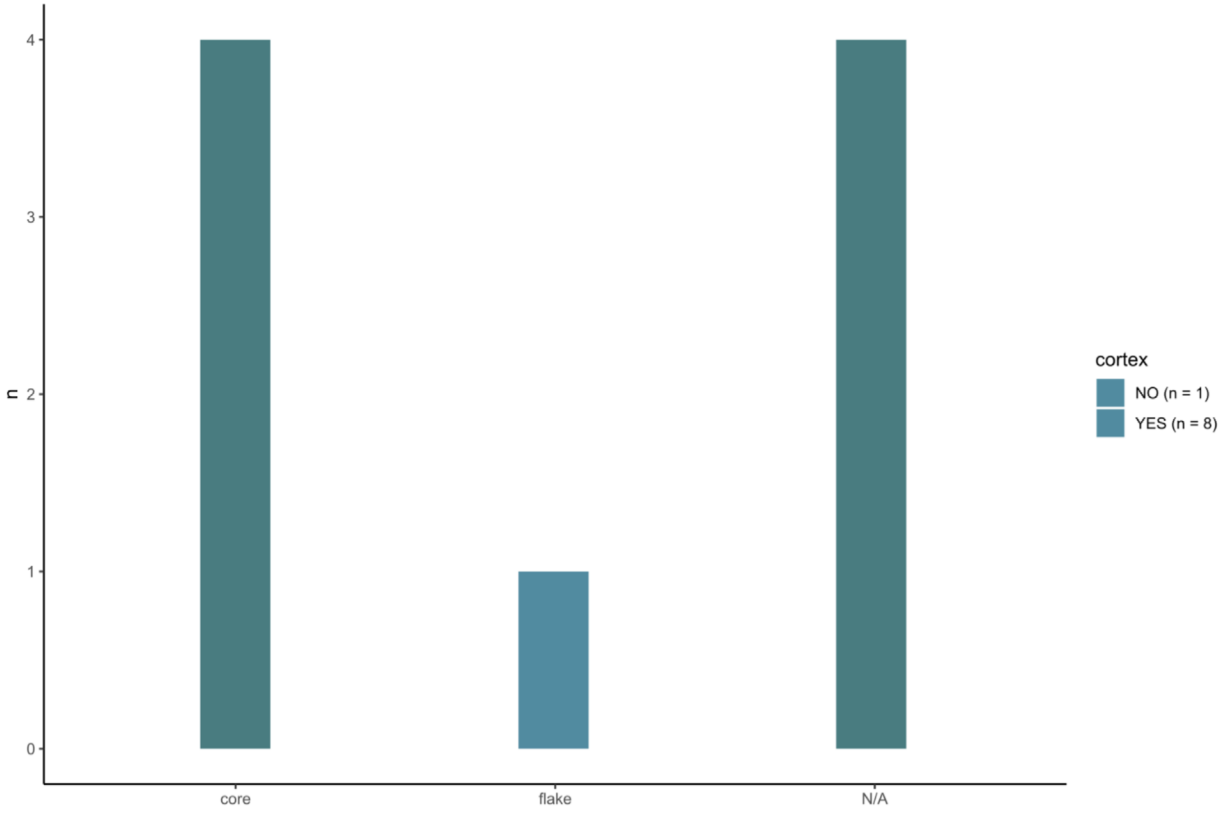

Fig. 46 Blank selection for the production of *Keilmesser* (n = 9) from Ramioul. Additionally, the figure includes the information whether an artefacts displays cortex or not.

These results combined for the three sites together illustrate a clear picture (**fig. 47**). The *Keilmesser* from these assemblages are by a majority of 68.8 % (n = 227) core tools. For only a small amount of 5.5 % (n = 18) a flake was used as a blank. For roughly a quarter (n = 85) of the tools the blank type could not be determined for sure.
Additionally, on the majority (69.8 %, n = 206) of the *Keilmesser,* cortex could be documented, covering up to 25 % of the surface (56.3 %, n = 116). Most often, the cortex was located on the back (68.0 %, n = 140) of the tools.
None of the *Prądnik scrapers* from the studied assemblages can be defined for sure as a core tool. In contrary, all *Prądnik scrapers* from Buhlen are clearly tools produced on a flake. The analysis for the quantity and location of cortex on the tool surfaces was done for the *Prądnik scrapers* as well. The results are contrasting to the ones from the *Keilmesser* though. However, considering the blanks chosen to produce the tools, the results are consistent. In Buhlen 79, 2 % (n = 19) of the *Prądnik scraper* do not show any cortex. The only n = 5 artefacts with cortex display up to 25 % cortex along the back (n = 4) or on the base (n = 1).
Also in Balve, n = 21 (77.8 %) artefacts could be documented as such. In the remaining n = 6 cases, the blank type was undeterminable. Nearly half (n = 13) of the *Prądnik scrapers* from the assemblage in Balve have no cortex. N = 8 artefacts display cortex along the back, n = 2 tools either has cortex in the medial or distal part of the tool. Except for one of these n = 10 *Prądnik scraper* the percentage of cortex per surface was less than 25 %. For n = 4 *Prądnik scraper* this analysis was not conducted.
The results for the *Prądnik scrapers* from Ramioul are equivalent to the ones from Buhlen; all *Prądnik scrapers* are produced from flakes. In Ramioul, no cortex could be documented on the *Prądnik scrapers.*
The results taken together illustrate that 88.9 % (n = 48) of the *Prądnik scrapers* are produced from flakes (**fig. 48**). For the other 10.1 % (n = 6) the blank type is unknown. With only 27.8 % (n = 15) the quantity of tools with cortex is lower than compared to the *Keilmesser*.

Morphometric quantitative analysis

The dimensions to address first are the length, width and thickness measurements. In general, the fragmented *Keilmesser* were omitted in this part of the analysis. The measurements of these tools can be found on GitHub [https://github.com/lschunk/Lithic_analysis_archaeology]. Additionally, the results from the complete *Keilmesser* are separated from the ones from the *Keilmesser* tips.
The complete *Keilmesser* from the here studied assemblage from Buhlen (n = 111) can be classified in a size range from 30.0 mm to 113.5 mm length (**figs 49. 52**). The arithmetic mean of the length is 53.0 mm. Concerning the width, the minimum and maximum are extending between 14.0 mm and 71.9 mm, with an arithmetic mean value of 32.9 mm (**fig. 53**). The thickness is ranging between 7.0 mm and 31.0 mm (**fig. 54**). The arithmetic mean amounts to 16.1 mm.
These measurements considered for the *Keilmesser* tips only, lead to the following picture. As to be expected, the n = 15 *Keilmesser* tips are significantly smaller in terms of the artefact length. The length ranges between 13.0 mm and 46.0 mm. The arithmetic mean is 28.1 mm. The minimum width measurement is 19.0 mm while the maximum is 42.0 mm. The arithmetic mean is similar to the one from the complete *Keilmesser* with 30.0 mm. The thickness is ranging from 8.0 mm to 20.0 mm with an arithmetic mean value of 12.6 mm.
In Balve, the results of the length, width and thickness measurements are based on n = 158 complete *Keilmesser*. The arithmetic mean of the length measurements is 55.5 mm with a minimum length of 29.7 mm and a maximum of 135.6 mm (**figs 50. 52**). With these values, the margin is bigger than in Buhlen, but

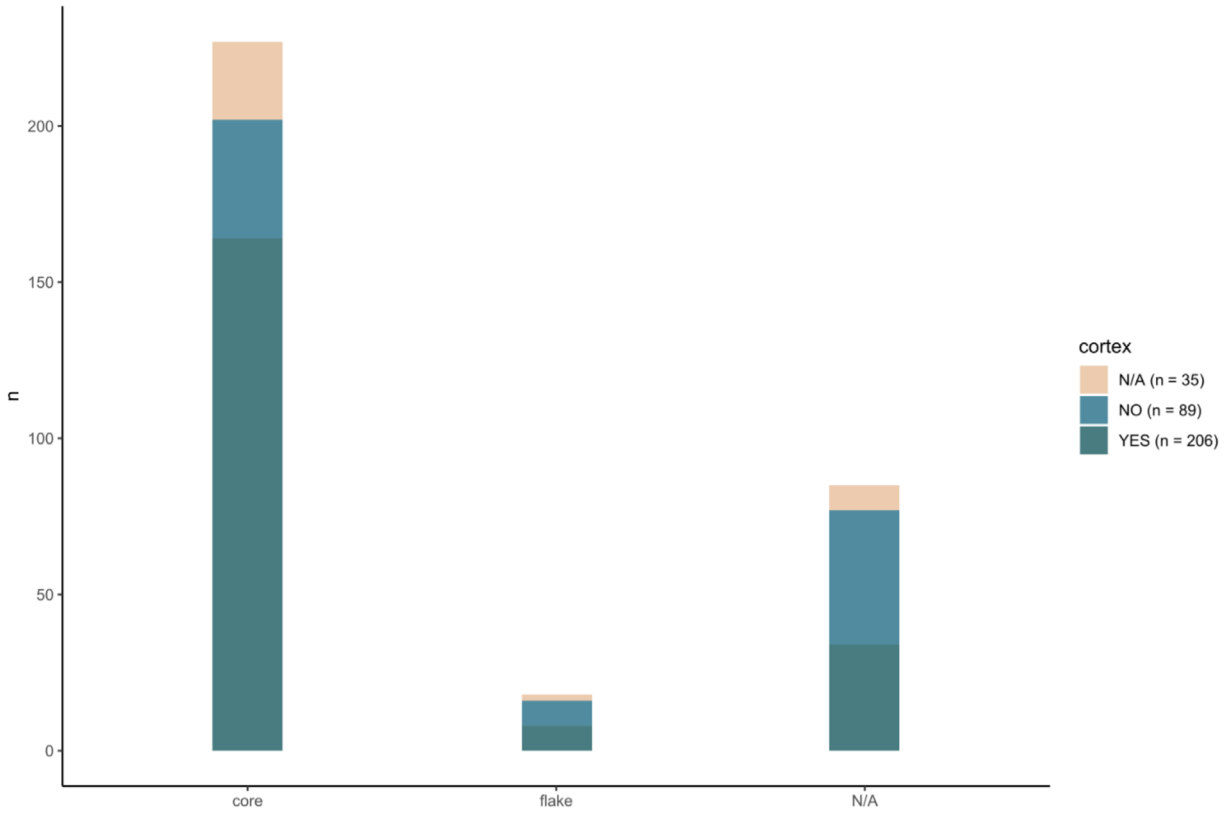

Fig. 47 Blank selection for the production of *Keilmesser* from Buhlen (n = 130), Balver Höhle (n = 191) and Ramioul (n = 9). Additionally, the figure includes the information whether an artefacts displays cortex or not. For some artefacts, this analysis was not done. Thus, these artefacts are labelled as N/A.

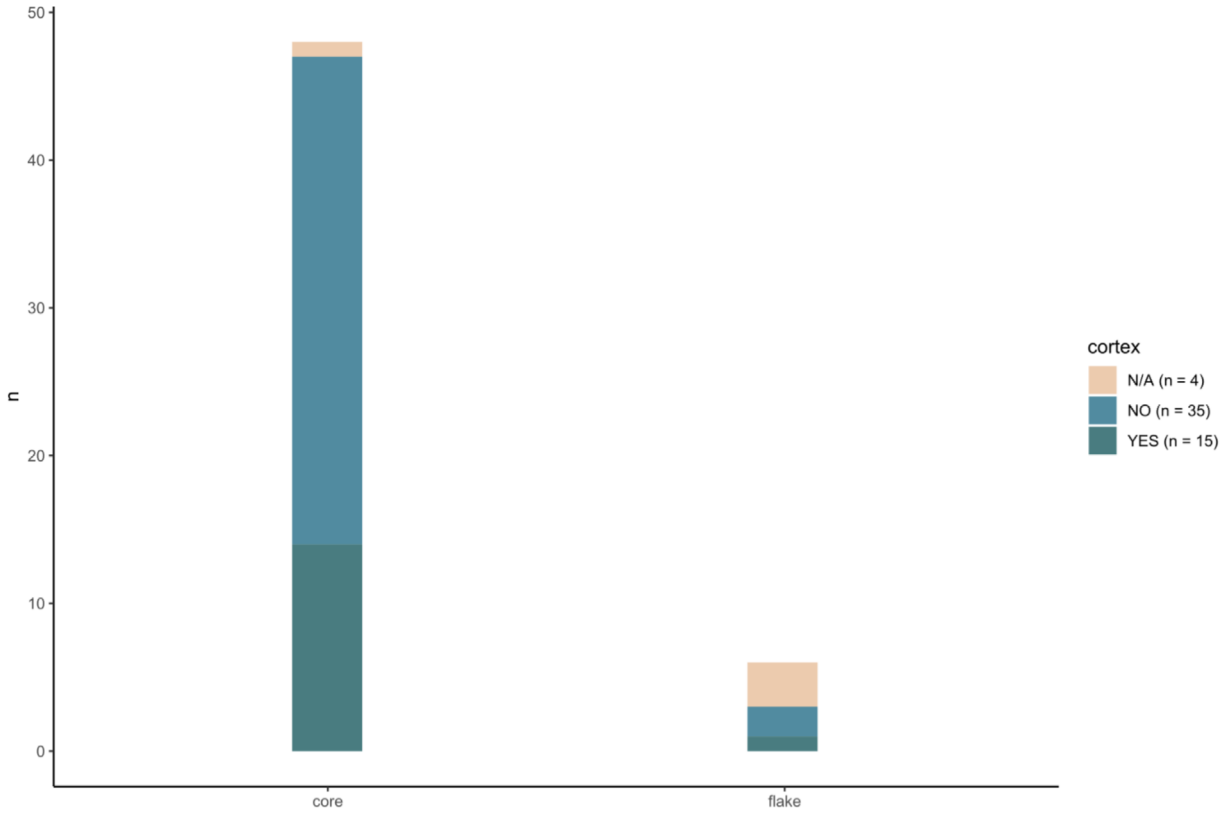

Fig. 48 Blank selection for the production of *Prądnik scraper* from Buhlen (n = 24), Balver Höhle (n = 27) and Ramioul (n = 3). Additionally, the figure includes the information whether an artefacts displays cortex or not. For some artefacts, this analysis was not done. Thus, these artefacts are labelled as N/A.

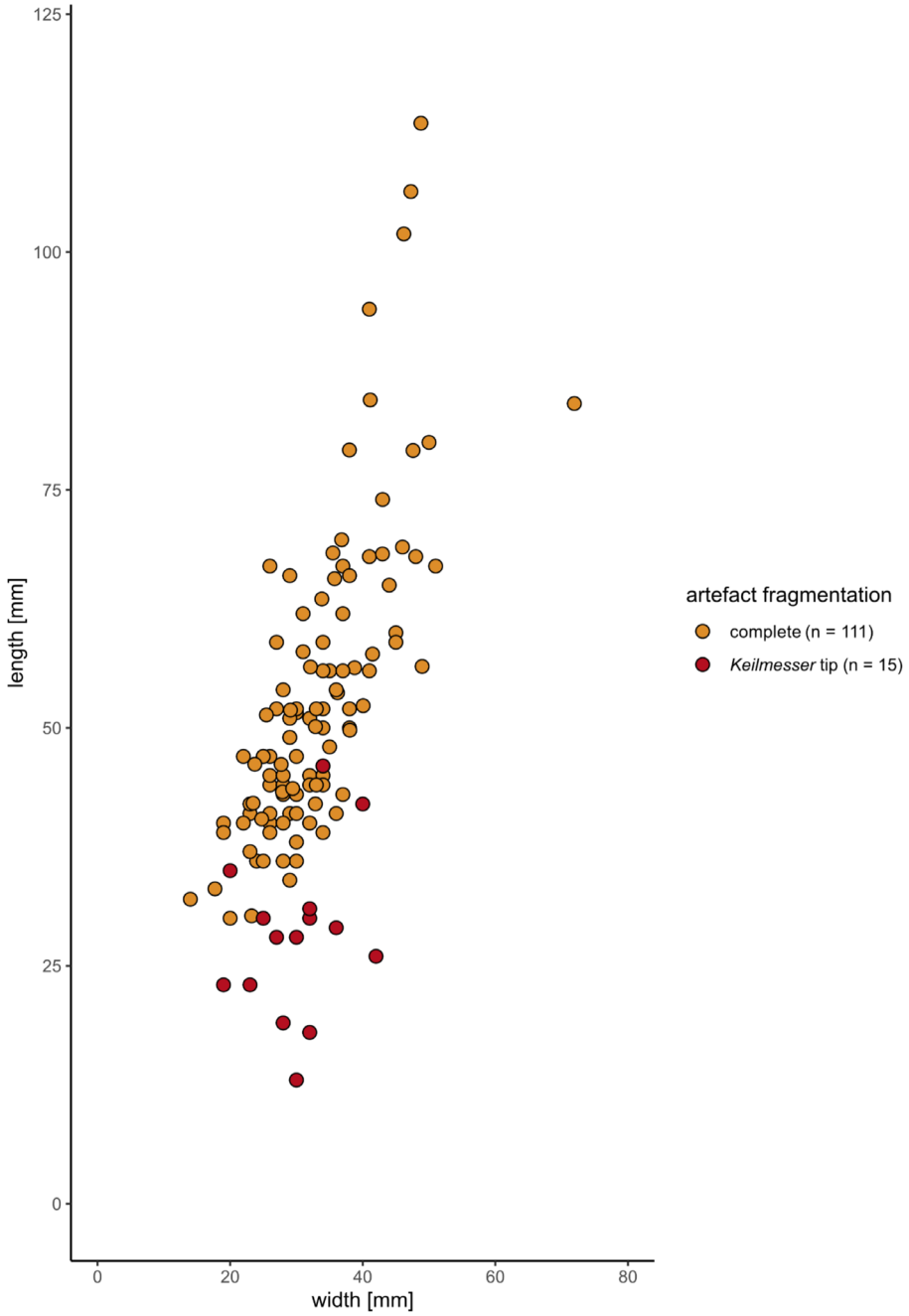

Fig. 49 Length-width ratio of the complete *Keilmesser* (n = 111) and *Keilmesser* tips (n = 15) from Buhlen.

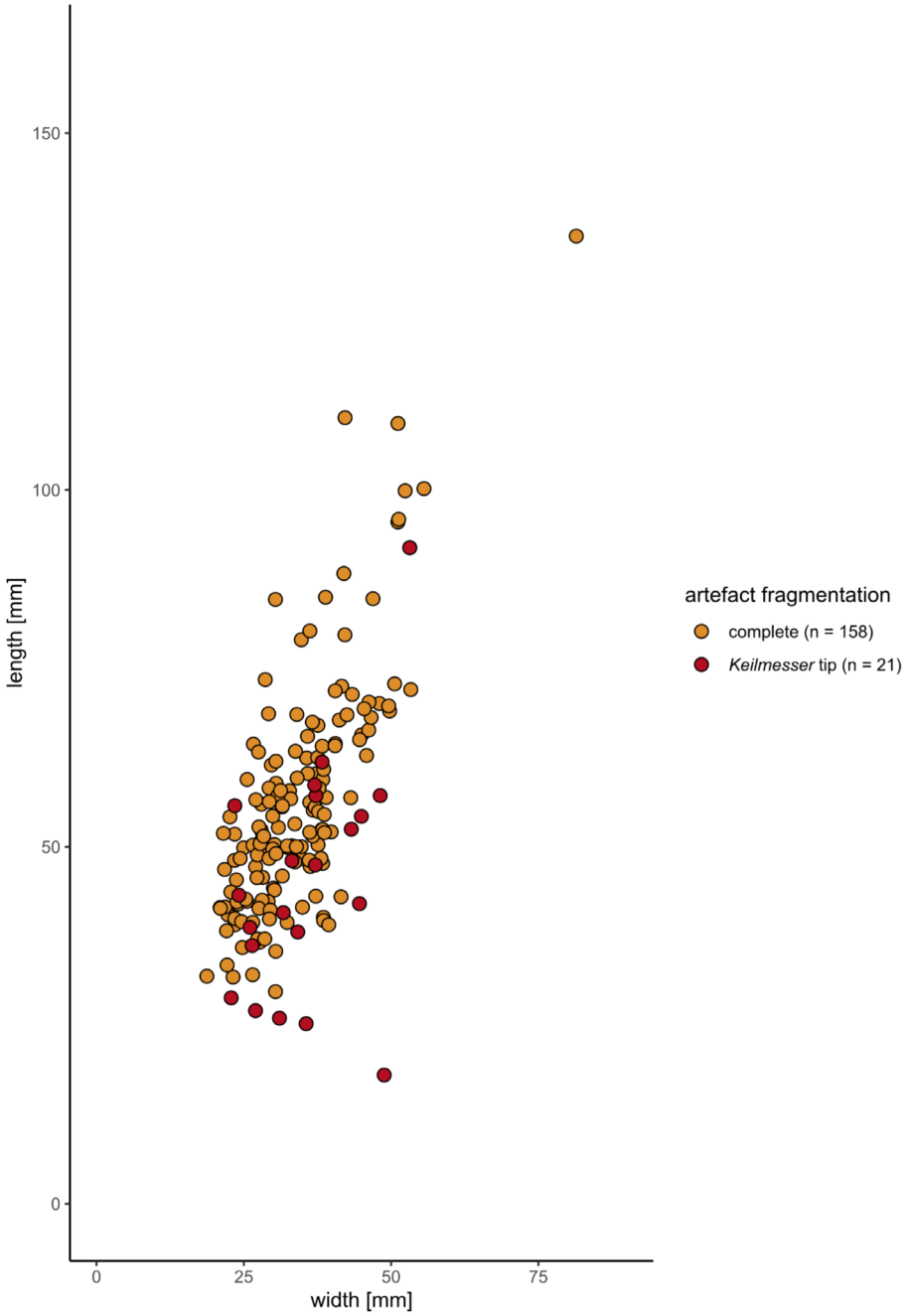

Fig. 50 Length-width ratio of the complete *Keilmesser* (n = 158) and *Keilmesser* tips (n = 21) from Balver Höhle.

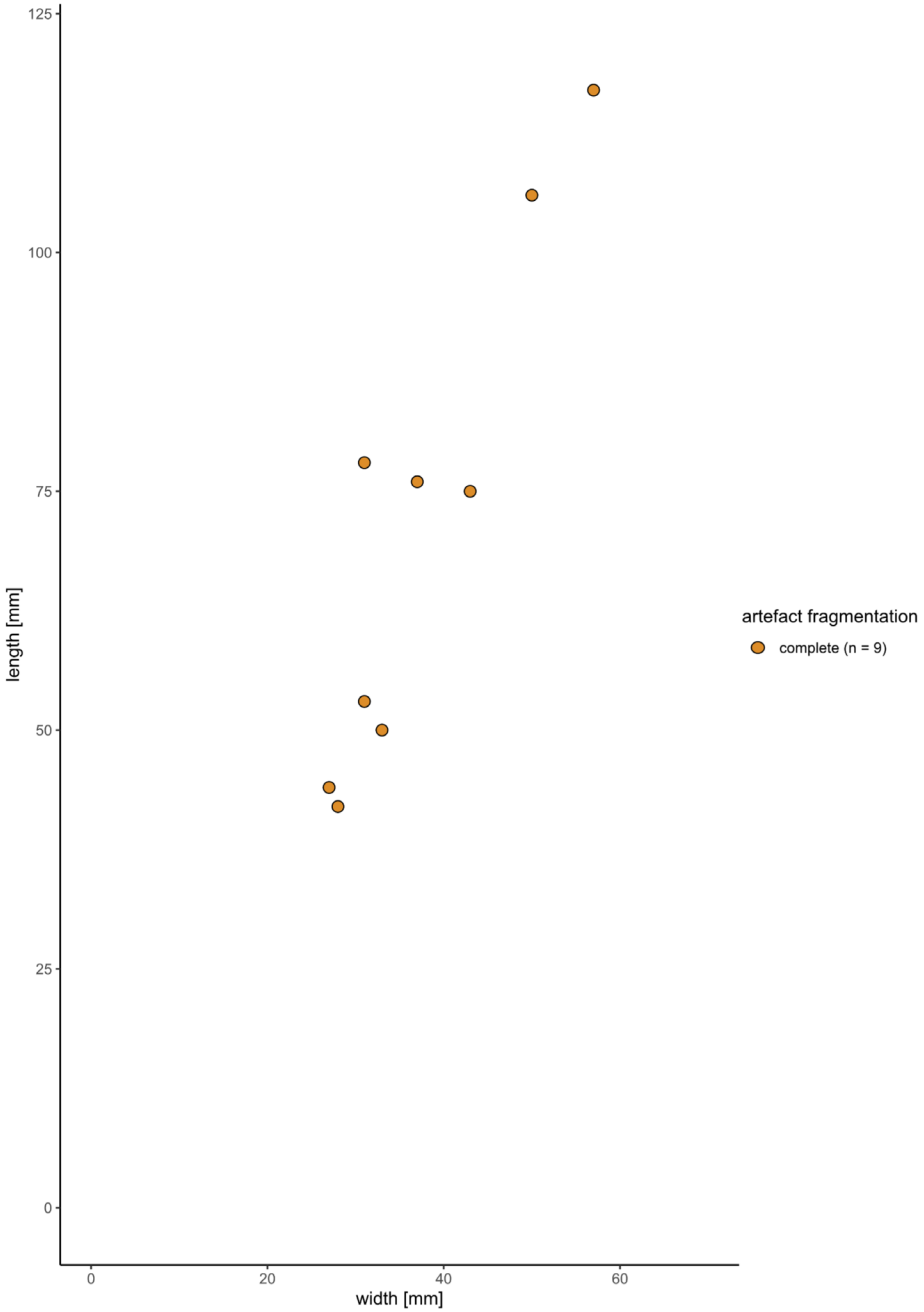

Fig. 51 Length-width ratio of the complete *Keilmesser* (n = 9) from Ramioul.

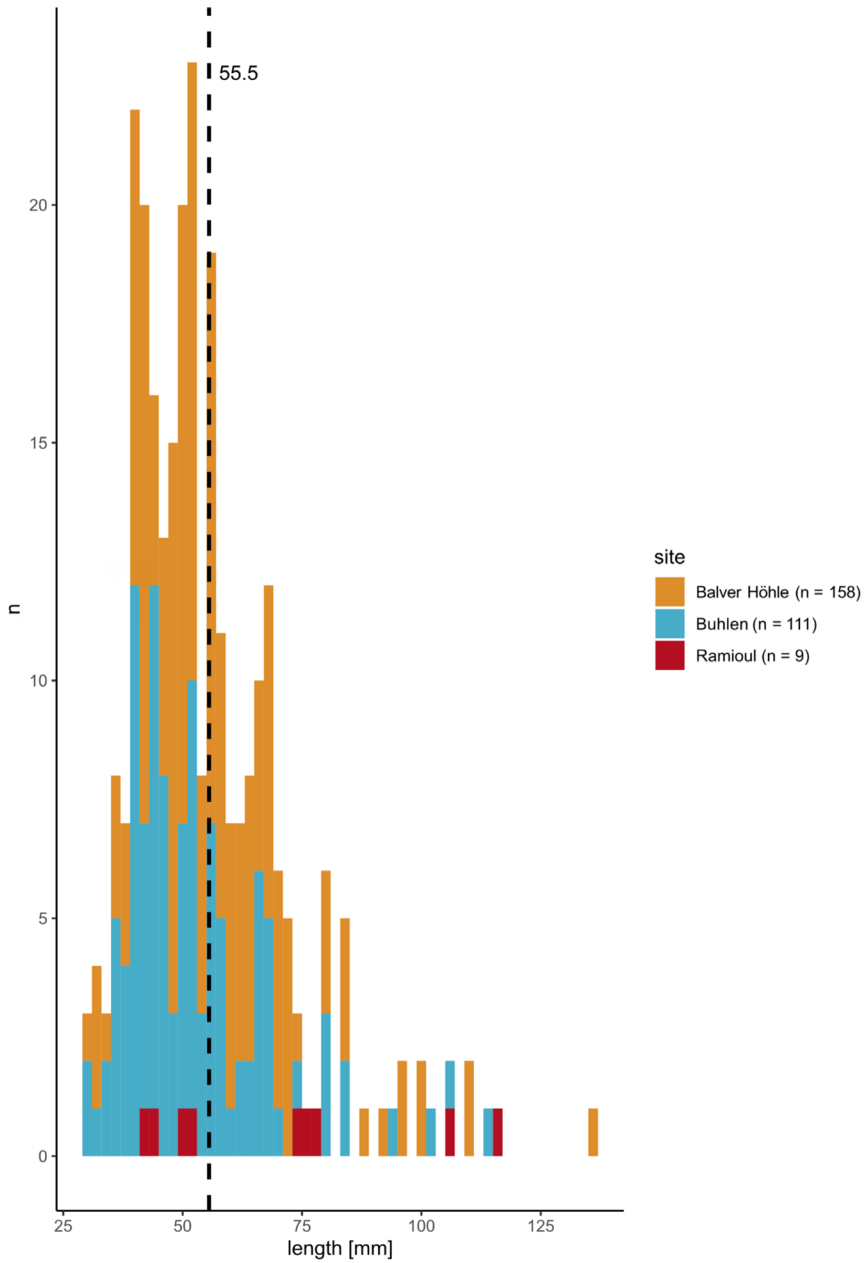

Fig. 52 Maximal length of the complete *Keilmesser* from Buhlen (n = 111), Balver Höhle (n = 158) and Ramioul (n = 9). The dashed line indicates the arithmetic mean value.

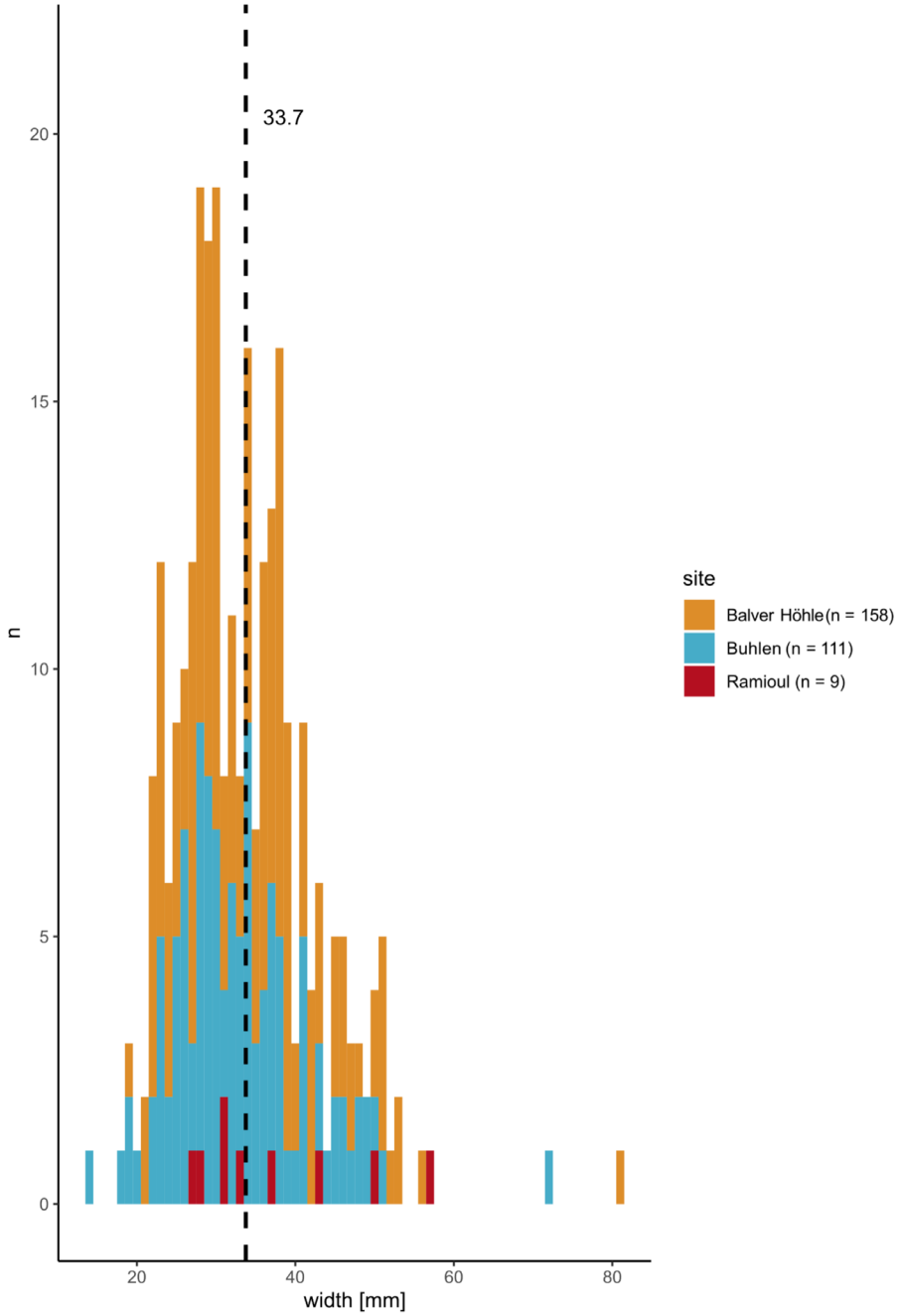

Fig. 53 Maximal width of the *Keilmesser* from Buhlen (n = 158), Balver Höhle (n = 111) and Ramioul (n = 9). The dashed line indicates the arithmetic mean value.

the mean values are comparable. The width is ranging between 18.7 mm and 81.4 mm with an arithmetic mean of 34.1 mm (**fig. 53**). The measured thickness values are similar to the ones from Buhlen (**fig. 54**). The margin is between 7.4 mm and 29.3 mm. The arithmetic mean value is 16.3 mm.

When looking at the *Keilmesser* tips only (n = 21), the measurements result in the following values. The length is ranging from 18.0 mm to 91.0 mm. The arithmetic mean amounts to 45.2 mm. The arithmetic mean value concerning the width is slightly higher than the one for the complete *Keilmesser* with 35.6 mm. The measured minimum value is thereby 22.9 mm and the maximum value 53.9 mm. The thickness margin is between 9.5 mm and 23.6 mm. The arithmetic mean is 15.5 mm.

In the same way as for Buhlen and Balve, the measurements were recorded for the *Keilmesser* from Ramioul. The results deviate not much from the results already mentioned, but since the assemblage from Rami-

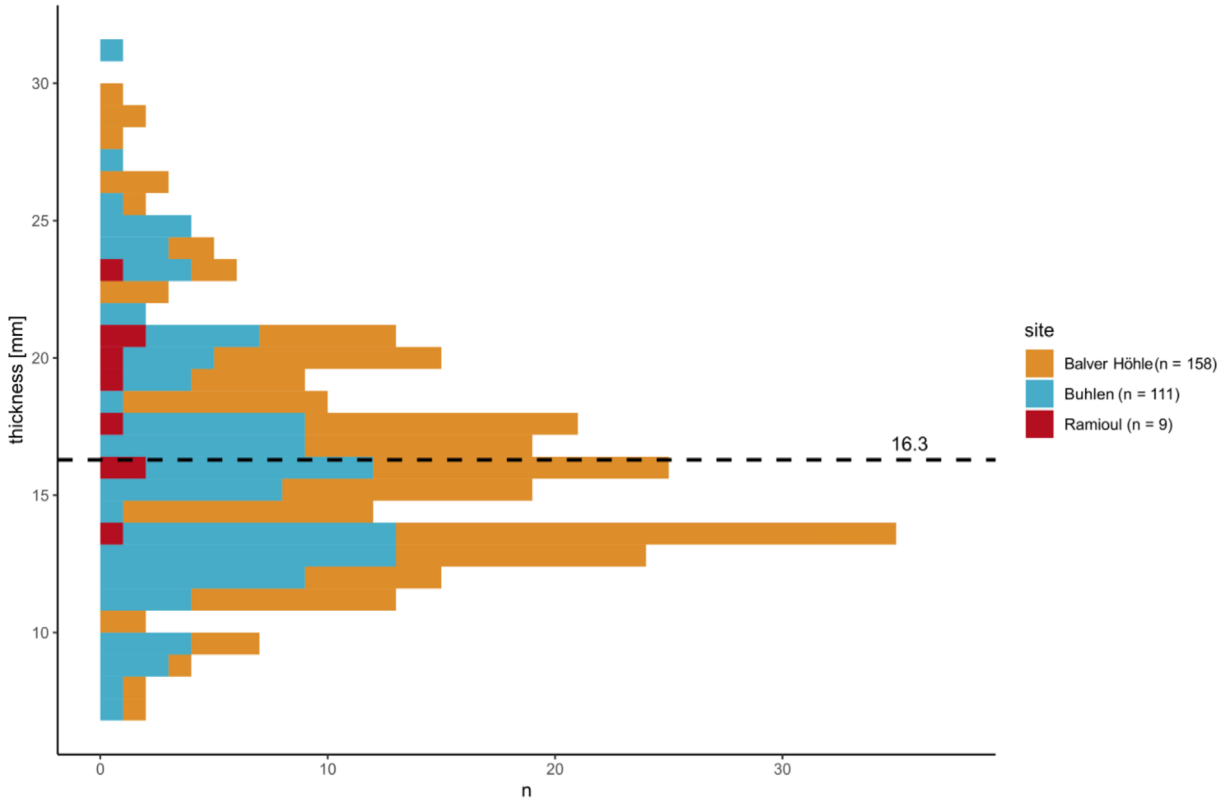

Fig. 54 Maximal thickness of the *Keilmesser* from Buhlen (n = 158), Balver Höhle (n = 111) and Ramioul (n = 9). The dashed line indicates the arithmetic mean value.

oul is significantly smaller (n = 9), the results are of little consequence (**figs 51-52**). The minimum length is 42.0 mm, while the maximum is 117.0 mm. The arithmetic mean can be calculated as 71.2 mm. Concerning the width, the minimum and maximum values extend between 27.0 mm and 57.0 mm, with an arithmetic mean value of 37.4 mm (**fig. 53**). The thickness of the *Keilmesser* ranges between 14.0 mm and 23.0 mm (**fig. 54**). The arithmetic mean is 18.7 mm.

The results from the three sites taken together reveal the following picture. *Keilmesser* (n = 278) extend in their length from 29.7 mm to 135.6 mm (**figs 52. 55**). The arithmetic mean is 55.5 mm. The width measurements ranging from 14.0 mm to 81.4 mm with an arithmetic mean value of 33.7 mm (**fig. 53**). The range for the thickness is between 7.0 mm and 31.0 mm (**fig. 54**). The arithmetic mean is 16.3 mm.

The dimensions – length, width and thickness – were measured for all *Prądnik scrapers.*

In Buhlen, the results of the length measurements are in a range between 27.0 mm and 78.0 mm (**figs 56. 59**). The arithmetic mean of the length is 43.5 mm. The mean value for the width is 28.5 mm with a minimum measurement of 18.0 mm and a maximum of 48.0 mm (**fig. 60**). The thickness of *Prądnik scrapers* is ranging between 4.0 mm and 15.8 mm with an arithmetic mean of 9.2 mm (**fig. 61**).

The *Prądnik scrapers* from Balve can be classified in a size range from 33.4 mm to 75.7 mm length (**figs 57. 59**). The arithmetic mean of the length is 50.5 mm. The width extends from 20.6 mm to 53.3 mm, with an arithmetic mean value of 32.8 mm (**fig. 60**). The thickness is ranging between 1.2 mm and 20.4 mm (**fig. 61**). The arithmetic mean is 13.9 mm.

The margins for the *Prądnik scraper* length from Ramioul are 45.0 mm and 52.0 mm (**figs 58-59**). The arithmetic mean value adds up to 48.3 mm. The minimum and maximum width values extend between 35.0 mm and 37.0 mm, with an arithmetic mean value of 35.7 mm (**fig. 60**). The arithmetic mean of the thickness is 12.0 mm (**fig. 61**). The measurements range from 11. 0 mm to 14.0 mm.

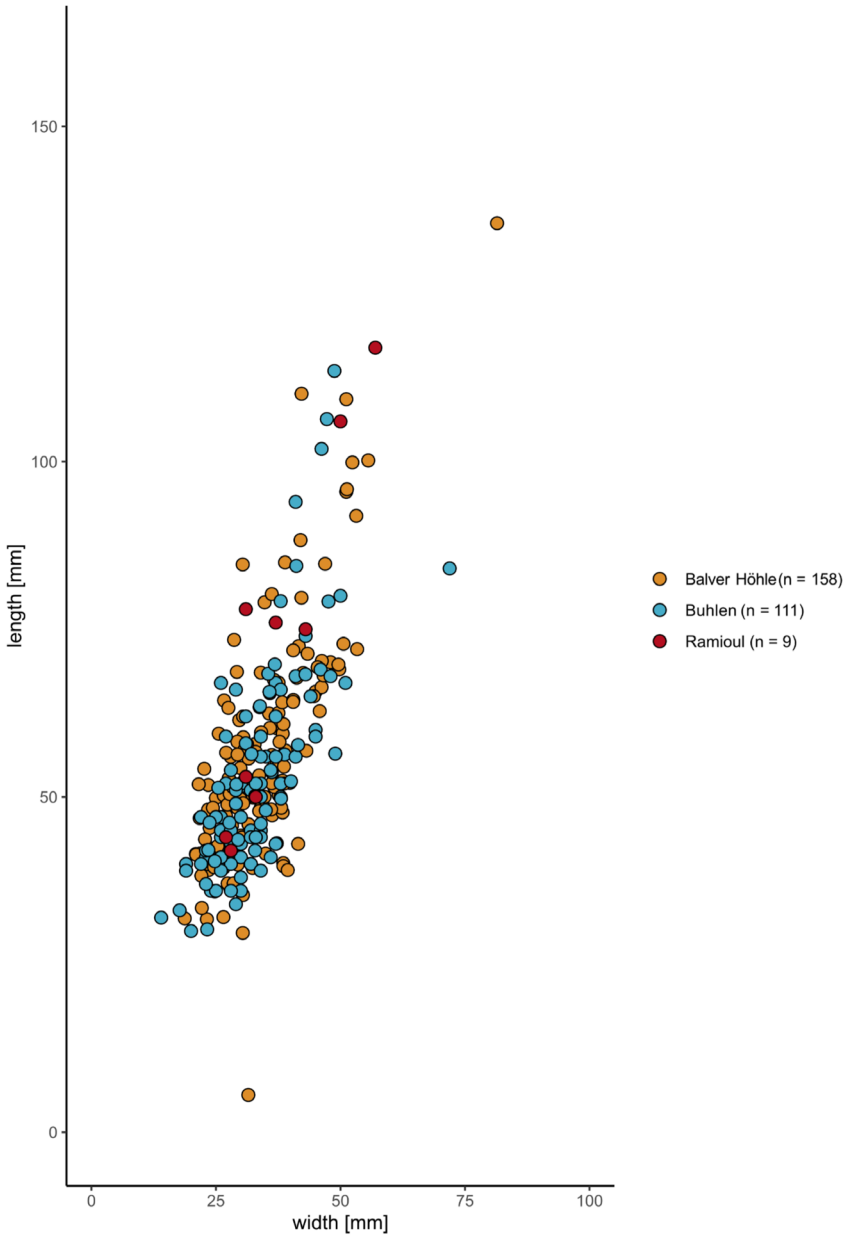

Fig. 55 Length-width ratio of the complete *Keilmesser* from Buhlen (n = 111), Balver Höhle (n = 158) and Ramioul (n = 9).

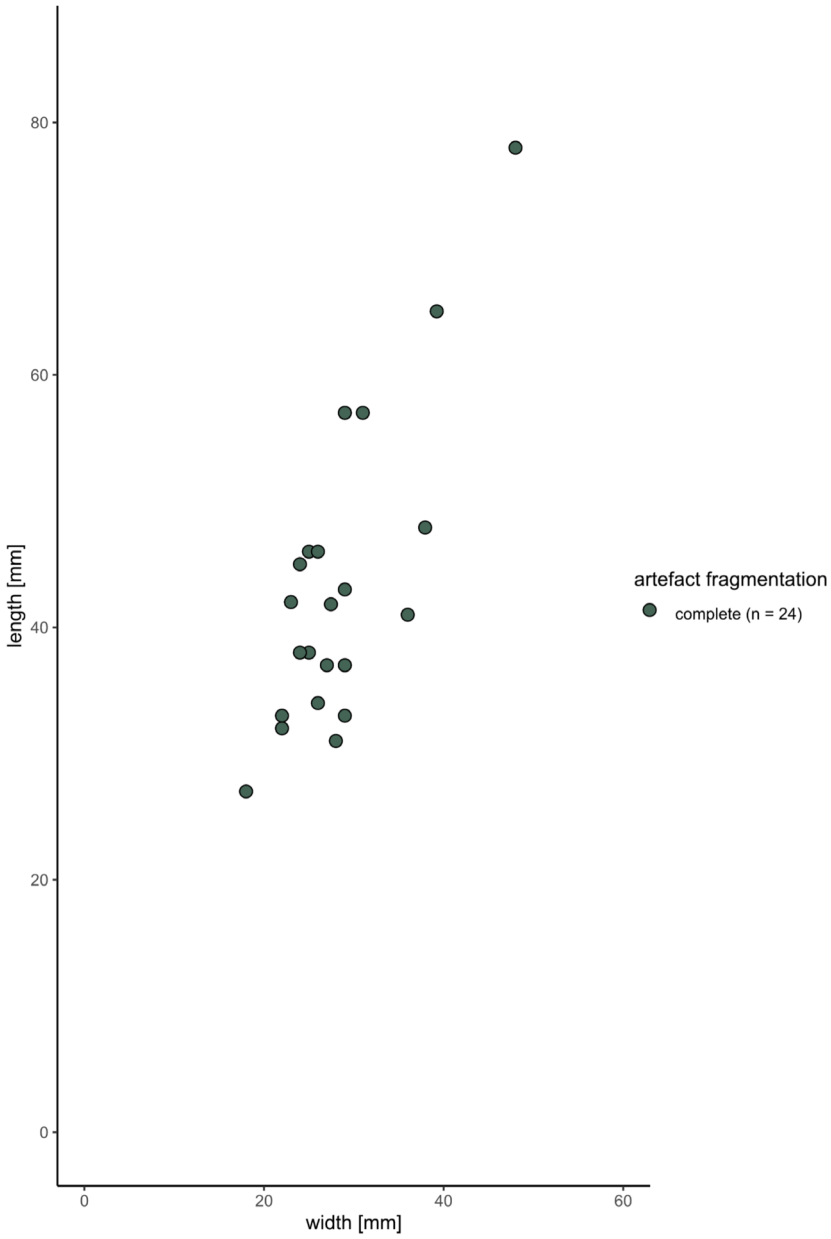

Fig. 56 Length-width ratio of the *Prądnik scrapers* (n = 24) from Buhlen.

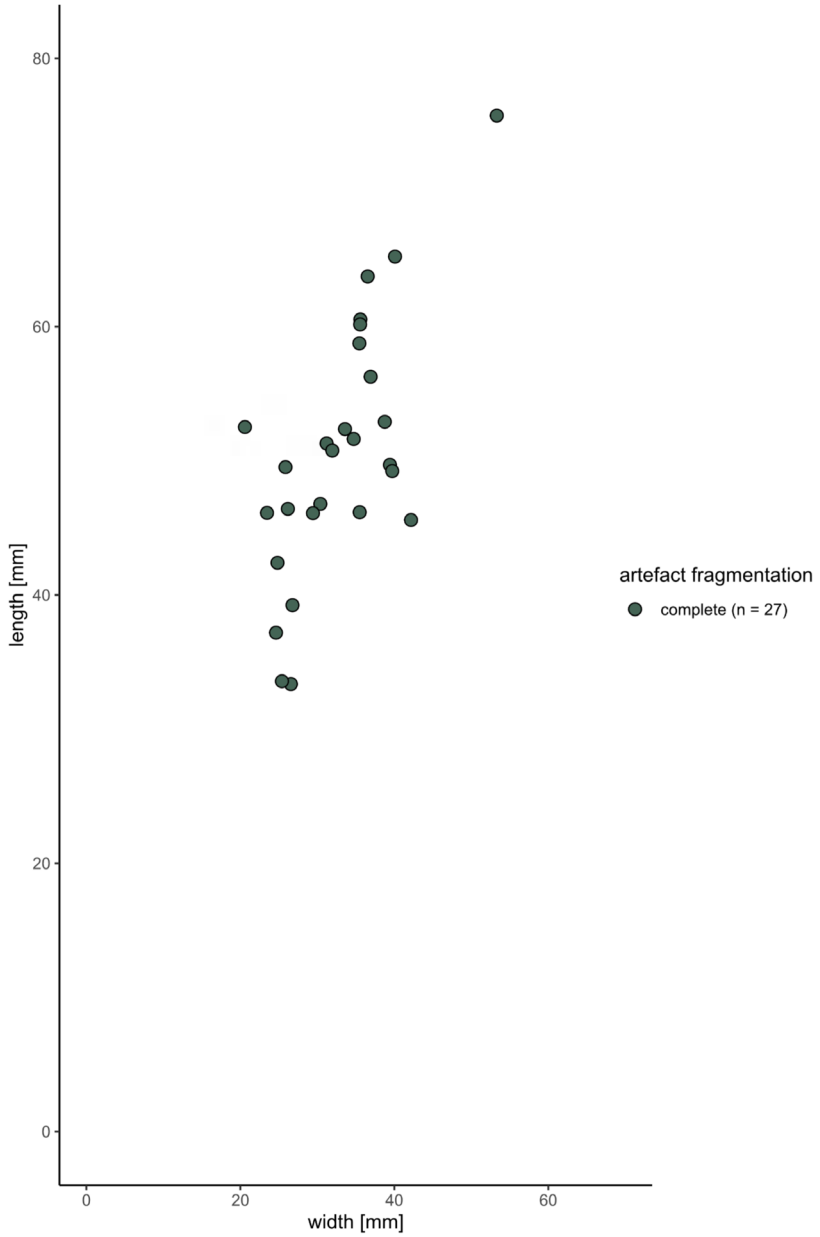

Fig. 57 Length-width ratio of the *Prądnik scrapers* (n = 27) from Balver Höhle.

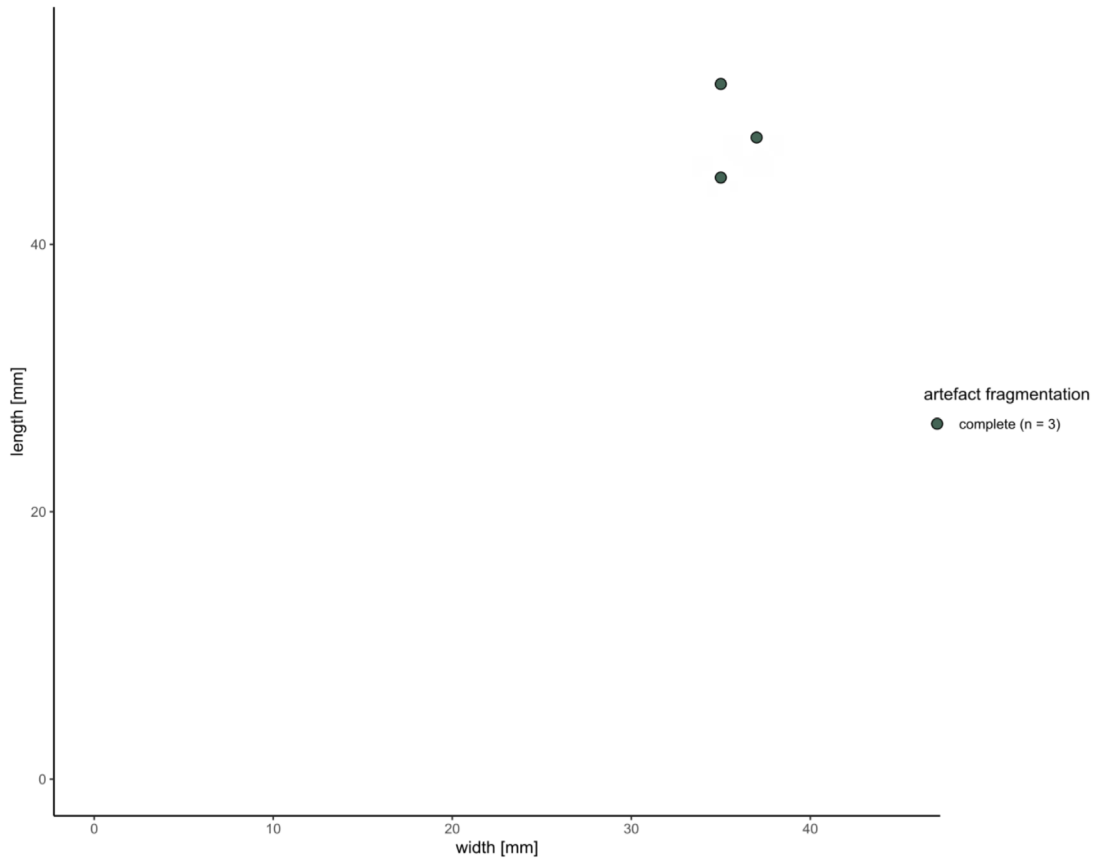

Fig. 58 Length-width ratio of the *Prądnik scrapers* (n = 3) from Ramioul.

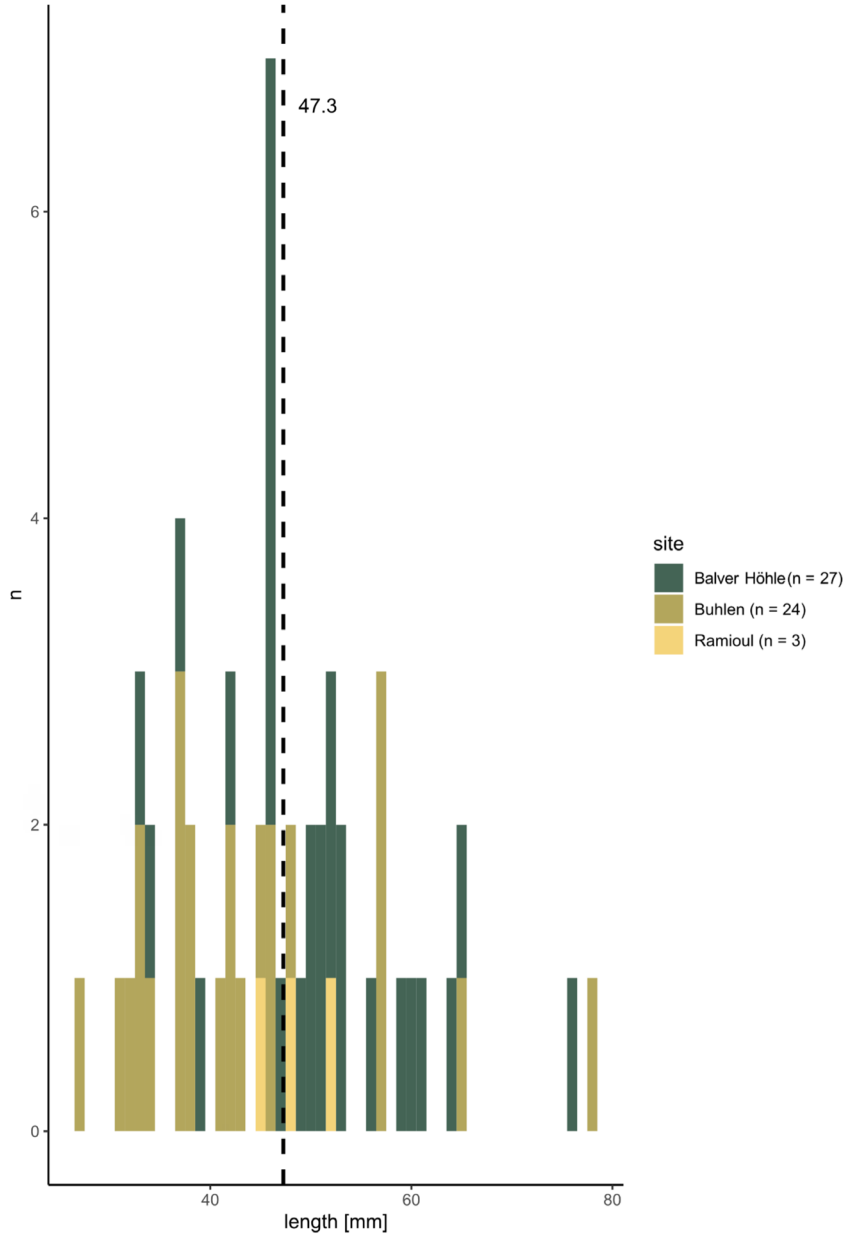

Fig. 59 Maximal length of the *Prądnik scrapers* from Buhlen (n = 24), Balver Höhle (n = 27) and Ramioul (n = 3). The dashed line indicates the arithmetic mean value.

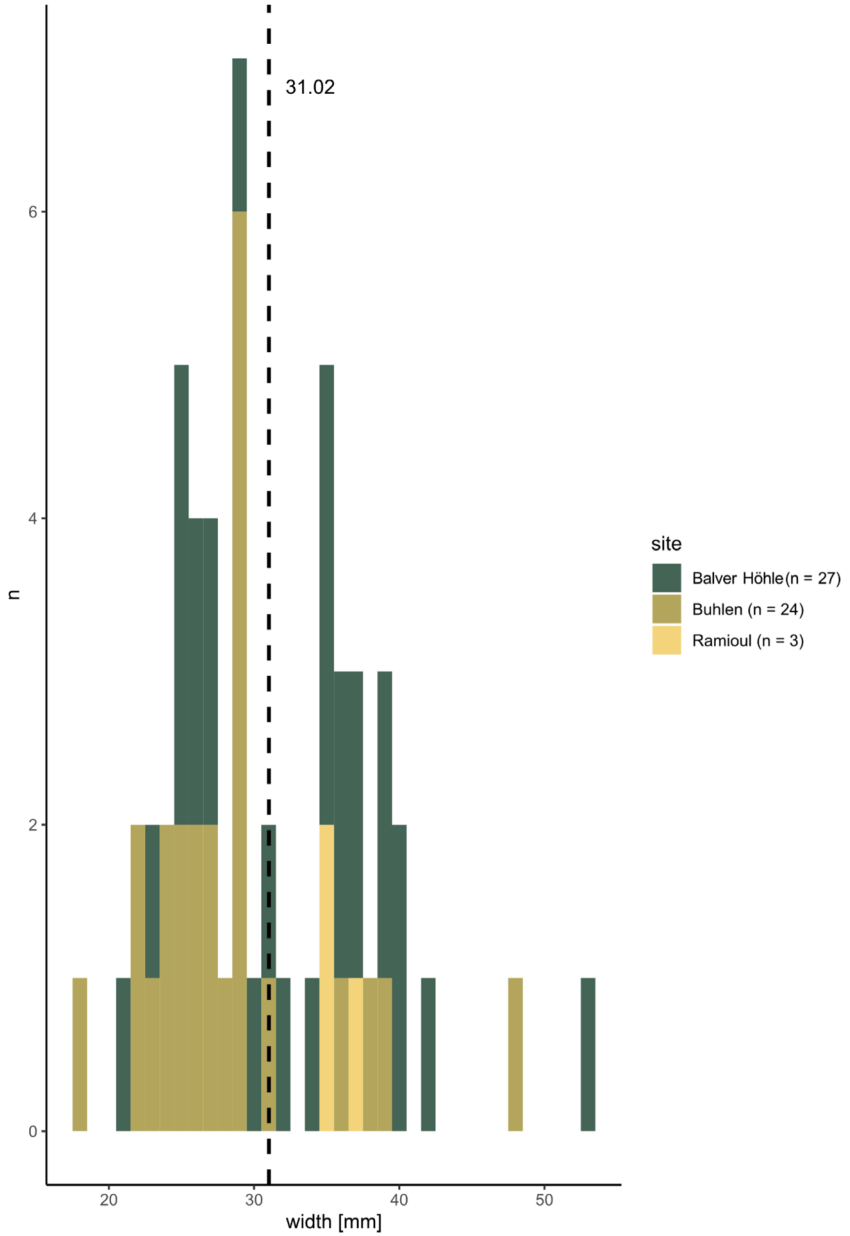

Fig. 60 Maximal width of the *Prądnik scrapers* from Buhlen (n = 24), Balver Höhle (n = 27) and Ramioul (n = 3). The dashed line indicates the arithmetic mean value.

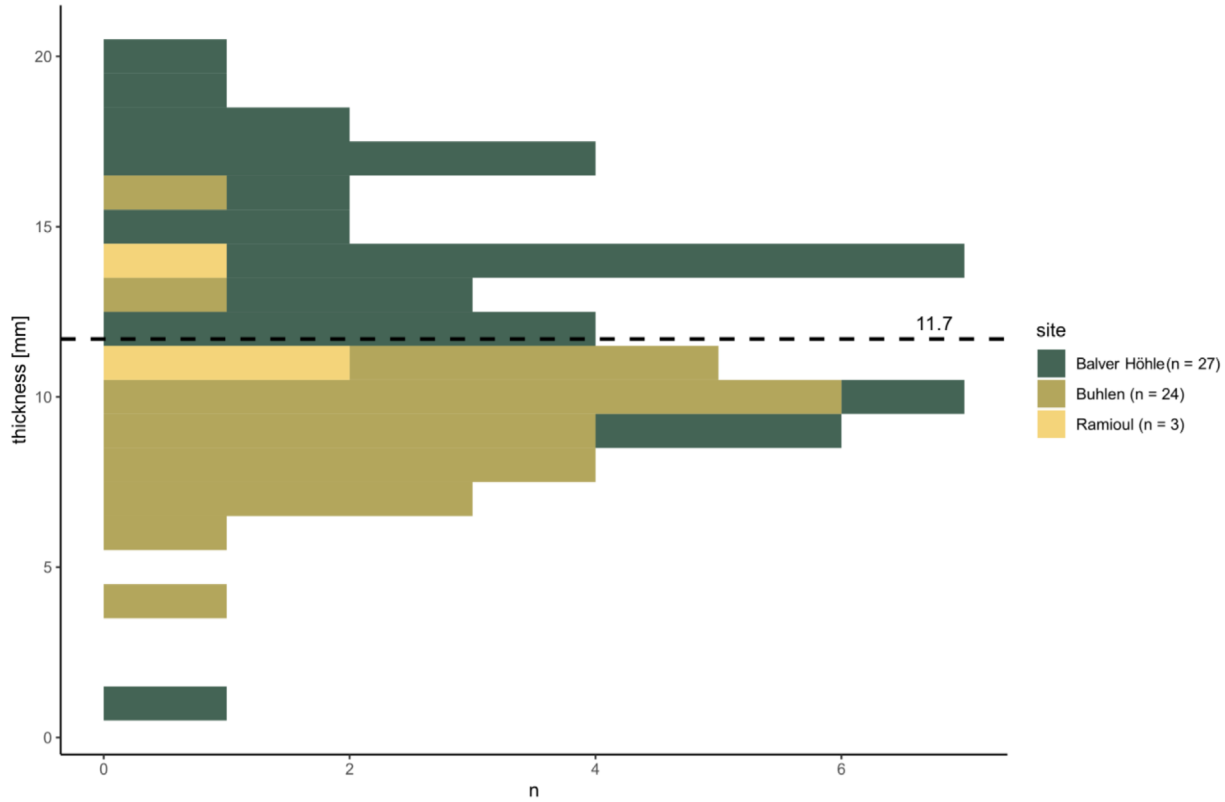

Fig. 61 Maximal thickness of the *Prądnik scrapers* from Buhlen (n = 24), Balver Höhle (n = 27) and Ramioul (n = 3). The dashed line indicates the arithmetic mean value.

Taken together, the measurements for the *Prądnik scrapers* length from the three sites result in a range from 27.0 mm to 78.0 mm with a mean value of 47.3 mm (**figs 59. 62**). All together, the *Prądnik scrapers* have a minimum width of 18.0 mm and a maximum of 53.3 mm (**fig. 60**). The arithmetic mean is 31.0 mm. The thickness of *Prądnik scrapers* ranges between 1.2 mm and 20.4 mm, with an arithmetic mean of 11.7 mm (**fig. 61**). The measurements from the *Prądnik scrapers* are in general smaller than the ones taken from the *Keilmesser.*

Tool back

This part of the qualitative analysis is about the characteristics of the back of the *Keilmesser*. Because locally used siliceous schist is mostly found in blocks, plates or barely rounded pebbles, the raw material piece itself mostly offers convenient striking angles for directed retouch. This aspect is the base to argue that the piece of raw material was carefully selected (Jöris 2001; Jöris/Uomini 2019). Following this argument, the raw material shape was integrated into the overall tool design. As a result, only few *Keilmesser* show clear traces of distinct knapping along the back.

This general observation is applicable to the studied assemblage from Buhlen. N = 46 pieces of the n = 111 complete *Keilmesser* are characterised by a natural back that is either unworked or covered with cortex (**fig. 63**). Some pieces with a natural cortex back display additional minimal retouch (n = 29). N = 18 artefacts can be described as partly retouched, n = 18 as retouched.

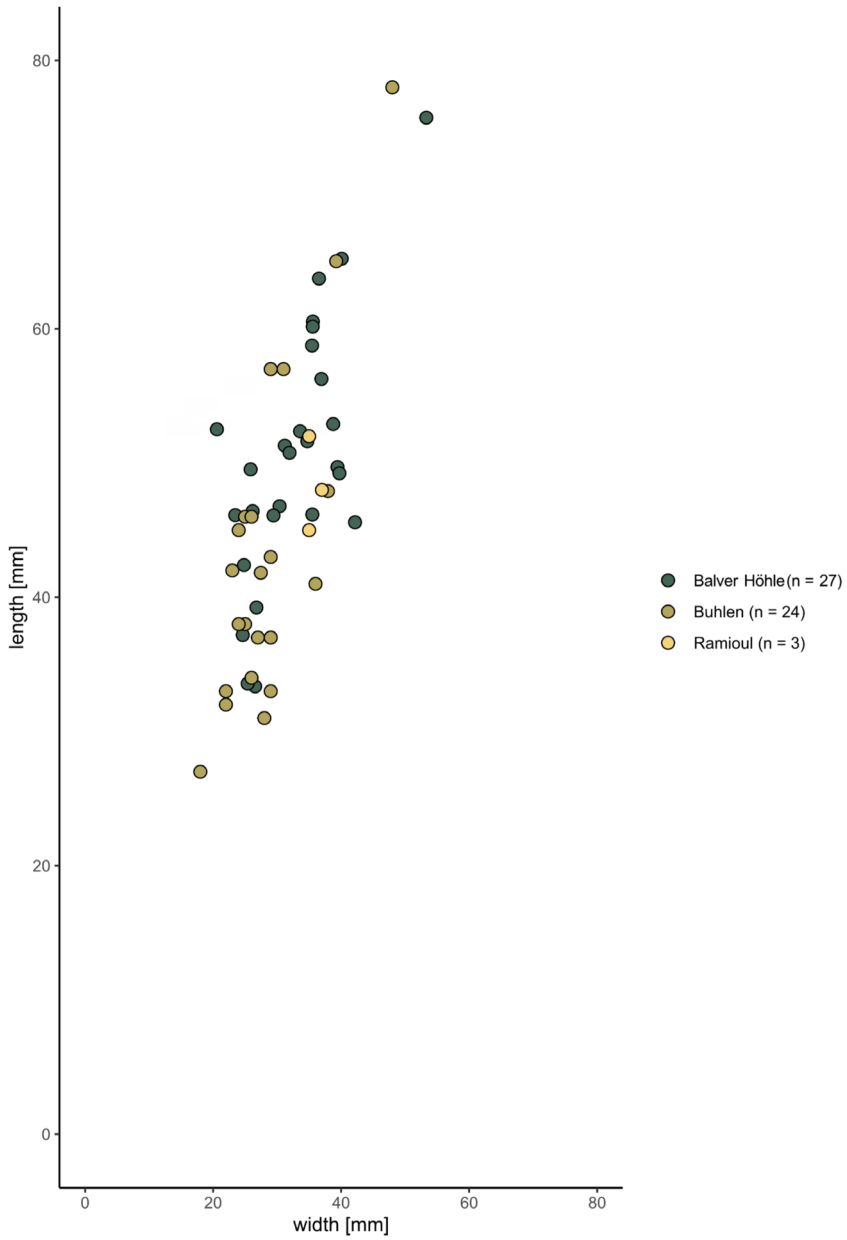

Fig. 62 Length-width ratio of the *Prądnik scrapers* from Buhlen (n = 24), Balver Höhle (n = 27) and Ramioul (n = 3).

Additionally, the thickness of the tool back was also recorded at the most pronounced part of the back (**fig. 67**). The thickness of the back ranges for the complete *Keilmesser* from 4.0 mm to 26.8 mm with an arithmetic mean of 11.9 mm.

A similar situation can be found for the *Keilmesser* from Balver Höhle (**fig. 64**). The majority of the tools with n = 77 artefacts do not display any work traces along the back of the tool. Frequently, the tools show small areas of retouch combined with the natural, unworked cortex (n = 35). The partly retouched back is characteristic for n = 23 artefacts, while n = 23 pieces show distinct retouch.

The thickness measurements of the back at its maximum extend was taken for all complete *Keilmesser* from Balve (**fig. 67**). The values ranging between 2.9 mm and 27.9 mm. The arithmetic mean amounts to 12.2 mm.

In Ramioul, n = 2 of the entire nine *Keilmesser* do not show work traces and thus display a natural back (**fig. 65**). Minimal traces of retouch along the back, showing also cortex, can be found on n = 5 artefacts.

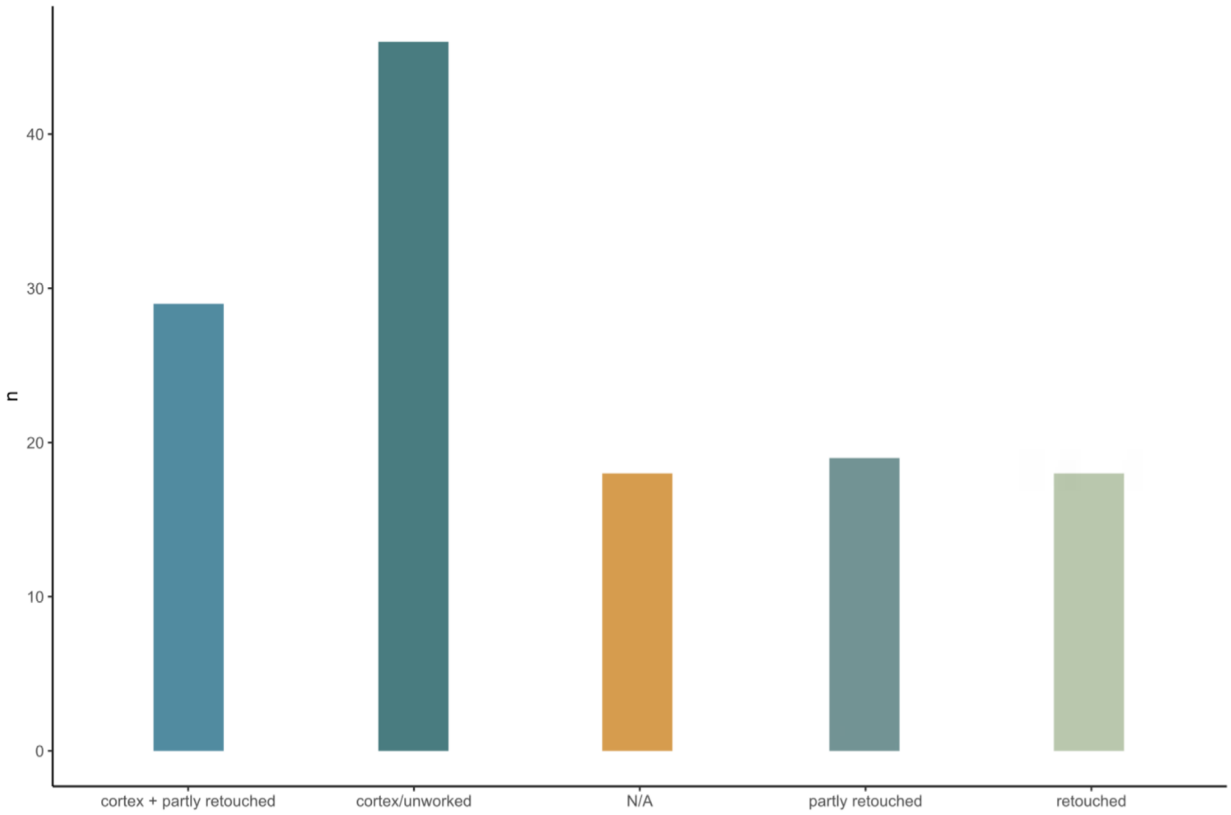

Fig. 63 Characteristics of the back of the complete *Keilmesser* (n = 111) from Buhlen.

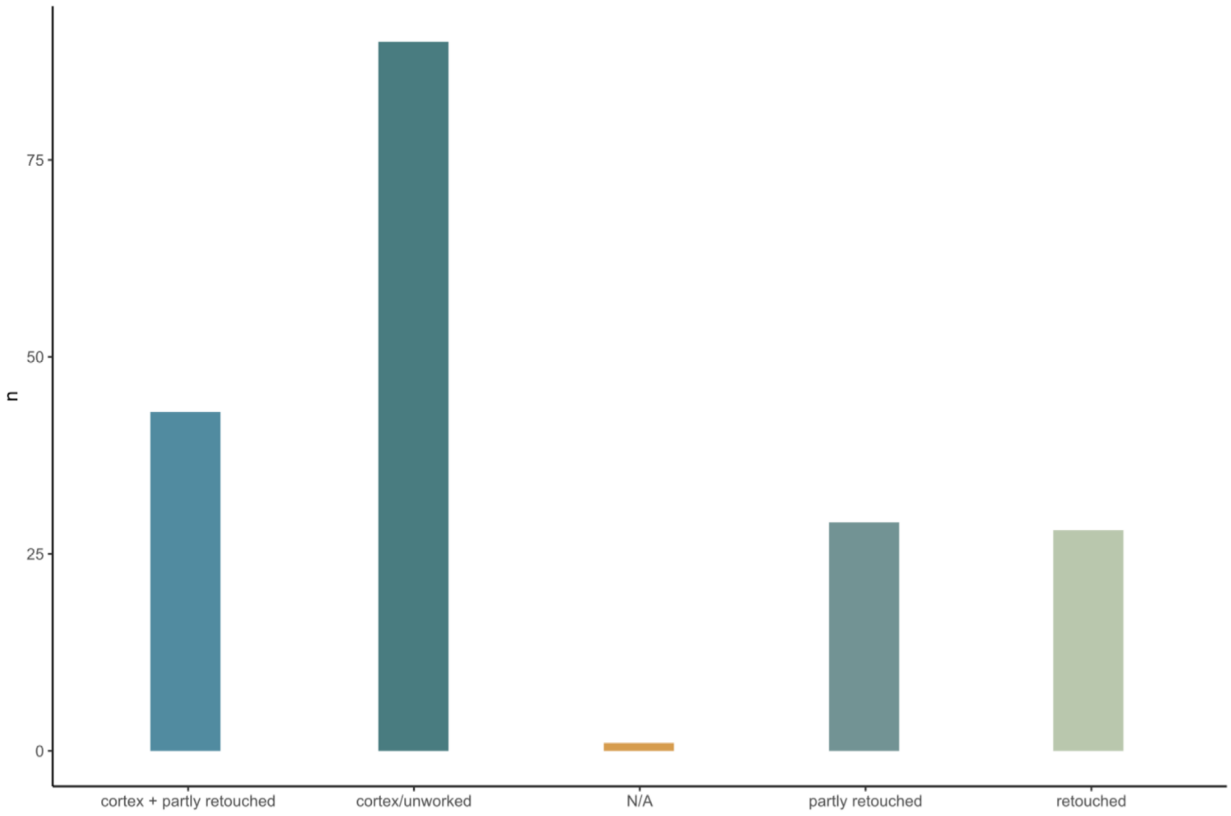

Fig. 64 Characteristics of the back of the complete *Keilmesser* (n = 158) from Balver Höhle.

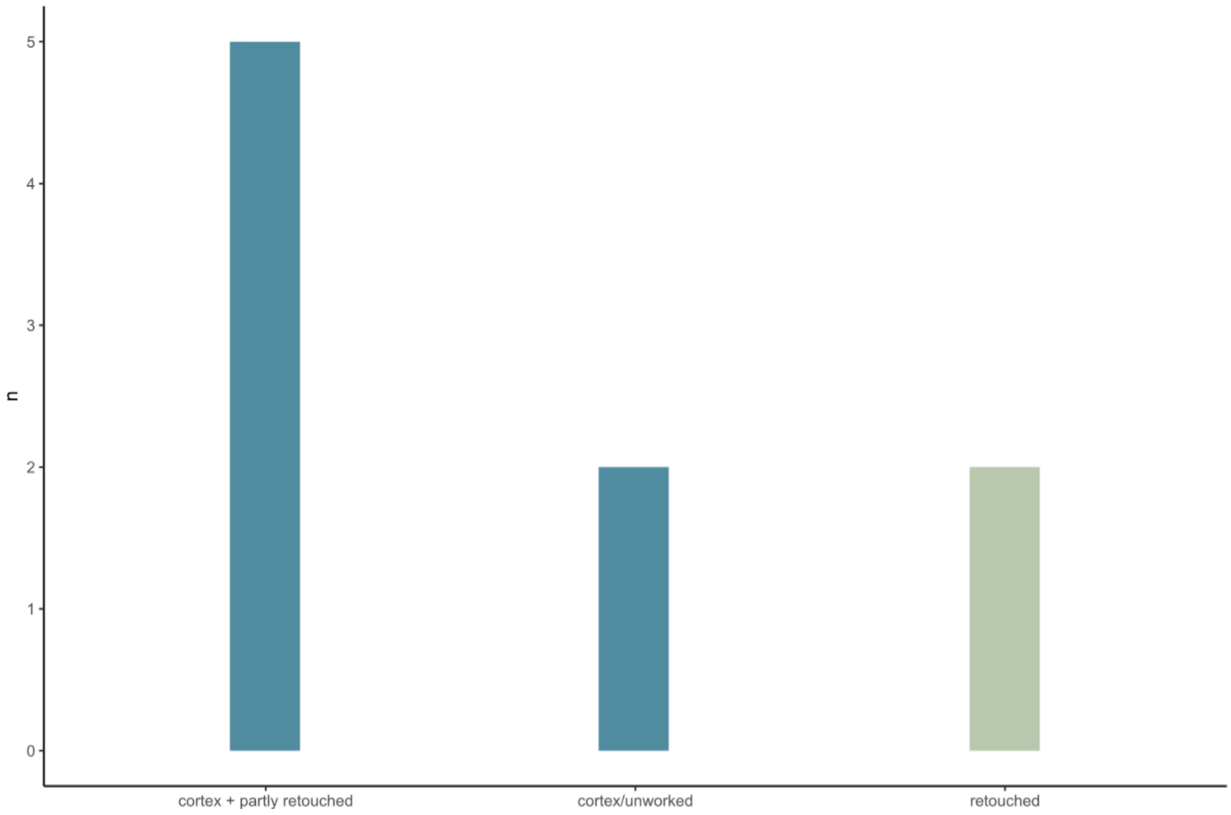

Fig. 65 Characteristics of the back of the complete *Keilmesser* (n = 9) from Ramioul.

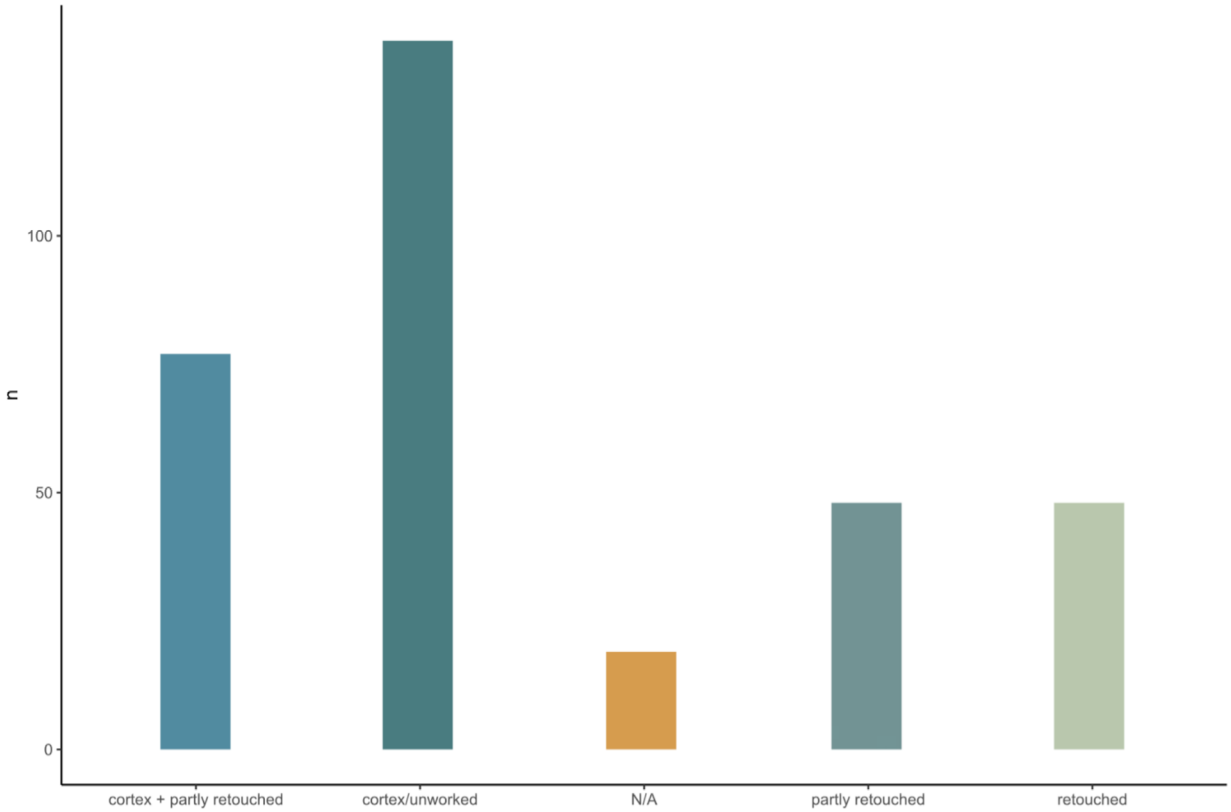

Fig. 66 Characteristics of the back of the complete *Keilmesser* from Buhlen (n = 111), Balver Höhle (n = 158) and Ramioul (n = 9).

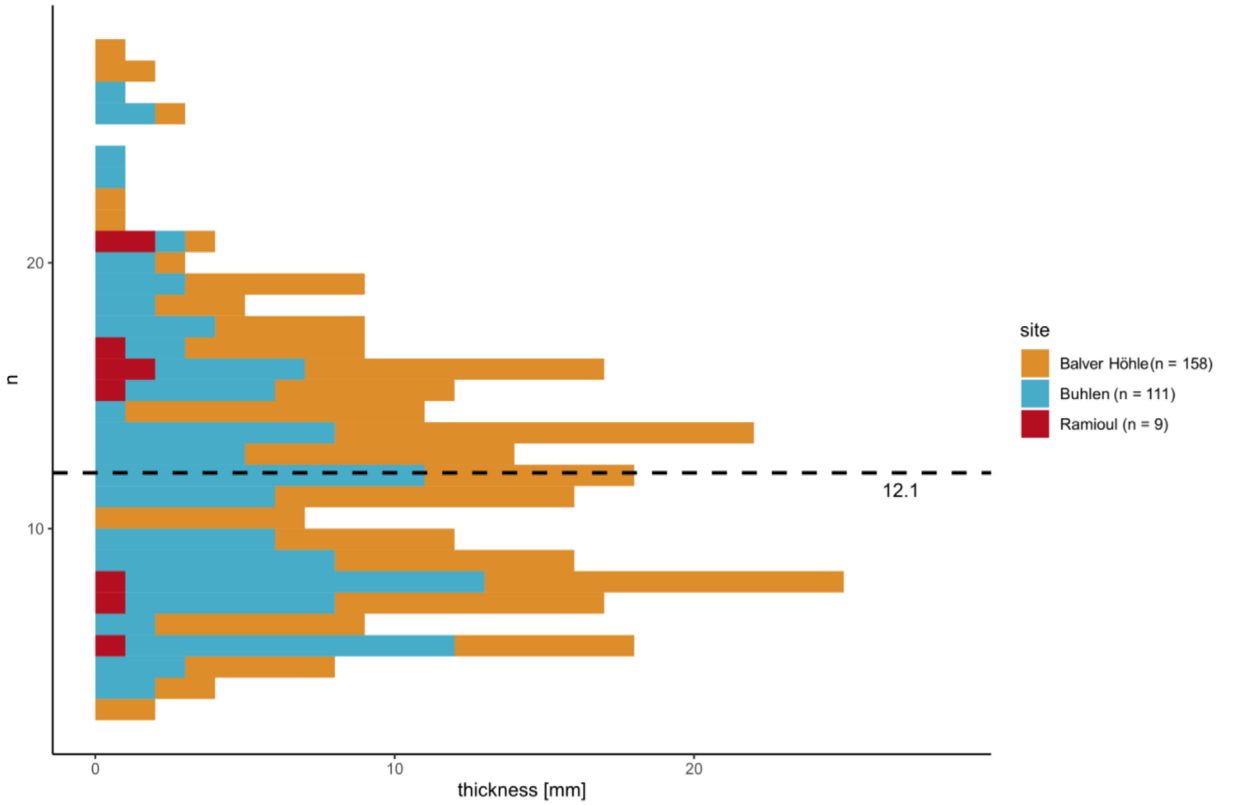

Fig. 67 Maximal thickness back of the *Keilmesser* from Buhlen (n = 111), Balver Höhle (n = 158) and Ramioul (n = 9). The dashed line indicates the arithmetic mean value.

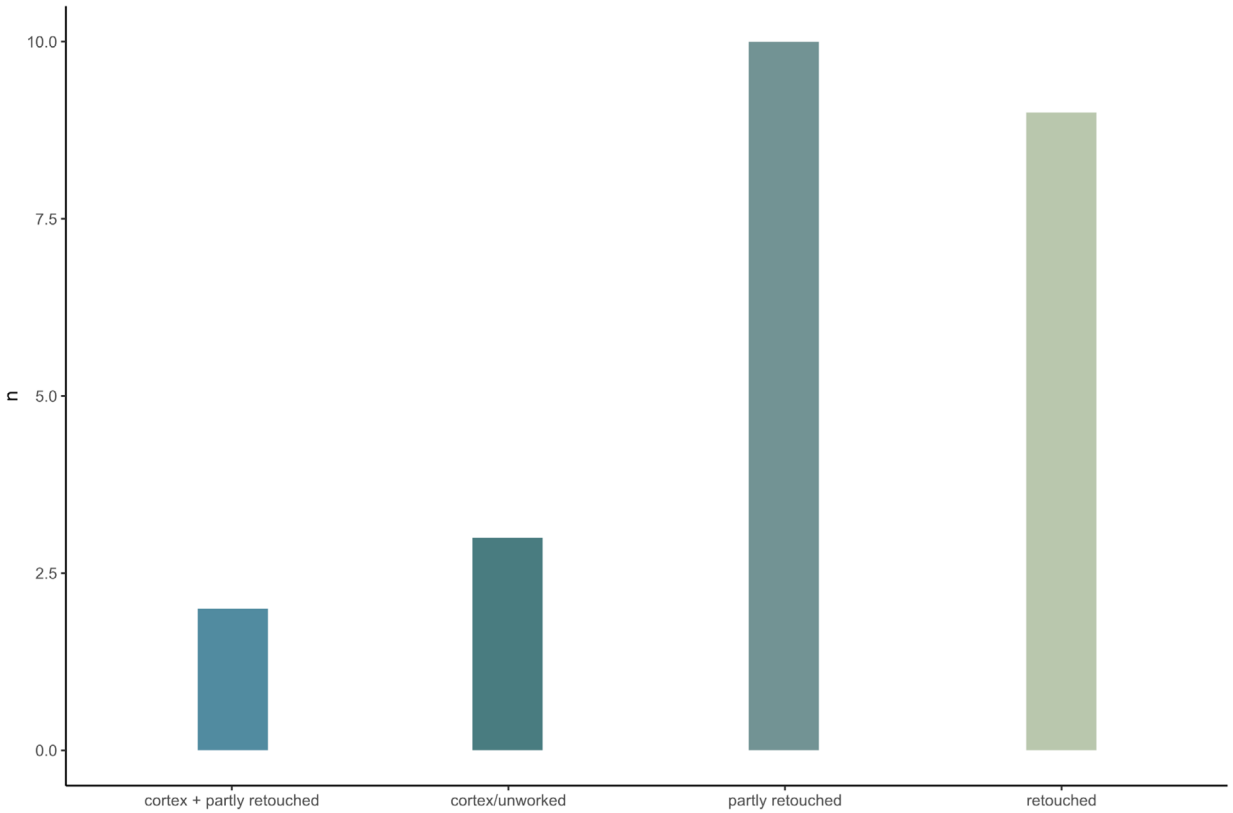

Fig. 68 Characteristics of the backs of the complete *Prądnik scrapers* (n = 24) from Buhlen.

N = 2 artefacts document clear retouch. Interestingly, the integration of the raw material piece in the tool manufacturing concept also seems to count for the artefacts which are made of flint and not only for the silicified schist tools. The assemblages from Ramioul is extremely small, but it shows that six out of eight flint *Keilmesser* are characterised by an either natural or slightly retouched back.
Additionally, the thickness of the tool back was also recorded, leading to a minimum value of 6.0 mm and a maximum of 21.0 mm for the artefacts from Ramioul (**fig. 67**). The mean value is 14.1 mm.
The three assemblages together document a clear picture (**fig. 66**). The back of these analysed *Keilmesser* is predominantly characterised by the absence of working traces (n = 125) or minimal modifications (n = 69). This makes 69.8 % of the artefacts, which can be described as tools with a natural back. Only for a small amount of 15.5 % of all *Keilmesser,* a distinct modification (retouch) can be documented.
Additionally, the thickness measurements of the back measured on all complete *Keilmesser* lead to similar ranges and arithmetic mean values for the three sites (**fig. 67**). The measurements taken together result in a range from 2.9 mm to 27.9 mm. The arithmetic mean value is reflected by the value 12.1 mm.
The characteristics of the tool back are also of interest concerning the *Prądnik scrapers*. Additionally, the retouch of the active edge opposed to the back is mentioned, too.
In Buhlen, the backs of the *Prądnik scrapers* are most often partly retouched (n = 10), sometimes even entirely retouched (n = 9; **fig. 68**). The fewest tools still display cortex (n = 3) or cortex with little retouch (n = 2) along the back. At the most pronounced part, the backs of the *Prądnik scrapers* have a thickness of 1.0 mm to 11.0 mm (**fig. 72**). The arithmetic mean amounts to 5.5 mm.
Comparable is the situation in Balve (**fig. 69**). The *Prądnik scrapers* from Balve are also mainly partly retouched (n = 11) along the back. Definite retouch is visible on n = 5 *Prądnik scrapers.* On the remaining tools could either cortex (n = 8) or cortex combined with slight retouch (n = 3) be documented. The minimum back thickness for the *Prądnik scrapers* is 4.6 mm and the maximum is 18.1 mm with a mean value of 9.9 mm (**fig. 72**).
The *Prądnik scrapers* from the assemblage in Ramioul are retouched (n = 3) in the back area (**fig. 70**). Additionally, the thickness of the tool back was recorded, leading to a minimum value of 5.0 mm and a maximum of 6.0 mm (**fig. 72**).
The results from this analysis are contrary to the ones from the *Keilmesser* (**fig. 71**). While the *Keilmesser* were most often not worked along the back, the *Prądnik scrapers* clearly display working traces and modifications. Modifications such as (partial) retouch taken together lead to a ratio of 70.4 % (n = 38) to 29.6 % (n = 16) of the tools. The 29.6 % of the *Prądnik scrapers* are thus natural or only slightly modified along the back.
The backs of all *Prądnik scrapers* from Buhlen, Balve and Ramioul have a thickness at its most pronounced part of 4.0 mm up to 20.4 mm, leading to a mean value of 7.7 mm (**fig. 72**).

Active edge retouch

Another recorded attribute was the retouch along the active edge. The active edges of the *Keilmesser* from Buhlen are to a percentage of 81.5 % (n = 106) bifacially retouched, some artefacts are semi-bifacially retouched (14.6 %, n = 19).
The *Keilmesser* from Balve do also mainly display a bifacially edge retouch (74.4 %, n = 142), followed by tools with a semi-bifacial retouch (20.4 %, n = 39).
In Ramioul, the *Keilmesser* are either bifacially retouched (44.4 %, n = 4) or semi-bifacially retouched (44.4 %, n = 4).

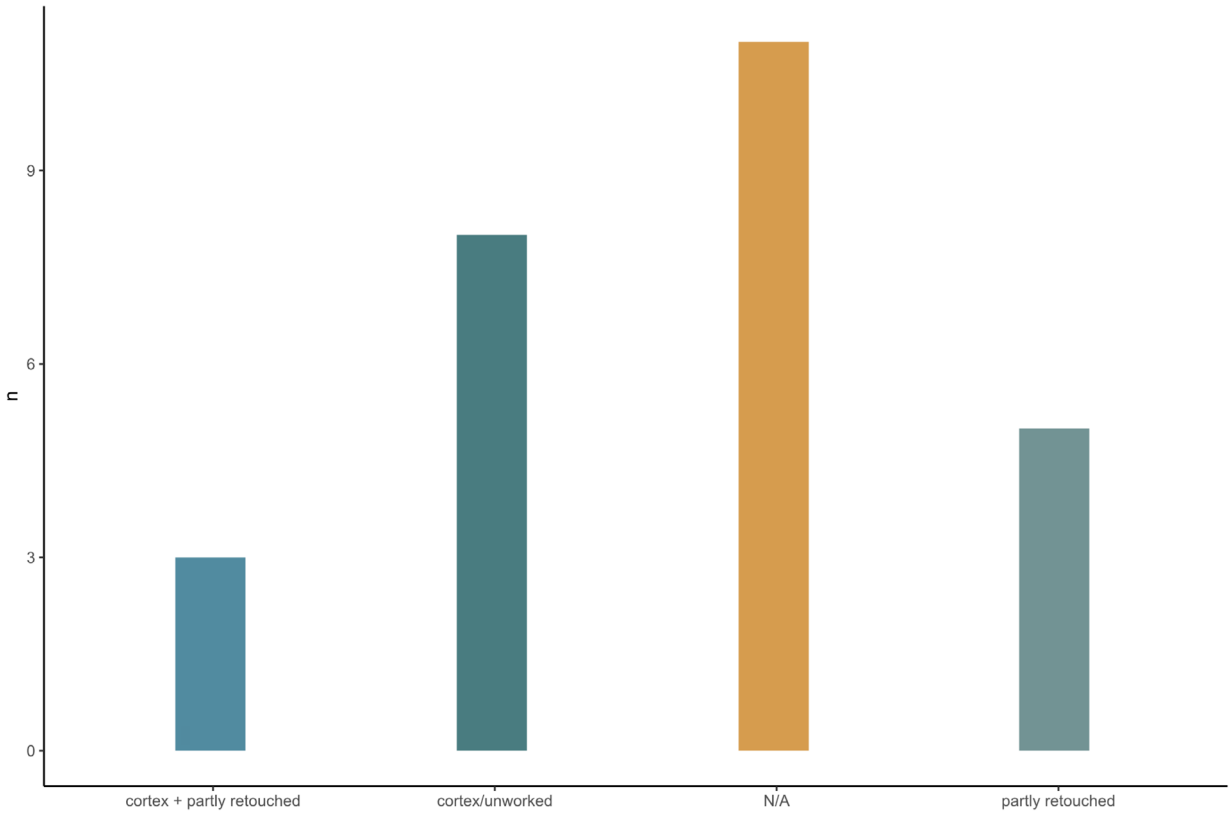

Fig. 69 Characteristics of the backs of the complete *Prądnik scrapers* (n = 27) from Balver Höhle.

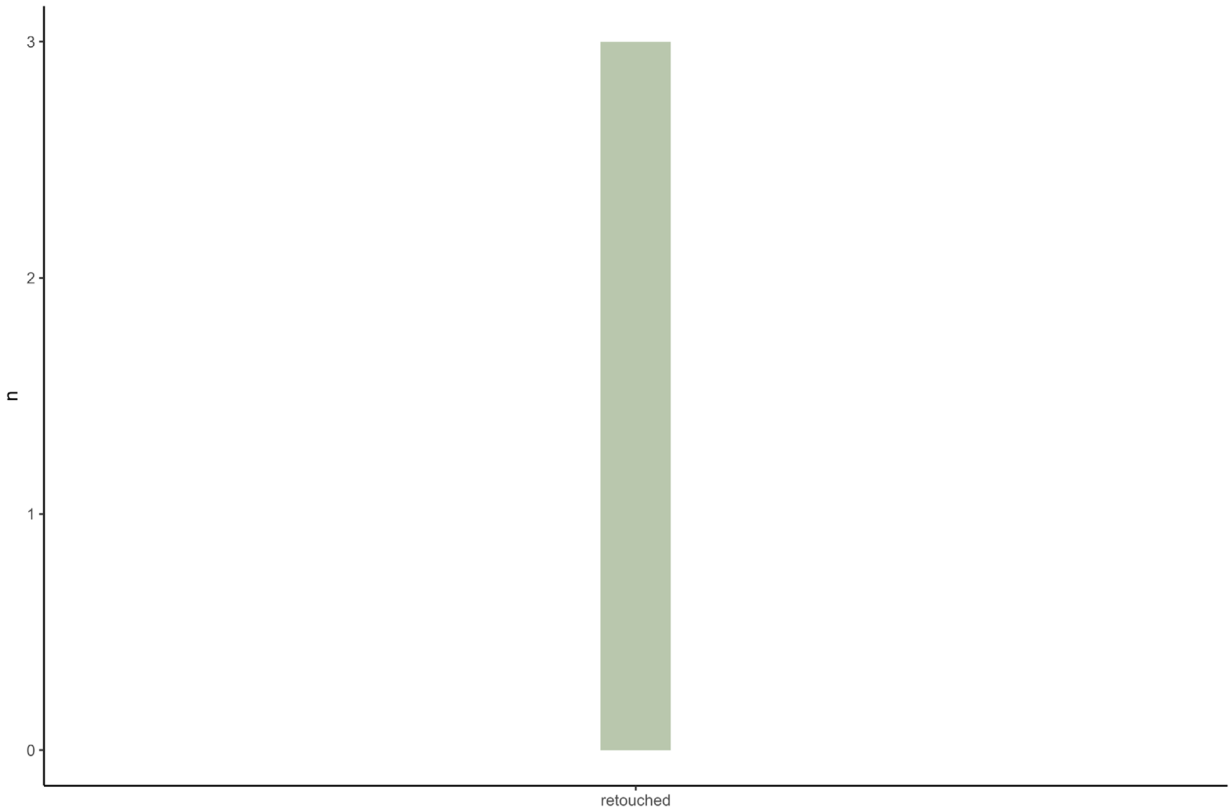

Fig. 70 Characteristics of the back of the complete *Prądnik scrapers* (n = 3) from Ramioul.

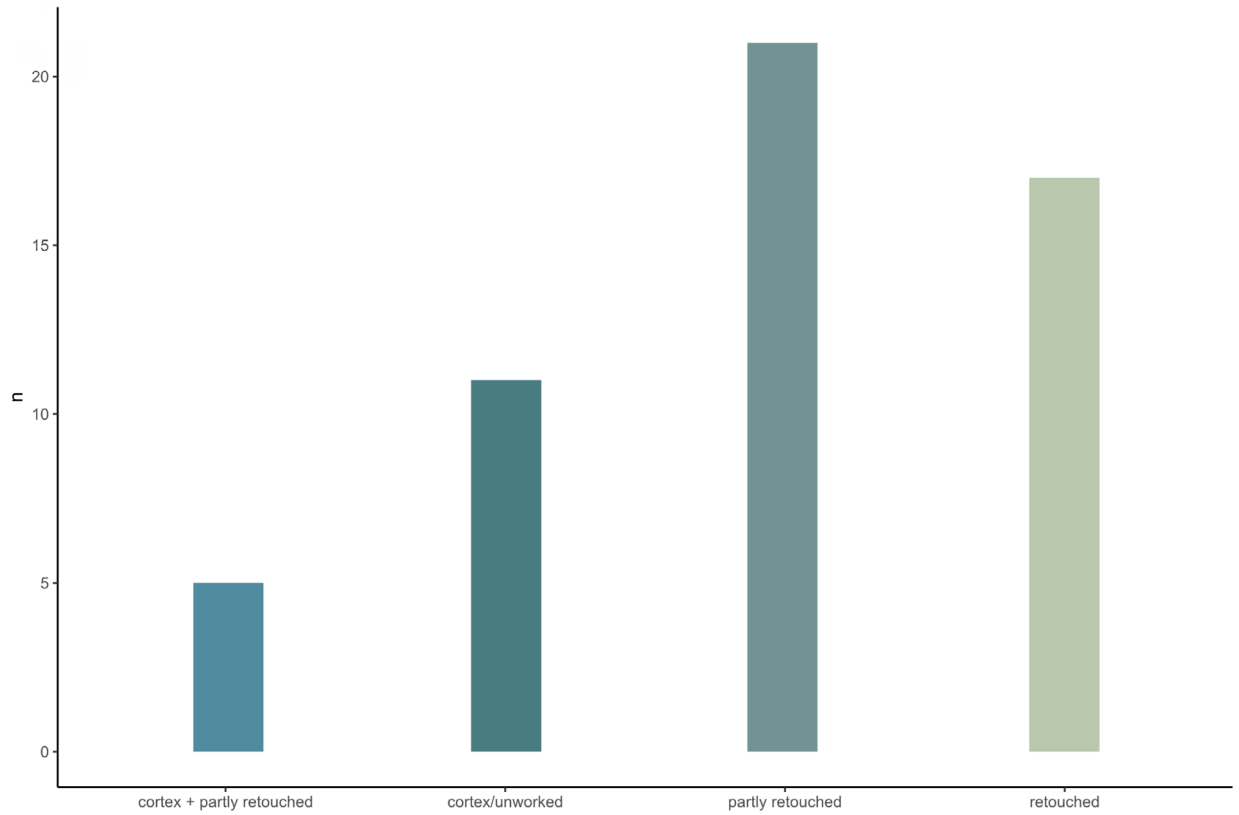

Fig. 71 Characteristics of the backs of the complete *Prądnik scrapers* from Buhlen (n = 24), Balver Höhle (n = 27) and Ramioul (n = 3).

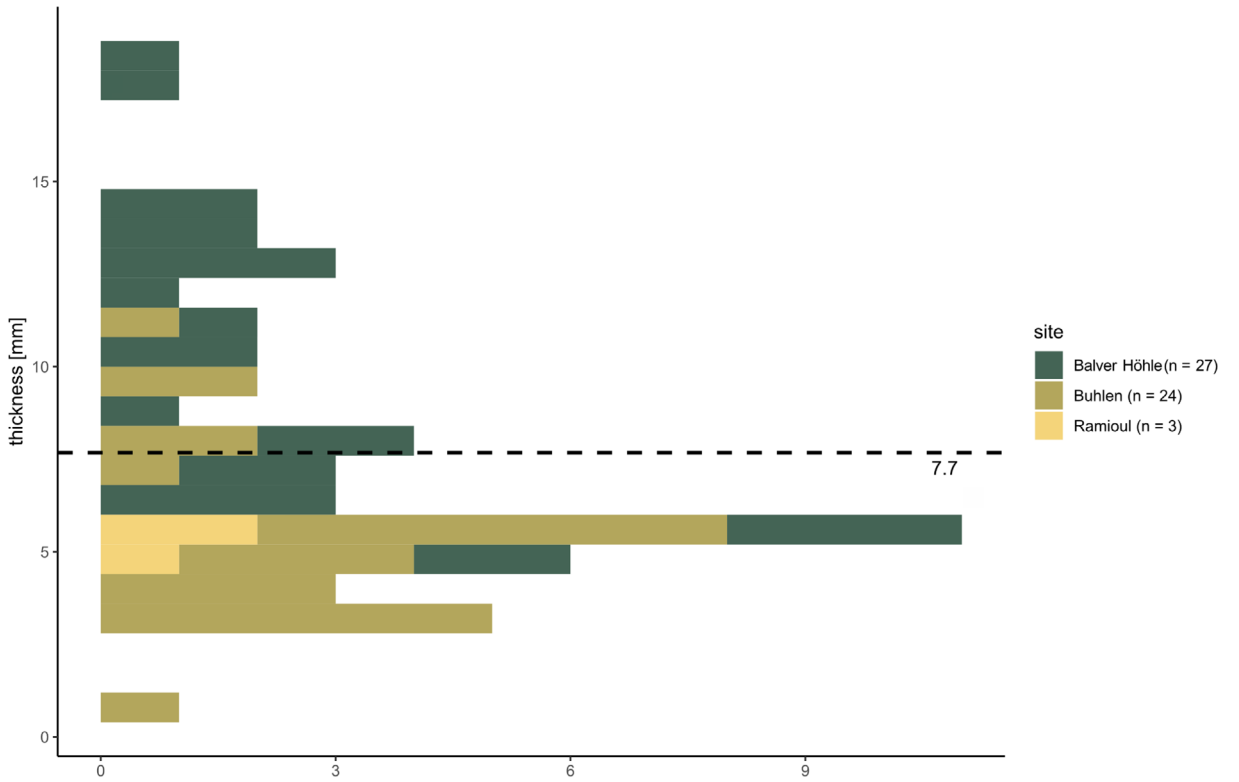

Fig. 72 Maximal back thickness of the *Prądnik scrapers* from Buhlen (n = 24), Balver Höhle (n = 27) and Ramioul (n = 3). The dashed line indicates the arithmetic mean value.

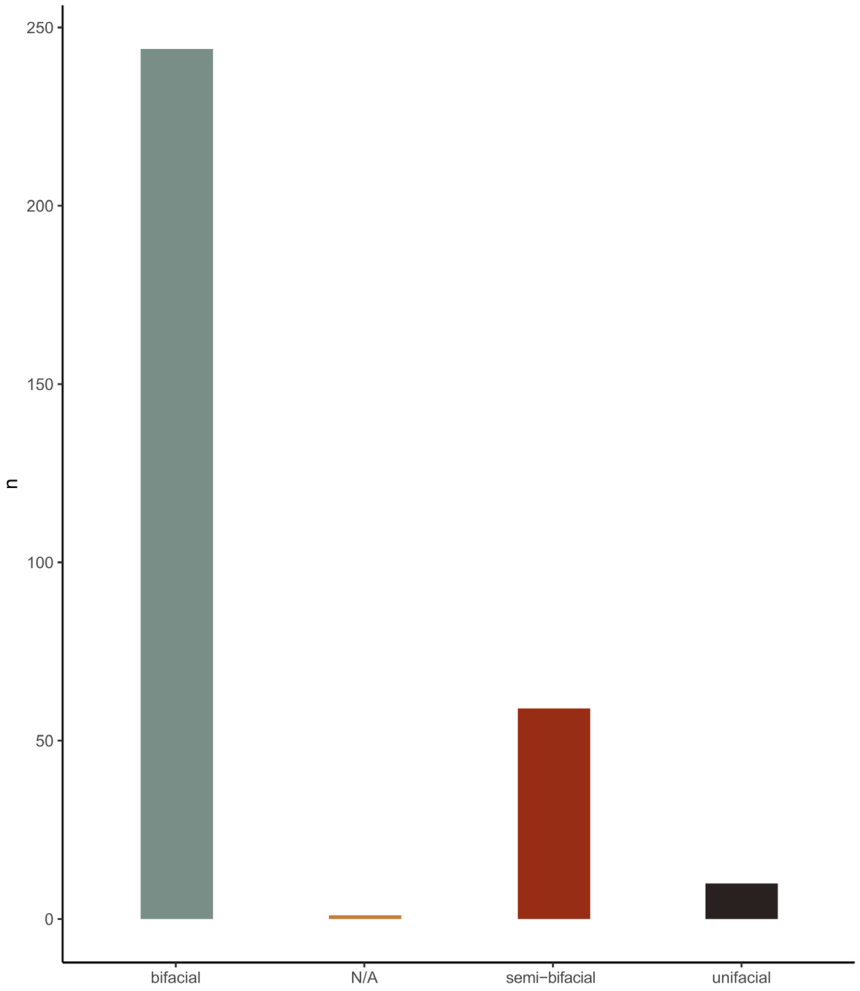

Fig. 73 Retouch type along the active edge of complete *Keilmesser* and *Keilmesser* tips from Buhlen (n = 111; n = 15), Balver Höhle (n = 158; n = 21) and Ramioul (n = 9). For a small part of the assemblage, this analysis was not done (N/A).

Keilmesser from the three sites are by a majority bifacially retouched (76.4 %, n = 252), some are semi-bifacially retouched (18.8 %, n = 62) and only a few pieces are unifacially retouched (3.3 %, n = 11; **fig. 73**). The active edge retouch was also documented for the *Prądnik scrapers* involved within this study. In Buhlen, the back of the *Prądnik scrapers* is most often (45.8 %, n = 11) opposed to a unifacially retouched active edge. Some artefacts are semi-bifacially retouched (29.2 %, n = 7) or bifacially retouched (25.0 %, n = 6).
In Balve, the active edge opposed to the back is mostly semi-bifacially retouched (44.4 %, n = 12), sometimes unifacially retouched (33.3 %, n = 9). One artefact is bifacially retouched. This analysis was initially not done for a small part of the assemblage (n = 5) and thus the data is missing.
The active edge of the studied *Prądnik scrapers* from Ramioul is either unifacially retouched (66.7 %, n = 2) or semi-bifacially retouched (33.3 %, n = 1).
To summarise these observations, the results concerning the active edge retouch of the *Prądnik scrapers* from the three analysed assemblages stands in contrast to the data recorded for the *Keilmesser* (**fig. 74**). A majority of 40.7 % (n = 22) of the *Prądnik scrapers* are only unifacaill retouched or 37.0 % (n = 20) are semi-bifacially retouched. Some artefacts display a bifacial edge retouch (13.0 %, n = 7).

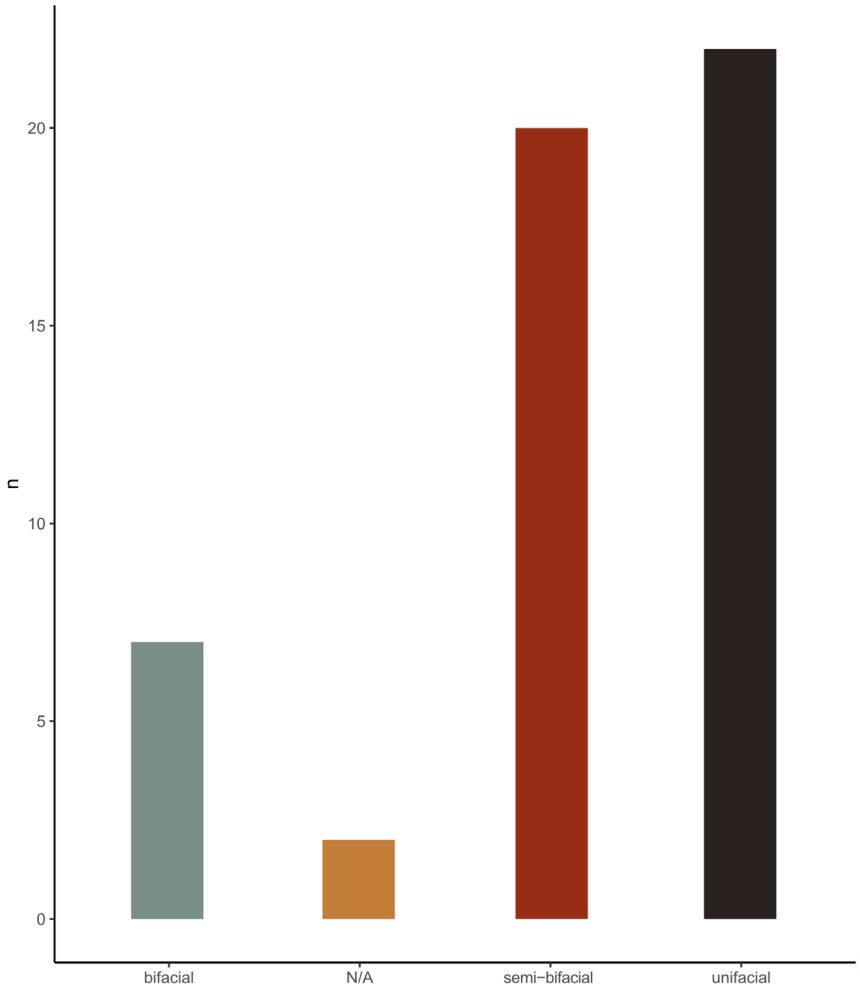

Fig. 74 Retouch type along the active edge of *Prądnik scrapers* from Buhlen (n = 24), Balver Höhle (n = 27) and Ramioul (n = 3). For a small part of the assemblage, this analysis was not done (N/A).

Lateralisation

Based on the asymmetry of *Keilmesser*, tool lateralisation can be defined.

A clear dominance of right-lateral tools can be documented in Buhlen (**tab. 12**). With n = 117 artefacts, the right-sided *Keilmesser* represent 90.0 % of the studied assemblage. A small amount of n = 10 artefacts were classified as left-lateral tools. For n = 3 *Keilmesser* the lateralisation could not be defined with certainty. Here, it should be pointed out again, that the studied assemblage from Buhlen does not reflect the entire amount of artefacts found in Buhlen. In particular the quantity of selected *Prądnik spalls* is considerably smaller. Thus, the mentioned results differ from already published ones (Jöris 2001; Jöris/Uomini 2019).

The same trend can be found in the *Keilmesser* assemblage from Balver Höhle (**tab. 12**). A clear majority (71.2 %, n = 136) of the tools were identified

site		*Keilmesser*			
		sin.	*dex.*	N/A	total
Buhlen	n	10	117	3	**130**
	%	7.7	90.0	2.3	100.0
Balve	n	50	136	5	**191**
	%	26.2	71.2	2.6	100.0
Ramioul	n	1	8	0	**9**
	%	11.1	88.9	0.0	100.0
total	**n**	**61**	**261**	**8**	**330**
	%	18.5	79.1	2.4	100.0

Table 12 Determination of the tool lateralisation for the *Keilmesser* from Buhlen, Balver Höhle and Ramioul.

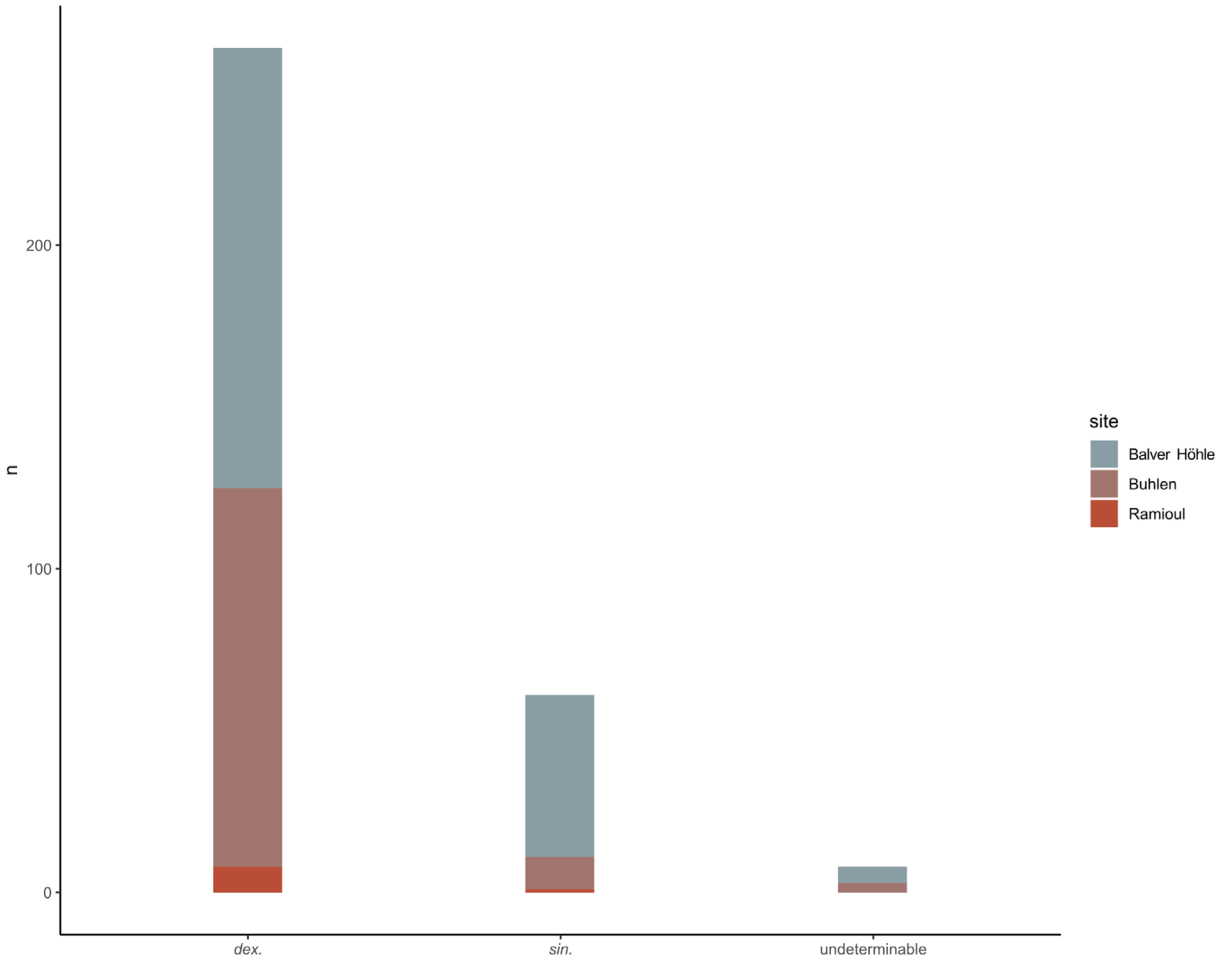

Fig. 75 Determination of the tool lateralisation for the *Keilmesser* from Buhlen (n = 130), Balver Höhle (n = 191) and Ramioul (n = 9).

as right-sided artefacts. As left-sided tools count 26.2 % (n = 50) of the *Keilmesser* in Balve. The laterality of n = 5 pieces could not be defined.

The right-sidedness of the *Keilmesser* also prevails in the assemblage from Ramioul (**tab. 12**). N = 8 tools could be documented as right-lateral tools, whereas only n = 1 counts as a left-sided tool.

In the three analysed sites, a clear tendency can be named (**fig. 75**; **tab. 12**). The *Keilmesser* are predominantly right-sided, represented by 79.1 % of the assemblages. Left-laterality is documented in 18.5 % of all *Keilmesser* only.

As *Keilmesser*, *Prądnik scrapers* display a morphological asymmetry. Therefore, the laterality of the *Prądnik scrapers* can be defined in the same way (**tab. 13**). The *Prądnik scraper* from Buhlen illustrate a clear dominance (n = 19) of right lateral tools. Only n = 3 *Prądnik scrapers* are documented as left lateral tools. For n = 2 of the in total n = 24 artefacts the tool laterality could not be defined.

site		*Prądnik scraper*			
		sin.	*dex.*	N/A	total
Buhlen	n	3	19	2	**24**
	%	12.5	79.2	8.3	100.0
Balve	n	4	23	0	**27**
	%	14.8	85.2	0.0	100.0
Ramioul	n	1	2	0	**3**
	%	33.3	66.7	0.0	100.0
total	**n**	**8**	**44**	**2**	**54**
	%	14.8	81.5	3.7	100.0

Table 13 Determination of the tool lateralisation for the *Prądnik scrapers* from Buhlen, Balver Höhle and Ramioul.

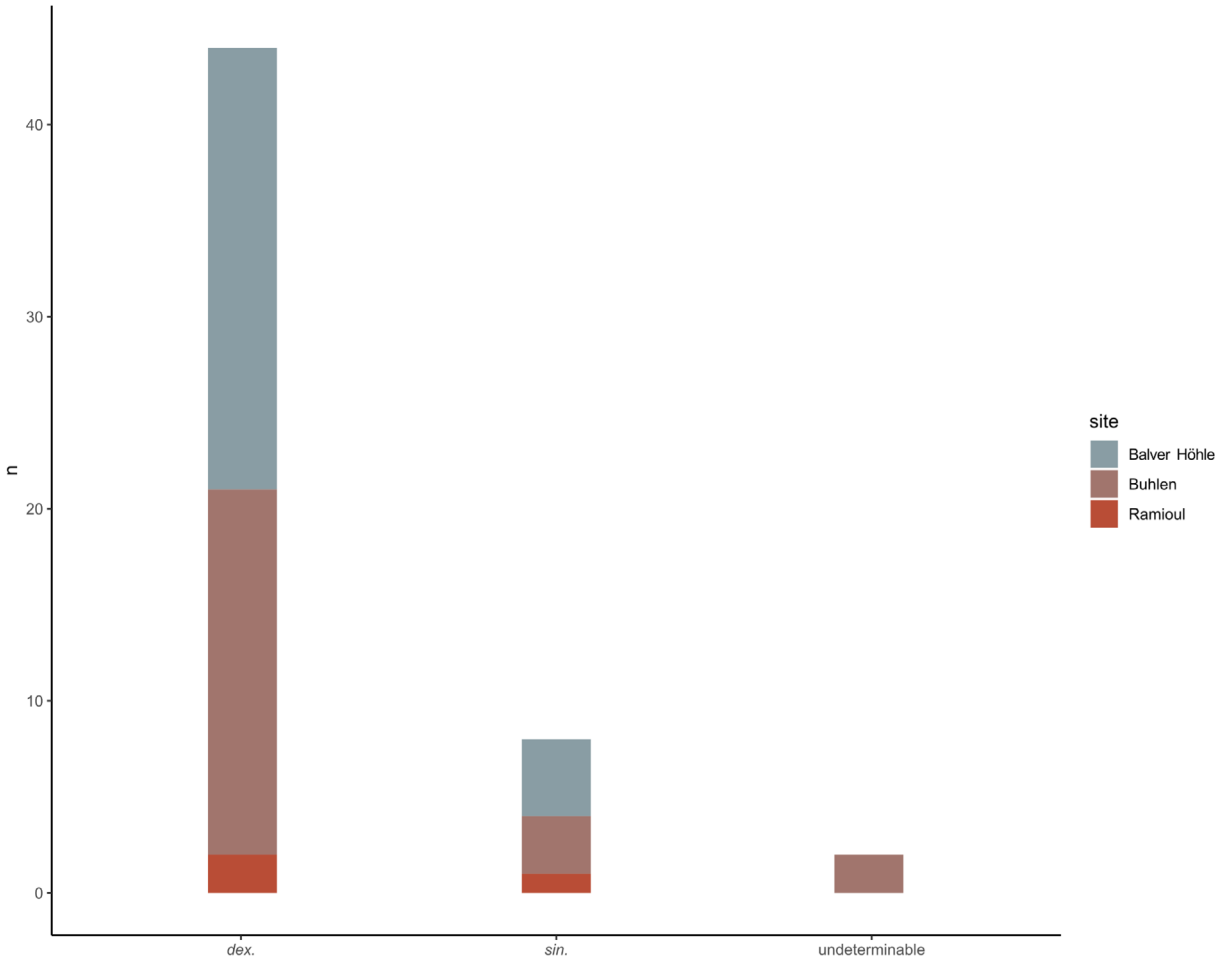

Fig. 76 Determination of the tool lateralisation for the *Prądnik scrapers* from Buhlen (n = 24), Balver Höhle (n = 27) and Ramioul (n = 3). The laterality of n = 2 artefacts could not be determined. These artefacts are excluded from the figure.

A similar picture is becoming evident for the *Prądnik scrapers* from Balve. By a majority of 85.2 % (n = 23), the tools are right-sided. N = 4 *Prądnik scrapers* count as left-sided artefacts.
N = 2 of the n = 3 *Prądnik scraper* from Ramioul display a right laterality, the other *Prądnik scraper* is left lateral.
To summarise, a predominance of right lateral *Prądnik scrapers* can be documented for the three studied sites Buhlen, Balve and Ramioul (**fig. 76**). The ratio of right lateral to left lateral tools is 81.5 % (n = 44) to 14.8 % (n = 8).

Morphological shape variability

The idea, to assign each *Keilmesser* to one of the previously described seven *Keilmesser* shapes were taken up in this subchapter. Only complete *Keilmesser* were involved in this part of the analysis. Due to some transitional morphology, it was not possible to ascribe every artefact strictly to one of the *Keilmesser* shapes. These tools are marked as undeterminable.
In Buhlen n = 111 *Keilmesser* could be assigned to a *Keilmesser* shape (**fig. 77**). While there is no *Königsaue Keilmesser* within the Buhlen assemblage, all other *Keilmesser* shapes are represented. Out of the remaining

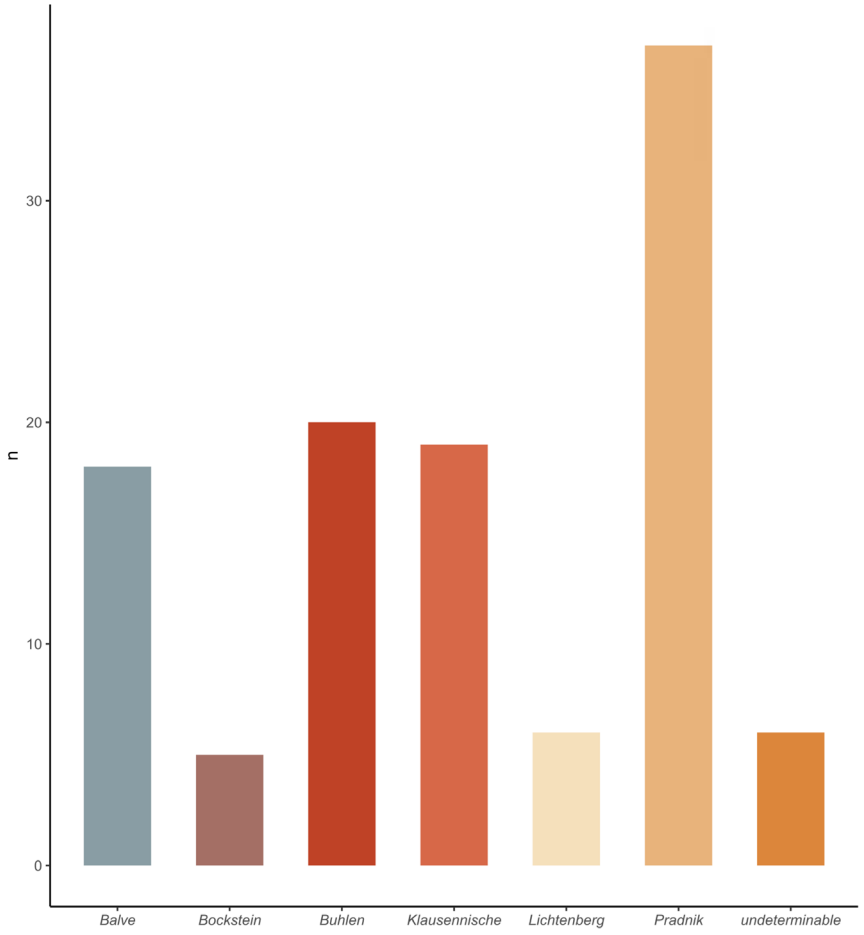

Fig. 77 Distribution of the complete *Keilmesser* (n = 111) from Buhlen to one of the described *Keilmesser* shapes.

six different types, one stands out slightly. Exactly one third (n = 37) of the tools are *Prądnik knives*. Subsequently, the *Keilmesser* shapes *Buhlen* (n = 20), *Klausennische* (n = 19) and *Balve* (n = 18) a part of the assemblage in about the same sum. Much scarcer are those tools, which can be morphologically assigned to the *Keilmesser* shapes *Bockstein* (n = 5) and *Lichtenberg* (n = 6).

A slightly different picture reveals the assignment of the *Keilmesser* shapes for the *Keilmesser* inventory from Balve (**fig. 78**). The type *Lichtenberg* is not represented at all. As in the Buhlen assemblage, the majority of *Keilmesser* can be ascribed as *Prądnik knives* (n = 47). This is followed by the *Keilmesser* shapes *Klausennische* (n = 37), *Balve* (n = 36) and *Bockstein* (n = 29). *Keilmesser* which can be morphologically defined as type *Buhlen* (n = 8) and *Königsaue* (n = 1) are rarely represented.

In Ramioul, the *Keilmesser* assemblage can only be ascribed to three of the seven *Keilmesser* shapes (**fig. 79**). The *Keilmesser* shapes *Balve, Klausennische and Prądnik* are present in equal parts (each n = 3).

Taken together, this means, the most often represented *Keilmesser* shape in the three studied assemblages is the *Prądnik knife* (n = 87; **fig. 80**). Together with the types *Balve* (n = 65) and *Klausennische* (n = 59) they compose three quarter of the artefacts.

In an additional step, the perimeter sections were measured for the *Keilmesser* from the three assemblages. For this analysis, only complete artefacts were suitable.

In Buhlen, the artefacts have a base and back length of minimum 33.0 mm and maximum 120.0 mm. The second perimeter section, the distal posterior part ranges from 6.0 mm to 92.0 mm. Some artefacts (n = 2), however, are characterized by a lack of this area. The determined values are therefore 0.0 cm. The active edge, as the third perimeter area, shows a size range from 21.0 mm to a maximum of 113.0 mm.

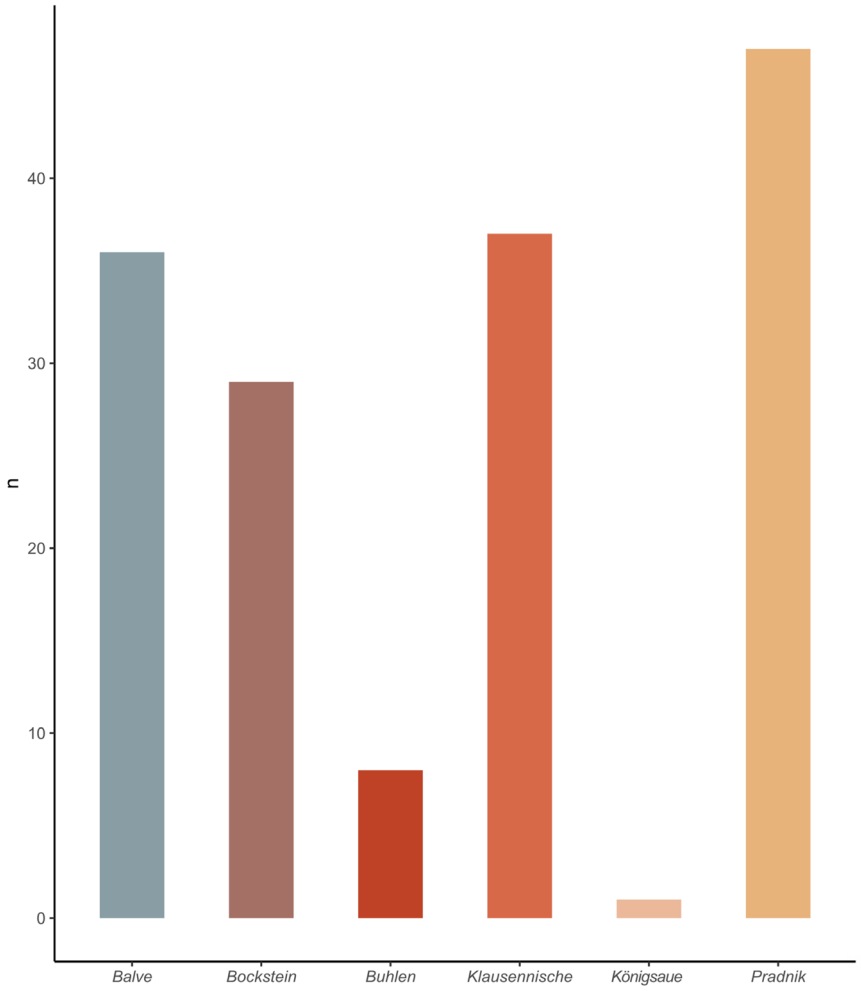

Fig. 78 Distribution of the complete *Keilmesser* (n = 158) from Balver Höhle to one of the described *Keilmesser* shapes.

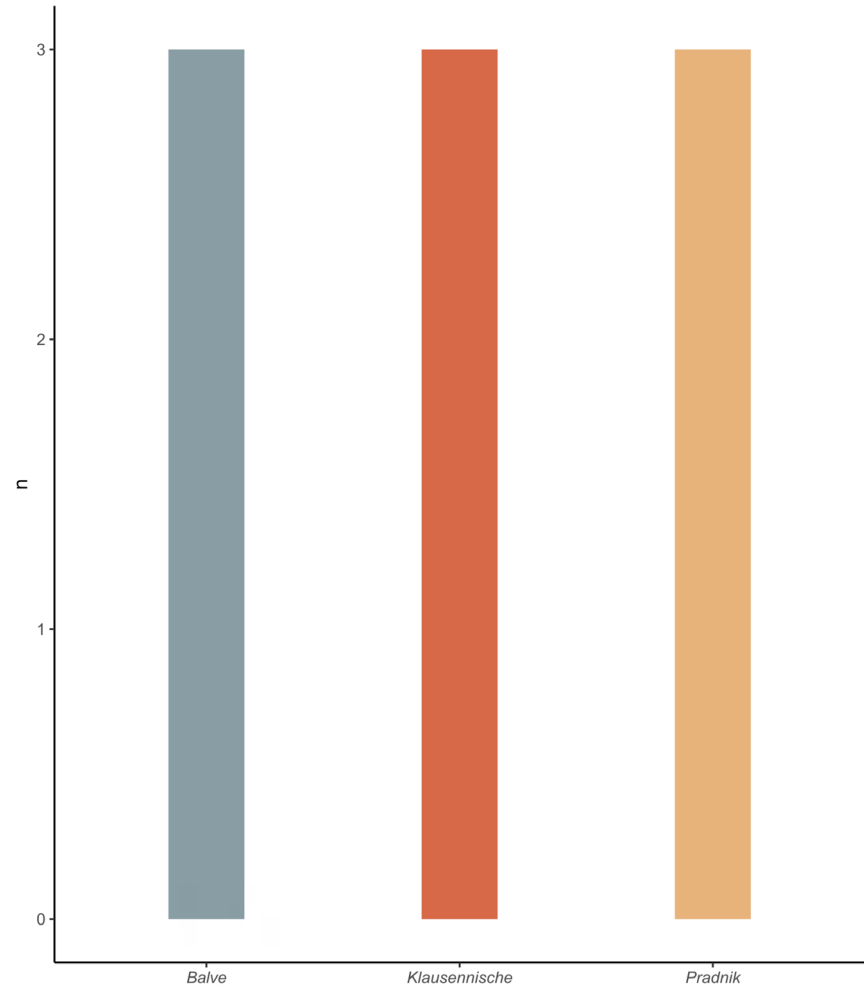

Fig. 79 Distribution of the complete *Keilmesser* (n = 9) from Ramioul to one of the described *Keilmesser* shapes.

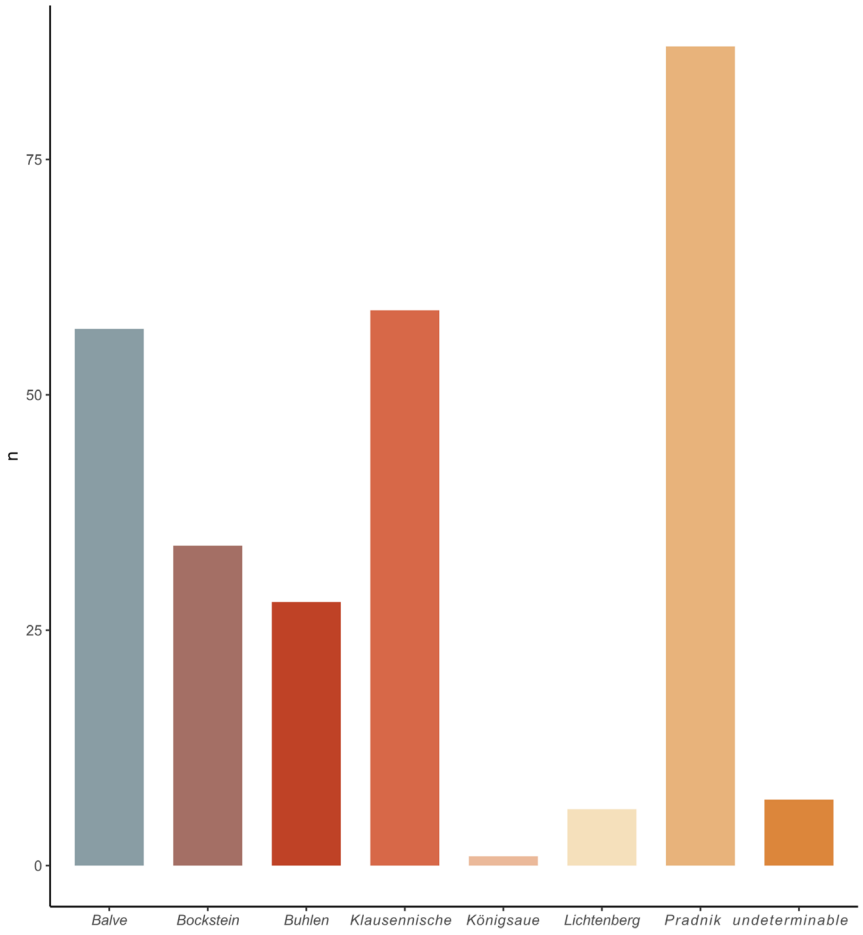

Fig. 80 Distribution of the complete *Keilmesser* from Buhlen (n = 111), Balver Höhle (n = 158) and Ramioul (n = 9) to one of the described *Keilmesser* shapes.

The results from the measurements taken from the Balve assemblage illustrate similar proportions. The section that spans from the base to the back ranges from 30.0 mm to 142.0 mm. The connecting section, the distal posterior part, has a minimum of 10.0 mm and maximum of 93.0 mm. Again, some artefacts do not have this section. In these cases (n = 24) the back directly connects to the active edge. The active edge displays a range between 26.0 mm and 127.0 mm.

In Ramioul, the first section – base and back – ranges from 57.0 mm to 105.0 mm. The margins for the distal posterior part are between 19.0 mm and 82.0 mm. The minimum measurement for the active edge is 13.0 mm while the maximum is 113.0 mm.

The analysis of the determined perimeter sections measured on all *Keilmesser* from the three sites illustrates the following: The proportions of the first section – base and back and the second perimeter section – the distal posterior part – seem to be closely related. The smaller the second section, the larger the dimensions of the back and base. Regardless of this, the length of the working edge is almost constant and occupies on average between 33 and 37 percent of the total perimeter.

In order to determine the actual relationship between the morphologically defined *Keilmesser* shapes and the metrically measured perimeter sections, the data was combined in one graph (**figs 81-84**). The dimensions were plotted in a ternary plot, comprising the mm measurements of the three perimeter sections together at once. The ascribed *Keilmesser* shapes were highlighted in different colours. In case, distinct *Keilmesser* shapes exist, they should cluster graphically grouped together. However, these clusters are not visible as such. Instead of clear clusters, there is a transition between the *Keilmesser* shapes represented by the individual data points. Only the *Keilmesser* classified as shape *Bockstein* separate from the rest of the

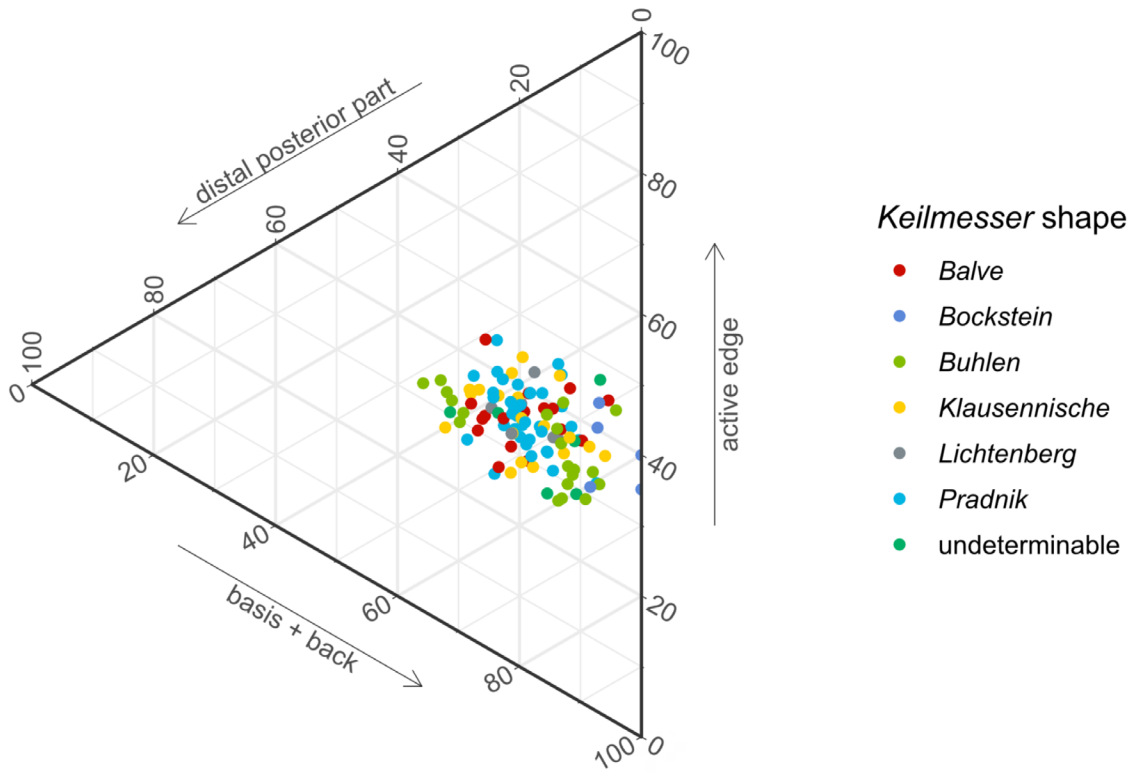

Fig. 81 Size-independent comparison of the shape variation in the perimeter of the complete *Keilmesser* from Buhlen, showing the ratio of the perimeter sections back and base, distal posterior part and active edge. The data points are coloured based on the assigned *Keilmesser* shape.

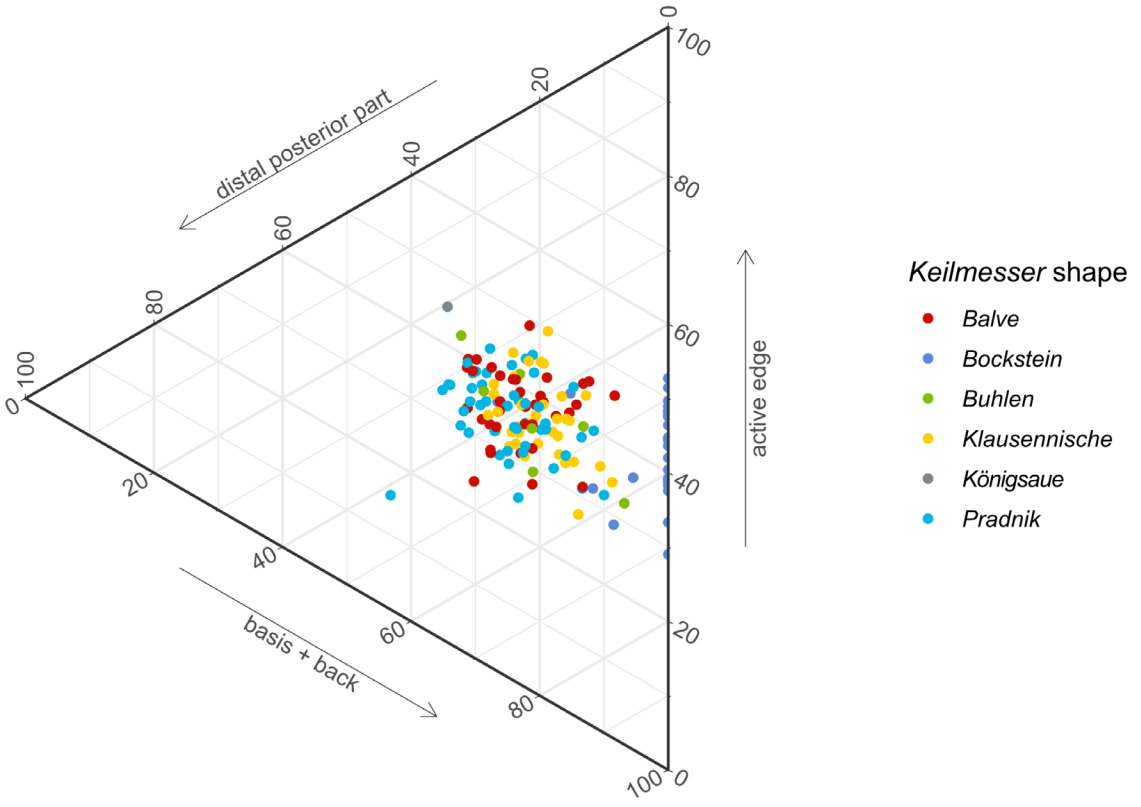

Fig. 82 Size-independent comparison of the shape variation in the perimeter of the complete *Keilmesser* from Balver Höhle, showing the ratio of the perimeter sections back and base, distal posterior part and active edge. The data points are coloured based on the assigned *Keilmesser* shape.

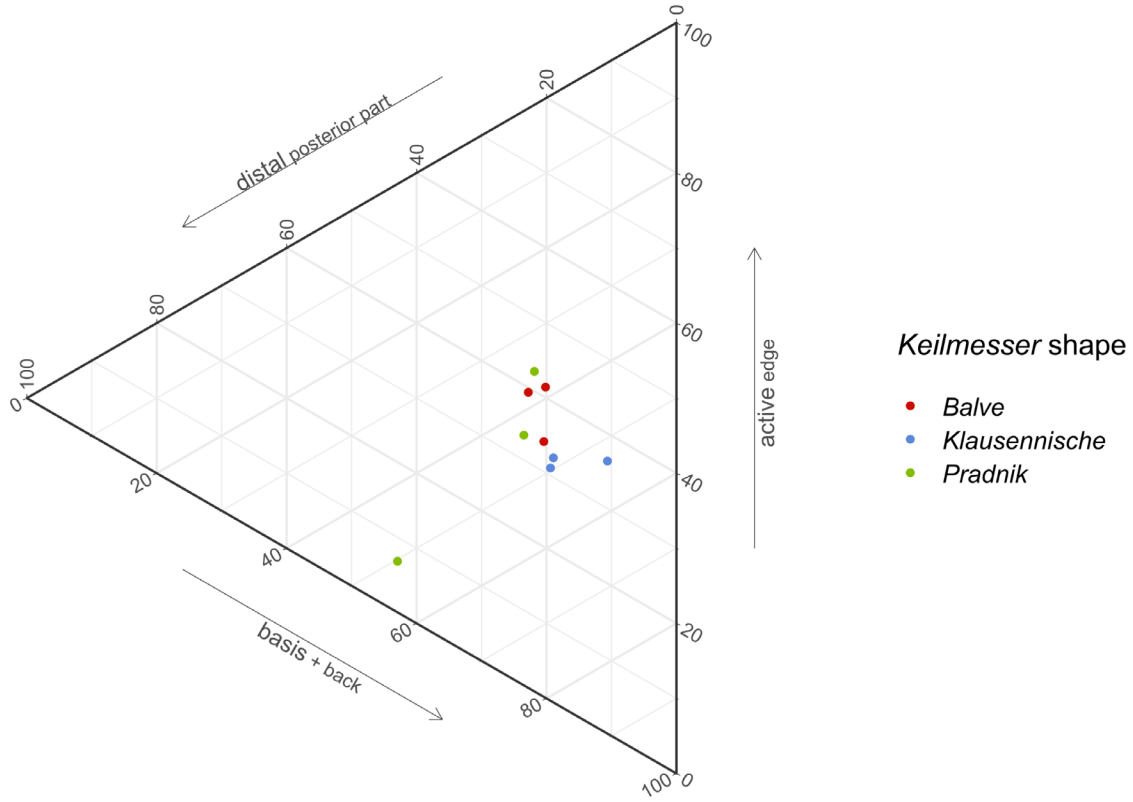

Fig. 83 Size-independent comparison of the shape variation in the perimeter of the complete *Keilmesser* from Ramioul, showing the ratio of the perimeter sections back and base, distal posterior part and active edge. The data points are coloured based on the assigned *Keilmesser* shape.

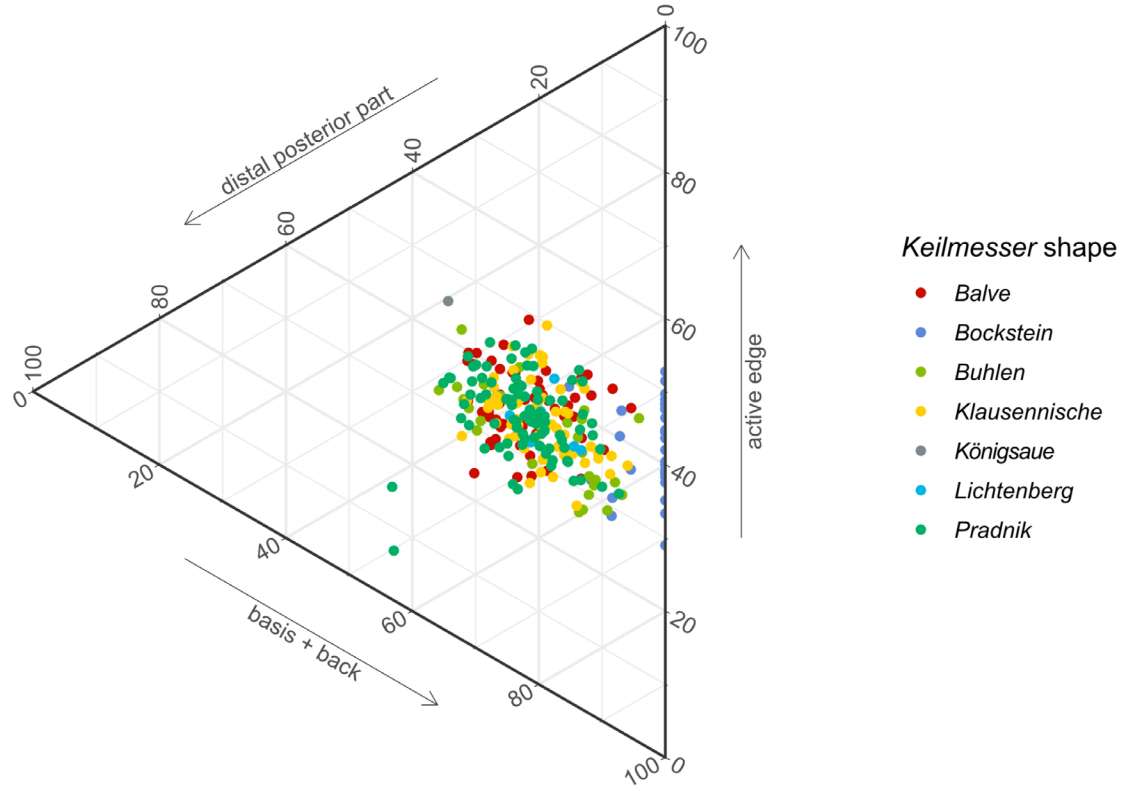

Fig. 84 Size-independent comparison of the shape variation in the perimeter of the complete *Keilmesser* from Buhlen, Balver Höhle and Ramioul, showing the ratio of the perimeter sections back and base, distal posterior part and active edge. The data points are coloured based on the assigned *Keilmesser* shape.

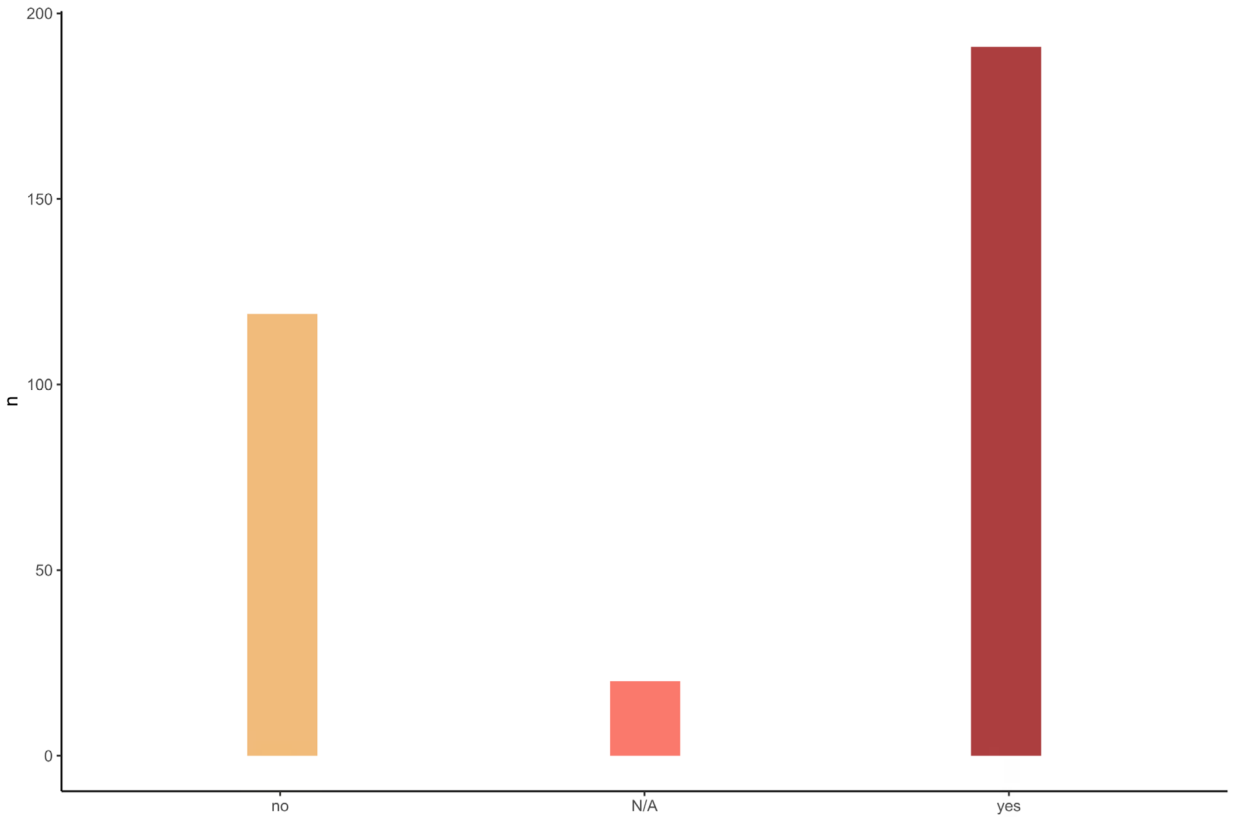

Fig. 85 Tool modification by the application of the *Prądnik method* for the complete *Keilmesser* and *Keilmesser* tips from Buhlen (n = 111, n = 15), Balver Höhle (n = 158, n = 21) and Ramioul (n = 9). In some cases (N/A), it was not possible to approve the application with certainty.

data. In the case of the *Bockstein Keilmesser*, the distal posterior part is missing (± 0 mm). Consequently, the *Keilmesser* of this shape can be found on one axis and not somewhere in the middle of the graph.
The described distribution of the data is relevant for the analysed *Keilmesser* from all three sites. The data taken together displays all data points distributed »randomly« together without clustering into distinct groups. Noticeable is the location of the plotted points. The data plots are not in the middle of the ternary plot, they all tend to be closer to the active edge axis. The other scenario would be expected if the proportions of the three perimeter sections are equal in length.
The fact that the measured values do not match with the morphologically defined *Keilmesser* shapes raises the question of the relevance or correctness of this classification. Rather, it should be questioned why the *Keilmesser* shapes seem to reflect some transitional stages and whether processes such as reworking, sharpening or transformation may cause the differences in the morphology of *Keilmesser* (Jöris 2001; 2004; Jöris/Uomini 2019).

Application of the *Prądnik method*

The majority of the *Keilmesser* from the three sites Buhlen, Balver Höhle and Ramioul display a special modification in the distal part of the tool. The application of the so-called *Prądnik method* is evident by one or multiple negatives on the tool surface resulting from the removal of an elongated lateral spall. For this part of the analysis, only complete and not fragmented *Keilmesser* were considered.

Nearly three quarter (73.0 %, n = 92) of the *Keilmesser* assemblage from Buhlen attests the edge modification by the application of the *Prądnik method*. Out of these, n = 77 display only one negative. It is therefore likely that the *Prądnik method* was applied only once. The remaining n = 15 artefacts of the assemblage are characterised by two or more superimposed negatives. A small amount of n = 26 *Keilmesser* show no evidence of a modification in the distal tool part. Some pieces are classified as undetermined. For these n = 8 artefacts it is not possible to approve the modification or not. In some of these cases, the artefacts are *Keilmesser tips*.
As mentioned above, also at Balve the *Prądnik method* was regularly applied to the *Keilmesser*. With n = 91 artefacts, this counts for half of the artefacts (50.8 %). Recognisable by superimposed negatives, n = 8 of these tools show evidence for the repeated application. More *Keilmesser* than in Buhlen, n = 82, do not display a modification in the distal tool part. For n = 6 *Keilmesser*, a point could not be made.
The same overall picture can be found in Ramioul. Almost all (n = 8) *Keilmesser* clearly document the application of the *Prądnik method*. One of these artefacts also displays a multiple application. Only one *Keilmesser* does not show a modification by the *Prądnik method* in the distal area of the tool.
The majority of *Keilmesser* from the three sites are bifacially retouched, but more interestingly regarding the edge design is the special modification in the distal area of the tool's active edge. The numbers taken together result in the following percentage distribution: 60.8 % (n = 191) of all *Keilmesser* are modified by the *Prądnik method* whereas 34.7 % (n = 109) are not (**fig. 85**). The reaming 4.5 % (n = 14) artefacts are undetermined regarding the application. A small percentage of 12.6 % (n = 24) is clearly characterised be a repeated application, indicated by superimposed negatives.

Prądnik spalls

The so-called *Prądnik spalls,* which result from the application of the *Prądnik method* on *Keilmesser* or *Prądnik scrapers,* are part of the studied inventories. In total, n = 159 *Prądnik spalls* were analysed. Due to the fact, that no *Prądnik spalls* from the assemblage in Ramioul could be selected for this study, this part of the analysis only focuses on the artefacts from Buhlen (n = 42) and Balve (n = 117).
The results presented in the following are based on a classification of the *Prądnik spalls* as primary or secondary spalls and the determination of the artefact laterality. In a further step, the dimensions of the *Prądnik spalls* will be addressed.

Morphometric quantitative analysis

The length, width and thickness of the *Prądnik spalls* was measured on the maximum extend, respectively. Only n = 36 of the n = 42 studied *Prądnik spalls* from Buhlen are complete and thus relevant for the analysis. The other *Prądnik spalls* are either distal (n = 3) or proximal (n = 3) fragments. The measurements of these pieces can be found on GitHub [https://github.com/lschunk/Lithic_analysis_archaeology]. The complete *Prądnik spalls* can be classified in a size range from 21.0 mm to 56.0 mm length (**figs 86. 89**). The arithmetic mean of the length is 35.1 mm. The minimum and maximum extension of the width are 8.0 mm and 31.0 mm, with an arithmetic mean value of 16.0 mm (**fig. 90**). The thickness is ranging between 2.0 mm and 13.0 mm (**fig. 91**). The arithmetic mean amounts to 4.7 mm.
As in Buhlen, not all *Prądnik spalls* from Balve are complete pieces. While the majority of the *Prądnik spalls* are complete (n = 110), also n = 4 distal and n = 3 medial fragments belong to the *Prądnik spall* assem-

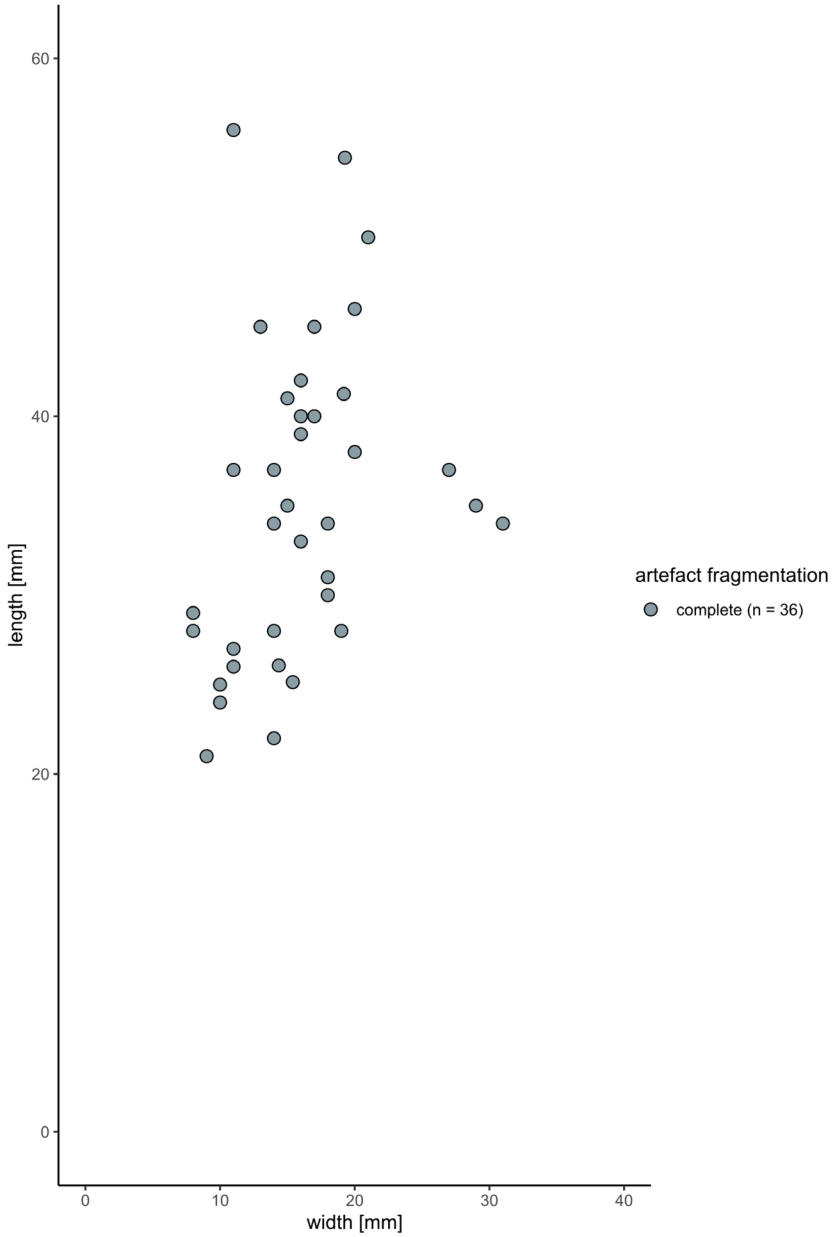

Fig. 86 Length-width ratio of the complete *Prądnik spalls* (n = 36) from Buhlen.

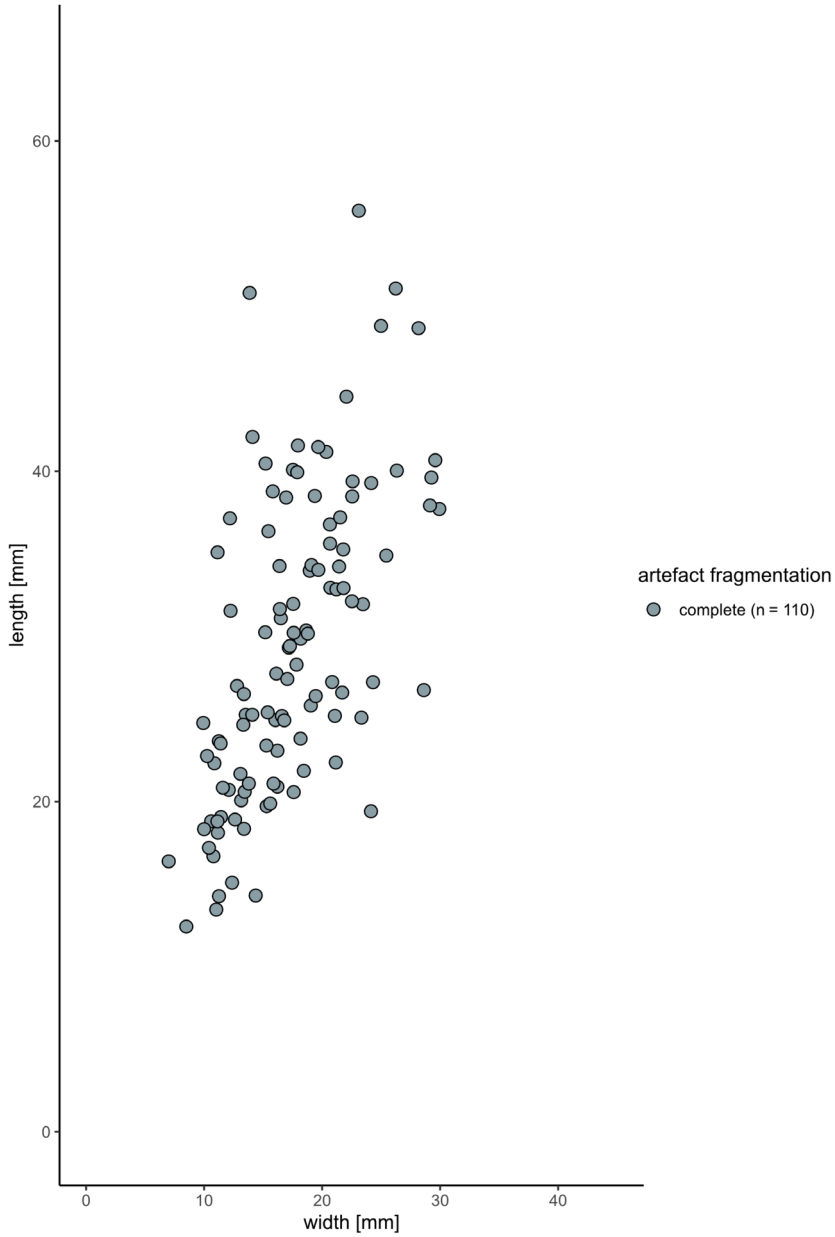

Fig. 87 Length-width ratio of the complete *Prądnik spalls* (n = 110) from Balver Höhle.

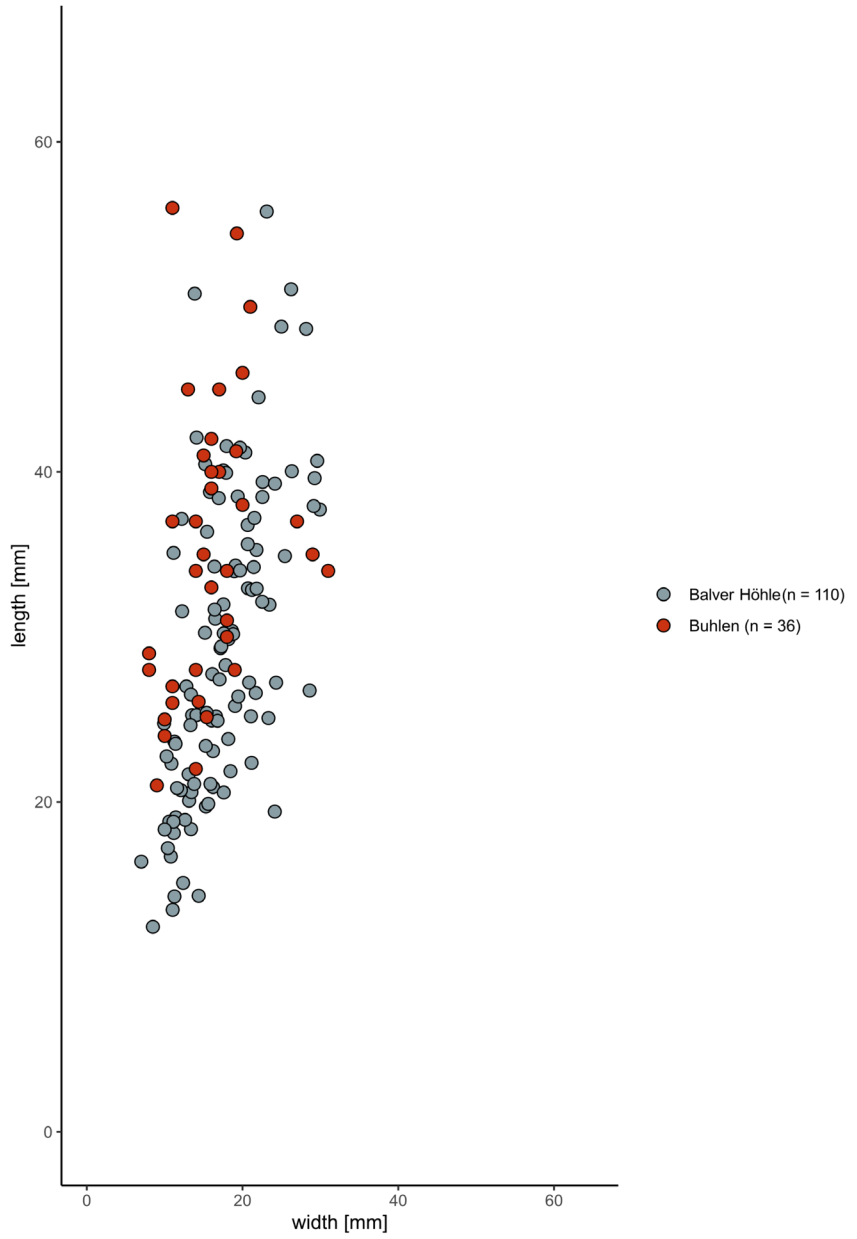

Fig. 88 Length-width ratio of the complete *Prądnik spalls* from Buhlen (n = 36) and Balver Höhle (n = 110).

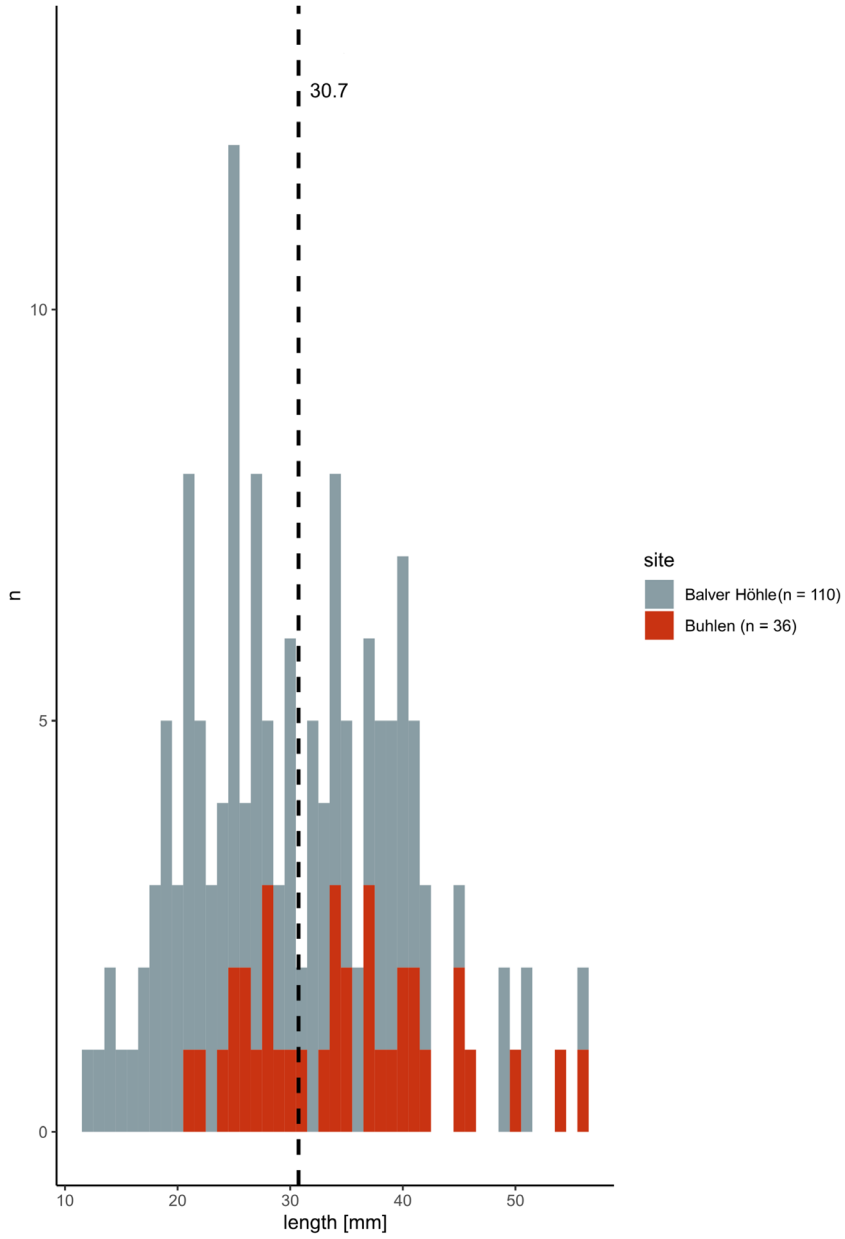

Fig. 89 Maximal length of the complete *Prądnik spalls* from Buhlen (n = 36) and Balver Höhle (n = 110). The dashed line indicates the arithmetic mean value.

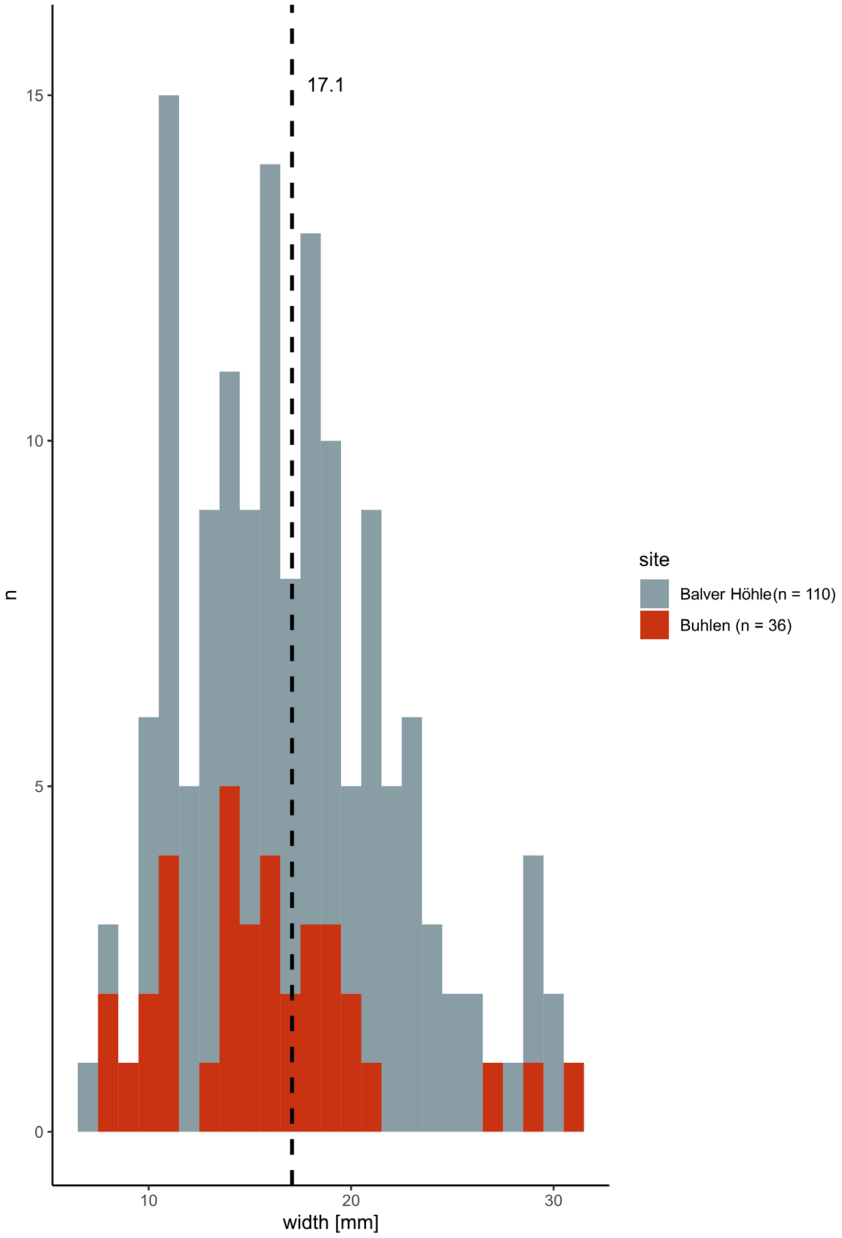

Fig. 90 Maximal width of the complete *Prądnik spalls* from Buhlen (n = 36) and Balver Höhle (n = 110). The dashed line indicates the arithmetic mean value of the complete and fragmented *Prądnik spalls* together.

blage. In Balve, the complete *Prądnik spall* length ranges between 12.4 mm and 55.8 mm (**figs 87. 89**). The arithmetic mean is 29.3 mm. The margin concerning the width is 7.0 mm and 29.3 mm with an arithmetic mean value of 17.4 mm (**fig. 90**). The minimum thickness of the *Prądnik spalls* is 2.14 mm and the maximum is 11.0 mm (**fig. 91**). The arithmetic mean amounts to 6.0 mm.

The data generated from the two sites shows, that the *Prądnik spalls* from Buhlen and Balve have comparable dimensions. To summarize, the analysed complete *Prądnik spalls* from the two sites together (n = 146) are between 12.4 mm and 56.0 mm long (**figs 88-89**). The arithmetic mean value thereby is 30.7 mm. The width extends from minimum 7.0 mm to maximum 31.0 mm with an arithmetic mean of 17.1 mm (**fig. 90**). The thickness is ranging between 2.0 mm and 13.0 mm (**fig. 91**). The arithmetic mean value for the thickness is 5.7 mm.

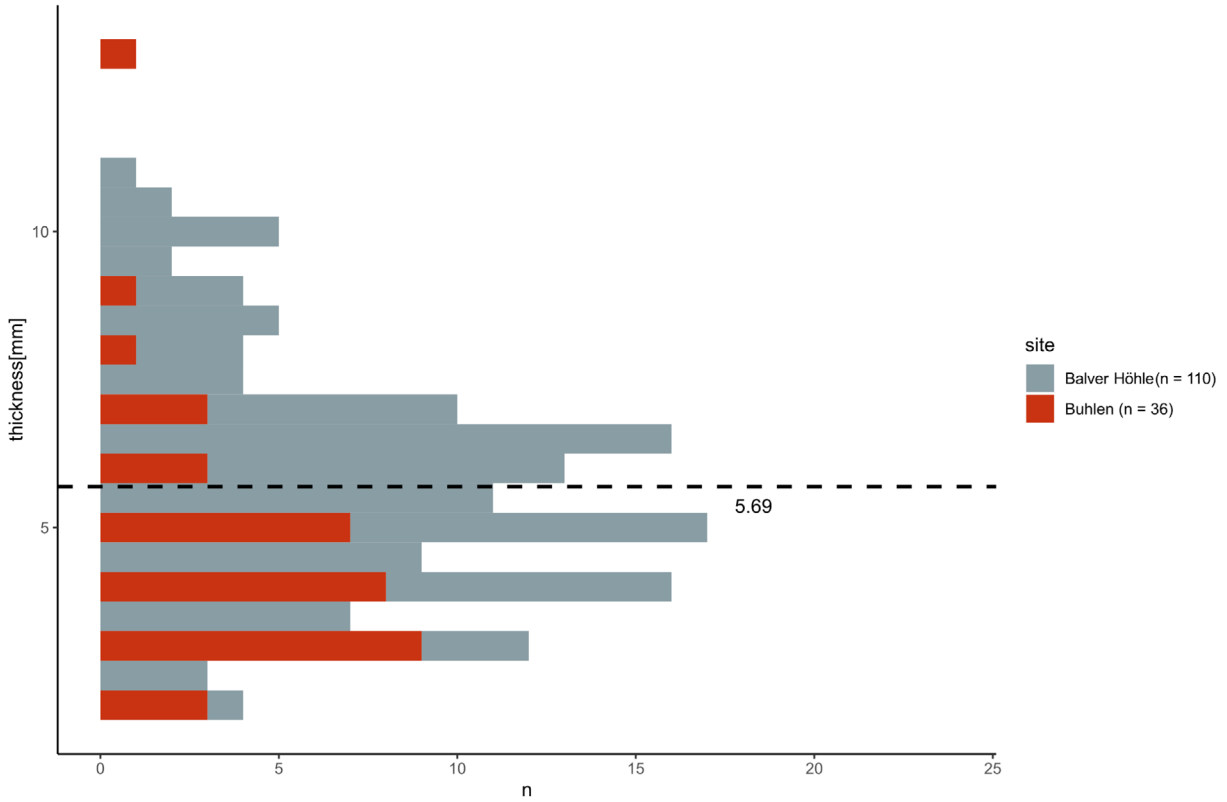

Fig. 91 Maximal thickness of the complete *Prądnik spalls* from Buhlen (n = 36) and Balver Höhle (n = 110). The dashed line indicates the arithmetic mean value of the complete and fragmented *Prądnik spalls* together.

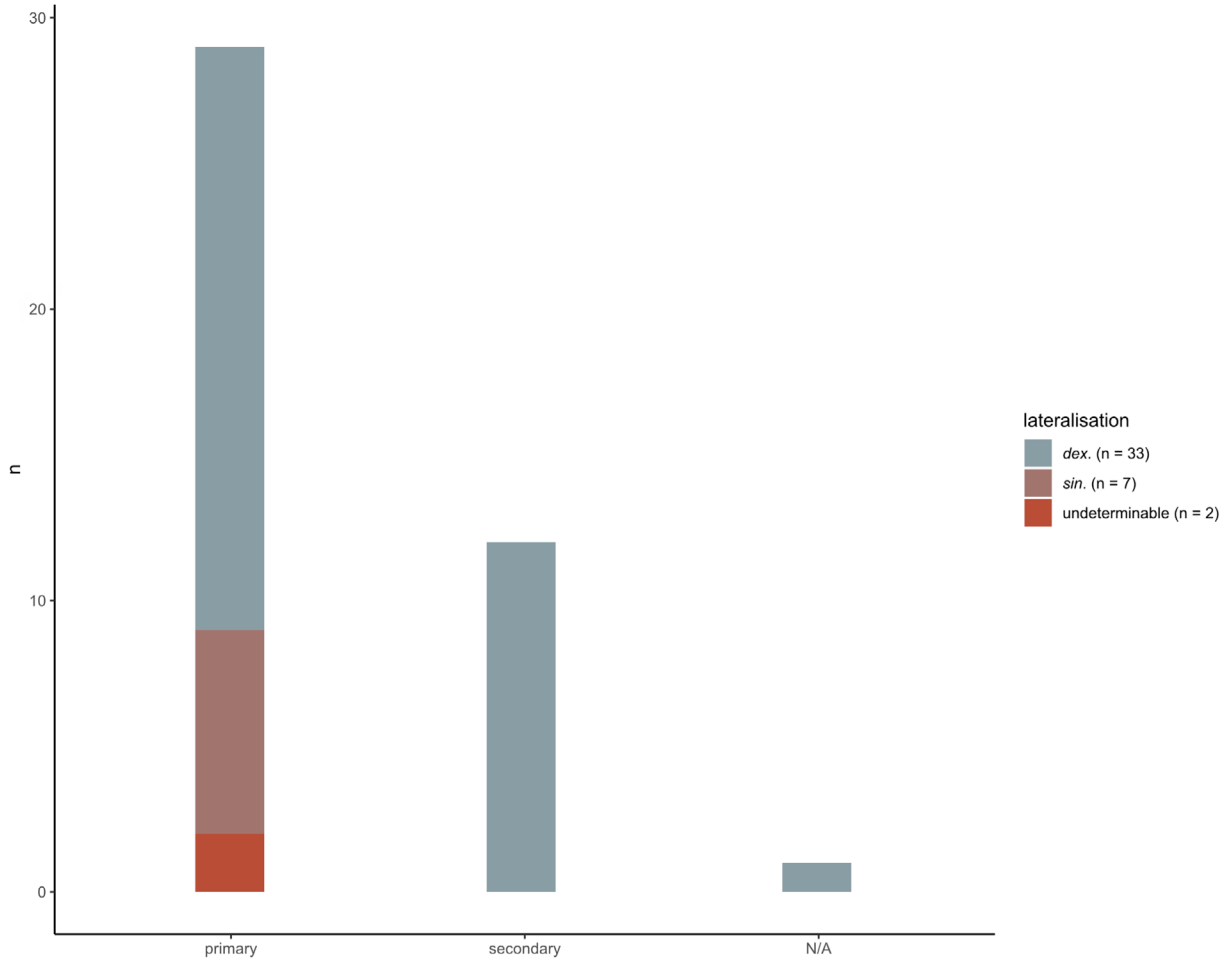

Fig. 92 Classification of the *Prądnik spalls* (n = 42) from Buhlen. The colours indicate the laterality of the artefacts.

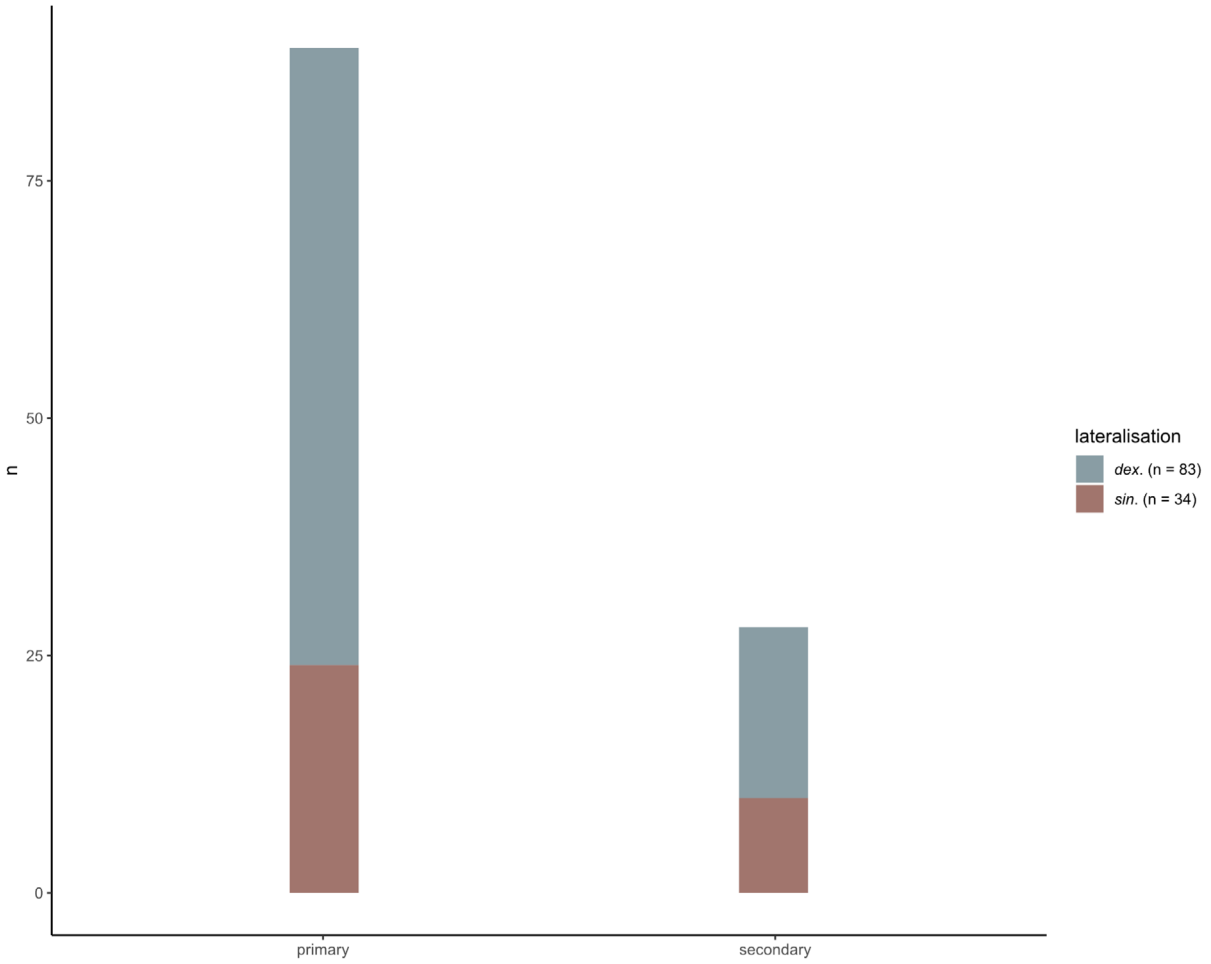

Fig. 93 Classification of the *Prądnik spalls* (n = 117) from Balver Höhle. The colours indicate the laterality of the artefacts.

Classification

The *Prądnik spalls*, which emerge by the application of the *Prądnik method*, can be subdivided in primary and secondary spalls. The n = 42 analysed *Prądnik spalls* from the Buhlen inventory can be separated in n = 29 primary and n = 12 secondary spalls (**fig. 92**). One artefact could not be attributed due to its fragmentation.
In Balve, in total n = 117 *Prądnik spalls* were analysed (**fig. 93**). Here, the primary *Prądnik spalls* predominate with n = 89 pieces, too. Secondary *Prądnik spalls* are represented with n = 28 artefacts.
The results from the two sites taken together lead to a percentage of 74.2 % primary to 25.2 % secondary *Prądnik spalls* (**fig. 94**).

Lateralisation

Similar as for the *Keilmesser* and *Prądnik scrapers*, a lateralisation can also be determined for the *Prądnik spalls* removed from these tools (**tab. 14**).

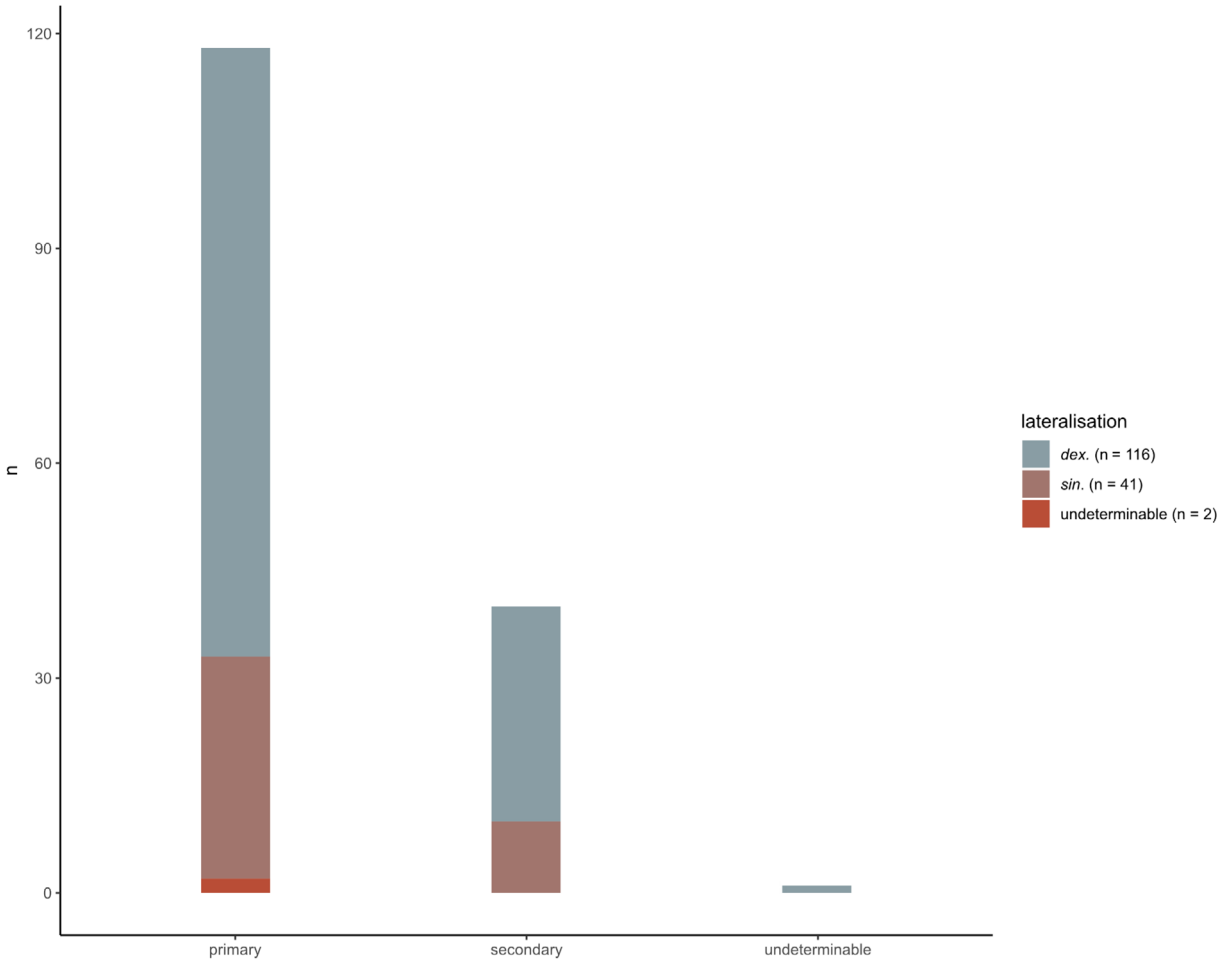

Fig. 94 Classification of the *Prądnik spalls* from Buhlen (n = 42) and Balver Höhle (n = 117). The colours indicate the laterality of the artefacts.

As for the tools, the *Prądnik spalls* from Buhlen are by a majority right-sided spalls (**fig. 94**). Next to the n = 29 right-lateral artefacts, n = 13 pieces are documented as left-lateral. These left-lateral *Prądnik spalls* are without exception primary spalls. However, the right-sided *Prądnik spalls* can be categorised as primary (n = 20) and secondary (n = 7) pieces.

A dominance of right-sided *Prądnik spalls* becomes also evident in the assemblage from Balve with n = 69 pieces. A description as left-lateral *Prądnik spalls* is possible for n = 28 artefacts. Both, right- as well as left-sided *Prądnik spalls* consist of primary and secondary spalls.

site		*Prądnik spall*		
		sin.	*dex.*	total
Buhlen	n	13	29	**130**
	%	31.0	69.1	100.0
Balve	n	34	83	**117**
	%	29.1	70.9	100.0
total	**n**	**47**	**112**	**159**
	%	29.6	70.4	100.0

Table 14 Determination of the tool lateralisation of the *Prądnik spalls* from Buhlen and Balver Höhle.

In total, 74.2 % (n = 118) of the analysed *Prądnik spalls* from Buhlen and Balve are documented as primary spalls, whereas 25.2 % (n = 40) of the pieces count as secondary spalls. The overall predominating right-sidedness of the *Keilmesser* and *Prądnik scrapers* is also reflected in the laterality of the *Prądnik spalls.* 61.2 % (n = 98) of the pieces are right-lateral, 25.8 % (n = 41) are left-lateral.

QUANTIFICATION OF EDGE DESIGN

One relevant aspect concerning tool design is the edge angle. Edge angle measurements have been taken on selected artefacts. The sampling strategy thereby was explained in the previous method chapter, resulting in a sub-sample of n = 226 artefacts (**tab. 8**). Only complete artefacts were selected. These artefacts can be divided in n = 157 *Keilmesser*, n = 18 *Keilmesser* tips, n = 20 *Prądnik scrapers* and n = 21 *Prądnik spalls*. Also for the edge angle measurements, artefacts not belonging to the selected artefact categories were relevant. Thus, n = 8 scraper as well as n = 2 flakes were sampled for reference as outgroup. The edge angles here was measured with a semi-automated, script-based method. Hence, the n = 226 artefacts have been scanned with a 3D scanner (AICON smartScan-HE R8, Hexagon, Germany) in order to create 3D models for the application of the method.

Edge angle variability

The edge angles of the scanned tools were calculated in order to understand the variability of the angle along the entire tool edge. Moreover, the specific method was also applied to document the changes of the edge angle from the intersection of dorsal and ventral surfaces towards the middle of the artefact. As pointed out already earlier, one mean value *per* tool is thus not sufficient and does not allow for any interpretation concerning the internal variability of the edge design within and between tools. In order to explain the resulting data, certain arithmetic mean values need to be mentioned here, though. Every individual measured angle can be review on GitHub [https://github.com/lschunk/edge_angle_analysis]. There, the raw data, the derived data and a plot of each single artefact can be found and accessed.
For each scanned artefact, ten horizontal sections were defined. Starting at the edge of the tool, each section had a length of 12 mm towards both surfaces (ventral and dorsal) (**figs 23-25**). Based on these horizontal sections, the measurements were taken in 1 mm steps starting at the intersection. Meaning, up to twelve measurements per section were taken.
As explained in the methods chapter, three different measurement procedures were applied for each tool. From earlier tests, which also have been done on objects with a known edge angle, it could be noticed, that the different measurement system led to slightly different results. While the »2-line« and the »best-fit« procedures produce similar results, the results from the »3-point« procedure vary more strongly. It is likely that the »3-point« measurement procedure deals well with simple structures and smooth surfaces. For instance, the »3-point' procedure works perfectly well on the experimental standard samples. The other two measurement procedures seem to be more suitable and reliable for complex structures and surface irregularities.
The results for the different artefact categories involved is presented and illustrated exemplarily for the three different measurement procedures respectively in the following. The data is split in the usual artefact categories *Keilmesser*, *Prądnik scrapers*, *Prądnik spalls*, scrapers and flakes. Additionally, the *Keilmesser* are furthermore separated in *Keilmesser* with and without negative of the *Prądnik spall* removal and *Keilmesser* tips. The data calculated for the *Prądnik spalls* refers always to the edge on the dorsal surface, which was the former active edge of the *Keilmesser* or *Prądnik scraper* before the spall was detached (**fig. 95**). In order to make the herein explained quantity of data a little more comprehensible, only the results for the measurements at 2 mm, 5 mm and 10 mm distance to the intersection will be mentioned. Moreover, when analysing the data, it became obvious, that the results of the first section (distal) as well as the tenth section (proximal) most often deviate from the results of the other eight sections. The reason for that can likely be found in the

length of the vertical polyline that follows the tool edge. This polyline often slightly extents toward the distal posterior part and the base of the tool. Meaning, these results would actually reflect not the edge angle measurements for the active edge, but rather for the adjacent perimeter section. Thus, to avoid any doubts, these two sections will be excluded when presenting the data. Whenever there will be a range discussed, it always refers to the range from the second (distal) to the ninth (proximal) horizontal section. The range does not necessarily reflect the minimum and maximum values. All mentioned edge angle values are in degrees.

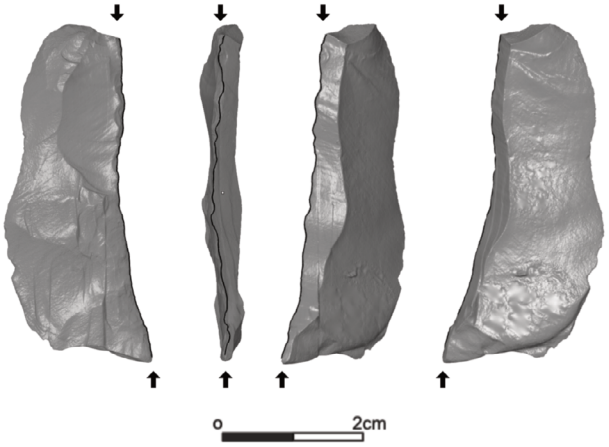

Fig. 95 3D scan of a secondary *Prądnik spall* from Buhlen (left: dorsal surface; middle: edge, right: ventral surface) illustrating on which edge (black line; indicated by the arrows) the angles have been calculated. – Not to scale.

»3-point« procedure

First, the results from the »3-point« measuring procedure is presented. The results for the *Keilmesser* are based on n = 57 artefacts (**tab. 8**). To start with the 2 mm distance, the edge angle ranges from 86.8° to 92.2° (**tab. 15**). The measurements at 5 mm distance result in a range from 70.4° to 79.6°. At the 10 mm distance, the values are 51.4° to 66.8°. For these three distances, the arithmetic mean is 89.1°, 75.3° and 61.6° respectively.

Keilmesser with a negative from the application of the *Prądnik method* are with n = 100 pieces part of the analysis (**tab. 16**). These measurements result in lower edge angles. At a distance of 2 mm from the intersection, the measurements are ranging from 79.8° to 86.1°, with an arithmetic mean value of 82.9°. The range for the 5 mm distance is from 67.0° to 74.0°. The arithmetic mean is 71.0°. At the 10 mm distance, the measurements are 54.6° to 61.2° and the arithmetic mean is 59.7°.

The next category is the *Keilmesser* tips. N = 18 pieces were scanned and analysed for the edge angle measurements (**tab. 17**). The results for the *Keilmesser* tips are similar to the previously mentioned results. Interesting here is, that n = 10 of the *Keilmesser* tips also display a negative resulting from the application of the *Prądnik method*. At the 2 mm distance, the values are 83.8° to 83.0°. The range at 5 mm is from 67.3°

section	distance to origin [in degrees]			mean per section (2-5)	mean per section (all)
	2 mm	5 mm	10 mm		
1	89.5	73.6	57.4	73.5	72.9
2	86.8	70.4	51.4	69.5	69.4
3	88.2	73.0	60.4	73.9	73.4
4	86.1	72.1	61.5	73.2	72.6
5	89.1	75.9	65.0	76.7	76.1
6	88.6	76.1	58.6	74.4	75.6
7	87.6	75.9	63.5	75.7	75.7
8	94.4	79.4	65.4	79.7	78.9
9	92.2	79.6	66.8	79.5	78.8
10	98.4	84.2	67.5	83.4	82.3

Table 15 Edge angle arithmetic mean values for *Keilmesser* (n = 57). The edge angles are calculated with the »3-point« measurement procedure.

section	distance to origin [in degrees]			mean per section (2-5)	mean per section (all)
	2 mm	5 mm	10 mm		
1	81.7	65.2	50.8	65.9	65.1
2	79.8	67.0	54.6	67.1	66.5
3	80.7	67.6	54.9	67.7	67.1
4	76.3	68.2	57.8	67.4	67.4
5	80.4	71.8	62.2	71.5	71.0
6	85.9	72.4	62.3	73.5	72.8
7	86.7	73.8	63.1	74.5	74.2
8	87.2	72.9	61.7	73.9	73.4
9	86.1	74.0	61.2	73.8	73.0
10	98.8	81.1	64.9	81.6	80.4

Table 16 Edge angle arithmetic mean values for *Keilmesser* modified by the *Prądnik method* (n = 100). The edge angles are calculated with the »3-point« measurement procedure.

section	distance to origin [in degrees]			mean per section (2-5)	mean per section (all)
	2 mm	5 mm	10 mm		
1	68.3	66.1	49.9	61.4	65.1
2	83.8	67.3	50.9	67.3	66.5
3	79.2	64.9	52.3	65.5	67.1
4	80.0	67.6	55.8	67.8	67.4
5	76.5	64.5	57.0	66.0	71.0
6	81.2	69.4	56.0	68.9	72.8
7	80.7	71.0	58.9	70.2	74.2
8	82.7	71.2	57.4	70.4	73.4
9	83.0	71.0	59.9	71.3	73.0
10	85.3	66.5	53.9	68.6	80.4

Table 17 Edge angle arithmetic mean values for *Keilmesser tips* (n = 18). The edge angles are calculated with the »3-point« measurement procedure.

section	distance to origin [in degrees]			mean per section (2-5)	mean per section (all)
	2 mm	5 mm	10 mm		
1	65.6	42.2	31.6	46.5	45.7
2	55.7	43.0	33.3	44.0	44.2
3	53.4	46.0	38.5	46.0	46.2
4	63.0	51.7	42.6	52.4	52.4
5	76.4	59.3	43.1	59.6	59.4
6	75.7	54.7	42.3	57.6	56.7
7	81.4	57.0	44.6	61.0	59.9
8	74.4	62.9	46.2	61.2	60.6
9	80.0	66.4	48.3	64.9	63.9
10	85.8	67.8	49.2	67.6	65.8

Table 18 Edge angle arithmetic mean values for *Prądnik scrapers* (n = 20). The edge angles are calculated with the »3-point« measurement procedure.

to 71.0°. At a distance of 10 mm from the intersection, the values are 50.9 to 59.9°. The arithmetic mean values amount to 80.9°, 68.4° and 56.0°.

N = 20 *Prądnik scrapers* were included in the analysis (**tab. 18**). From 55.7° to 80.0° is the range at the 2 mm distance. The measurements ranging from 43.0° to 66.4° at the 5 mm distance. Significantly lower are the values at 10 mm. They range from 33.3° to 48.3°. This leads to arithmetic mean values of 70.0°, 55.1° and 42.4° per mentioned distance.

Table 19 Edge angle arithmetic mean values for *Prądnik spalls* (n = 21). The edge angles are calculated with the »3-point« measurement procedure.

section	distance to origin [in degrees]			mean per section (2-5)	mean per section (all)
	2 mm	5 mm	10 mm		
1	54.3	32.1	19.6	35.3	37.4
2	59.5	38.8	17.9	38.7	38.9
3	63.4	41.6	17.2	40.7	40.8
4	64.4	40.0	18.9	41.1	41.0
5	64.5	41.8	19.5	41.9	41.6
6	72.0	46.6	20.9	46.5	45.5
7	72.5	44.7	22.0	46.4	45.0
8	73.4	45.6	22.3	47.1	45.1
9	69.4	42.1	20.4	44.0	42.7
10	56.4	35.4	18.4	36.7	36.8

Table 20 Edge angle arithmetic mean values for scrapers (n = 9). The edge angles are calculated with the »3-point« measurement procedure.

section	distance to origin [in degrees]			mean per section (2-5)	mean per section (all)
	2 mm	5 mm	10 mm		
1	79.4	55.2	52.5	62.4	59.4
2	72.3	58.5	47.1	59.3	58.3
3	89.0	65.3	55.3	69.9	69.4
4	56.8	51.2	48.6	52.2	51.8
5	74.3	57.5	49.5	60.4	59.5
6	78.8	60.3	53.6	64.2	63.3
7	76.0	59.9	50.4	62.1	61.1
8	82.4	62.6	55.7	66.9	66.2
9	80.7	71.9	61.6	71.4	70.3
10	108.9	106.7	95.6	103.7	105.1

The analysed n = 21 *Prądnik spalls* result in measurements of 59.5° and 69.4° at 2 mm distance with an arithmetic mean of 67.4° (**tab. 19**). At a distance of 5 mm, the values are 38.8° to 42.1°. The arithmetic mean values for the 5 mm distance is 42.7°. The range for the 10 mm distance is 17.9° to 20.4°. The arithmetic mean is 19.9°.

Additionally, n = 9 scrapers and n = 2 flakes were analysed as outgroup (**tab. 20**). The scrapers range at the 2 mm distance from 93.7° to 85.2°. At the 5 mm distance, the values are 74.9° to 75.2°. The measurements for the 10 mm distance are 55.0° and 75.8°. These measurements result in arithmetic mean values of 94.8°, 77.0° and 59.8° per distance respectively.

The flakes have a range of 72.3° to 80.7° at the 2 mm distance with an arithmetic mean of 76.3° (**tab. 21**). The measurements at 5 mm distance reach from 58.5° to 71.9°. The arithmetic mean value is 60.9°. At the 10 mm distance, the values are lower and range from 47.1° to 61.6°. The arithmetic mean is 52.7°.

»2-lines« procedure

With the second measuring procedure, the so-called »2-lines« procedure, deviating edge angle values were calculated.

section	distance to origin [in degrees]			mean per section (2-5)	mean per section (all)
	2 mm	5 mm	10 mm		
1	95.9	79.4	50.0	75.1	75.1
2	93.7	74.9	55.0	74.5	74.6
3	93.3	74.1	58.1	75.2	74.5
4	96.9	76.4	58.7	77.3	76.5
5	95.7	80.3	62.3	79.4	79.1
6	94.8	81.4	64.4	80.2	79.3
7	93.6	76.6	62.5	77.6	77.5
8	95.5	76.9	60.2	77.5	76.9
9	95.2	75.2	57.0	75.8	74.8
10	99.5	81.4	56.9	79.3	78.0

Table 21 Edge angle arithmetic mean values for flakes (n = 2). The edge angles are calculated with the »3-point« measurement procedure.

section	distance to origin [in degrees]			mean per section (2-5)	mean per section (all)
	2 mm	5 mm	10 mm		
1	76.5	53.9	28.2	52.9	52.6
2	73.7	51.3	28.2	51.1	49.5
3	71.9	59.2	39.2	56.8	55.9
4	72.3	58.4	45.0	58.6	58.4
5	74.3	60.8	47.0	60.7	61.1
6	77.3	59.3	45.7	60.8	59.9
7	73.7	62.8	43.8	60.1	59.7
8	81.3	60.2	40.6	60.7	60.8
9	78.4	62.7	43.1	61.4	61.9
10	83.9	66.1	43.9	64.6	63.0

Table 22 Edge angle arithmetic mean values for *Keilmesser* (n = 57). The edge angles are calculated with the »2-lines« measurement procedure.

section	distance to origin [in degrees]			mean per section (2-5)	mean per section (all)
	2 mm	5 mm	10 mm		
1	63.4	48.9	30.8	47.7	46.8
2	66.3	52.9	30.9	50.0	50.4
3	66.7	50.6	35.3	50.9	51.3
4	68.3	55.3	43.8	55.8	55.1
5	69.6	62.8	46.8	59.7	58.4
6	71.3	58.4	45.0	58.2	58.8
7	74.5	59.3	44.4	59.4	59.5
8	72.5	59.3	44.3	58.7	58.1
9	74.6	59.9	41.9	58.8	57.5
10	82.8	59.8	42.0	61.5	59.9

Table 23 Edge angle arithmetic mean values for *Keilmesser* modified by the *Prądnik method* (n = 100). The edge angles are calculated with the »2-lines« measurement procedure.

For *Keilmesser*, the range at 2 mm is from 73.7° to 78.4° (**tab. 22**). At a distance of 5 mm from the intersection, the values are 51.3° and 62.7°. The range at 10 mm is from 28.2° to 43°. The arithmetic means for these three distances are 75.4°, 59.3° and 41.5° respectively.

Keilmesser with a negative from the removed *Prądnik spall* do have slightly smaller values at the 2 mm and 5 mm distance compared to the beforehand mentioned results for the *Keilmesser* (**tab. 23**). At 2 mm dis-

Table 24 Edge angle arithmetic mean values for *Keilmesser* tips (n = 18). The edge angles are calculated with the »2-lines« measurement procedure.

section	distance to origin [in degrees]			mean per section (2-5)	mean per section (all)
	2 mm	5 mm	10 mm		
1	65.0	41.6	28.5	45.0	46.8
2	64.8	50.5	30.3	48.5	50.4
3	62.8	52.1	32.1	49.0	51.3
4	68.2	54.7	34.2	52.4	55.1
5	64.6	60.9	31.7	52.4	58.4
6	68.2	57.3	33.2	52.9	58.8
7	64.9	66.1	31.6	54.2	59.5
8	70.3	57.8	34.3	54.1	58.1
9	71.2	60.7	42.2	58.0	57.5
10	61.9	47.2	35.4	48.2	59.9

Table 25 Edge angle arithmetic mean values for *Prądnik scrapers* (n = 20). The edge angles are calculated with the »2-lines« measurement procedure.

section	distance to origin [in degrees]			mean per section (2-5)	mean per section (all)
	2 mm	5 mm	10 mm		
1	41.5	26.2	25.8	31.2	30.3
2	42.3	33.6	15.8	30.6	30.6
3	43.8	37.1	17.2	32.7	34.7
4	49.5	40.9	24.1	38.2	39.4
5	59.5	40.5	23.8	41.3	39.4
6	55.8	36.9	20.5	37.7	38.0
7	59.9	36.1	24.4	40.1	41.2
8	62.6	45.6	21.8	43.3	41.4
9	64.8	50.9	16.2	44.0	42.5
10	67.6	47.5	16.7	43.9	43.7

tance, these *Keilmesser* have a range of 66.3° to 74.6 ° with a mean value of 70.5°. The measurements at 5 mm range from 52.9° to 59.9°. The arithmetic mean is 57.3°. At the 10 mm distance, the measurements are 30.9° to 41.9° and the arithmetic mean is 41.6°. Thus, the arithmetic means at the 10 mm distance for *Keilmesser* and *Keilmesser* with negative are nearly identical. It is likely that the negative often does not reach up to 10 mm width on the surface.

The measurements for the *Keilmesser* tips result in the following values (**tab. 24**). The range at the 2 mm distance from the intersection is 64.8° to 71.2°. For the measurements at the 5 mm distance, the values are 50.5° and 60.7°. At 10 mm distance to the intersection, the values ranging from 30.3° to 42.2°. The edge angle measurements lead to arithmetic mean values of 66.9°, 57.5° and 33.7° per mentioned distance.

The calculated edge angles for the *Prądnik scrapers* result in measurements of 42.3° and 64.8° at 2 mm distance with an arithmetic mean of 54.8° (**tab. 25**). At a distance of 5 mm, the values are 33.6° to 50.9°. The arithmetic mean values for the 5 mm distance is 40.0°. The range for the 10 mm distance is 15.8° to 16.2°. The arithmetic mean is 20.5°.

For *Prądnik spalls*, the values measured at the 2 mm distance are 44.4° and 50.7° (**tab. 26**). At the 5 mm distance to the intersection, a range from 20.7° to 14.9° could be calculated. The values at 10 mm are ranging from 21.4° to 16.1°. The arithmetic mean for these three distances are 47.6°, 18.5° and 18.8° respectively. The measured scrapers display a range of 71.7° to 75.6° at the 2 mm distance with an arithmetic mean of 77.5° (**tab. 27**). The measurements at 5 mm distance reach from 53.7° to 52.2°. The arithmetic mean value is 55.2°. At the 10 mm distance, the values range from 22.9° to 25.8°. The arithmetic mean is 33.8°.

section	distance to origin [in degrees]			mean per section (2-5)	mean per section (all)
	2 mm	5 mm	10 mm		
1	32.8	18.3	21.7	24.3	24.9
2	44.4	20.7	21.4	28.8	28.5
3	43.9	20.5	21.1	28.5	28.5
4	44.4	18.1	20.3	27.6	26.7
5	43.9	17.7	17.8	26.5	26.5
6	53.1	18.5	21.3	31.0	29.5
7	47.5	20.3	16.9	28.2	27.6
8	52.7	17.3	15.6	28.5	27.6
9	50.7	14.9	16.1	27.2	25.6
10	35.3	10.2	13.3	19.6	20.5

Table 26 Edge angle arithmetic mean values for *Prądnik spalls* (n = 21). The edge angles are calculated with the »2-lines« measurement procedure.

section	distance to origin [in degrees]			mean per section (2-5)	mean per section (all)
	2 mm	5 mm	10 mm		
1	74.4	42.4	18.7	45.2	44.4
2	71.7	53.7	22.9	49.4	51.0
3	74.9	52.2	36.8	54.6	54.0
4	78.5	51.8	36.5	55.6	54.9
5	83.3	55.7	43.7	60.9	59.2
6	81.3	58.8	41.5	60.5	60.3
7	76.5	59.5	32.9	56.3	57.1
8	78.2	57.5	30.1	55.3	54.1
9	75.6	52.2	25.8	51.2	51.3
10	83.1	56.4	14.5	51.3	49.0

Table 27 Edge angle arithmetic mean values for scrapers (n = 9). The edge angles are calculated with the »2-lines« measurement procedure.

section	distance to origin [in degrees]			mean per section (2-5)	mean per section (all)
	2 mm	5 mm	10 mm		
1	54.3	30.3	24.8	36.5	39.5
2	59.6	39.7	35.5	44.9	43.3
3	69.4	48.2	39.2	52.3	53.0
4	49.9	47.3	33.9	43.7	46.2
5	55.6	44.2	40.2	46.7	46.8
6	58.3	48.7	43.3	50.1	50.7
7	60.7	42.0	44.2	49.0	48.8
8	58.3	50.6	42.8	50.6	52.5
9	78.4	52.7	51.0	60.7	59.1
10	99.9	109.9	61.5	90.4	91.3

Table 28 Edge angle arithmetic mean values for flakes (n = 2). The edge angles are calculated with the »2-lines« measurement procedure.

The flakes, also belonging to the selected outgroup, range at a distance of 2 mm to the intersection from 59.3° to 78.4° (**tab. 28**). The values displayed at the 5 mm distance are 39.7° and 52.7°. At the 10 mm distance, the measurements are 35.5° and 51.0°. For the three mentioned distances, the arithmetic means are 61.3°, 46.7° and 41.3°.

Table 29 Edge angle arithmetic mean values for *Keilmesser* (n = 57). The edge angles are calculated with the »Best-fit« measurement procedure.

section	distance to origin [in degrees]			mean per section (2-5)	mean per section (all)
	2 mm	5 mm	10 mm		
1	76.0	55.1	38.4	56.5	56.6
2	73.4	54.6	27.8	51.9	51.7
3	71.7	59.3	45.6	58.9	58.8
4	72.7	58.5	47.3	59.5	59.5
5	73.7	61.5	47.4	60.9	61.6
6	77.5	59.0	45.9	60.8	59.8
7	73.9	63.3	44.1	60.4	60.0
8	80.2	59.6	41.0	60.3	61.3
9	78.4	62.6	46.8	62.6	63.4
10	84.2	66.3	47.4	66.0	65.2

Table 30 Edge angle arithmetic mean values for *Keilmesser* modified by the *Prądnik method* (n = 100). The edge angles are calculated with the »Best-fit« measurement procedure.

section	distance to origin [in degrees]			mean per section (2-5)	mean per section (all)
	2 mm	5 mm	10 mm		
1	63.4	50.0	30.8	48.1	49.5
2	66.4	54.9	35.2	52.2	53.0
3	66.3	51.2	37.1	51.5	52.3
4	67.6	56.0	44.5	56.0	56.9
5	69.4	63.2	48.6	60.4	59.9
6	71.4	57.9	50.5	59.9	59.4
7	74.4	59.0	44.0	59.1	59.9
8	71.9	59.0	45.3	58.7	59.2
9	74.3	59.9	43.7	59.3	58.3
10	82.8	59.6	43.7	62.0	60.8

»Best-fit« procedure

Lastly, the results from the »best-fit« measurement procedure will be presented. These results are similar to the ones from the »2-lines« measurements. Since the two procedures are almost identical, except that the »best-fit« procedure interpolates the points between the 2 mm line, the similarity between the results is not surprising.

The measurements for the *Keilmesser* display a range from 73.4° to 78.4° at the 2 mm distance to the intersection (**tab. 29**). At 5 mm distance, the values range from 54.6° to 62.6°. The measurements for the 10 mm distance are 27.8° and 46.8°. The arithmetic means for these three distances are 75.2°, 59.8° and 43.2°.

Keilmesser with a negative from the application of the *Prądnik method* result again in lower edge angle values than the *Keilmesser* without modification (**tab. 30**). At a distance of 2 mm from the intersection, the measurements are ranging from 66.4° to 74.3°, with an arithmetic mean value of 70.2°. The range for the 5 mm distance is from 54.9° to 59.9°. The arithmetic mean is 57.6°. At the 10 mm distance, the measurements are 35.2° and 43.7° and the arithmetic mean is 43.6°. Also, in this case, the arithmetic mean value at the 10 mm distance is similar to the one from the *Keilmesser* without modification while the mean values at 2 mm and 5 mm are lower.

The calculated edge angles for the *Keilmesser* tips result in measurements of 63.8° and 71.1° at 2 mm distance (**tab. 31**). At a distance of 5 mm, the values are 50.4° and 62.5°. The range for the 10 mm distance is 42.5° to 41.7°. The arithmetic mean values amount to 66.7°, 58.6° and 40.3°.

section	distance to origin [in degrees]			mean per section (2-5)	mean per section (all)
	2 mm	5 mm	10 mm		
1	64.8	47.5	41.1	51.1	49.5
2	63.8	50.4	42.5	52.2	53.0
3	63.6	58.3	43.3	55.1	52.3
4	68.8	54.5	39.6	54.3	56.9
5	64.5	60.1	31.8	52.1	59.9
6	67.8	57.9	50.4	58.7	59.4
7	64.2	65.2	31.6	53.7	59.9
8	69.7	59.6	41.7	57.0	59.2
9	71.1	62.5	41.7	58.4	58.3
10	60.8	48.0	35.1	48.0	60.8

Table 31 Edge angle arithmetic mean values for *Keilmesser* tips (n = 18). The edge angles are calculated with the »Best-fit« measurement procedure.

section	distance to origin [in degrees]			mean per section (2-5)	mean per section (all)
	2 mm	5 mm	10 mm		
1	41.0	27.6	30.0	32.9	37.3
2	42.6	34.0	19.9	32.2	33.7
3	44.0	37.5	22.1	34.5	37.1
4	50.3	46.1	27.1	41.2	42.1
5	58.5	40.6	30.2	43.1	43.4
6	57.7	36.4	24.8	39.6	38.5
7	61.0	37.5	29.2	42.6	43.9
8	61.3	45.5	30.0	45.6	43.2
9	65.5	51.7	19.4	45.5	43.7
10	66.3	47.3	74.6	62.7	50.2

Table 32 Edge angle arithmetic mean values for *Prądnik scrapers* (n = 20). The edge angles are calculated with the »Best-fit« measurement procedure.

section	distance to origin [in degrees]			mean per section (2-5)	mean per section (all)
	2 mm	5 mm	10 mm		
1	37.0	19.3	23.9	26.7	34.0
2	46.0	21.9	33.3	33.7	36.6
3	43.4	20.6	23.7	29.2	31.0
4	53.5	27.5	34.0	38.3	38.7
5	43.6	18.8	27.3	29.9	32.0
6	54.0	33.6	32.0	39.9	36.6
7	47.7	19.8	24.4	30.6	33.0
8	55.1	27.3	15.6	32.7	35.0
9	54.9	15.4	25.2	31.8	33.8
10	47.4	21.0	38.3	35.6	28.0

Table 33 Edge angle arithmetic mean values for *Prądnik spalls* (n = 21). The edge angles are calculated with the »Best-fit« measurement procedure.

For the *Prądnik scrapers*, the following results were calculated with the »best-fit« measuring procedure (**tab. 32**). At the 2 mm distance to the intersection, the values are 42.6° and 65.0° with an arithmetic mean of 55.1°. The measurements at 5 mm range from 34.0° to 51.7°. The mean value is 41.2°. At the 10 mm distance, the measurements are 19.9° and 19.4° and the arithmetic mean is 25.3°.

Table 34 Edge angle arithmetic mean values for scrapers (n = 9). The edge angles are calculated with the »Best-fit« measurement procedure.

section	distance to origin [in degrees]			mean per section (2-5)	mean per section (all)
	2 mm	5 mm	10 mm		
1	72.7	41.3	34.2	49.4	46.6
2	71.1	67.8	23.1	54.0	53.6
3	74.7	50.8	53.9	59.8	55.4
4	77.7	51.6	35.9	55.1	54.9
5	82.9	55.9	45.0	61.3	59.3
6	81.8	58.0	41.3	60.4	61.6
7	76.7	60.8	32.2	56.6	57.1
8	77.6	58.4	30.5	55.5	55.7
9	74.9	52.1	43.8	56.9	54.6
10	82.6	56.5	14.3	51.1	49.3

Table 35 Edge angle arithmetic mean values for flakes (n = 2). The edge angles are calculated with the »Best-fit« measurement procedure.

section	distance to origin [in degrees]			mean per section (2-5)	mean per section (all)
	2 mm	5 mm	10 mm		
1	54.5	33.2	25.4	37.7	39.6
2	60.5	40.7	35.9	45.7	43.2
3	71.3	48.7	39.4	53.1	53.1
4	48.9	48.0	33.6	43.5	46.8
5	53.7	44.5	41.1	46.4	46.8
6	56.1	48.7	45.6	50.1	50.7
7	61.3	40.7	43.3	48.4	48.9
8	55.7	50.2	43.0	49.6	52.5
9	77.2	53.5	52.3	61.0	59.2
10	96.0	109.1	60.7	88.6	91.8

The analysed *Prądnik spalls* display at the 2 mm distance a range of 46.0° to 54.9° (**tab. 33**). At the 5 mm distance, the values range from 21.9° to 15.4°. The measurements at the 10 mm distance are 33.3° and 25.2°. The calculated arithmetic mean values of these three distances are 49.8°, 23.1° and 26.9°.
The scrapers, representing one artefact category of the sampled outgroup, display at the 2 mm distance measurements of 71.1° and 74.9° with an arithmetic mean value of 77.2 (**tab. 34**). The range for the 5 mm distance is from 67.8° to 52.1°. The arithmetic mean is 56.9°. At the 10 mm distance, the measurements are 23.1° and 43.8° and the arithmetic mean is 38.2°.
The measurements for the flakes result in a range of 60.5° to 77.2° at the 2 mm distance from the intersection (**tab. 35**). For the measurements at the 5 mm distance, the values are 40.7° and 53.5°. At 10 mm distance to the intersection, the values ranging from 35.9° to 52.3°. The edge angle measurements result in arithmetic mean values of 60.6°, 46.9° and 41.8° per mentioned distance.

Edge angle analysis

When taking all the data concerning the edge angle analysis into account, the differences in the results from the three measurement procedures are primarily noticeable. The differences between the »2-lines« and the »best-fit« procedures are comparable small. The measurements at 2 mm and 5 mm distance from the inter-

section display a variance of 0.2° up to 3.6°. Only at the 10 mm distance, a difference of 8.1° is noticeable between the results of the »2-lines' and the »best-fit« measurement procedures. The variance between these results and the results of the »3-point« measurement procedure is significantly higher. However, the results reflect the same tendencies and are not randomly different. Instead, the results calculated with the »3-point« procedure are always around 10° to 20° higher. Beforehand conducted, controlled tests with an artefact, an experimental flake and a calibrated standard angle (gauge block; edge angle known) led to the exact same conclusion. These tests were done in order to validate the reliability of the method. The results of the three measurement procedures reflect the same tendencies and patterns although the calculated edge angles with the »3-point« procedure are always higher. As mentioned earlier, it seems like the »3-point« measurement is leading to reliable results when edge angles of simple objects are measured. As soon as the object is more complex and does not have plain surfaces, the »2-lines« and the »best-fit« procedures seem to lead to more precise data.

Another striking aspect regarding the data are the different results calculated for the three presented distances to the intersection. In general, the variance between the distances is for all artefact categories higher that the variance along the edge. When considering all artefact categories, especially the distance at 2 mm stands out. This is not entirely unexpected. Two aspects are relevant when interpreting the data. The first one is the resolution of the 3D model. The data can only be as good as the resolution of 3D model. In particular, the acute edges of the artefacts are often difficult to document with a 3D scanner. When zooming extremely into a 3D model, the edges of the models always appear curved instead of sharp. Therefore, the results calculated for the first probably 1 to 3 mm should likely be higher than the edge angle values calculated for the following distances. The second aspect is the human factor. Although the method is predominantly script- and algorithm-based, some steps need to be done manually. One of these steps is the digitalisation of the edge by defining a vertical polyline. Placing this polyline in the correct position is complicated when the edge of the scanned artefact is curved. Thus, it can happen that the line was placed for instance 1 mm too far towards one tool surface. As a result, the edge angle value will be higher than it would be in reality. To summarize, the measurements taken really close to the edge are likely to be affected by at least one of the described issues. This should be reflected by higher edge angle values at the first few distances from the intersection.

After highlighting some general aspects, aspects concerning specific artefact categories are discussed in the following. First of all, it has to be mentioned that not only the edge angles for the active edge were calculated. *Per* tool, two edges (E1 and E2) have been digitalised. In the case of *Keilmesser* often even three edges (E3). The distinction between a back and an active edge is mostly simple. *Keilmesser* in particular often have such a pronounced and thick back, that the back can only be defined by two edges. Nevertheless, the idea was to calculate the edge angles from all existing edges *per* artefact in order to be as objective as possible. The results of this second and/or third edge per tool can be found on GitHub [https://github.com/lschunk/edge_angle_analysis]. The graphic representation of the measured edge angles for each artefact also includes all edges. Since the focus, when presenting the data, was only on the active edge, the results for the *Keilmesser* edges representing the back will be addressed here only briefly. In general, there is no recognisable trend that shows the edge angle values change along the edge. There is a variance along the edge, but the values do not increase towards the proximal part of the tool. The edge angle values along the edge as well as the ones from the different distances seem to be slightly higher compared to the values from the *Keilmesser* active edge. Although edge angle values around 70° were calculated, also values above 100° were documented.

The second topic refers to the artefact morphology. The tool morphology seems to be reflected in the data. Tools including *Keilmesser* and *Prądnik scrapers* but also scrapers have deviating edge angle values at 5 mm

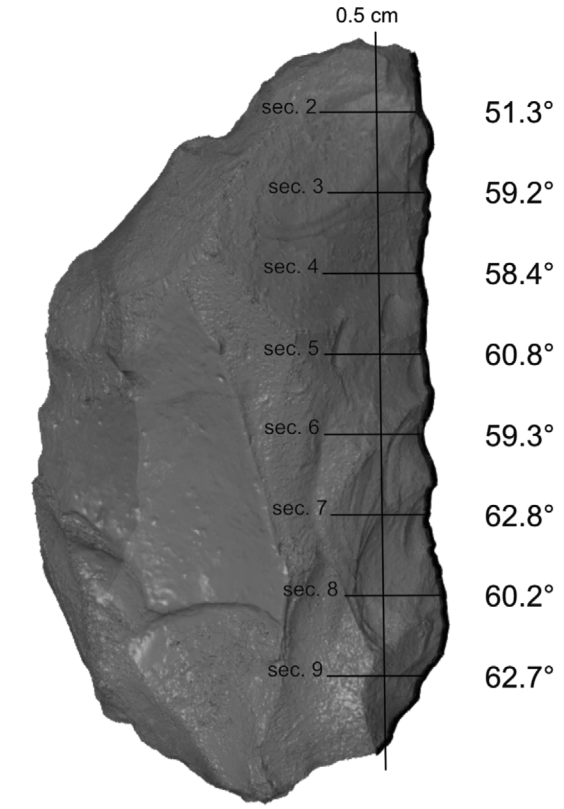

Fig. 96 Edge angle variability at 0.5 cm distance from the intersection for all measured *Keilmesser* (n = 57) without *Prądnik method* modification. The edge angle values display mean values calculated with the »2-lines« procedure. The 0.5 cm vertical line is only schematic. Normally, this line follows the shape of the digitalised active edge.

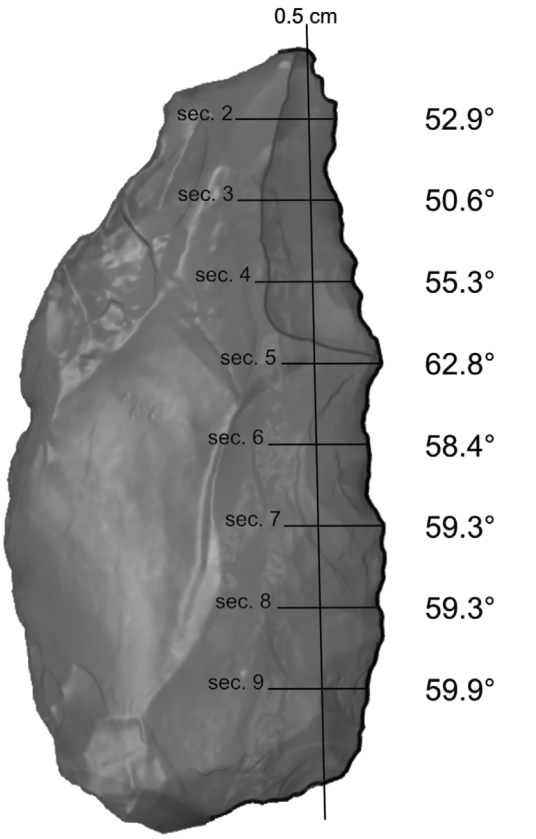

Fig. 97 Edge angle variability at 0.5 cm distance from the intersection for all measured *Keilmesser* (n = 100) with *Prądnik method* modification. The edge angle values display mean values calculated with the »2-lines« procedure. The 0.5 cm vertical line is only schematic. Normally, this line follows the shape of the digitalised active edge.

and 10 mm distance, while *Prądnik spalls* and flakes display no remarkable differences between the measurements. Since bifacially worked tools or especially *Keilmesser* and *Prądnik scrapers* do not necessarily have flat surfaces, the curvature of the surface will be reflected by changing edge angle values with increasing distance to the intersection. The *Prądnik spalls* and flakes do not reflect this change between the measurements at 5 mm and 10 mm distance.

Another aspect is the edge angle variability along the edge of *Keilmesser* (**figs 96. 98**). The data calculated for the *Keilmesser* (with and without modification) illustrates a change in the edge angle from the distal to the proximal part of the *Keilmesser* around approximately 10°. According to the data, the edge is on average more acute in the distal part of the tool than in the proximal area. The same is documented for the *Prądnik scrapers*.

Additionally, the *Keilmesser* with a modification through the *Prądnik method* do display a lower, sharper edge angle in the distal tool area than *Keilmesser* without the modification (**fig. 97**). This difference is only small and does not exceed 10°.

Prądnik scrapers do have more acute edge angles than *Keilmesser* (**fig. 99**). The calculated edge angles for the *Prądnik scraper* are on average 20° lower.

The *Prądnik spalls*, when excluding the measurements at the 2 mm distance to the intersection for the mentioned reasons, display significantly lower edge angles values compared to the tools (**fig. 100**). The values range

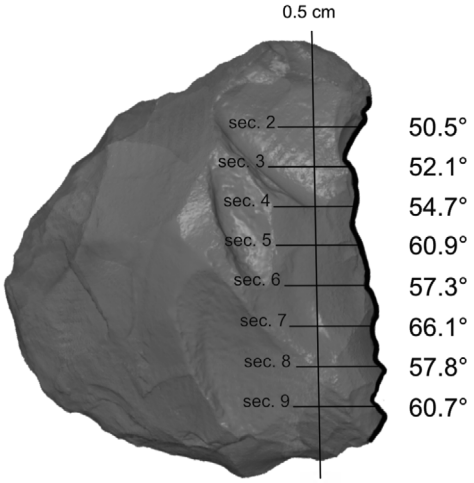

Fig. 98 Edge angle variability at 0.5 cm distance from the intersection for all measured *Keilmesser* tips (n = 18). The edge angle values display mean values calculated with the »2-lines« procedure. The 0.5 cm vertical line is only schematic. Normally, this line follows the shape of the digitalised active edge.

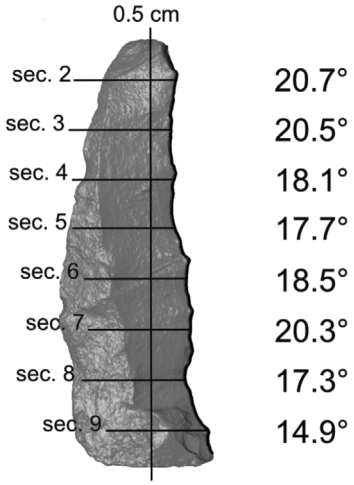

Fig. 100 Edge angle variability at 0.5 cm distance from the intersection for all measured *Prądnik spalls* (n = 21). The edge angle values display mean values calculated with the »2-lines« procedure. The 0.5 cm vertical line is only schematic. Normally, this line follows the shape of the digitalised active edge.

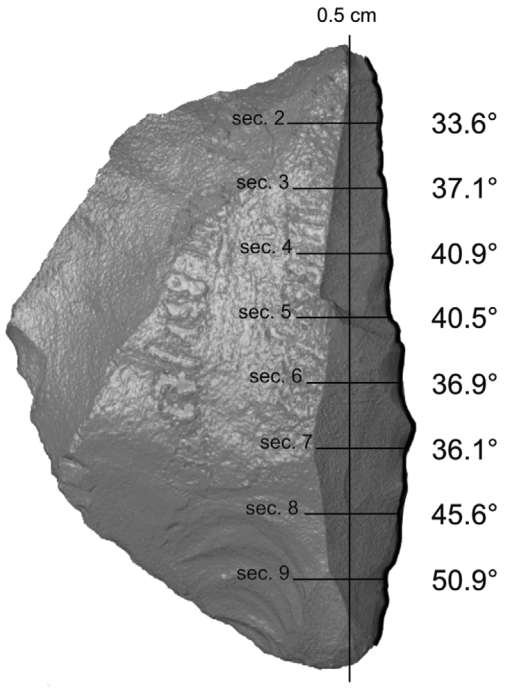

Fig. 99 Edge angle variability at 0.5 cm distance from the intersection for all measured *Prądnik scrapers* (n = 20). The edge angle values display mean values calculated with the »2-lines« procedure. The 0.5 cm vertical line is only schematic. Normally, this line follows the shape of the digitalised active edge.

between 20° and 25°. Additionally, the edge angle values for the *Prądnik spalls* display in general only a small variance (~ 5°) and are in comparison more constant along the edge and towards the surface.

The last aspect to address is the result from the outgroup. A small quantity of scrapers (**fig. 101**) and flakes (**fig. 102**) were included in the edge angle measurements in order to have a possibility to put the results from the *Keilmesser* and *Prądnik scraper* in context. The variability along the edge with the tendency of an increasing edge angle towards the proximal part of the tool as noticed for the *Keilmesser* and *Prądnik scraper* cannot be documented for the scrapers and flakes. Moreover, the edge angle values are in general lower. In particular, the flakes with edge angle values between 30° and 40° have more acute edges than *Keilmesser*. However, these values are similar to the measurements from the *Prądnik scrapers*.

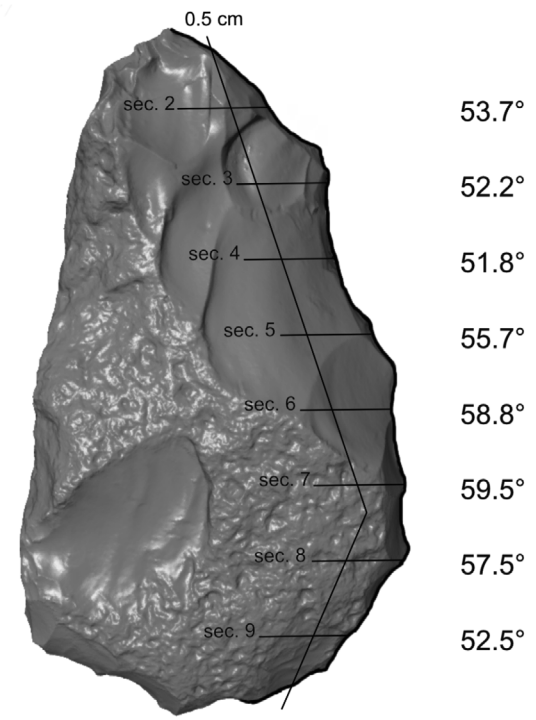

Fig. 101 Edge angle variability at 0.5 cm distance from the intersection for all measured scraper (n = 9). The edge angle values display mean values calculated with the »2-lines« procedure. The 0.5 cm vertical line is only schematic. Normally, this line follows the shape of the digitalised active edge.

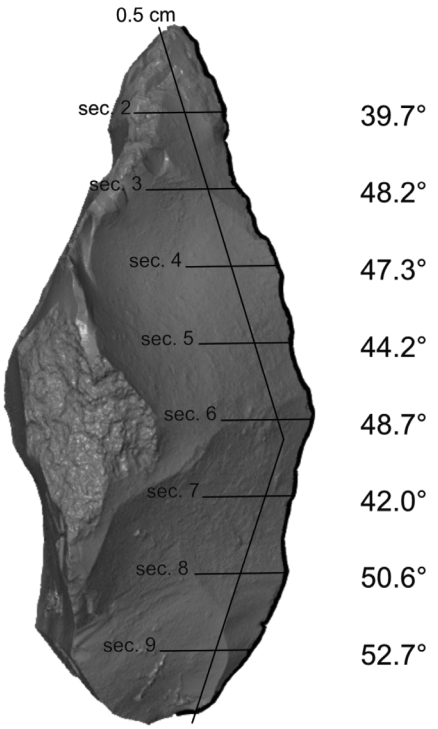

Fig. 102 Edge angle variability at 0.5 cm distance from the intersection for all measured flakes (n = 2). The edge angle values display mean values calculated with the »2-lines« procedure. The 0.5 cm vertical line is only schematic. Normally, this line follows the shape of the digitalised active edge.

USE-WEAR ANALYSIS

This subchapter addresses the results of the conducted use-wear analysis. First, the results of the qualitative assessment are presented. This includes the location, the orientation and the description of the use-were traces. Subsequently, the results of the quantitative use-wear are addressed.

Qualitative use-wear analysis

Use-wear analysis is a time-consuming approach. For that reason, a sub-sampling of the assemblage under study was needed. The sampling was done during the techno-typological analysis. The base for the sampling was thereby the research question. Since the research question focusses on specific tools – *Keilmesser* and *Prądnik scrapers* – these tools were predominantly selected. Also relevant in order to address the research question are the *Prądnik spalls*, which have been removed from the *Keilmesser* and *Prądnik scrapers* at a certain stage within the use-life history of the tools. In order to be able to put the results in relation with other artefact categories afterwards, some other tools were additionally sampled. A small number of scrapers and flakes was selected as outgroup. Only complete and well-preserved artefacts from the three archaeological assemblages were chosen for the use-wear analysis and all *Keilmesser* shapes were selected.

sites	use-wear	artefact category						
		Keilmesser	*Keilmesser* tip	*Prądnik* scraper	*Prądnik* spall	scraper	flake	total
Buhlen	with traces [n]	34 (33.6 %)	7 (6.9 %)	12 (11.9 %)	11 (10.9 %)	1 (1.0 %)	0 (0.0 %)	65 (64.3 %)
	without traces [n]	24 (23.8 %)	1 (1.0 %)	3 (3.0 %)	7 (6.9 %)	1 (1.0 %)	0 (0.0 %)	36 (35.7 %)
Balve	with traces [n]	40 (50.6 %)	2 (2.5 %)	2 (2.5 %)	16 (20.3 %)	8 (10.1 %)	0 (0.0 %)	68 (86.1 %)
	without traces [n]	2 (2.5 %)	0 (0.0 %)	3 (3.8 %)	5 (6.3 %)	1 (1.3 %)	0 (0.0 %)	16 (13.9 %)
Ramioul	with traces [n]	8 (40.0 %)	0 (0.0 %)	3 (15.0 %)	0 (0.0 %)	5 (25.0 %)	1 (5.0 %)	17 (85.0 %)
	without traces [n]	1 (5.0 %)	0 (0.0 %)	0 (0.0 %)	0 (0.0 %)	1 (5.0 %)	1 (5.0 %)	3 (15.0 %)
total	with traces [n]	82 (41.0 %)	9 (4.5 %)	17 (8.5 %)	27 (13.5 %)	14 (7.0 %)	1 (0.5 %)	150 (75.0 %)
	without traces [n]	27 (13.5 %)	1 (0.5 %)	6 (3.0 %)	12 (6.0 %)	3 (1.5 %)	1 (0.5 %)	50 (25.0 %)

Table 36 Numbers of artefacts per site and artefact category studied with a qualitative use-wear analysis. The percentages in brackets relate to the number of artefacts per assemblage.

Having this as a prerequisite, with n = 200 artefacts, more than one third of the entire assemblage was sampled for the qualitative use-wear analysis (**tab. 9**). These n = 200 sampled artefacts divide in n = 119 *Keilmesser*, whereas n = 10 of these are *Keilmesser* tips, n = 23 *Prądnik scrapers* as well as n = 39 *Prądnik spalls*. This means, more than one third (36.1 %) of the entire *Keilmesser* assemblage was part of the qualitative use-wear analysis, while nearly half of the *Prądnik scrapers* (42.6 %) have been studied. *Prądnik spalls* were less frequently involved in this analysis with 24.5 %. less frequently. The outgroup consist of n = 17 scrapers and n = 2 flakes. The n = 200 artefacts are not sampled equally from the three archaeological sites. Since the assemblage from Ramioul is comparatively small, the entire n = 20 samples were included for the qualitative use-wear analysis. The macroscopic preservation (e. g. no edge damage) in Buhlen seemed better than the one in Balve. Therefore, more artefacts from Buhlen were sampled. Thus, the sampled artefacts are to 50.5 % (n = 101) from Buhlen, to 39.5 % (n = 79) from Balve and to 10.0 % from Ramioul.

The samples were studied with an upright light microscope (ZEISS Axio Scope.A1 MAT) under a 5×, 10× and 20× magnification. By doing so, traces could be found on n = 150 pieces out of the sampled n = 200 artefacts (**tab. 36**). Although Buhlen was samples most numerously, the artefacts from Buhlen displayed the fewest use-wear traces. On only n = 65 artefacts traces could be documented. The preservation for the material from Balve was estimated as poorer and therefore less suitable for a use-wear analysis. Surprisingly, n = 68 out of n = 79 selected pieces displayed use-wear traces. The complete studied assemblage from Ramioul (n = 20) was selected for the use-wear analysis. The material from Ramioul appeared as less well preserved. Most of the edges and higher micro topographical areas seemed rounded and affected. Moreover, the light coloured, almost white flint made the detection of use-wear traces more complicated. Nevertheless, on n = 17 artefacts traces could be documented.

The tool areas displaying use-wear traces were documented as EDF stitching images with a digital microscope (ZEISS Smartzoom 5) by using a 1.6× objective and 34-× zoom. All use-wear traces are illustrated as figures in the supplementary material.

Analysis use-wear traces and spatial pattern recognition

During the performance of the qualitative use-wear analysis, all traces were documented in the beforehand described scheme (see chapter Qualitative use-wear analysis; **fig. 26**). Hence, not only the location of each trace on the artefacts was recorded, but also, if possible, the type (polish, striation or impact marks) and the orientation (perpendicular, parallel or oblique to the edge). After performing the qualitative use-wear, all documented traces of the n = 150 artefacts with use-wear were sorted and visually categorised (**appendix I**). Important criteria for the categorisation were the appearance of the traces, their extension, their orientation as well as the abrasiveness on the surface. In this way, nine types of traces were defined (described below).

The different types were named in a simple way by giving, as soon as a category was defined, a letter as a name, starting with the letter »A«. When two categories were nearly identical, but for instance, only the orientation of the striations was different, the addition »2« was given. In three cases, no clear category could be given. These traces appeared like a combination out of two already defined categories. Therefore, next to the seven categories, also »C/E«, »C/D« and »C/A« exist.

Afterwards, a reordering of these types was done in order to make the descriptions more comprehensible and the order more logical. However, the former names of the categories are additionally given since these names also appear in the plots. A description of the traces is given in the following (**fig. 103**; **tab. 37**).

I. The first category is characterised by small polished spots. These spots appear as bright, intact circles. The polish is only slightly abrasive and affects only the highest micro topography. An orientation is indeterminable. [A]
II. The second category is also a polish. This time the polish is not limited to a spot, instead it is extended to a small area. Again, only the highest topographical locations are affected. The abraded, polished areas appear bright and slightly scattered. The polish can be parallel or perpendicular to the tool edge or without clear orientation. [B]
III. The third type of polish is in its appearance identical to the second category (II/B), but the distribution is more extensive. The polished areas occur most often parallel to the tool edge. [B2]
IV. The fourth category is another type of polish. The polish is smooth and distinctly more compact. In terms of the extension, the polish is comparable with the second category (II/B) and only appears in small, sometimes elongated areas. Despite the compact appearance, the polish can be found only on the highest topographical locations. This polish has either no orientation or is parallel to the edge orientated. [E]
V. The fifth category is again a polish. The polish is extensive and continual and appears as bright and shiny. Not only the highest topographical locations are abraded, but also lower topography. The orientation is most often indeterminable or otherwise parallel to the edges. [C]
VI. Category six combines a smooth polish with randomly orientated striations. The traces are not selected, instead they are extended over small areas. The polish is abrasive, affects all topographical locations, the highest and the lowest topography. The striations do not reach deeper than the polish. In the majority, the traces do not have an orientation. [D]
VII. The seventh category is identical to the category described before (VI/D). The only difference can be found in the orientation. The striations are not randomly orientated, they are orientated towards one direction. Since the striations do have an orientation, it was also possible to define the orientation of the traces in general. Most often, the traces are orientated perpendicular to the tool edges. [D2]
VIII. The eighth category can be described by orientated striations, which are not extensive and limited in their dimensions. The linear scratches affect the lowest as well as the highest topographical locations. These traces can be either parallel, perpendicular or oblique towards the edges. [F]

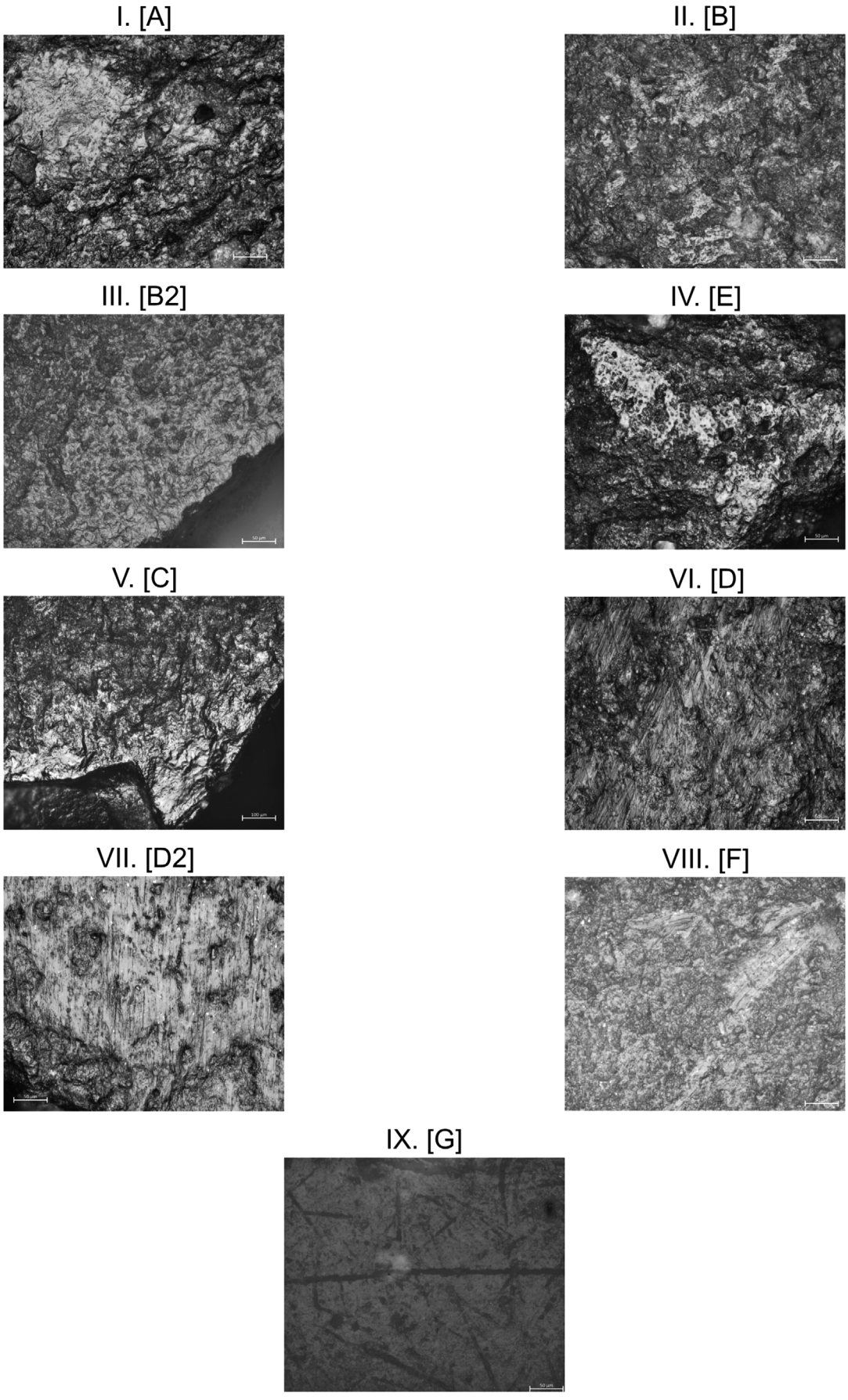

Fig. 103 Documented qualitative use-wear types (all images are taken with a 20× optical objective).

type	main features	description	topographical location
I. [A]	polish	small & bright polished circle	highest micro topography
II. [B]	polish	small & bright area of polish	highest micro topography
III. [B2]	polish	extended area of polish	highest micro topography
IV. [E]	polish	small areas of smooth & compact polish	highest micro topography
V. [C]	polish	extensive & continues and bright & shiny polish	lowest and highest micro topography
VI. [D]	polish & striation	smooth polish with randomly orientated striations; small area	lowest and highest micro topography
VII. [D2]	polish & striation	smooth polish with orientated striations; small area	lowest and highest micro topography
VIII. [F]	striation	small & orientated striations	lowest and highest micro topography
IX. [G]	polish, furrows & groves	dull & abrasive polish, deep furrows and groves	lowest and highest micro topography

Table 37 Description of the documented use-wear traces including their topographical location.

IX. The ninth and thus the last category displays a dull and abrasive polish. The polish is additionally combined with shallow or deep furrows and groves. The linear striations are randomly orientated and sometimes reach deeper than the polish. These traces are extensive and cover big areas of the surface while affecting all topographical locations, causing a surface deformation. The orientation is indeterminable. The category can be found close to the edge, but also extending towards the surface. [G]

Although the studied silicified schist samples clearly outnumber the flint samples, the mentioned use-wear types were documented on silicified schist as well as on flint samples. The categories do not differ depending on the raw material. However, one type was only documented on silicified schist, not on flint. This is type II. (B). However, type III. (B2) was documented and only differs concerning the extension of the trace.
In qualitative use-wear analysis, the first step is the recognition and the characterisation of use-wear types on the analysed artefacts. The aim of a use-wear analysis is to identify the observed traces in order to gain a functional interpretation of the different tools. In a qualitative use-wear analysis, this is solely based on visual identifications and characterisation. It is known that not only the worked material (Keeley 1980; Haslam 2009; Rots 2013), but also the raw material, the use intensity and the performed task haven an impact on the formation of the use-wear traces (Buc 2011; Marreiros et al. 2020). Without a widespread and highly reliable reference collection, the aim of a functional interpretation of the observed use-wear traces can barely be observed. For silicified schist, there is no such reference collection existing yet. Thus, the aspiration of identifying the use-wear traces based on a qualitative use-wear analysis will not be fulfilled within this project.
Despite this, one single interpretation regarding the described use-wear categories will be made. The interpretation refers to the ninth category (IX/G). The described features of the traces are distinctly different from the other categories. These features do not look like use-wear traces, instead, they will be interpreted as post-depositional traces.
After analysing the artefacts, observing, categorising and describing the traces, the location of these traces was transformed from the manually filled scheme into a geographical information system (QGIS, version 3.14.16). Each use-wear trace was illustrated by a coloured point. The points were coloured according to the use-wear type categorisation.

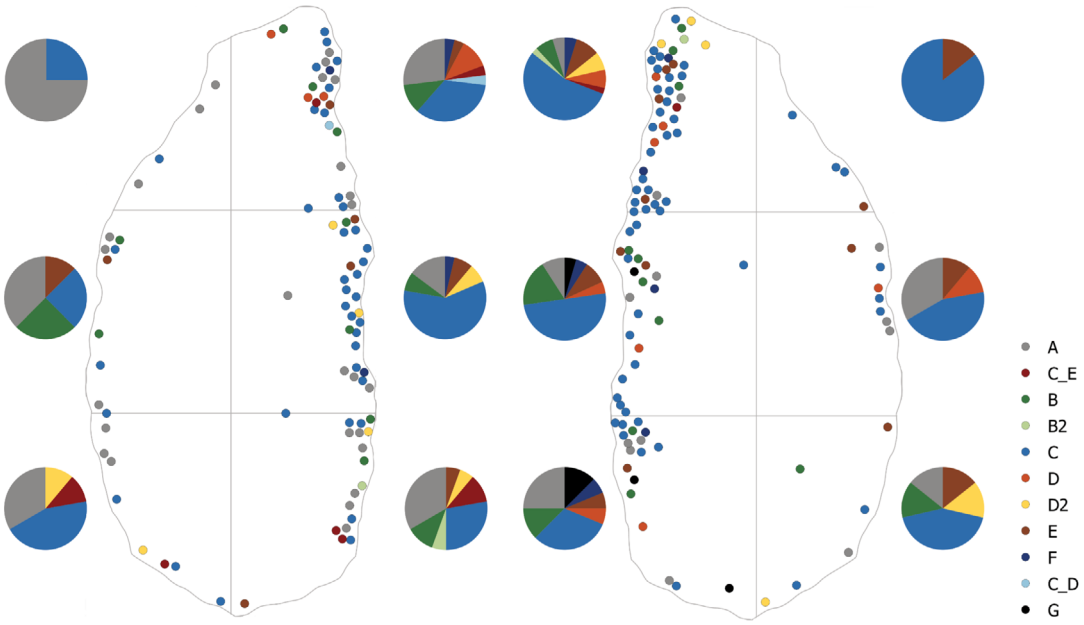

Fig. 104 Distribution of all the use-wear traces documented on *Keilmesser*. The left side illustrates the dorsal surfaces of the tool, the right side the ventral tool surface. The colours indicate the use-wear types.

The results of this graphical representation are presented in the following organised by artefact categories. Before doing so, one issue needs to be explained. Per tool category, one outline was used in order to locate the use-wear traces. These outlines were divided into areas, whereas A and B always displayed the dorsal and D and C the ventral surface of the tool. The orientation of these areas changed when looking at a left sided instead of a right sided tool. Since the specific lateralisation of the artefacts had no priority in the context of the location of the use-wear traces, all use-wear traces from left sided artefacts were transferred to the right sided scheme in order to fit a uniform scheme.

For *Keilmesser*, all described nine use-wear categories were documented (**fig. 104**). Surface modifications in the sense of use-wear or post-depositional traces could be documented on in total n = 195 locations (**tab. 38**). Although the surfaces of the tools were checked entirely, most of the use-wear traces can be found along the active edge. This counts for 77.4 % (n = 151) of the traces. The ventral surface shows thereby slightly more traces (n = 80) than the dorsal surface (n = 71). The traces are of all documented

artefact category	use-wear type [n]											
	I. (A)	II. (B)	III. (B2)	IV. (E)	V. (C)	VI. (D)	VII. (D2)	VIII. (F)	IX. (G)	V./ IV.	V./ VI.	total
Keilmesser	38	19	2	15	89	9	8	6	3	5	1	**195**
Prądnik scraper	9	0	0	0	19	0	1	0	3	1	0	**33**
Prądnik spall	7	4	0	0	33	2	0	2	0	5	0	**53**
scraper	4	3	1	5	18	0	2	2	4	1	0	**40**
total	**58**	**26**	**3**	**20**	**159**	**11**	**11**	**10**	**10**	**12**	**1**	321

Table 38 Number of documented use-wear traces on artefacts from Buhlen, Balver Höhle and Ramioul per use-wear type and artefact category.

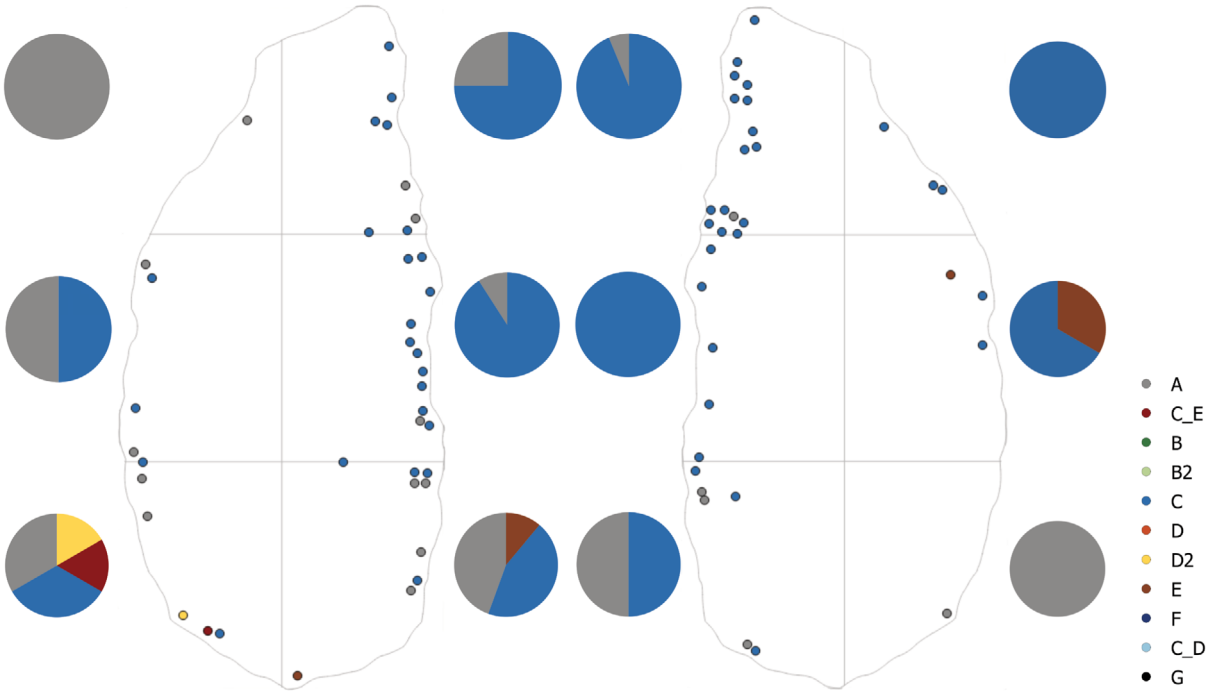

Fig. 105 Distribution of all the use-wear traces documented on *Keilmesser* from Buhlen. The left side illustrates the dorsal surfaces of the tool, the right side the ventral tool surface. The colours indicate the use-wear types.

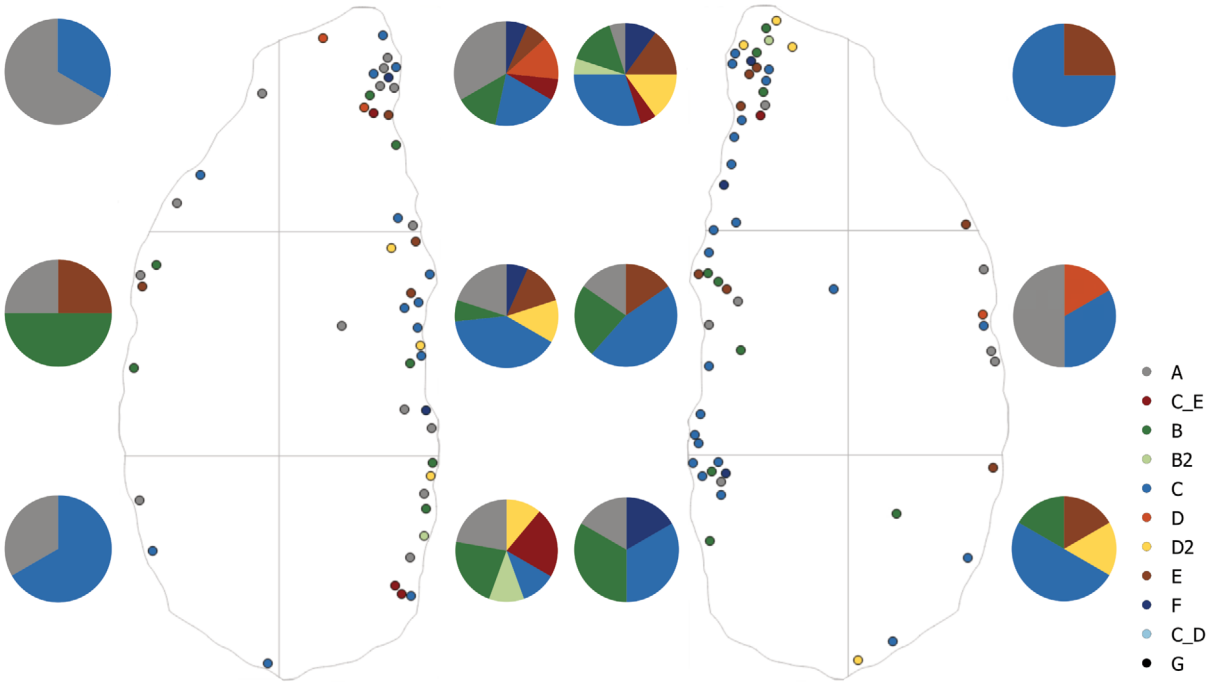

Fig. 106 Distribution of all the use-wear traces documented on *Keilmesser* from Balver Höhle. The left side illustrates the dorsal surfaces of the tool, the right side the ventral tool surface. The colours indicate the use-wear types.

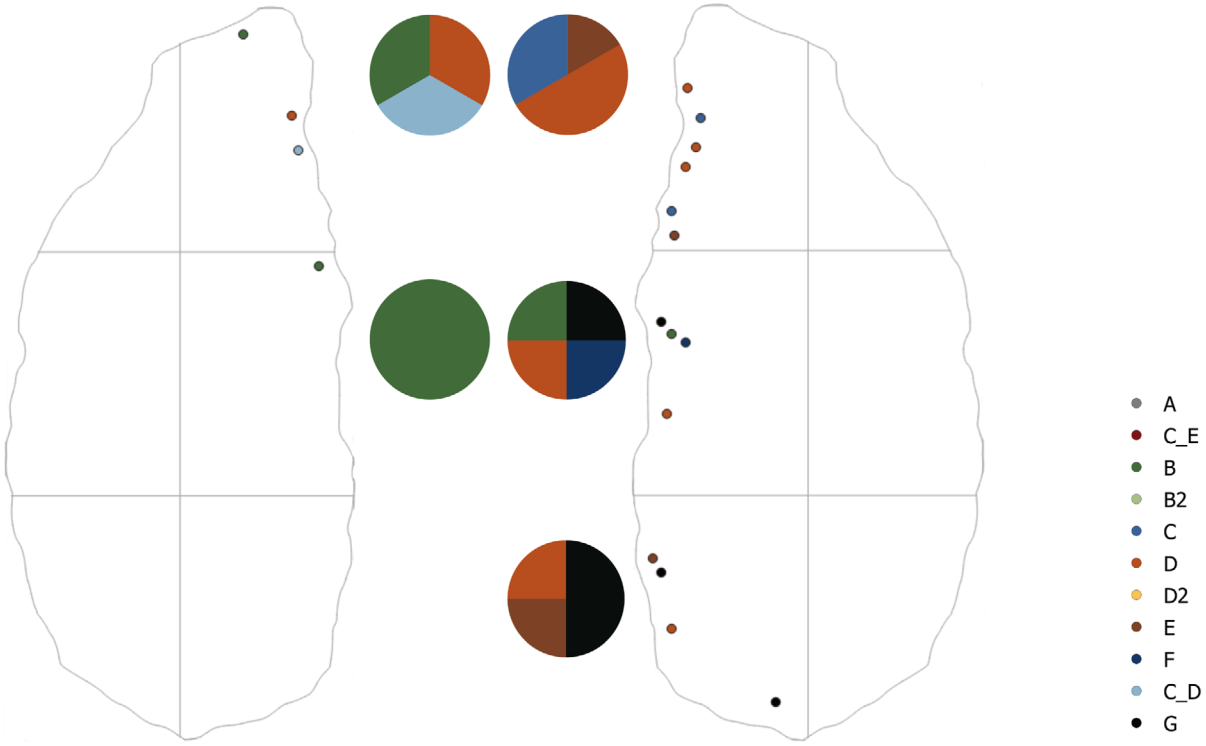

Fig. 107 Distribution of all the use-wear traces documented on *Keilmesser from Ramioul*. The left side illustrates the dorsal surfaces of the tool, the right side the ventral tool surface. The colours indicate the use-wear types

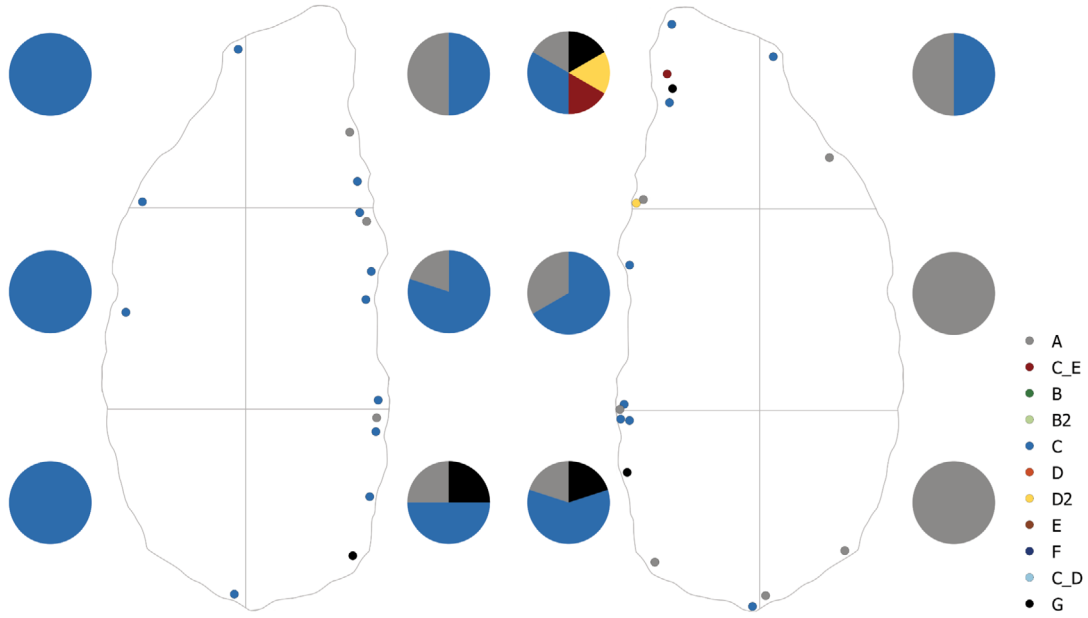

Fig. 108 Distribution of all the use-wear traces documented on *Prądnik scrapers*. The left side illustrates the dorsal surfaces of the tool, the right side the ventral tool surface. The colours indicate the use-wear types.

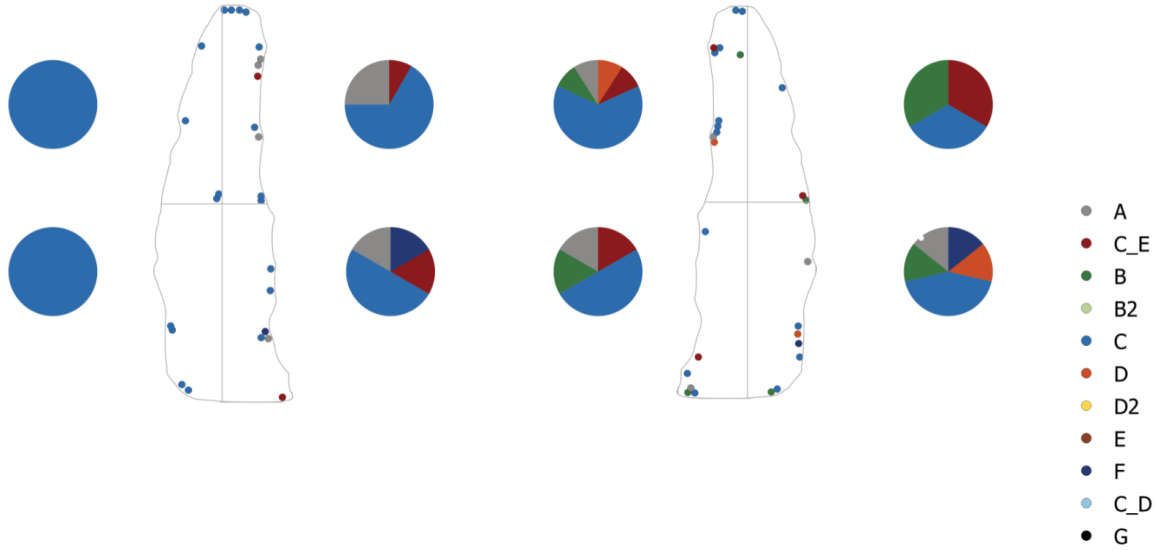

Fig. 109 Distribution of all the use-wear traces documented on *Prądnik spalls*. The left side illustrates the dorsal surfaces of the tool, the right side the ventral tool surface. The colours indicate the use-wear types.

types, but the majority (n = 37) can be categorised as V. (C). Conspicuously often (n = 26) along the edge is also the category I. (A). A third category, type II. (B), sticks out a little with n = 9 documented spots. The remaining categories could be documented on one to five locations.

These results differ when looking at the plotted traces from the three studied sites individually. All the aforementioned observations concerning the location of the use-wear traces is still valid. However, the occurrence of the documented use-wear types differ from site to site. The diversity of use-wear types reflected on all analysed *Keilmesser* together is not present on the *Keilmesser* from Buhlen only (**fig. 105**). Besides a few exceptions in the proximal part of the tools on the dorsal surface, the *Keilmesser* from Buhlen display solely use-wear traces of the category I. (A) or V. (C).

The documented traces on the artefacts in Balve do reflect the variety of use-wear types noticed for all *Keilmesser* from the three sites together (**fig. 106**). Eight of the nine use-wear categories can be found on the *Keilmesser* from Balve. The only missing category is type IX. (G), the type interpreted as post-depositional trace.

Despite the small quantity of analysed *Keilmesser* from the site Ramioul, the variety of documented use-wear traces is nearly comparable to the results from Balve (**fig. 107**). The observed traces are located only along the active edge. Except for the three use-wear categories I. (A), III. (B2) and VIII. (D2), all other types could be documented on the artefacts.

The results for the analysed *Prądnik scrapers* do look different (**fig. 108**). First of all, not many traces (n = 33) could be documented as measured by the smaller number of tools, compared to the *Keilmesser*. Most of the traces could be found again along the active edge (n = 25) with a majority of traces on the ventral surface (n = 14). Moreover, the diversity of use-wear types is also different. The surface modifications on *Prądnik scrapers* can be attributed to 84.9 % (n = 27) to the types V. (C) and I. (A), but type V. clearly predominates (n = 19). Three times, the category IX., interpreted as post-depositional traces, was found on two tools.

Within the qualitative use-wear analysis, n = 39 *Prądnik spalls* were microscopically checked for surface modifications. In total, n = 53 traces on n = 27 artefacts could be documented (**fig. 109**). The variance is higher than documented for the *Prądnik scrapers*, but not as high as for the *Keilmesser*. Five of the nine categories were found on the *Prądnik spalls*. The main frequency of the use-wear types is the same as for

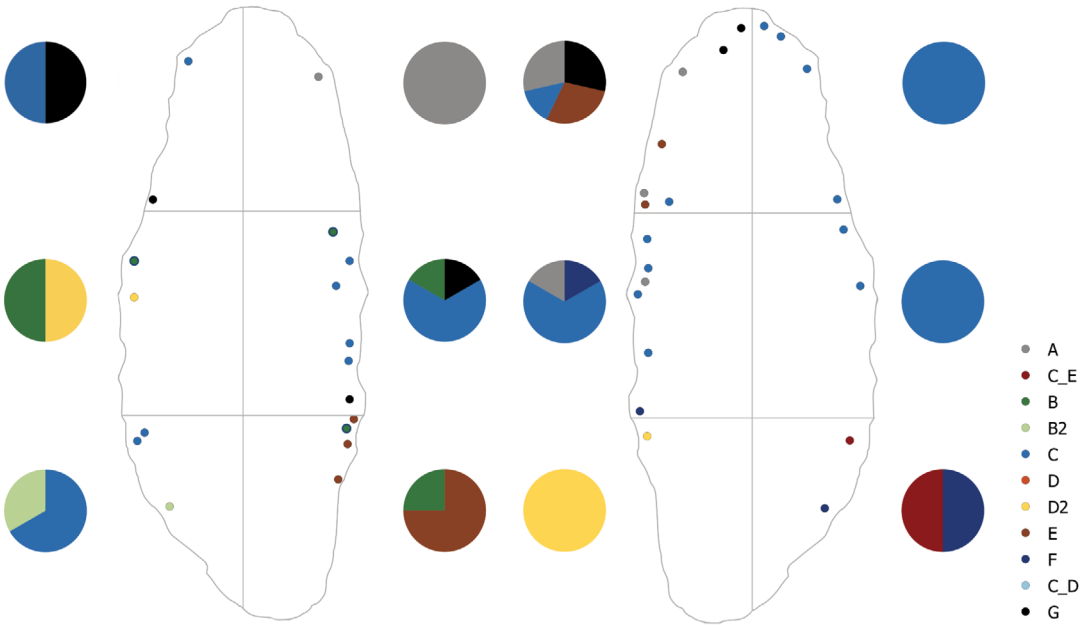

Fig. 110 Distribution of all the use-wear traces documented on scrapers. The left side illustrates the dorsal surfaces of the tool, the right side the ventral tool surface. The colours indicate the use-wear types.

Keilmesser. Category V. is again the most often documented use-wear type with n = 33 locations. The frequency of type I. (n = 7) is also slightly higher compared to other types as well as type II. (n = 4). The combination of category V. and category IV. was also documented for n = 5 locations. The distribution of the traces is not as clear as described for *Keilmesser* and *Prądnik scrapers*. The traces are still most often orientated along the active edge (former active edge of the tool) but also the number of traces along the opposite edge is proportionally high. The percentage distribution is 52.8 % for the active edge to 47.2 % for the opposed edge.

Additionally, the orientation of the striations on *Keilmesser*, *Prądnik scarpers* and *Prądnik spalls* was reviewed. This was done in order to see, whether the striations can support or contradict the interpreted tool lateralisation. To do so, only striations along the active edge with a clear orientation (type VII. and VIII.) can provide information. Furthermore, these striations have to be oblique towards the edge. Oblique striations could reflect the tool handling of the tool during its action in the sense of which surface was used. Therefore, striations of left-lateral tools should be thereby mirrored, compared to the ones on right-lateral tools. Unfortunately, none of the documented striations with an oblique orientation is located along the edge. Thus, the tool laterality cannot be correlated with results of the qualitative use-wear analysis.

The results of the analysed scrapers illustrate again a different picture (**fig. 110**). For the small number of analysed tools with some surface modification (n = 14), the quantity of documented traces is comparably high (n = 37). Additionally, the variance of use-wear types is also high. Seven of the nine categories are displayed on the scrapers. Although the most frequent category is again type V. (n = 18), there is no other prominent use-wear type. The other categories are all present with one to five locations. The distribution of these traces is more even towards all edges, although the traces along the active edge still prevail slightly (n = 25).

The only flake with use-wear traces displayed type V. on three different locations.

For all artefact categories from the three archaeological sites together, the following picture emerges. The traces clearly prevail along the active edges. About 38.9 % (n = 125) of the traces can be found close to the

site		artefact category						
		Keilmesser tip	*Prądnik scraper*	*Prądnik spall*	scraper	flake	total	
Buhlen	n	4	0	1	1	0	0	**6**
	%	66.7	0.0	16.7	16.7	0.0	0.0	100.1
Balve	n	25	2	0	3	3	0	**33**
	%	75.8	6.1	0.0	9.1	9.1	0.0	100.1
Ramioul	n	6	0	2	0	3	0	**11**
	%	54.6	0.0	18.1	0.0	27.3	0.0	100.0
total	n	**37**	**2**	**3**	**4**	**6**	**0**	**52**
	%	71.2	3.9	5.8	7.7	11.5	0.00	100.1

Table 39 Selected artefacts from Buhlen, Balve and Ramioul for the quantitative use-wear analysis.

active edge on the ventral surface, 34.6 % (n = 111) on the dorsal surface. The remaining 26.5 % of the traces are located on the edge opposed to the active edge, the posterior part, either on the ventral (n = 45) or on the dorsal surface (n = 40). The quantity of traces decreases in all areas (A to D) from the distal and medial to the proximal tool part. While the quantity of traces in the medial and proximal part is more or less equally distributed in the areas A, B and C, the frequency of traces in area D is considerably higher in the distal part of the tool (n = 66; medial n = 37, proximal n = 22).
Regarding the type of traces, there is also one category that clearly stands out. Out of the n = 321 in total documented traces on all tools, 49.5 % (n = 159) of the traces are ascribed as category V. The next more frequent category is I. with 18.1 % (n = 58). Worth mentioning are also use-wear type II. and IV., documented on 8.10 % (n = 26) and 6.2 % (n = 20) of the cases. The remaining categories are rarely present on the tools and make only up to 4 % of the traces respectively.
Some additional aspects should be highlighted, which are a consequence of the distribution and the occurrence of the different traces. As mentioned before, *Keilmesser* (Buhlen as an exception) display all of the aforementioned described use-wear categories. The only other artefact category that displays nearly all use-wear types too, are the scrapers. Interestingly, category VI. only appears on *Keilmesser* and *Prądnik spalls*. In general it seems the distribution of the use-wear types on *Prądnik spalls* are very similar to the distribution on *Keilmesser.* This makes sense when assuming that the traces result from tool use before the *Prądnik spalls* have been removed from the *Keilmesser*. At the same time, the traces on *Prądnik spalls* can be found on all edges, what makes it impossible to only be a consequence of a *Keilmesser* use. *Prądnik scrapers*, however, do not share these similarities with *Keilmesser* and *Prądnik spalls*. The use-wear types on *Prądnik scrapers* reflect almost no diversity and can be summarised be they types V. and I.

Quantitative use-wear analysis

The second part of the use-wear analysis was the quantitative use-wear analysis with the aim to acquire 3D surface topography data to measure and characterise the micro surface texture of the identified use-wear traces. The samples for the quantitative use-wear analysis have been selected based on the results from the previously performed qualitative use-wear analysis. From the n = 150 artefacts that displayed in total n = 321 traces, n = 50 traces provide the subsample for the quantitative use-wear analysis (**tab. 39**). These sampled traces correspond to n = 37 spots on *Keilmesser*, n = 3 on *Prądnik scrapers*, n = 4 on *Prądnik spalls*

and n = 6 traces on scrapers. This subsample does not only display the different artefact categories, but also the different use-wear types. Since the predominant use-wear type found on the artefacts was category V., this type was selected by a majority (n = 13). The remaining use-wear types were selected on the premise, that, if possible, the minimum number of use-wear types were represented by three samples. Each use-wear trace was measured three times. These measurements were taken at nearby but non-identical spots within the trace in order to review the homogeneity within each trace. Hence, n = 150 measurements were performed in total. As explained in the method chapter, the data was acquired with an upright light microscope coupled with a laser-confocal microscope (ZEISS Axio Imager.Z2 Vario + ZEISS LSM 800 MAT).

Surface micro texture data analysis

The acquired data was analysed according to the ISO 25178-2 parameters. Based on this international standard, 21 ISO 25178-2 parameters, three furrow parameters, three texture direction parameters, one texture isotropy parameter and the scale-sensitive fractal analysis (SSFA) parameters *epLsar, NewEplsar, Asfc, Smfc, HAsfc9 and HAsfc81* were calculated on each surface (**tab. 11**; further information about these parameters can be found in the »surface metrology guide« from Digital Surf; see Digital Surf, Besançon, France). Only one parameter, *Str*, could not be calculated on a small number of surfaces and is thus missing for n = 9 measurements. However, the parameter *isotropy* (texture direction parameter) is identical to the ISO 25178-2 *Str* parameter. The ConfoMap templates, the resulting data including plots for each measured parameter can be found on GitHub. In order to present the data here, nine out of the 34 parameters were considered. These nine parameters spanning the different categories of field parameters (Blateyron 2013) and some additional isotropy, furrow and SSFA parameters. The areal parameters separate in the three categories areal field, areal-scale and length-scale analysis. To start with the areal field parameters, *Sq* was chosen as an amplitude parameter expressing the root mean squared height. Thus, *Sq* is a measure of surface roughness. The higher the *Sq*, the higher the surface roughness. *Std*, a spatial parameter, calculates the main direction of the surface texture (texture direction). The parameter is defined relative to the y-axis. Thus, a surface with an orientation along the y-axis will return a *Std* of 0 degrees. Only when a surface is anisotropic, this parameter is of relevance or can be calculated. Interesting is, that *Std* can be used to detect the presence of a preliminary surface modification process, which is to be removed (succeeding modifications that lead to different texture directions). As a volume parameter of the areal field parameters, *Vmc* stands for the volume of the material. *Vmc* can be useful to understand how much material may be worn away for a given depth. *Sxp* is another functional parameter describing the peak extreme height. *Sxp* is a measure for the height differences between the average height of the surface and the highest peak by excluding 2.5 % of the highest points. High *Sxp* values indicate the existence of high peaks. A field parameter belonging to the category of areal scale analysis is the hybrid parameter *Sdr*. *Sdr* is a measure of surface complexity. The higher the value, the more complex the surface. Meaning, a value close to 0 % is equitable to a flat and smooth surface. Moreover, for the texture isotropy and periodicity the *isotropy* on surface was selected. The higher the *isotropy* value, the more the surface resembles itself in every direction. In other words, the *isotropy* decreases with an increasing directionality of the surface. For the furrow analysis, the *mean density of furrows* was selected as a parameter for detecting and characterising furrows on the surface. The last category are parameters of the fractal analysis. One of these parameters is *HAsfc9*. *HAsfc9* displays the heterogeneity of areal-scale fractal complexity. A high HAsfc9 value indicates a high-degree within-surface variation across different scales. EpLsar is another parameter of the fractal analysis, categorised as length-scale analysis. The parameter reflects the anisotropy of a texture and it thus the reverse of isotropy. The

epLsar values increase with increasing directionality. To summarise, for the quantitative characterisation of the surface micro texture these variables were considered: surface roughness, surface directionality, volume, height, surface complexity, isotropy, heterogeneity and anisotropy.

Based on these selected variables, representative for the different categories of parameters, some results are explained. Prior to this, it should be mentioned again that quantitative use-wear analysis is a comparable new approach in archaeology although the interest is clearly increasing (e. g. Martisius et al. 2018; Galland et al. 2019; Stemp/Macdonald/Gleason 2019; Álvarez-Fernández et al. 2020; Bradfield 2020; Martisius et al. 2020; Pedergnana et al. 2020b; Pedergnana/Ollé/Evan 2020). Following the international standards (ISO 25178-2) offers a secure way to analyse the data. However, which parameters are relevant or the most important ones to analyse use-wear traces on lithics, especially on silicified schist, is not sufficiently known yet. Quantitative use-wear analysis is a very promising approach with the great potential to be straightforward when explored and applied more regularly (Calandra et al. 2019b; Martisius et al. 2020; Pedergnana et al. 2020b). Large archaeological assemblages, such as the one presented here, have not been part of a qualitative use-wear analysis yet.

To check the results, the scatterplots (**figs 111-119**) of all measurements plotted *per* parameter give a first overview on the distribution of the values. The scatterplots show the measured values separated per artefact. Information about the raw material and the location (A to D, one to three) are given. The data points are coloured based on the interpreted use-wear types. In this way, different results within or between the raw materials, the artefact categories, the use-wear type classification and the locations can be compared. Unfortunately, the measured parameters lead to no obvious diagnostic results. No direct pattern between the results and the aforementioned variables is apparent. However, four measurements stand out. These measurements (MU-199 C3_01_a, MU-202 D2_01c, BU-173 C2-01_a and BU-173 C2-01_b) are noteworthy. Here, it should be pointed out again that from each trace, three measurements were taken in order to make an identification of measuring errors possible. The results of these three measurements *per* trace should be similar, otherwise the measurement is likely unreliable. However, this is the case for the four aforementioned samples. The variability within the results of the three measurements per traces respectively is conspicuous. A review of the four measurements could clearly identify them as outliers. When processing the data, existing noise is removed by a threshold. This data is interpreted as non-measured points. In a further step, such missing data gets filled. This is necessary in order to calculate some of the ISO and the SSFA parameters. In the case of the four outliers, the following happened: The measured areas were marginal and located closed to the tool edge. When scanning the surface, a small area beyond the edge was also included in the scan. Meaning, this area is treated as non-measured points. In order to calculate the parameters, the missing data needed to be filled in and the final results do not reflect the actual measured surfaces. Thus, these four measurements appear as outliers and should therefore be excluded when interpreting the data.

Although the data results in no immediately identifiable pattern, some aspects can be pointed out. The first aspect concerns the surface roughness (*Sq*). The *Sq* values calculated on flint are lower than the ones from lydite (**fig. 116**). The arithmetic mean values for flint is 98.6 µm while the mean value for lydite is 189.2 µm. It needs to be noted that the arithmetic mean value for lydite (n = 111) is based on more measurements than the flint (n = 39) one. When looking at the use-wear types, some can be categorised by higher *Sq* values then others. The surface roughness for the use-wear type I., II. and IV. seems slightly rougher compared to the other types. Contrary to that, the use-wear type V. appears to be smoother, which is reflected by lower *Sq* values.

In general, the three mentioned use-wear types I., II. and IV. differ from the other types not only concerning the surface roughness, but also concerning volume, height and surface complexity.

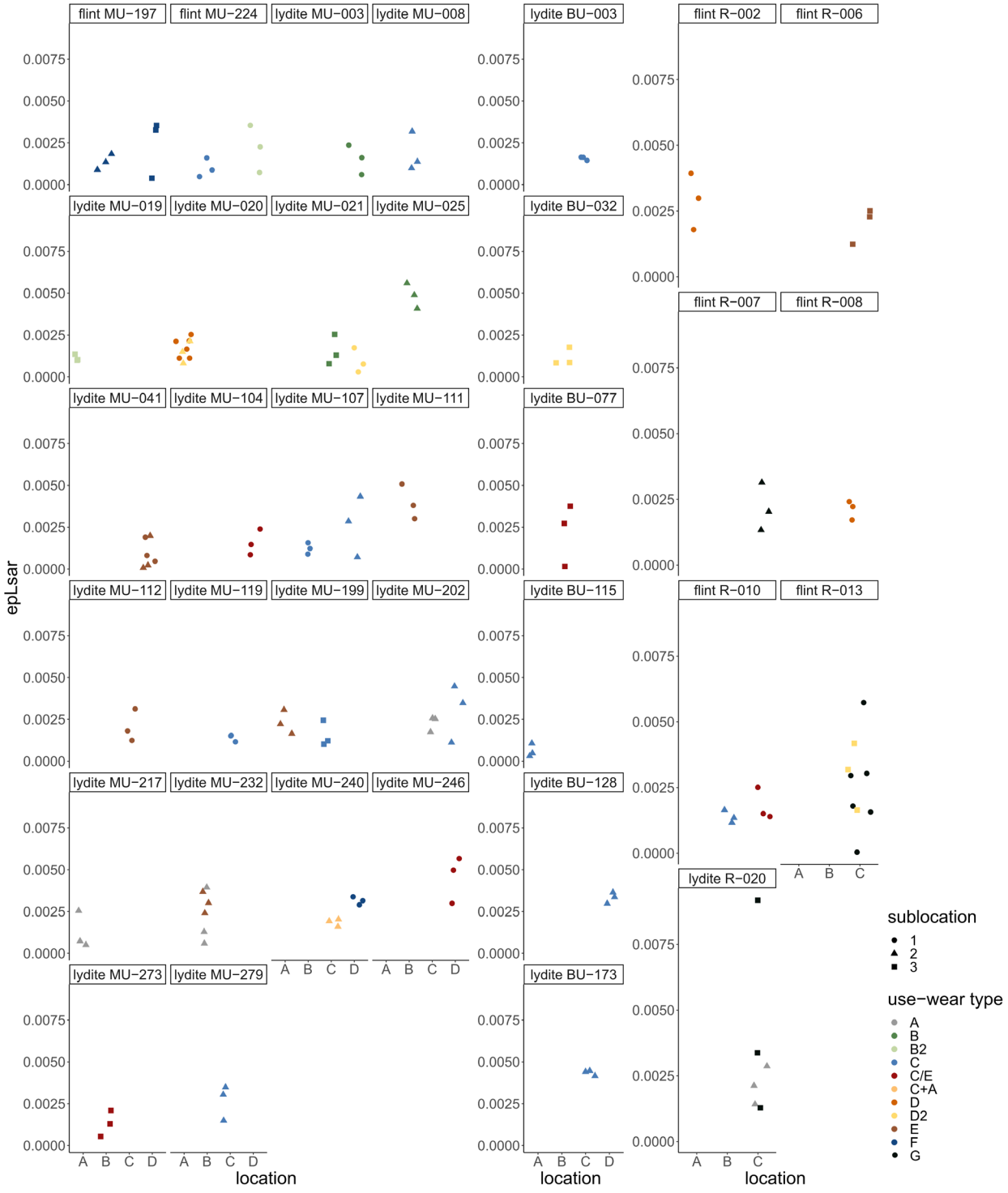

Fig. 111 *EpLsar* values for each analysed artefact (raw material [flint or lydite] plus ID). The parameter reflects the anisotropy of the texture. The epLsar value increases with increasing directionality. The plot indicates the location of the use-wear on the tool (A & B = dorsal, D & C = ventral) plus the sublocation (1, 2 or 3; sublocation stands for the number of use-wear traces *per* location). The three measurements per location and sublocation represent the three measurements *per* use-wear taken at non-identical but nearby spots. The data points are coloured based on the interpreted use-wear types.

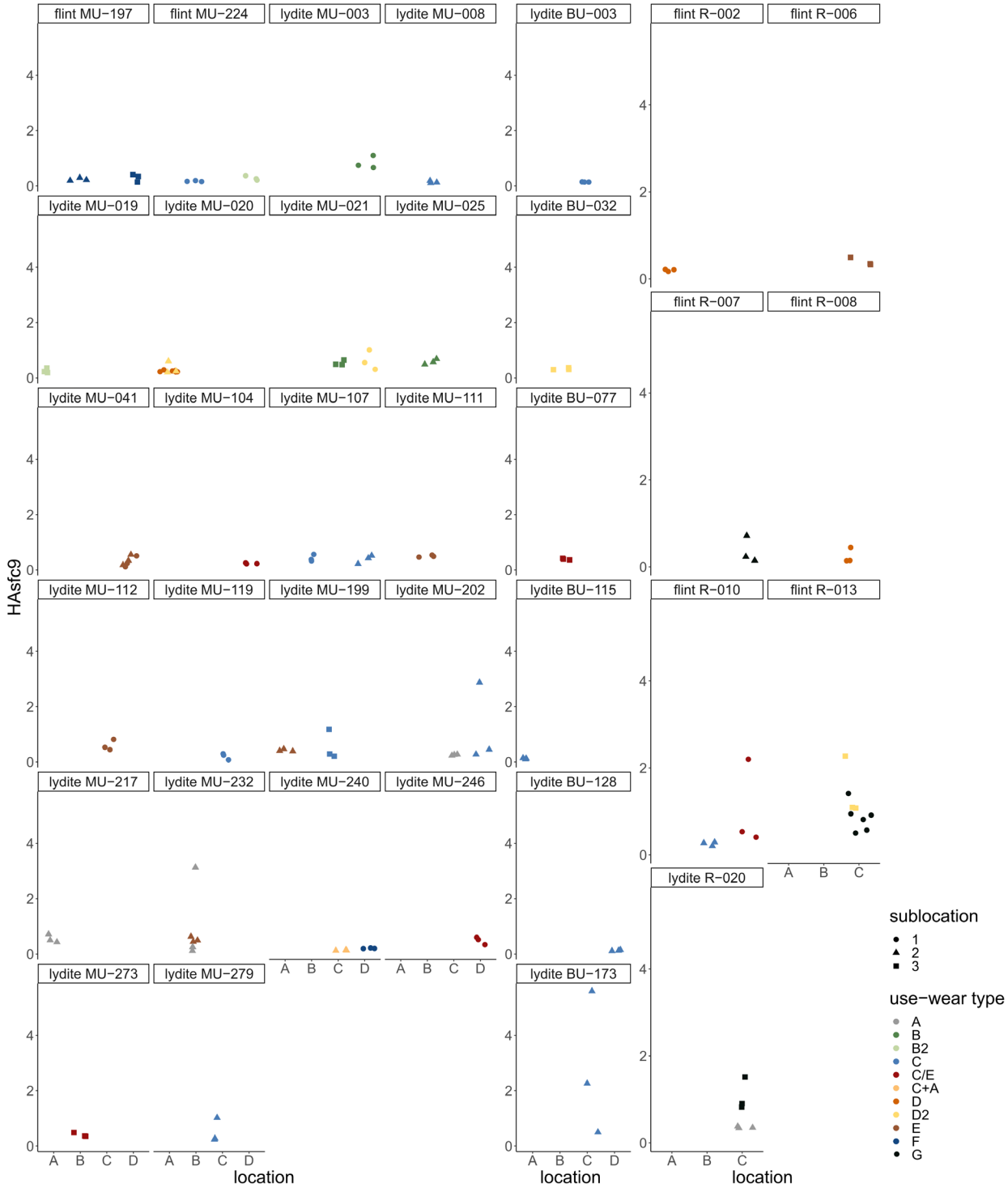

Fig. 112 *HAsfc9* values for each analysed artefact (raw material [flint or lydite] plus ID). HAsfc9 displays the heterogeneity of areal-scale fractal complexity. The plot indicates the location of the use-wear on the tool (A & B = dorsal, D & C = ventral) plus the sublocation (1, 2 or 3; sublocation stands for the number of use-wear traces *per* location). The three measurements per location and sublocation represent the three measurements *per* use-wear taken at non-identical but nearby spots. The data points are coloured based on the interpreted use-wear types.

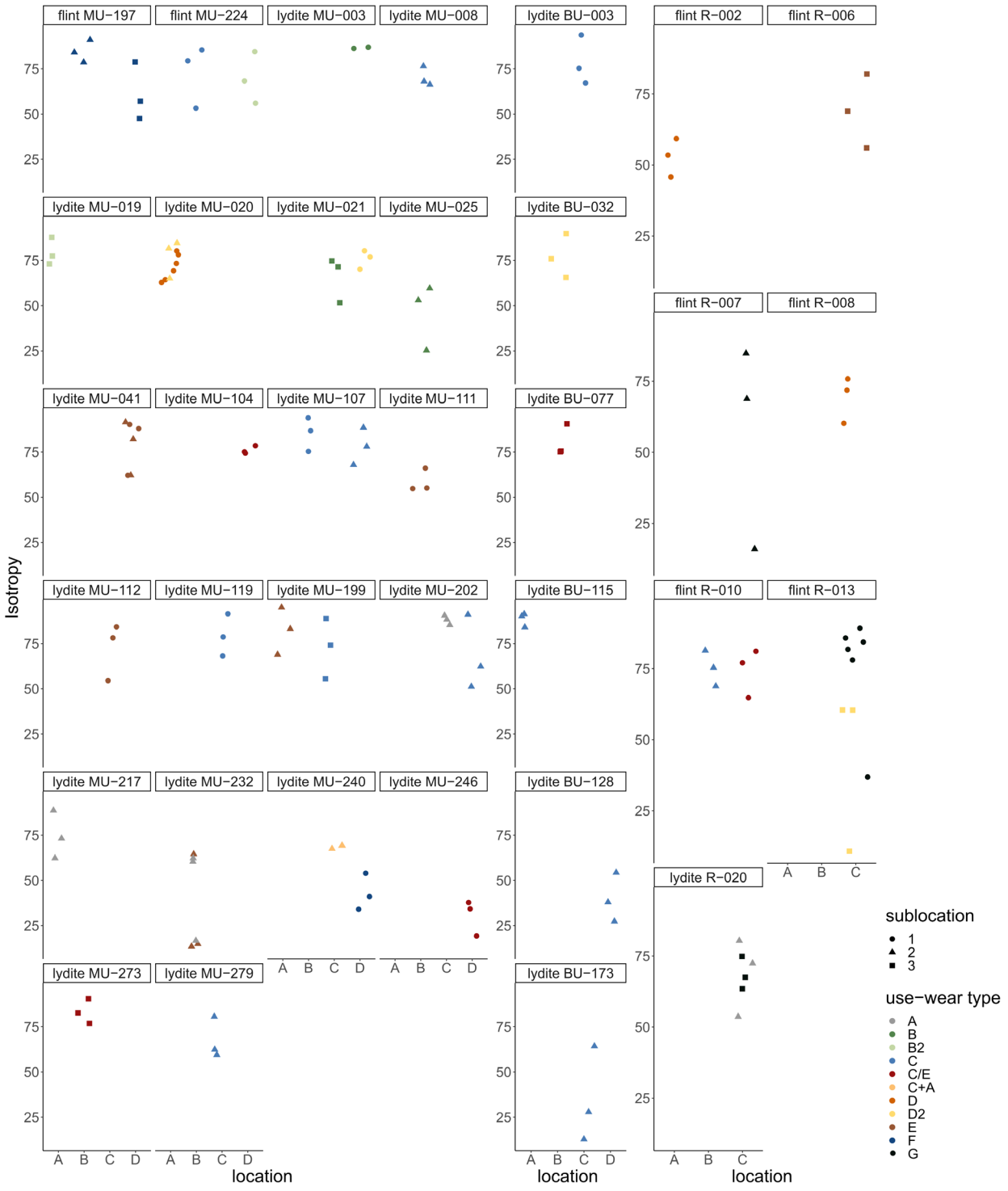

Fig. 113 *Isotropy* values for each analysed artefact (raw material [flint or lydite] plus ID). *Isotropy* reflects surface directionality. The value decreases with an increasing directionality of the surface. The plot indicates the location of the use-wear on the tool (A & B = dorsal, D & C = ventral) plus the sublocation (1, 2 or 3; sublocation stands for the number of use-wear traces *per* location). The three measurements per location and sublocation represent the three measurements *per* use-wear taken at non-identical but nearby spots. The data points are coloured based on the interpreted use-wear types.

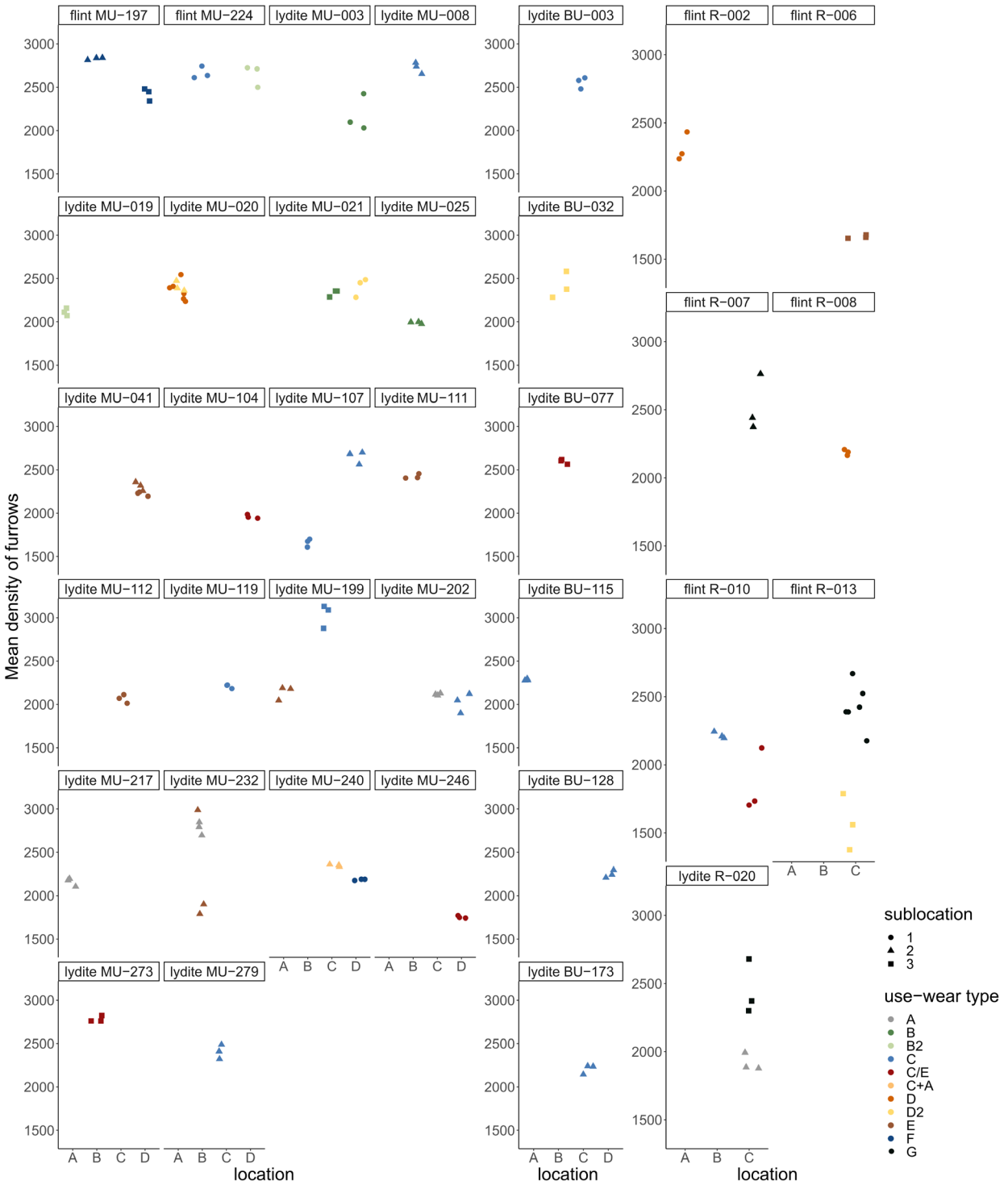

Fig. 114 *Mean density of furrow* values for each analysed artefact (raw material [flint or lydite] plus ID). *Isotropy* reflects surface directionality. The value reflects furrows on the surface. The plot indicates the location of the use-wear on the tool (A & B = dorsal, D & C = ventral) plus the sublocation (1, 2 or 3; sublocation stands for the number of use-wear traces *per* location). The three measurements per location and sublocation represent the three measurements *per* use-wear taken at non-identical but nearby spots. The data points are coloured based on the interpreted use-wear types.

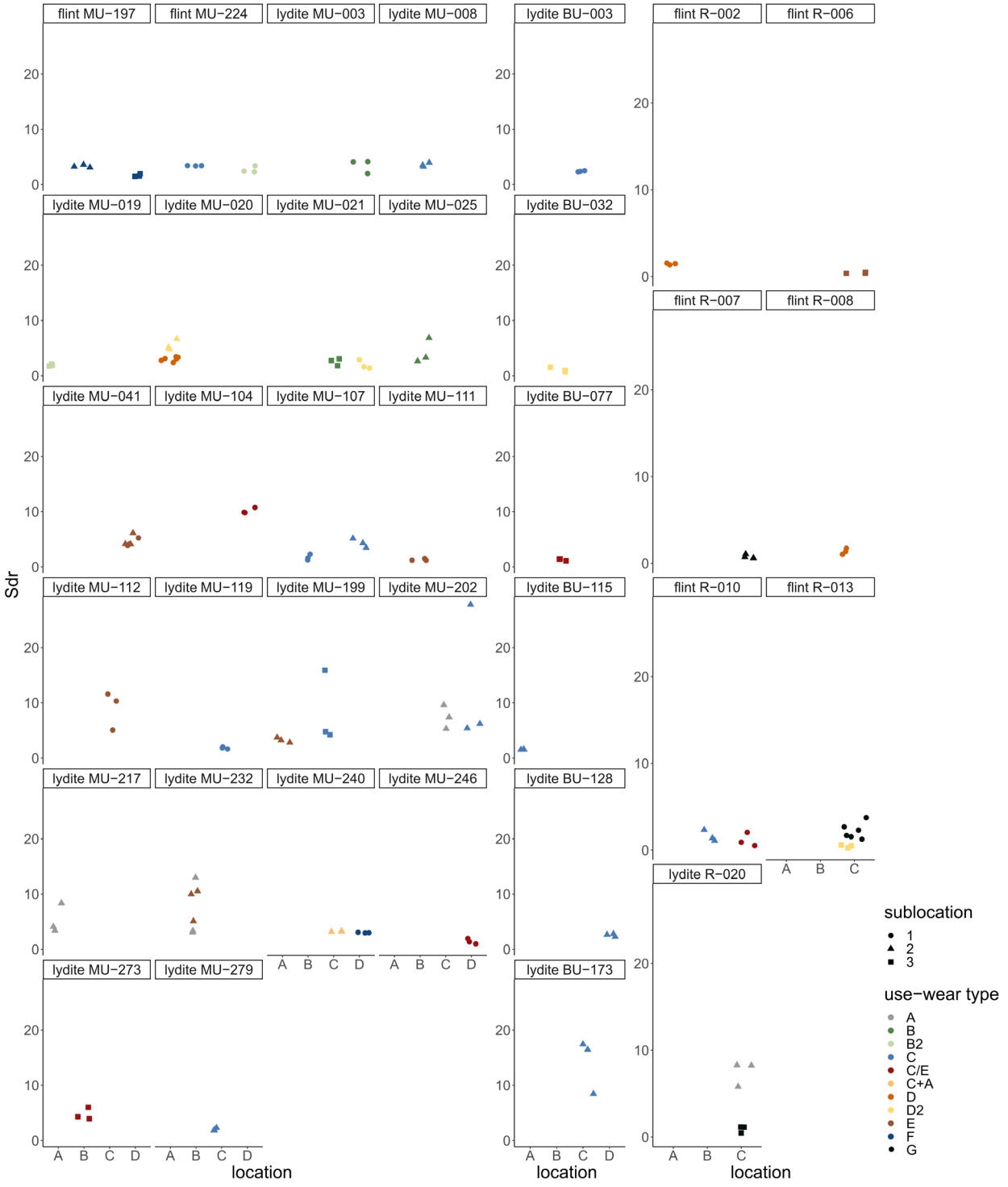

Fig. 115 *Sdr* values for each analysed artefact (raw material [flint or lydite] plus ID). *Sdr* is a measure of surface complexity. The higher the value, the more complex the surface. The plot indicates the location of the use-wear on the tool (A & B = dorsal, D & C = ventral) plus the sublocation (1, 2 or 3; sublocation stands for the number of use-wear traces *per* location). The three measurements per location and sublocation represent the three measurements *per* use-wear taken at non-identical but nearby spots. The data points are coloured based on the interpreted use-wear types.

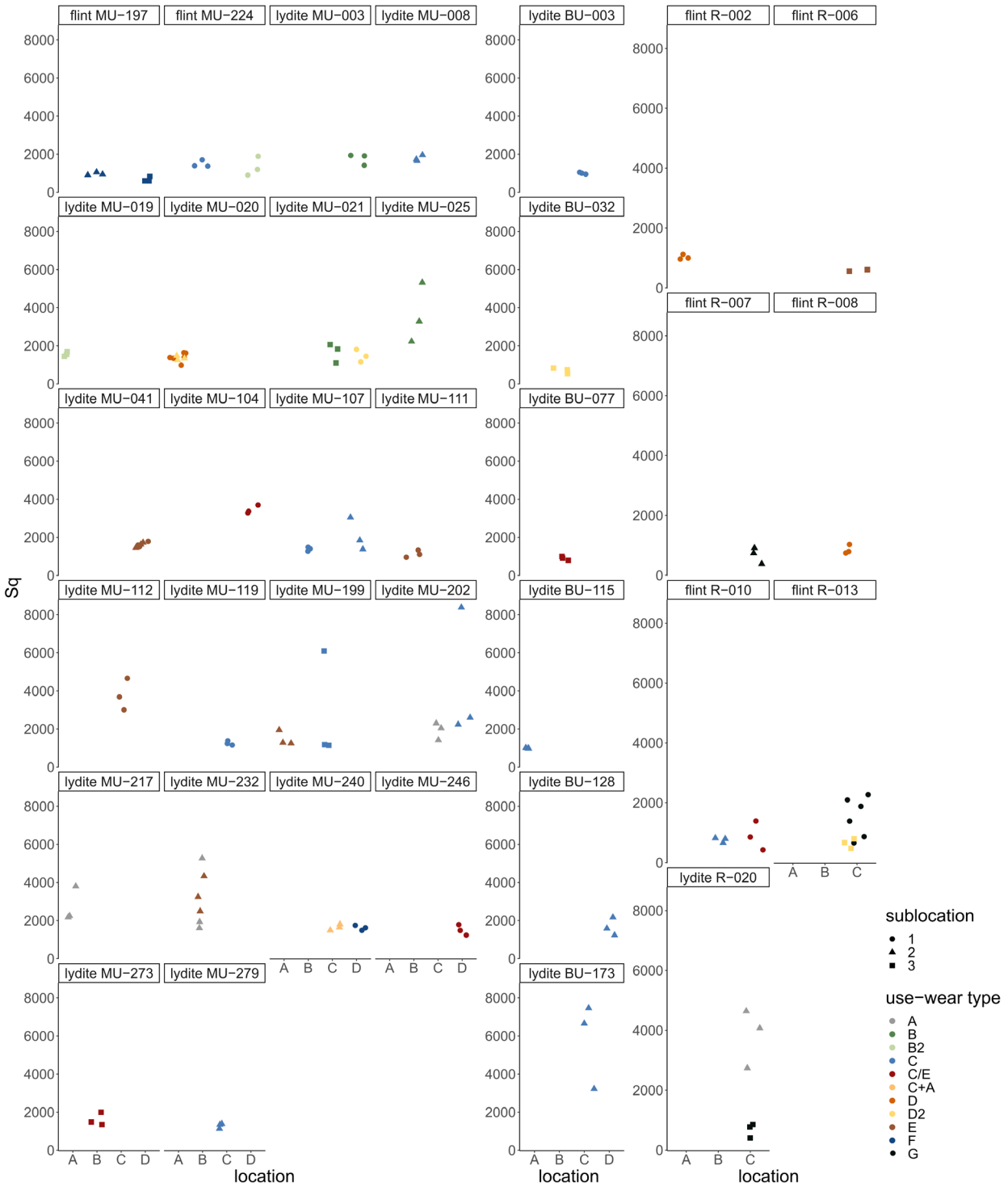

Fig. 116 *Sq* values for each analysed artefact (raw material [flint or lydite] plus ID). *Sq* is a measure of surface roughness. The higher the *Sq* value, the higher the surface roughness. The plot indicates the location of the use-wear on the tool (A & B = dorsal, D & C = ventral) plus the sublocation (1, 2 or 3; sublocation stands for the number of use-wear traces *per* location). The three measurements per location and sublocation represent the three measurements *per* use-wear taken at non-identical but nearby spots. The data points are coloured based on the interpreted use-wear types.

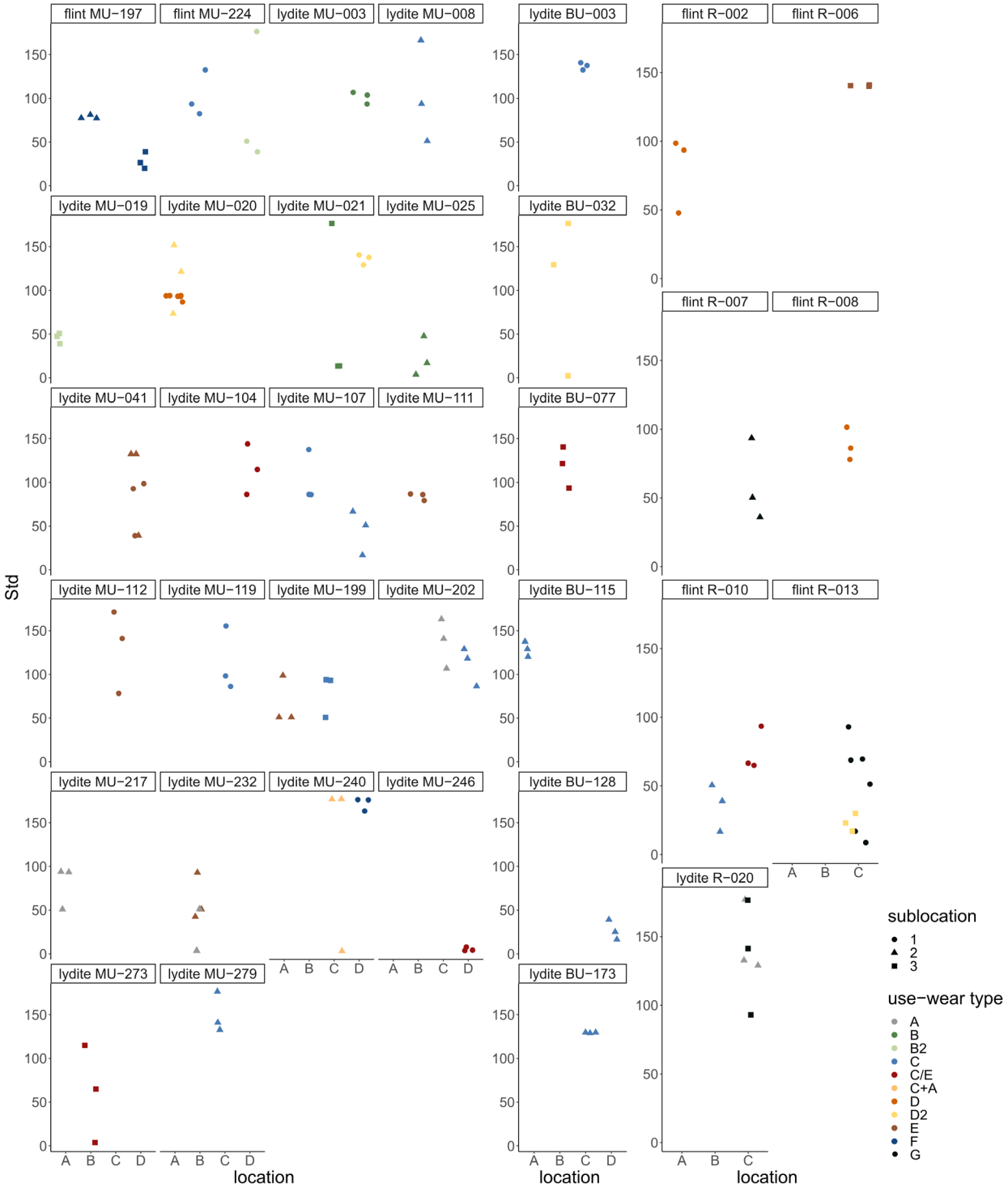

Fig. 117 *Std* values for each analysed artefact (raw material [flint or lydite] plus ID). *Std* reflects the main direction of the surface texture. The plot indicates the location of the use-wear on the tool (A & B = dorsal, D & C = ventral) plus the sublocation (1, 2 or 3; sublocation stands for the number of use-wear traces *per* location). The three measurements per location and sublocation represent the three measurements *per* use-wear taken at non-identical but nearby spots. The data points are coloured based on the interpreted use-wear types.

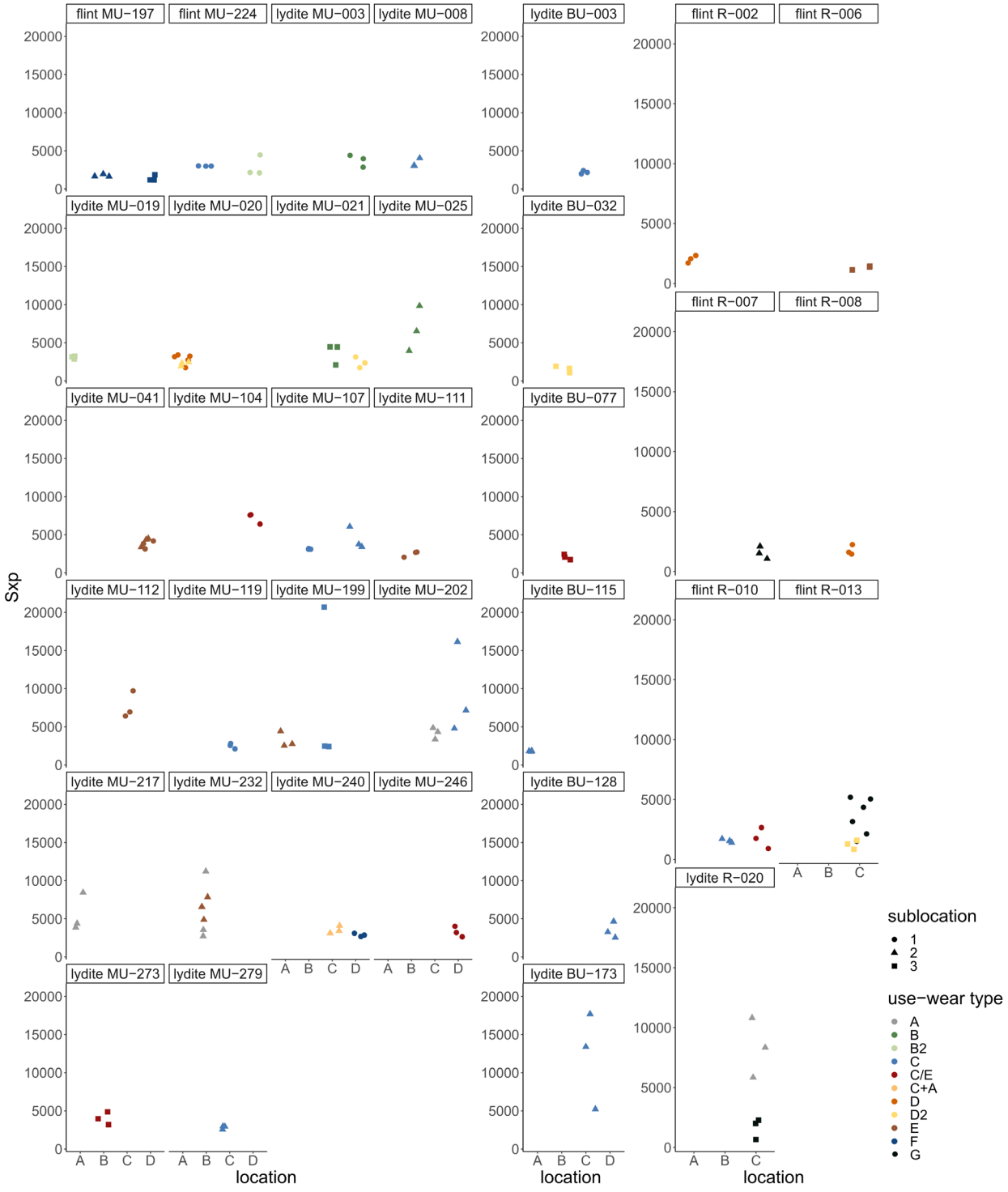

Fig. 118 *Sxp* values for each analysed artefact (raw material [flint or lydite] plus ID). *Sxp* is a measure for the height differences between the average height of the surface and the highest peak by excluding 2.5 % of the highest points. The plot indicates the location of the use-wear on the tool (A & B = dorsal, D & C = ventral) plus the sublocation (1, 2 or 3; sublocation stands for the number of use-wear traces *per* location). The three measurements per location and sublocation represent the three measurements *per* use-wear taken at non-identical but nearby spots. The data points are coloured based on the interpreted use-wear types.

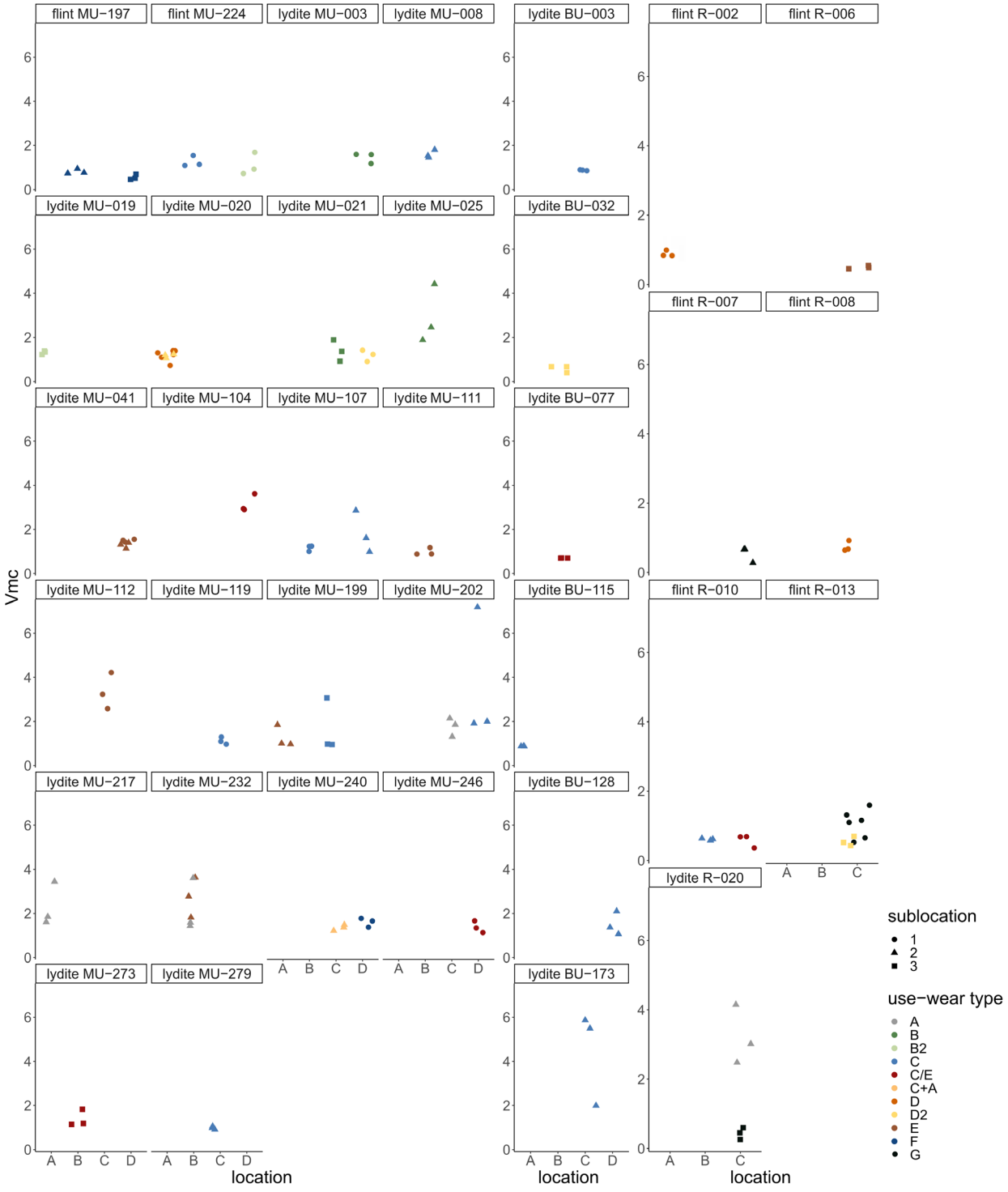

Fig. 119 *Vmc* values for each analysed artefact (raw material [flint or lydite] plus ID). *Vmc* stands for the volume of the material. The plot indicates the location of the use-wear on the tool (A & B = dorsal, D & C = ventral) plus the sublocation (1, 2 or 3; sublocation stands for the number of use-wear traces *per* location). The three measurements per location and sublocation represent the three measurements *per* use-wear taken at non-identical but nearby spots. The data points are coloured based on the interpreted use-wear types.

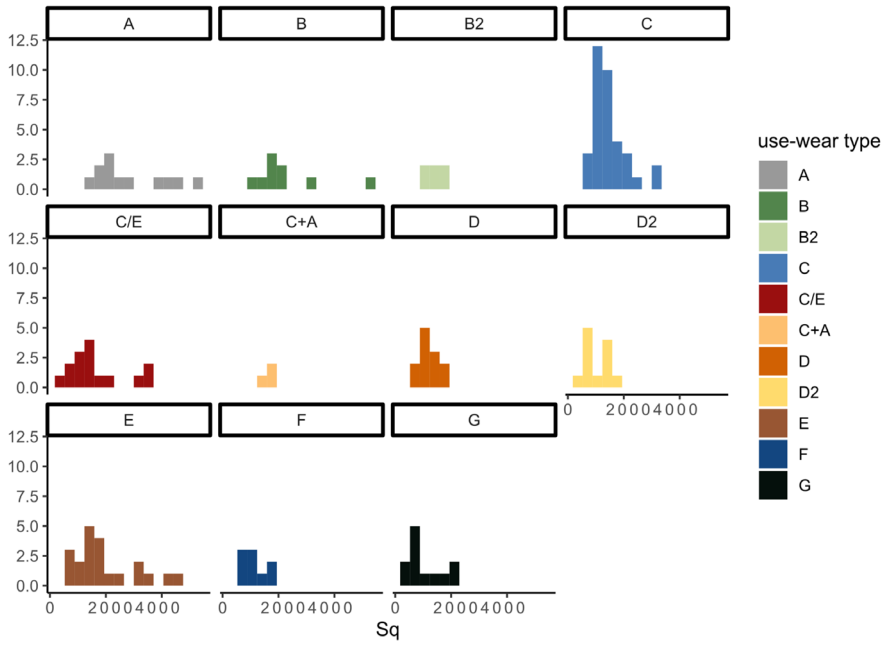

Fig. 120 *Sq* values and their frequency for the use-wear traces (n = 50) on the artefacts, categorised and coloured according to the interpreted use-wear types.

In order to bring the data a little more into question, the data was plotted in additional ways. For all these additional plots, the four measurements identified as outliers were excluded. Histograms of the use-wear types plotted *per* parameter support the aforementioned aspect (**fig. 120**). By a majority, the use-wear type V. displays a comparably low roughness based on the parameter *Sq*. Moreover, the observations that the types I., II. and IV. differ from other types, is also visible in the histograms.

The last mentioned aspect is also illustrated by the boxplots of the use-wear types plotted again per parameters (**fig. 121**). The boxplots include the information about the artefact category. Interestingly, the data measured on the scrapers set off against the other artefact categories.

Two parameters, *Vmc* and *Sq* were selected in order to plot the results of these parameters against each other in a scatterplot. In one plot, the data was coloured based on the interpreted use-wear types (**fig. 122**). The data points align in one direction without any significant correlation. The same can be reported for the second plot, in which the data points were coloured based on the two plotted artefact categories *Keilmesser* and *Prądnik scrapers* (**fig. 123**). The data representing the *Keilmesser* spread more over the plot, but is numerically also more represented. Other parameters were plotted in the similar way. The parameters are *epLsar* and *Asfc* (**fig. 124**) as well as *Mean density of furrows* against *mean depth of furrows* (**fig. 125**). The plots reflecting the different use-wear types lead to no new insights. However, in the plot *epLsar* against *Asfc* a separation of the use-wear types I. (A) and IV. (E) is visible. These two types do not cluster differently, but the data points spread further towards a higher *Asfc* value.

A last attempt to explore the data was done by a principal component analysis (PCA). A first PCA was applied on seven components reflecting the variance in the artefact categories (**fig. 126**). These components are the parameters *Sq, Ssk, Vmc, Mean density of furrows, Isotropy, Asfc* and *HAsfc9*, spanning the different categories of field parameters. The variance in *Sq, Vmc* and *Asfc* is represented by Principal Component 1 (PC1), which accounts for 38.55 %. Principal component 2 (PC2) reflected 21.29 % of the explained variance with *Ssk, Mean density of furrows, Isotropy* and *HAsfc9*. This dimensionality reduction illustrates an overlap of the data with the data scattering mainly on the right half of the PC1 axis. The data cluster from the four different artefact categories – *Keilmesser*, *Prądnik scraper*, *Prądnik spall* and *scraper* – clearly overlap, whereas the data points from the *Keilmesser* spread the most. The cluster built by the data points from the *Prądnik spacers* do differ from the other data.

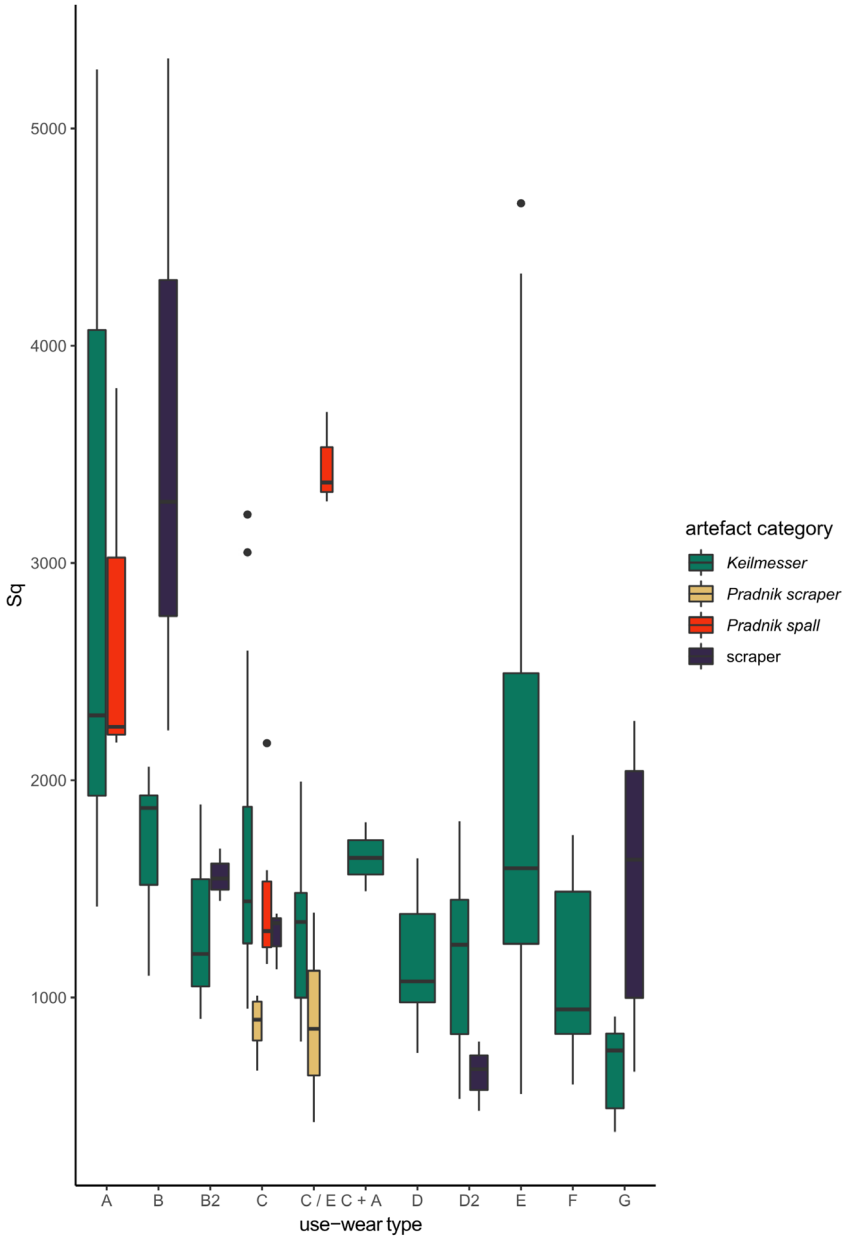

Fig. 121 Distribution of *Sq* values for the measured use-wear traces (n = 50) on the artefacts. The data is categorised according to the interpreted use-wear types and coloured based on the artefact type.

A second PCA visualises the variance of the different use-wear types based on the same seven components (**fig. 127**). Again, the data scatters mainly on the right part of the PC1 axis. However, the clusters illustrating the use-wear types I. (A), II. (B), IV. (E) and also the combination of V. (C) and IV. (E) stretch towards the left PC1 axis. In particular use-wear type I. (A) varies from the other clusters and does not overlap with the use-wear types III. (B2), VI. (D) and IX. (G).

Although the interpretation of these data enters a new field in archaeology and needs to be explored in more detail, the quantitative use-wear analysis proved to have the potential to complement and improve qualitative use-wear analysis. Based on the presented data, it can be noticed that *Sq* as a parameter for the surface texture roughness indicates differences when combined with the defined use-wear types. Some use-wear types (e. g. type V.) seem to reflect a lower surface-roughness than other types. However, the parameters associated with the surface directionality (e. *g. isotropy, epLsar* or *NewEpLsar*) are more complex and thus, the combination between the results of the qualitative and this quantitative use-wear analysis might be more complicated.

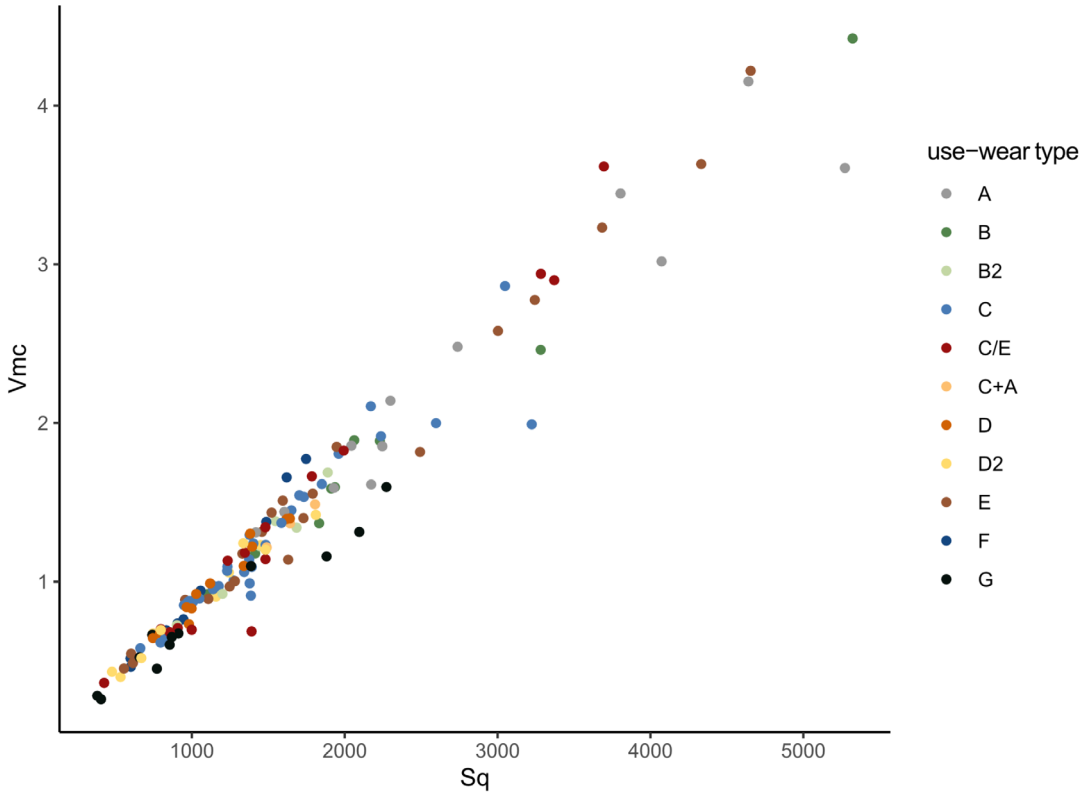

Fig. 122 *Vmc* and *Sq* values of the measured use-wear traces (n = 50) on the artefacts plotted against each other. The data points are coloured according to the interpreted use-wear type.

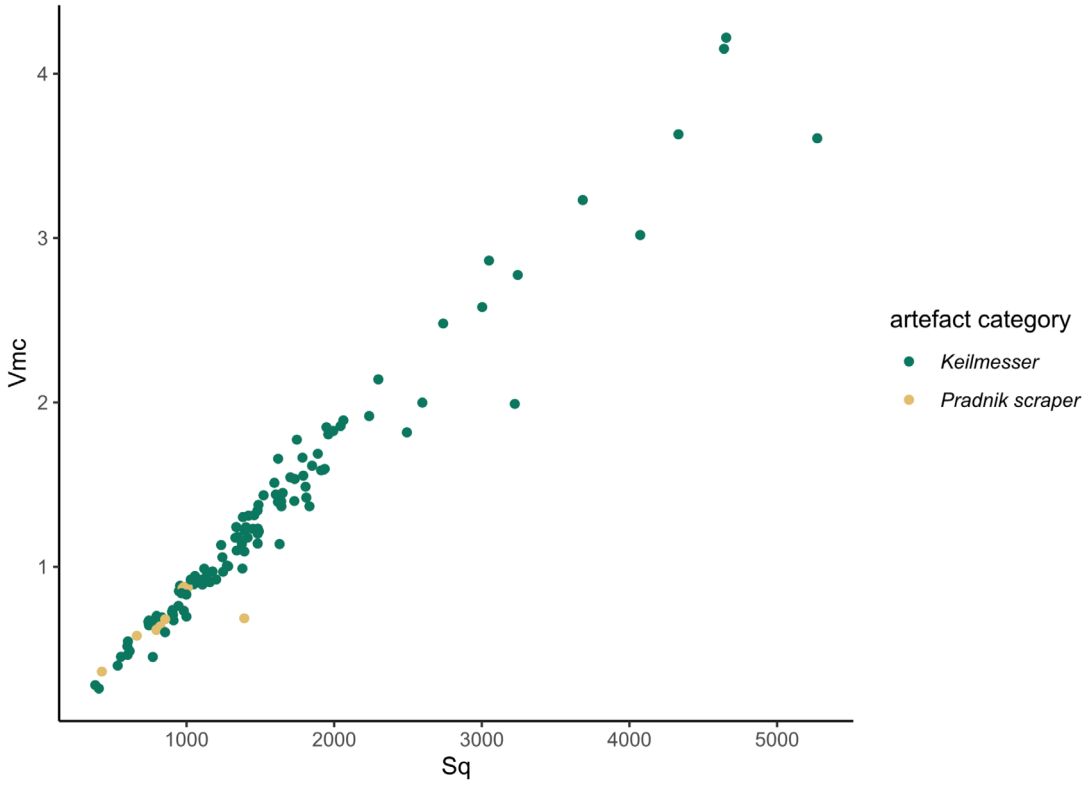

Fig. 123 *Vmc* and *Sq* values of the measured use-wear traces (n = 50) on the artefacts plotted against each other. The data points are coloured according to the artefact category.

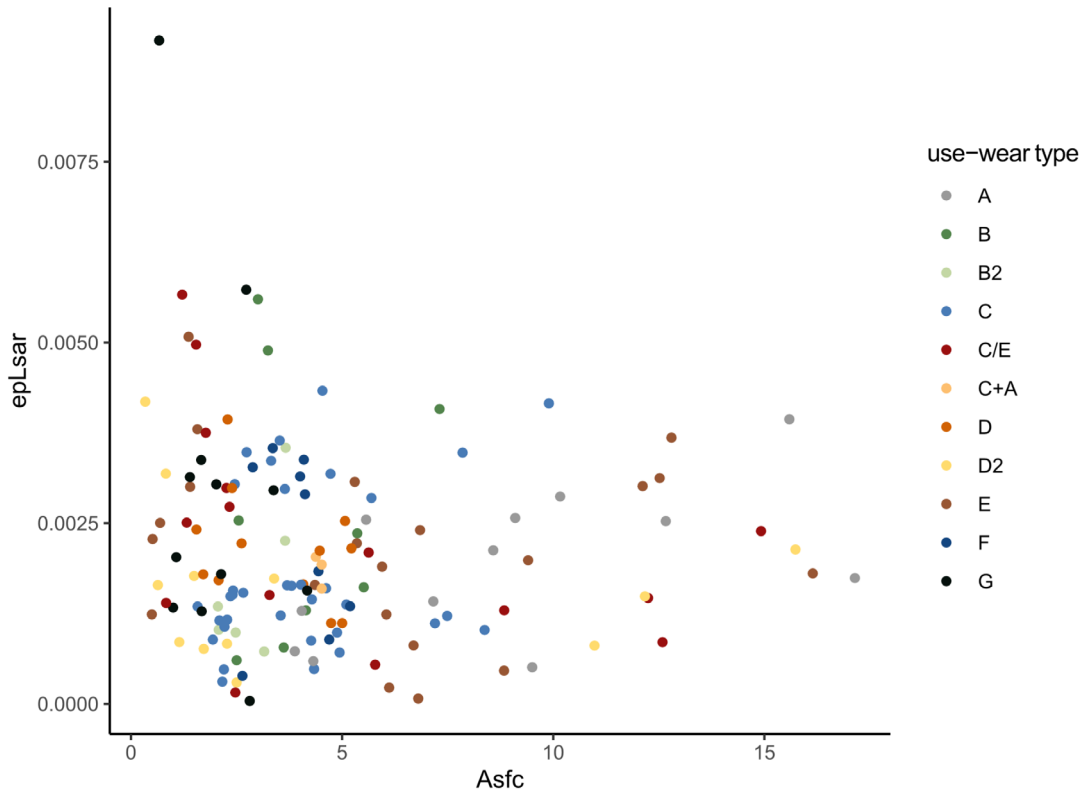

Fig. 124 *EpLsar* and *Asfc* values of the measured use-wear traces (n = 50) on the artefacts plotted against each other. The data points are coloured according to the interpreted use-wear type.

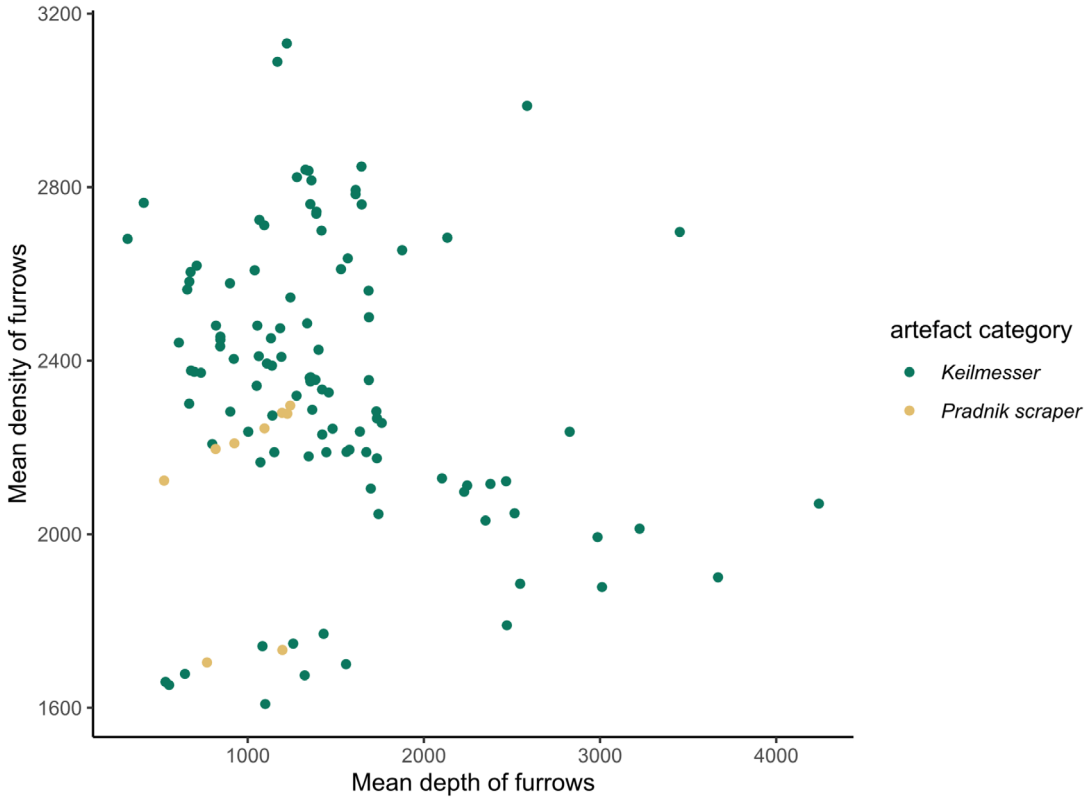

Fig. 125 *Mean density of furrows* and *Mean depth of furrows* values of the measured use-wear traces (n = 50) on the artefacts plotted against each other. The data points are coloured according to the artefact category.

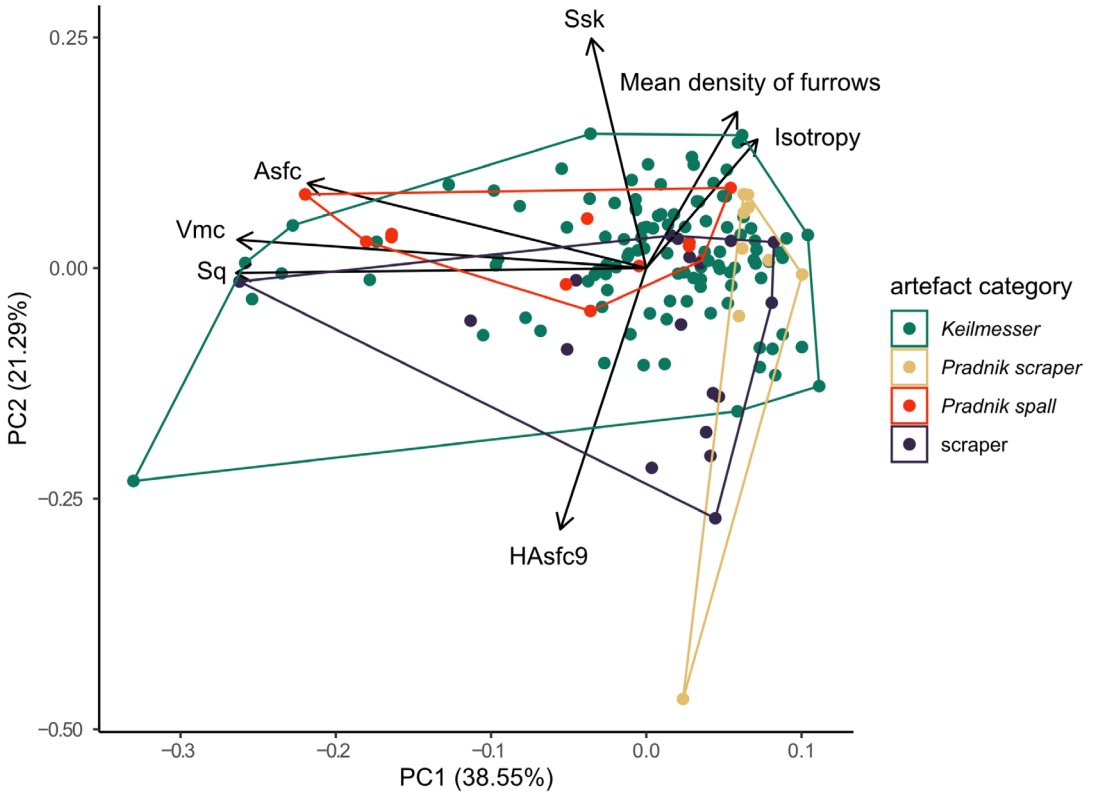

Fig. 126 Principal component analysis applied on the measured use-wear traces (n = 50) of the artefacts, reflecting variation regarding the artefact category.

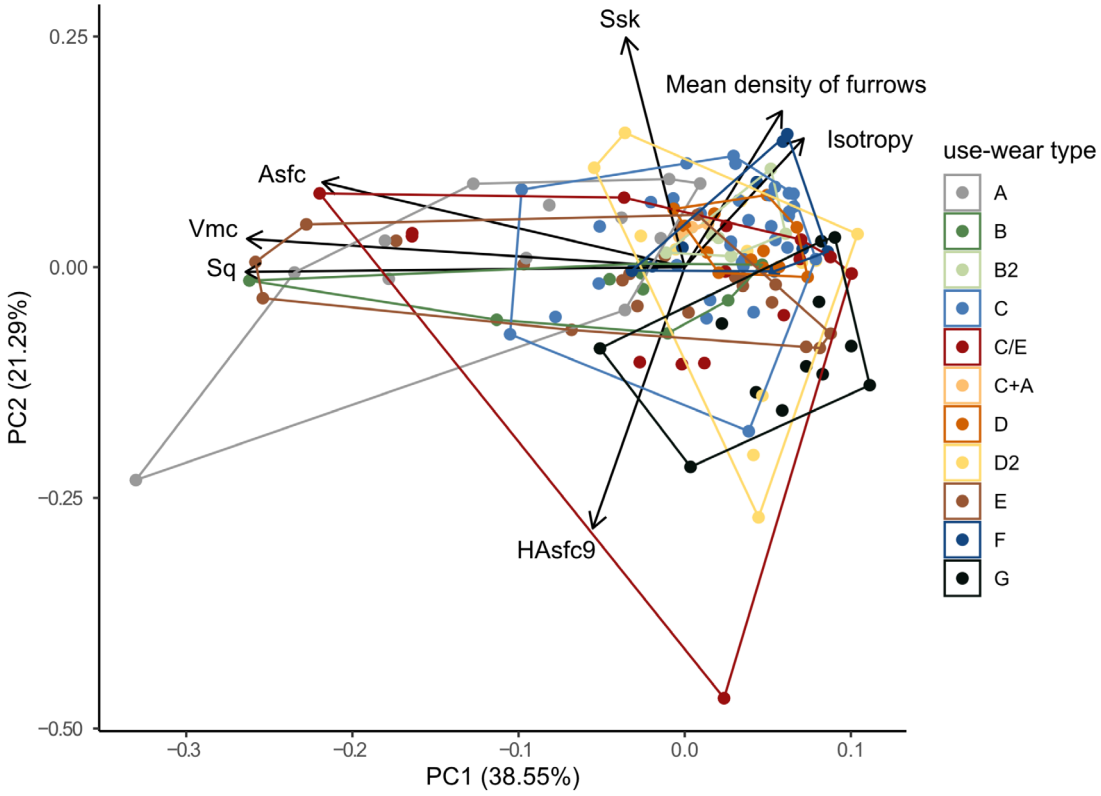

Fig. 127 Principal component analysis applied on the measured use-wear traces (n = 50) of the artefacts, reflecting variation regarding the interpreted use-wear types.

CONTROLLED EXPERIMENTS

The last subchapter refers to the results from the conducted so-called controlled or *second generation experiments* (*sensu* Marreiros et al. 2020). These experiments aimed at understanding the influence of specific, individually tested variables. These independent variables were the raw material and the edge angle of the standard samples, the contact material and the performed task. In order to test the effect-causation of these variables within a complex system, a mechanical device, the modular material tester SMARTTESTER®, was used to perform defined actions. Designed as sequential experiments, this also allowed for investigating the mechanics affecting tool performance and the formation of-use wear traces. Together, the execution of the experiments aimed at understanding the tool design of *Keilmesser* from a mechanical and practical point of view. At the same time, they were meant to test the possibility of successfully performing the two tasks, cutting and carving, with a specific edge design. In the following subchapter, the results are presented in the exact order, the experiments have been conducted: initial experiment, »artificial VS. natural« experiment and tool function experiment.

Data analysis – initial experiment

The first in the sequence of experiments was the so-called initial experiment (**fig. 36**). The purpose of this experiment was to test the experimental setup and to receive a first impression on the influence of the chosen variables within the setup. In total n = 7 standard samples (3× silicified schist 40°, 2× silicified schist 60°, 1× flint 40°, 1× flint 60°) were tested in a linear cutting movement on an artificial bone plate. Each sample had to perform in four cycles. Based on the uniform documentation of the standard samples before and after each cutting cycle it is possible to reveal precisely at which stage and location alteration in the sense of material loss, fractures, retouch etc. occur throughout the sequential experiment. In general, alteration has been documented via 3D scans and EDF images taken with a digital microscope as well as measurements based on the weight and the volume. However, the volume could not be calculated in the case of the samples from the initial experiment. The proximal part of the standard samples were fixed in a metal sample holder (**fig. 128**). This was done in order to guarantee that the samples can be fixed easily and cannot move in the sample holder of the SMARTTESTER®. During the course of the initial experiment, the metal attachment turned out as a weak point in the experimental setup. Thus, the metal attachment was slightly modified for the second experiment. After testing it on a few samples again, it was finally discarded. It became evident that an additional sample holder was not needed. Whenever a sample had this additional metal attachment, it was difficult to scan this area due to the high reflections of the material. Most of the time, the metal area was covered with a black fabric during the scanning process so that it was excluded from the documentation. Hence, the 3D models from the standard samples are missing their base. 3D models, which do not have an entirely closed mesh, are unsuitable for calculating the volume.
One important characteristic of a *second generation experiment* is the repeatability of the experiment and with thus the reproducibility of the data. As explained beforehand, the SMARTTESTER® was connected to five sensors throughout the experiments. In this way, the predetermined factors velocity, acceleration and force were sensor recorded. Two additional sensors measured the penetration depth and the friction. The initial experiment was meant to test the reliability of these controlling mechanisms. Thus, the data was checked frequently. The data set can be found on GitHub [https://github.com/lschunk/Initial_experiment-sensor_recording]. As shown by the data plot (**fig. 129**), force, friction, velocity (including acceleration) and depth are controlled throughout the experiment. Shown here are the measurements for one cycle of

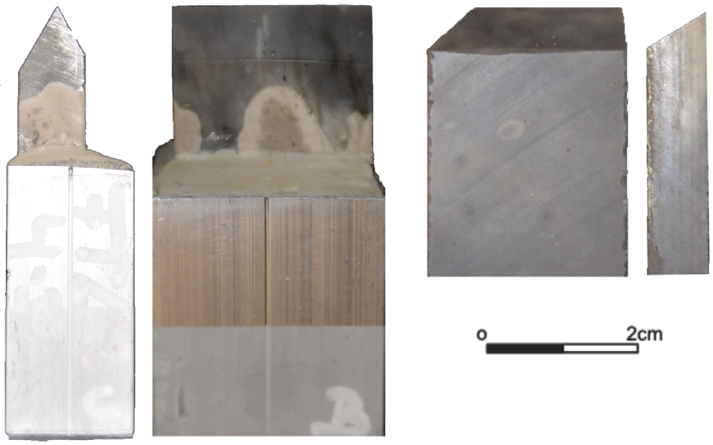

Fig. 128 Design of two standard sample (flint) illustrating the changes in design from the initial experiment to the later ones. The sample on the left side is fixed in a metal sample holder as used during the initial experiment. Moreover, the sample is bifacially cut. The sample on the right has no sample holder and is only unifacially cut. Additionally, this sample is modified by a 45° chamfered edge. – Scale 1:1.

50 strokes made with one standard sample (LYDIT1-2). Except for a few outliers in the force plot, the lines displaying each stroke are always following the same pattern. The data produced by the depth sensor at the bottom right, documents the increased depth of penetration by the standard sample with every cut.
All seven samples were used to perform the four cycles. Within these cycles of in total 2000 cutting strokes, the progressive alteration of the standard sample surfaces is recognisable (**fig. 130**). When looking at the samples with the 40° edge angle, the tool damage on the flint specimen is lower than the damage on the

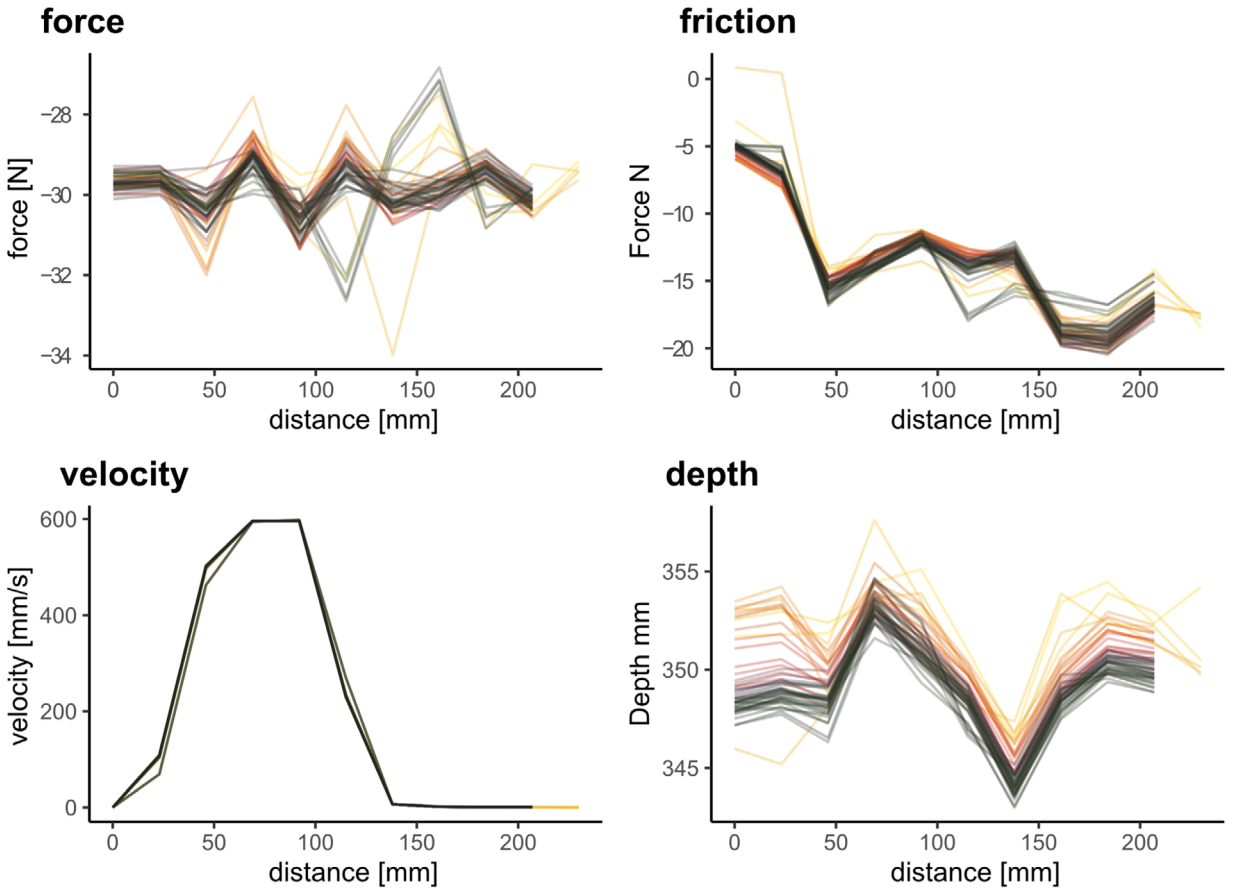

Fig. 129 Sensor data from a cycle of 50 cutting strokes performed with the SMARTTESTER® using the sample LYDIT4-2. Each line reflects one cutting stroke. The first stroke is in yellow and with increasing stroke number, the colour of the line turns darker. The graph illustrates that the predetermined factors force, friction and velocity stayed constant (as set) throughout the experiment. The graph in the lower right corner (depth) displays the achieved penetration depth, which increases throughout the 50 performed cutting stokes.

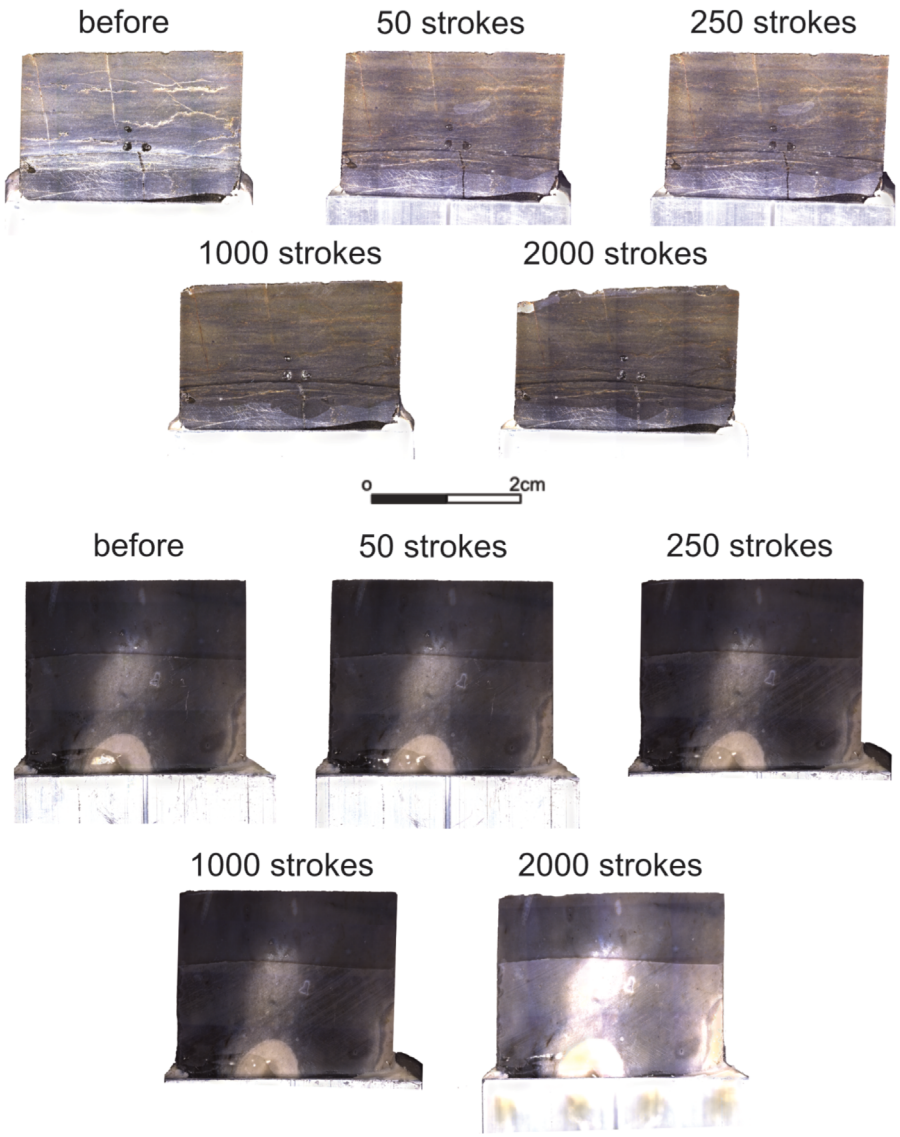

Fig. 130 Standard samples made of lydite (row one and two) and flint (row three and four) illustrating the alteration experience throughout the sequential experiment. – Scale 1:1

lydite samples. The material loss is also reflected in the weight measurements. In fact, one lydite sample (LYDIT1-4) performed only 1368 strokes instead of the targeted 2000 strokes. The cycle had to be ended at that point, because the sample could not perform the task anymore due to a breakage. Standard samples with the 60° edge angle do not show this difference between the raw materials. Only minor edge fragmentation (barley macroscopically visible) could be documented in both raw materials. Higher fragmentation changes the edge angle as well as the tool performance. Tool performance was only assessed based on visual estimations. As defined, tool performance describes how well a task, here the cutting, was accomplished. This can be assessed by correlating the cutting depth with the material loss on the standard sample and on the contact material. Since one factor, the calculation of the material loss based on the standard sample volume was not possible, this was not done for this initial experiment. Nevertheless, the tool performance can be partially assessed based on the contact material, the artificial bone plate. The first aspect that can be noticed is the quality of the cuts. The first three cuts on the bone plate are made by lydite samples, the fourth by a flint sample (**fig. 131**). All four samples had a 40° edge angle. While the flint sample cut appears as a thin line, the cut created with the lydite samples are broader and less fine. The same can be noticed for cuts produced with the 60° samples. The lydite cuts are not only wider they also achieve a greater cutting depth. A new line needed to be used for one sample (LYDIT3-2) during the last cycle. After

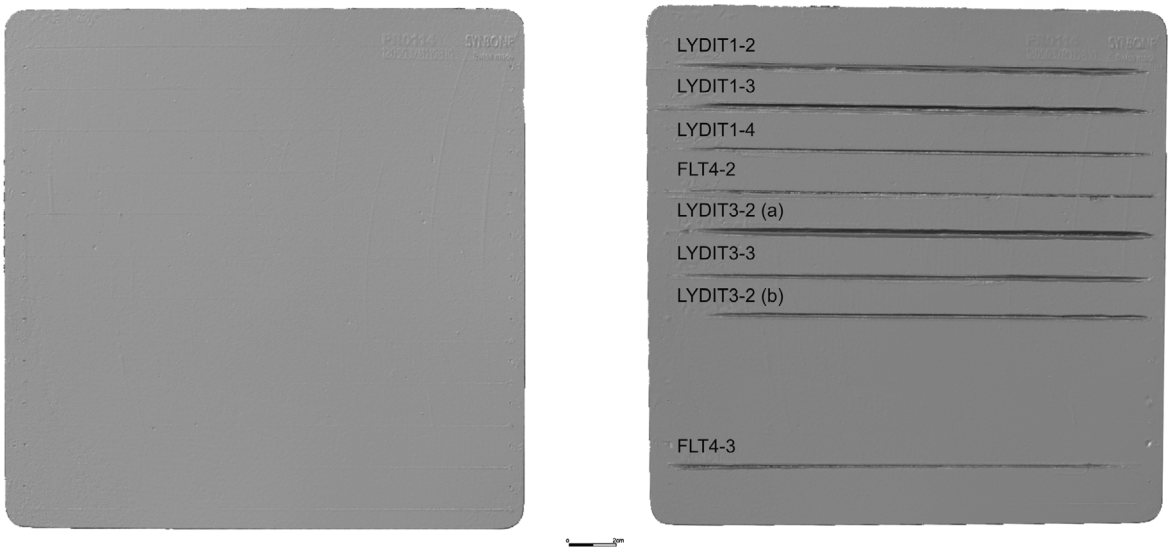

Fig. 131 3D scan of the artificial bone plate used during the initial experiment. The left side shows the plate before the use, the right side after 2000 strokes performed with seven standard samples.

1000 strokes, the generated cutting depth was nearly equal to the thickness of the bone plate. In order to avoid a damage of the mechanics below the bone plate, a new cutting track was started. Visually judged, this above mentioned lydite sample was not the only sample creating a deep cut. It seems as if the cutting depth generated by the lydite samples in general is deeper than the ones from the flint samples. Likely, this aspect can be combined with the edge angle changes of the samples.

The edge angles of all samples were calculated before and after each cycle. This was done based on the 3D models, as previously explained. Although the edge angles were calculated with the three different measurement procedures respectively, only the results from the »3-point« procedure will be presented here (fig. 132). The entire dataset can be found on GitHub [https://github.com/lschunk/edge_angle_experiments]. The data as well as the plot illustrates clearly, that the 40° and 60° flint samples change the edge angle in the course of the experiment only insignificantly. The same counts for the two 60° lydite samples. The change of the edge angles in these samples is about maximum 3° and thus also in the threshold of the expected inaccuracy of the measurement method. The 40° lydite samples did change more significantly. Throughout the first 250 strokes, the edge angles of the three lydite samples altered only slightly as described for the other samples. Distinct changes occurred during the penultimate and especially during the last cycle. While this means a difference of about 10° from the initial 40° edge angle in two lydite samples, one sample altered much more. The edge angle of the sample LYDIT1-4 changed from 40° to roughly 50° after 1000 strokes and above 100° throughout the last cycle.

Altogether, the preliminary observations made during the initial experiment show a reproducible trend: lydite breaks more easily than flint when the tool has a low edge angle (= 40°). With a higher edge angle of 60° this difference between flint and lydite can no longer be observed (Schunk et al. 2019). At the same time, lydite seems more efficient in the sense of the achieved cutting depth. The more fragile the raw material, the bigger the risk of damages, which can affect the durability. In the case of the more fragile lydite, increasing the edge angle leads to an improved durability. Efficiency and durability both play a role when evaluating tool performance.

Neither a qualitative nor a quantitative use-wear analysis was done on the samples from the initial experiment.

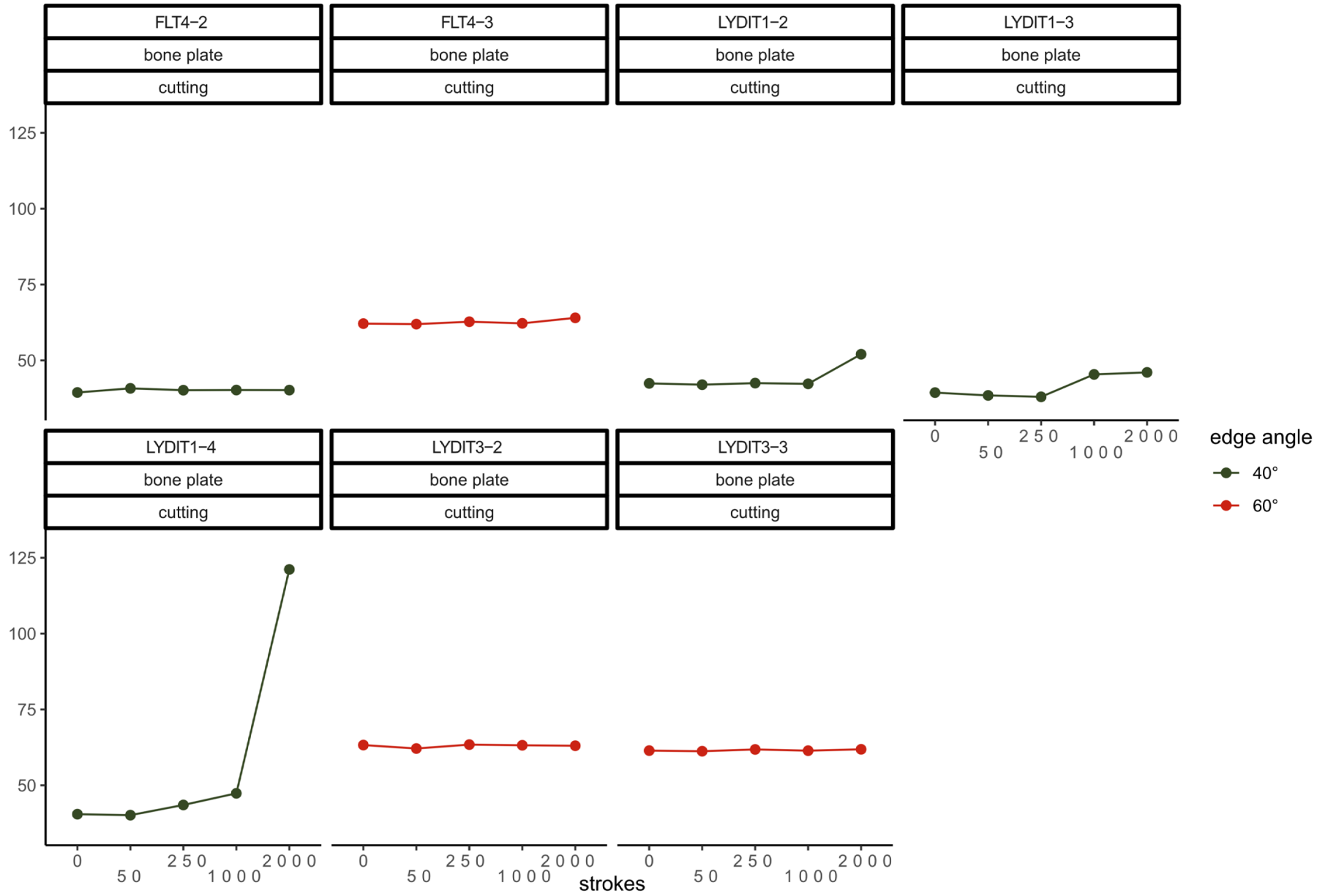

Fig. 132 Edge angle values calculated per sample used during the initial experiment (calculated with the »3-point« procedure; mean value of section 2 to 8 and distance 3 to 6). The data points per sample represent the values after the performance of each cycle (0, 50, 250, 1000 and 2000 cutting strokes).

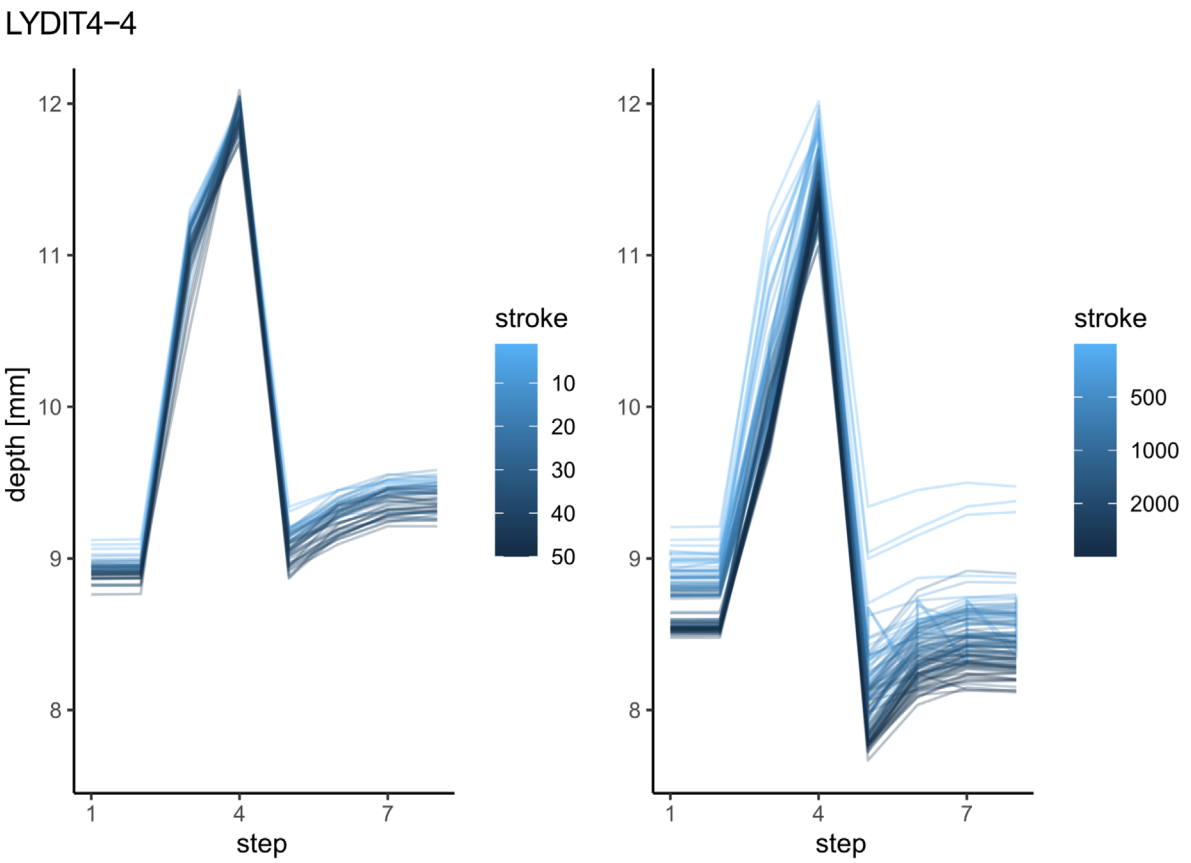

Fig. 133 Sensor recorded penetration depth achieved with a cutting movement performed with the SMARTTESTER® during the »artificial VS. natural« experiment. Exemplarily presented here the recording of sample LYDIT4-4. The left graph shows each cutting stroke within the first cycle (0 to 50 strokes). The right graph shows each 40th cutting stroke within all cycles (0 to 2000 strokes). The darker the colour, the greater the penetration depth.

Data analysis – »artificial VS. natural« experiment

The second experiment was the »artificial VS. natural« experiment (**fig. 37**). The goal of the experiment was to evaluate, whether standardised, artificial contact materials lead to comparable results as the use of natural contact material does. Simultaneously, this experiment was meant to add more data on how the independent variables – here raw material and contact material – influences tool efficiency, durability and performance. Concerning the use-wear, this experiment was also meant to provide data in order to test and understand the mechanics behind the formation of use-wear traces. Moreover, the reflection of these processes in the quantitative data should be investigated.

The twelve lydite and the twelve flint samples were all unifacially cut with a 60° edge angle. The samples were tested in four cycles on a bone plate with a rubber skin layer, a fresh cow scapula, a soft tissue pad and a piece of natural pork skin. All 24 samples passed through the four cycles and completed the 2000 cutting strokes respectively.

The first analysed aspects were the sensor data from the SMARTTESTER®. As explained in the method chapter, the focus thereby was lying on the data from the depth sensor. The penetration depth for each sample was recorded throughout the entire experiment. The data was plotted per sample (**fig. 133**). The plots always show in one plot each single stroke from the first cycle (n = 50 strokes) and every 40th stroke

from all the four cycles together in a second plot. These plots illustrated a continuous increase in depth with a rapid penetration during the first 250 strokes (dependant on the contact material). Unfortunately, some issues with the software of the SMARTTESTER® can be noticed similarly. Some of the plots show clear outliers with sudden changes in depth. These are part of the data, but could be identified as wrong recoding due to problems with the software. Moreover, the absolute penetration depth per sample was calculated (**figs 134-135**). The plots of these calculations reveal some interesting aspects. First of all, the samples reached a greater cutting depth on the natural contact materials compared to the artificial contact materials. More surprisingly is that the lydite samples performed better than the flint ones. Except for the skin pad, where the results are similar between the samples from the two raw materials, lydite tends to achieve a higher cutting depth.

Identical to the initial experiment, the edge angle values of all samples during the different stages were calculated (**fig. 136**). Before explaining the results, it has to be mentioned that a few data points are misleading. The scans from one sample, LYDIT4-9, are slightly problematic. The scans after 50 strokes and after 1000 strokes displayed some small holes on the edge, indicating that the edge was not perfectly scanned. These holes needed to be filled in order to calculate the edge angle values. Apparently, the filling was not accurate enough. These two data points are wrong and do not display the real edge angle values. That these data points are incorrect can be reconstructed by inspecting the raw data of the 3D models and the EDF pictures of the edge. For the mentioned two samples, no visible change occurred during the corresponding cycles. One other sample displays misleading results. The sample FLT4-7 got damaged right before it was used in the experiment. Due to this damage, the cutting edge of the standard sample was partly modified. One half of the edge was still complete and displayed the typical diamond band saw cut, the other half looked retouched (**fig. 137**). Since it takes many hours to produce such a standard sample, it was decided to use this sample as initially planned. The sample was documented again and treated as any other new sample. However, the edge angle of the retouched part of the standard sample was slightly higher than the targeted 60°. Therefore, the mean edge angle of sample FLT4-7 deviates with ~ 66° from the other standard samples. For the remaining edge angle calculations, no mistake could be identified. For the twelve samples (lydite and flint) used on the soft materials, natural pork skin and artificial soft tissue pad, no significant change could be documented. All edge angle changes are within the approximated 3° threshold of the expected impreciseness of the measurement method. The results differ when looking at the samples used to cut the hard contact material, fresh cow scapula. The samples used on the fresh cow scapula are characterised by alteration along the standard sample edge. The alteration occurs directly during the first cycle and proceeds continuously throughout each cycle. The edge angle values shift about 3° to 9°, whereas the edge alternation is slightly bigger for the lydite samples than for the flint samples. The results for the samples used on the second hard material, the artificial bone plate, are comparable to the results from the soft contact material. One exception should be mentioned. Sample LYDIT4-2 displays a small alternation of the edge of about 6° in total. Here, the modification is also characterised by a continuous process starting already during the first cycle. To summarize, the hard contact material favours alteration of the standard samples. This process was documented on the flint standard samples as well as on the lydite standard samples. However, this effect is stronger in lydite. The last aspect is emphasised by the results from sample LYDIT4-2.

The qualitative and quantitative use-wear analysis was done for eight samples from the »artificial VS. natural« experiment (see **appendix II**). These eight standard samples have been selected systematically so that four flint and four lydite samples were involved in the analysis. *Per* raw material, there was one sample respectively tested from each of the four contact materials. For the qualitative use-wear analysis, the »dorsal« (A and B) and the »ventral« surface (D and C) were analysed with the upright light microscope (ZEISS Axio Scope.A1 MAT). All use-wear traces are illustrated as figures in the supplementary material.

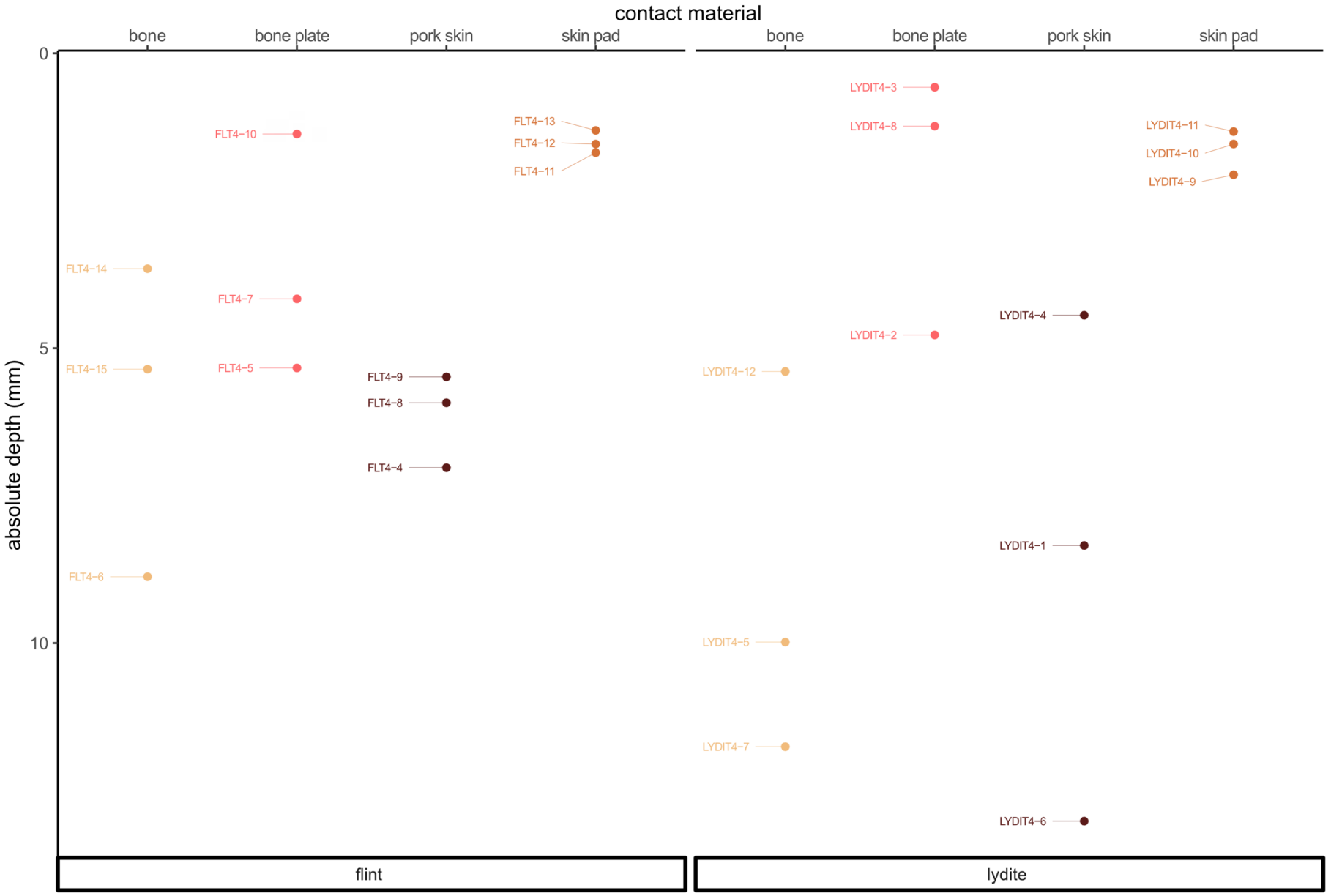

Fig. 134 Absolute cutting depth of all samples used during the »artificial VS. natural« experiment. The samples are organised according to the standard sample raw material and the contact material.

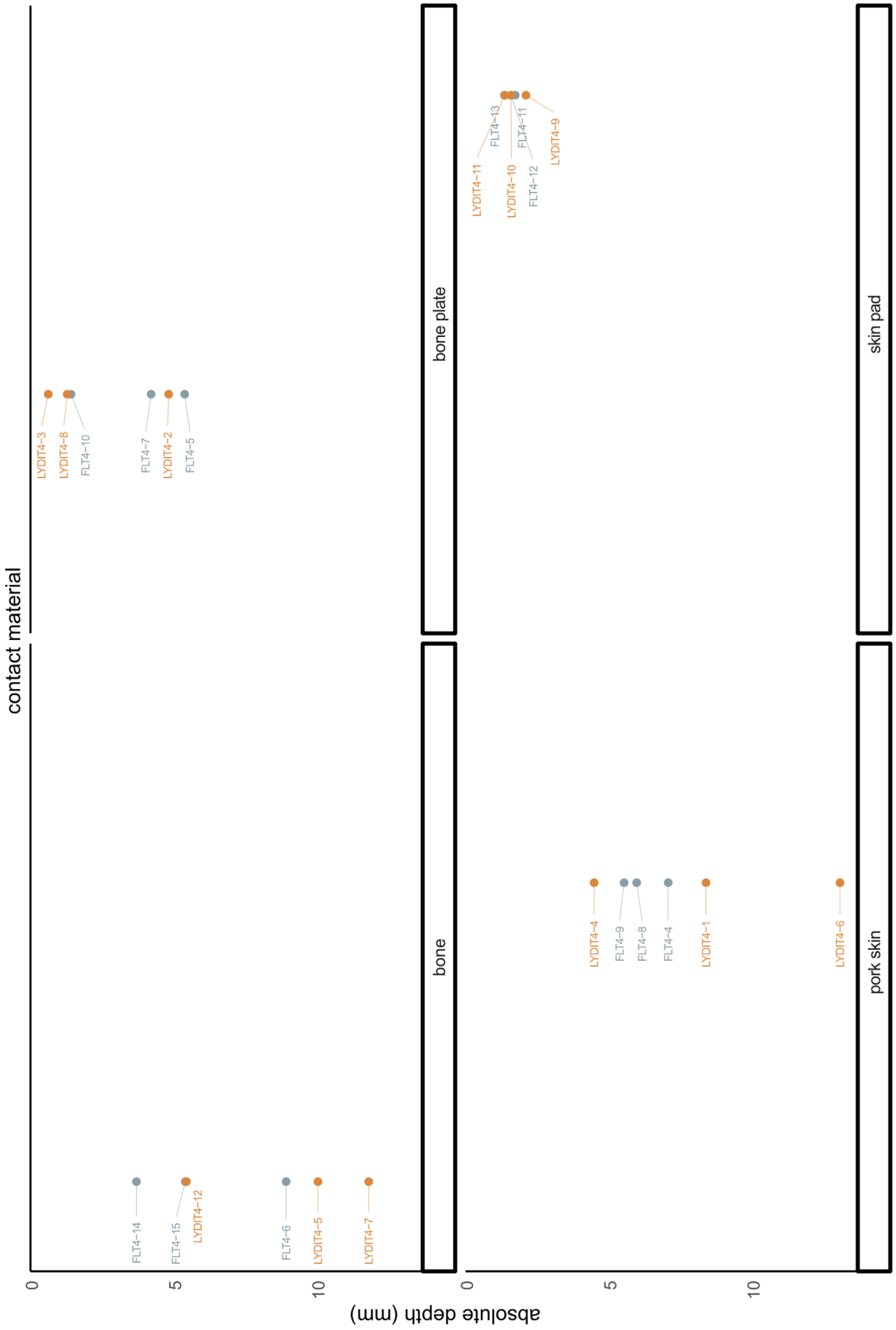

Fig. 135 Absolute cutting depth of all samples used during the »artificial VS. natural« experiment. The samples are organised according to the contact material.

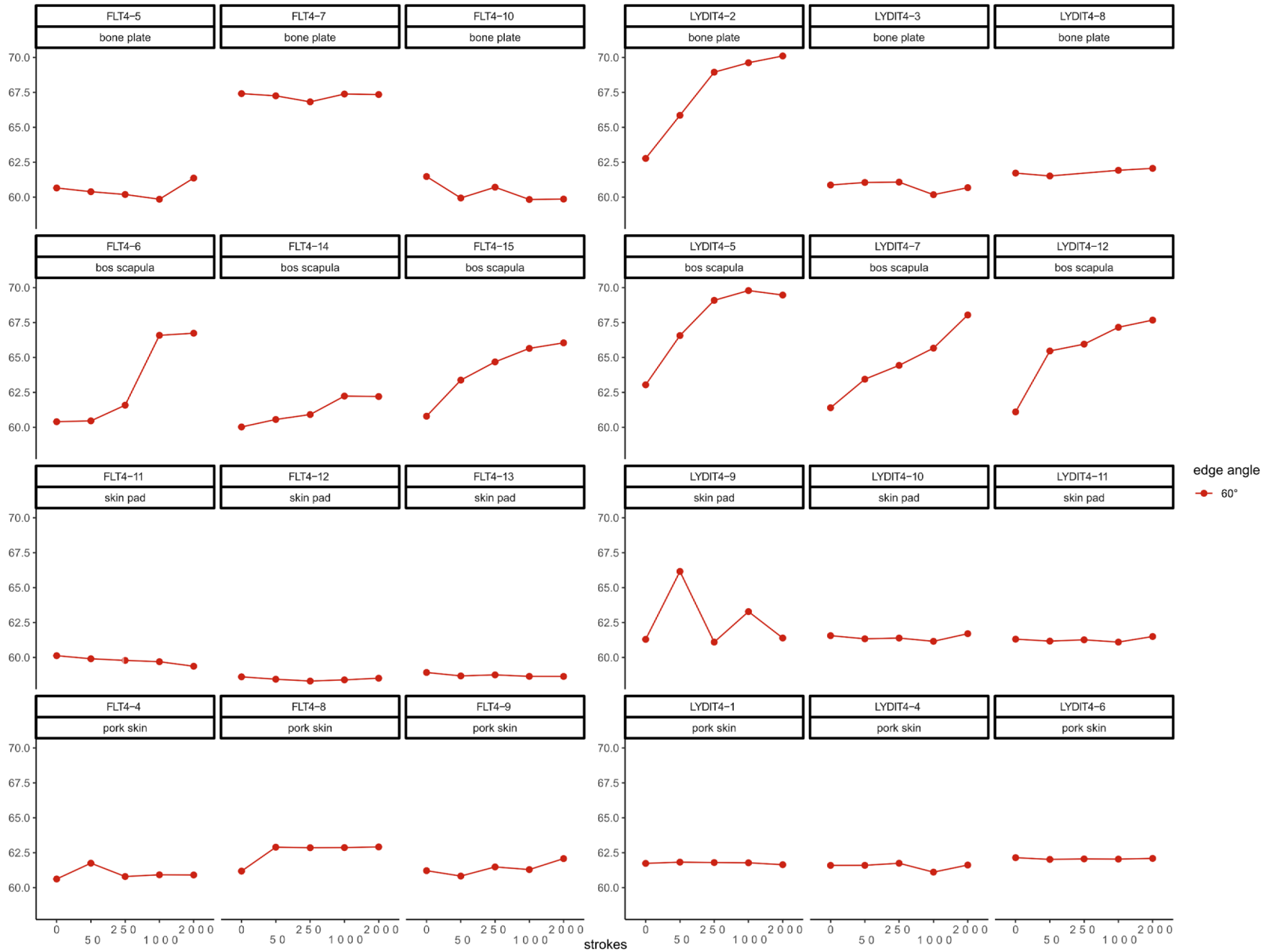

Fig. 136 Edge angle values calculated per sample used during the »artificial VS. natural« experiment (calculated with the »3-point« procedure; mean value of section 2 to 8 and distance 3 to 6). The data points per sample represent the values after the performance of each cycle (0, 50, 250, 1000 and 2000 cutting strokes).

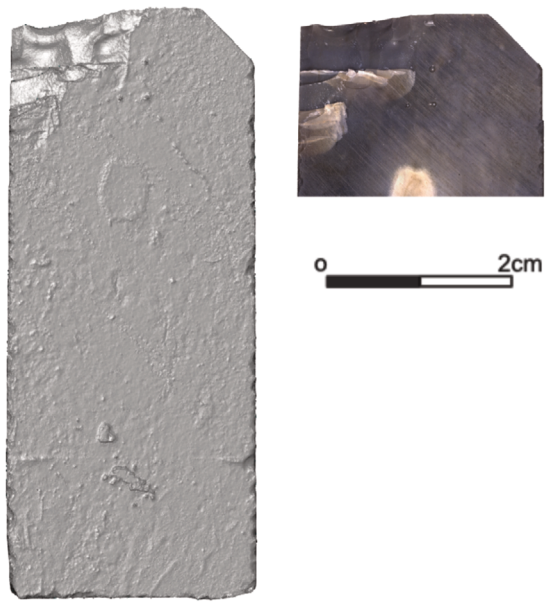

Fig. 137 Flint standard sample FLT4-7 as 3D scan (left) and EDF-stitching image of the edge (right) used during the »artificial VS. natural« experiment. The sample is damages on the left side. – Not to scale.

The question behind the use-wear analysis was to see how, where and when use-wear develops on the standard samples. Another question was, whether or not the use-wear traces produced with the natural contact material differ from the ones produced with the artificial contact material or vice versa. To answer these questions, the selected eight samples (moulds) were microscopically analysed before and after each cycle. To start with the soft contact material again, first the results for the natural pork skin will be explained (**figs 138-139**). On the flint sample (FLT4-4), there is no development of use-wear visible until 1000 strokes. Use-wear is visible on the »dorsal« (B) surface. The spot is further developed after 2000 strokes. The lydite sample (LYIT4-1) used on the natural pork skin starts to develop some use-wear traces after 250 strokes (D), but identifiable use-wear traces are only visible after 2000 strokes (A, B, D). However, the surface shows in the beginning clear traces of the diamond band saw cut and these traces turned weaker within the first cycles. The same can be noticed for the lydite sample (LYDIT4-9) used on the artificial soft tissue pad. Throughout the cycles, the initially visible traces from the diamond band saw abrade and disappear, the »natural« surface seems to appear and during the last cycle, use-wear traces develop (B). The situation is similar for the corresponding flint sample (FLT4-12). The flint sample (FLT4-7) used on the artificial bone plate only displays clear use-wear traces (A, B) after 2000 strokes. By contrast, use-wear traces (A, C) on the lydite sample (LYDIT4-2) are already visible after 50 strokes. Both samples (FLT4-15 and LYDIT4-5), which were used on the fresh cow scapula, show traces right after the first (lydite: A, B) and second cycle (flint: B, D). Only the traces on the »ventral« surface (D) of the lydite sample occur as distinct traces not until 1000 strokes.

The qualitative analysis could prove that use-wear traces do develop on the standard samples, although they are missing the surface texture characteristic for the material. Moreover, these observations clearly show that the harder the contact material, the easier is it for use-wear traces to develop. At the same time, a modification of the standard sample surface occurs faster on lydite than on flint. The answer for the comparability between natural and artificial contact materials is less straightforward though. Visually inspected, the traces produced by both groups of contact material do appear similar. The developed polished areas do look typical for hard and soft contact materials. However, the process, when the traces develop, is not always comparable. The results for the lydite samples are identical on the natural as well as on the artificial contact materials. The lydite samples used on both soft contact materials display use-wear traces after 250 and 1000 strokes, the ones used on both hard contact materials after 50 strokes. The situation for the flint samples is different. While cutting, the natural soft contact material led to use-wear traces after 1000 strokes, the artificial soft contact material did not produce use-wear traces before the 2000 stroke cycle. The sample used on the natural hard contact material developed traces after 50 strokes, while traces from the artificial hard contact material appeared not until 1000 strokes. Unfortunately, only one sample per raw material and contact material was analysed, so that the results are not statistically evaluable.

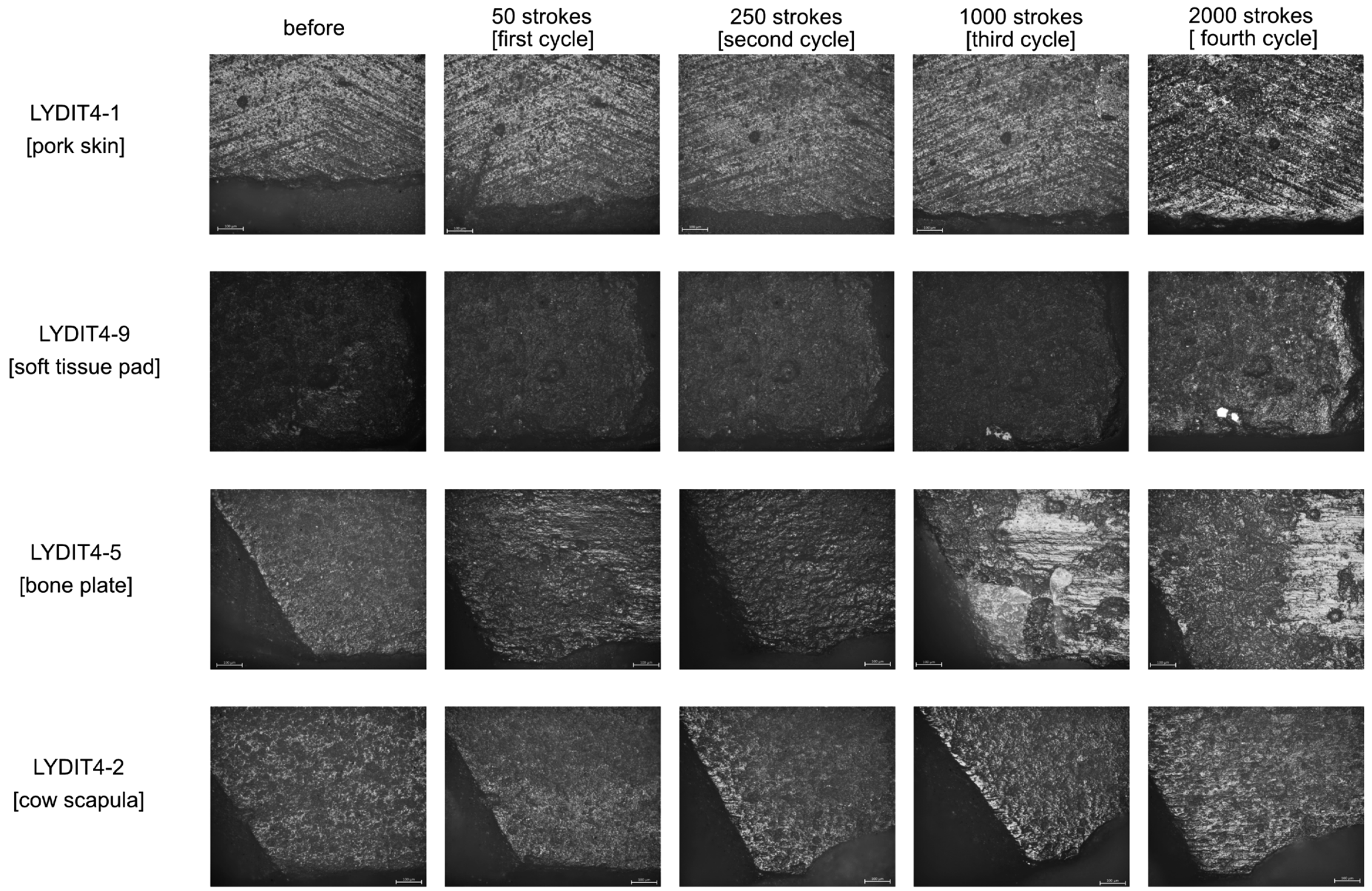

Fig. 138 Use-wear formation on the analysed lydite standard samples during the four cycles of the »artificial VS. natural« experiment (all images are taken with a 10× optical objective).

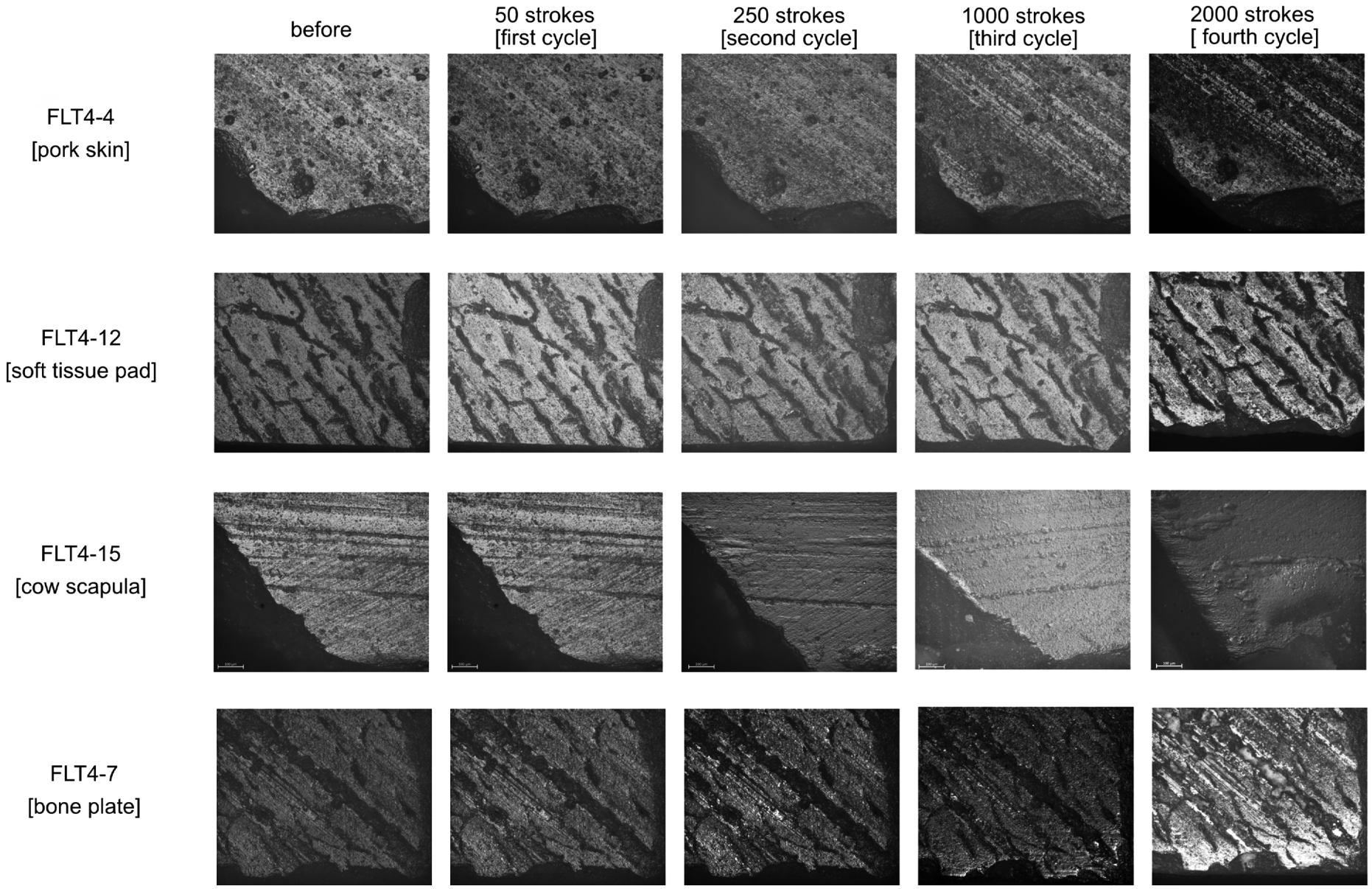

Fig. 139 Use-wear formation on the analysed flint standard samples during the four cycles of the »artificial VS. natural« experiment (all images are taken with a 10× optical objective).

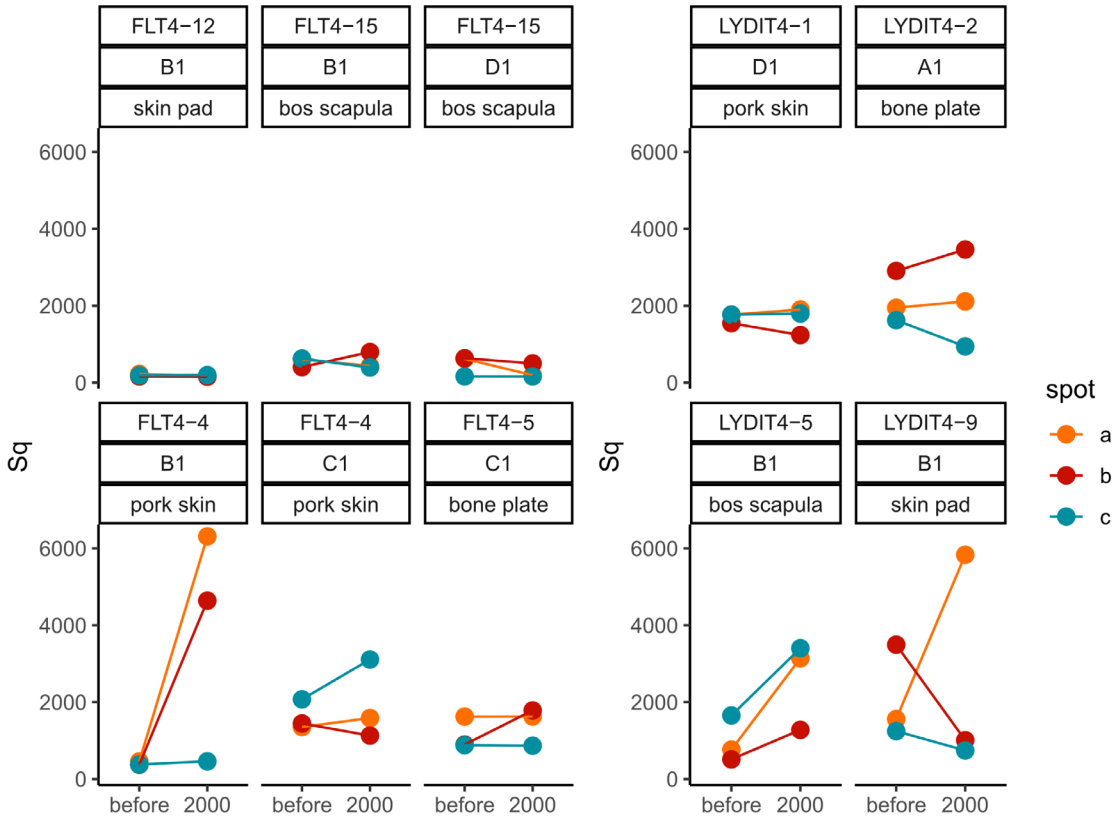

Fig. 140 *Sq* values before and after 2000 cutting strokes measured on identical spots on each standard sample used during the »artificial VS. natural« experiment respectively. Spot a, b and c refers to the three measurements taken per use-wear trace.

Additionally, a quantitative use-wear analysis was conducted. The same eight samples were used for the analysis, but only the moulds from before the experiment and after 2000 strokes were analysed. Thanks to the coordinate system (beads; Calandra et al. 2019a) on each tool surface, it was possible to relocate to the identical spot on the before and after surface. Thus, variability due to positional inaccuracy could be excluded. Generally, one spot per sample was selected for the quantitative use-wear analysis. Two samples constitute an exception: on two flint samples (FLT4-14 and FLT4-15) two instead of one spot were measured. Scans were acquired on well-developed polished areas (after 2000 strokes). As done already for the quantitative use-wear analysis from the archaeological material, each use-wear trace was measured three times (a-c) on nearby, but not identical spots. In total, n = 30 measurements were taken on the samples from before the experiments and n = 30 on the samples from after 2000 strokes. Identical to the qualitative use-wear analysis performed on the archaeological samples, the data was acquired to the ISO 25178-2. Furthermore, the same 21 ISO 25178-2 parameters, three furrow parameters, three texture direction parameters, one texture isotropy parameter and the SSFA parameters *epLsar, NewEplsar, Asfc, Smfc, HAsfc9 and HAsfc81* were calculated on each surface (**tab. 11**).

A first attempt to review the data was done by plotting the data in a scatterplot per parameter (**figs 140-141**). These scatterplots include information about the sample, the raw material and the contact material as well as the location (A-D). The data is illustrated in a way that the results from before and after 2000 strokes can be compared directly.

Four data points, identified as outliers, need to be mentioned. Since the use-wear on the standard samples is extremely marginal due to the low penetration depth into the contact material, it was often difficult to acquire the data without scanning beyond the edge. Whenever this happens, such areas are interpreted

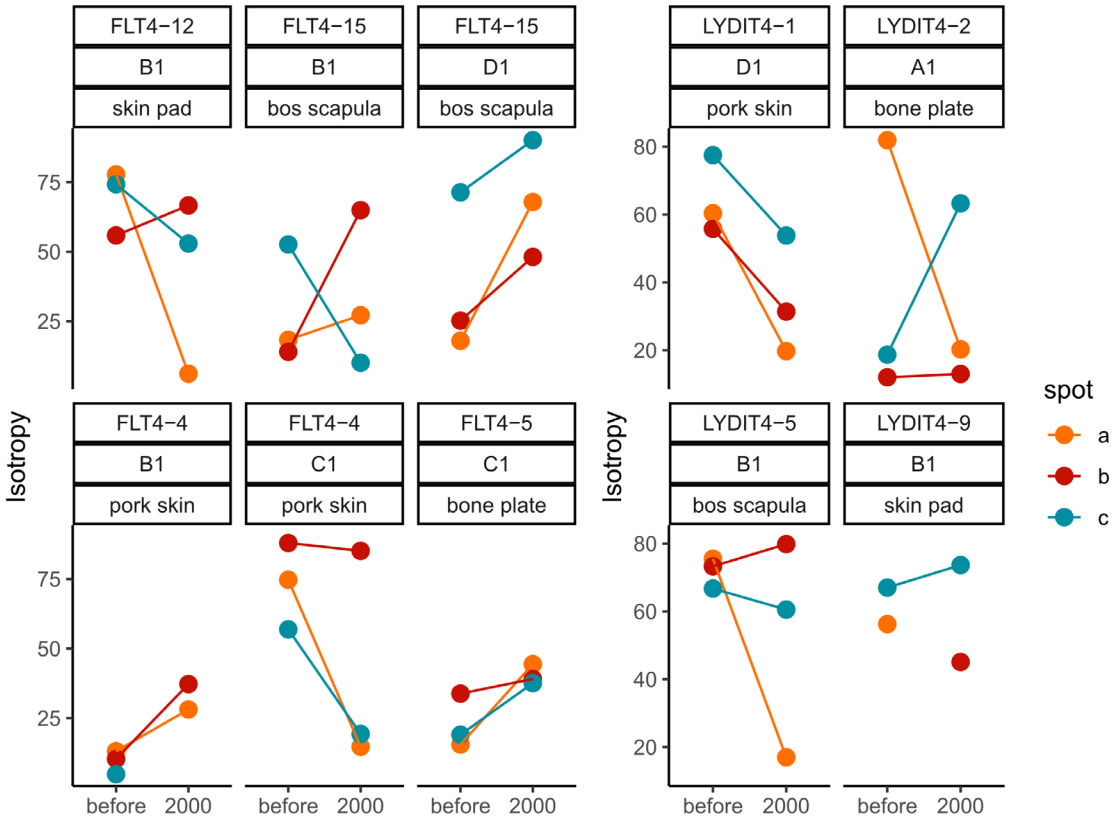

Fig. 141 *Isotropy* values before and after 2000 cutting strokes measured on identical spots on each standard sample used during the »artificial VS. natural« experiment respectively. Spot a, b and c refers to the three measurements taken per use-wear trace.

as non-measured points. Filling these data points to calculate the parameters leads to divergent results. Unfortunately, that happened in four cases. The samples LYDIT4-9-B1-b (before), FLT4-4-B1-a, FLT4-4-B1-b and LYDIT4-9-B1-a (all 2000 strokes) need to be treated as outliers and excluded from interpretations. Most of the parameters, as for instance *Sq*, *Vmc, Sxp* or *Sdr* change from before to after 2000 strokes only insignificantly. For single samples, as for example the sample LYDIT4-5, the surface roughness seems to increase after 2000 strokes. Clear changes are noticeable when looking at the *isotropy* or *epLsar* (equal to anisotropy) (**fig. 141**). With some exceptions within the flint samples (FLT4-5-C1, FLT4-15-D1), the *isotropy* values decrease from before towards 2000 strokes. This means, the directionality of the surface is getting higher, and the surface is getting less similar in all directions. It seems as if directionality of the surface, characterised by the diamond band saw cut, stands in contrast to the directionality of the use-wear traces. In another plot type, the three measurements per use-wear traces were taken together and the arithmetic mean values per use-wear trace were calculated (**fig. 142**). These plots only emphasize, what was pointed out before. Based on the calculated ISO parameters, there is no significant recognisable change between before and after the 2000 strokes. The only exception still, is sample LYDIT4-5 use on fresh bone. Nevertheless, it seems as if the initial surface texture roughness influences how significant the change from before to after the use is. Samples with an initially higher surface roughness seem to experience more change than samples with an initially lower surface roughness. However, a clear shift can be noticed concerning the texture isotropy parameter and the SSFA parameters.

On seven selected parameters, a principal component analysis (PCA) was applied. The same parameters as for the last PCA (see chapter Surface micro texture data analysis) were chosen in order to perform the PCA.

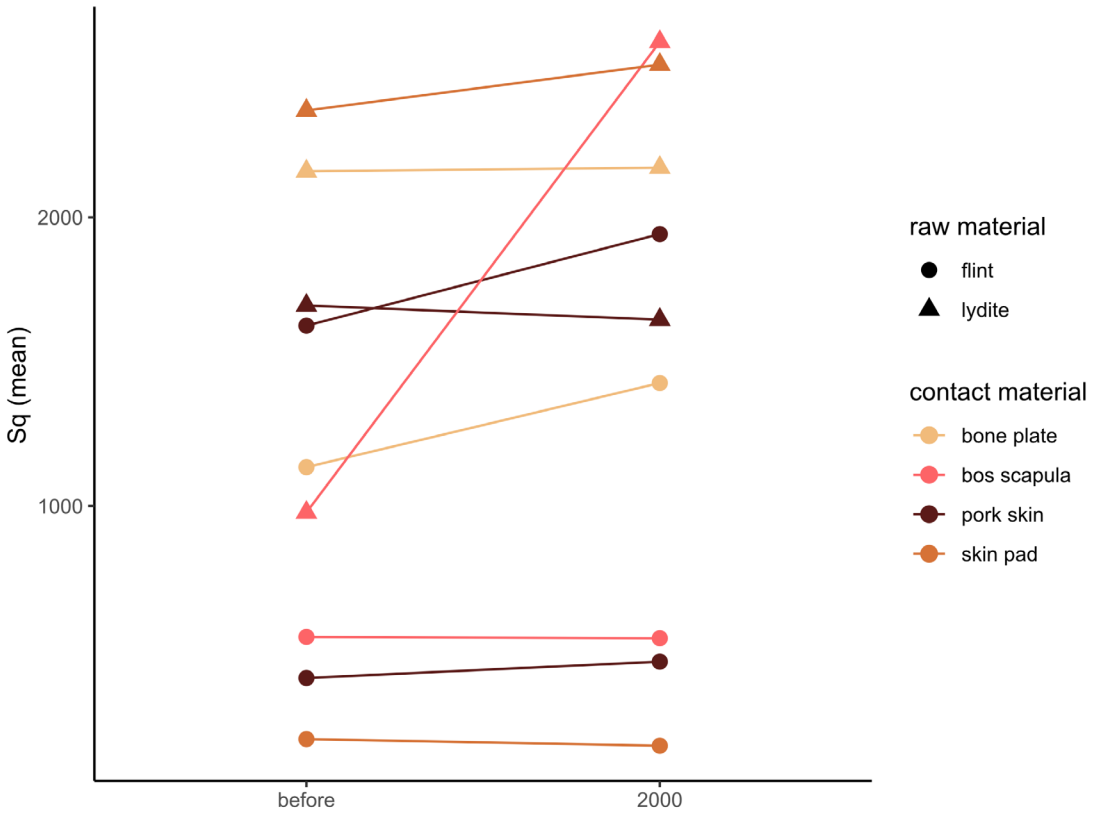

Fig. 142 *Sq* values before and after 2000 cutting strokes measured on identical spots on each standard sample used during the »artificial VS. natural« experiment, respectively. *Sq* reflects the mean value of the three measured spots taken per use-wear trace. The colours indicate the contact material the tool was used on.

These parameters are *Sq, Ssk, Vmc, Mean density of furrows, Isotropy, Asfc* and *HAsfc9*, spanning the different categories of field parameters. The first PCA reflects the variance between the samples used on the four contact materials (**fig. 143**). Principal component 1 (PC1) reflects 39.74 % of the variance in *Sq, Vmc*, and *Asfc*. The variance in *Ssk, Mean density of furrows, Isotropy* and *HAsfc9* is represented by Principal Component 2 (PC2), which accounts for 21.17 %. The data cluster from the four contact materials overlap. Unfortunately, the cluster from the natural contact material and the corresponding artificial contact material differ distinctly in both cases.

A second PCA visualises the variance in the two categories before and after 2000 strokes (**fig. 144**). The two cluster overlap mainly in the left part of the PC1 axis. At the same time, the data points from after 2000 strokes scatter more over the plot. The cluster from before is denser, pointing to more homogeneous data. The results of the quantitative use-wear analysis illustrate the diversity within the measured, individual use-wear traces. While the homogeneity for the three measured spots (a, b and c) *per* use-wear trace is given, this does not count for the use-wear traces on the different samples. The acquired data emphasise that within the selected use-wear traces, a variance exists. This means, the use-wear traces on the flint samples and the use-wear traces on the lydite samples produced on identical contact material respectively, already differ. The same results count for the comparison between the natural and the artificial contact material. The analysis highlights the importance of the amount of data and the relevance of replicas. Here, the acquired data is not statistically evaluable since only one sample per raw material and contact material was part of the quantitative use-wear analysis. Otherwise, it would be interesting to see, whether the data acquired on the replicas used within the experiment would lead to different results within each analysed category.

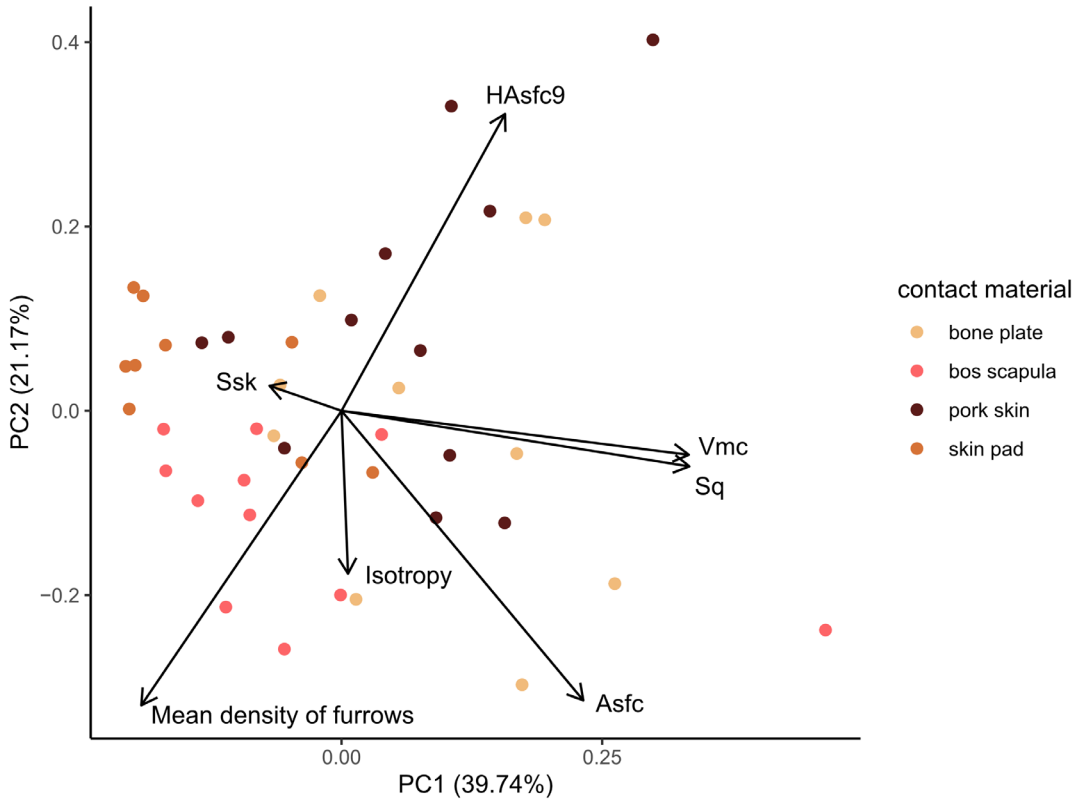

Fig. 143 Principal component analysis applied on the measured use-wear traces of the analysed standard samples from the »artificial VS. natural« experiment after 2000 cutting strokes, reflecting variation regarding the contact material.

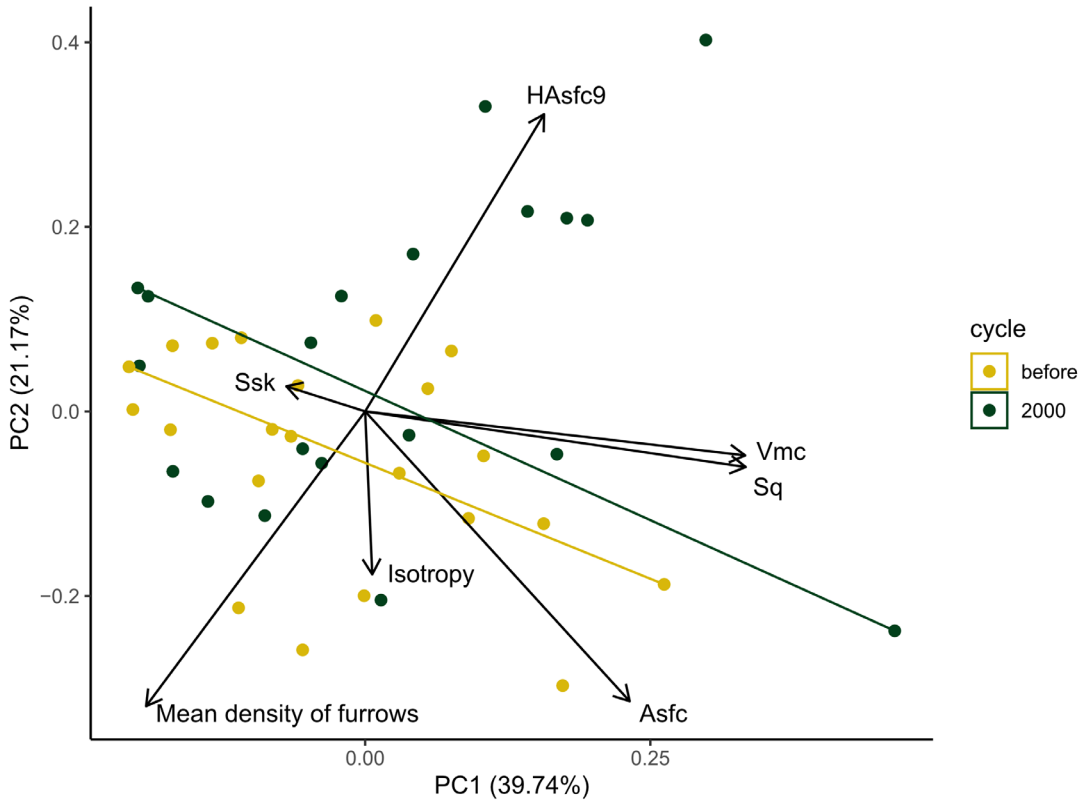

Fig. 144 Principal component analysis applied on the measured use-wear traces of the analysed standard samples from the »artificial VS. natural« experiment, reflecting variation regarding before and after 2000 cutting strokes.

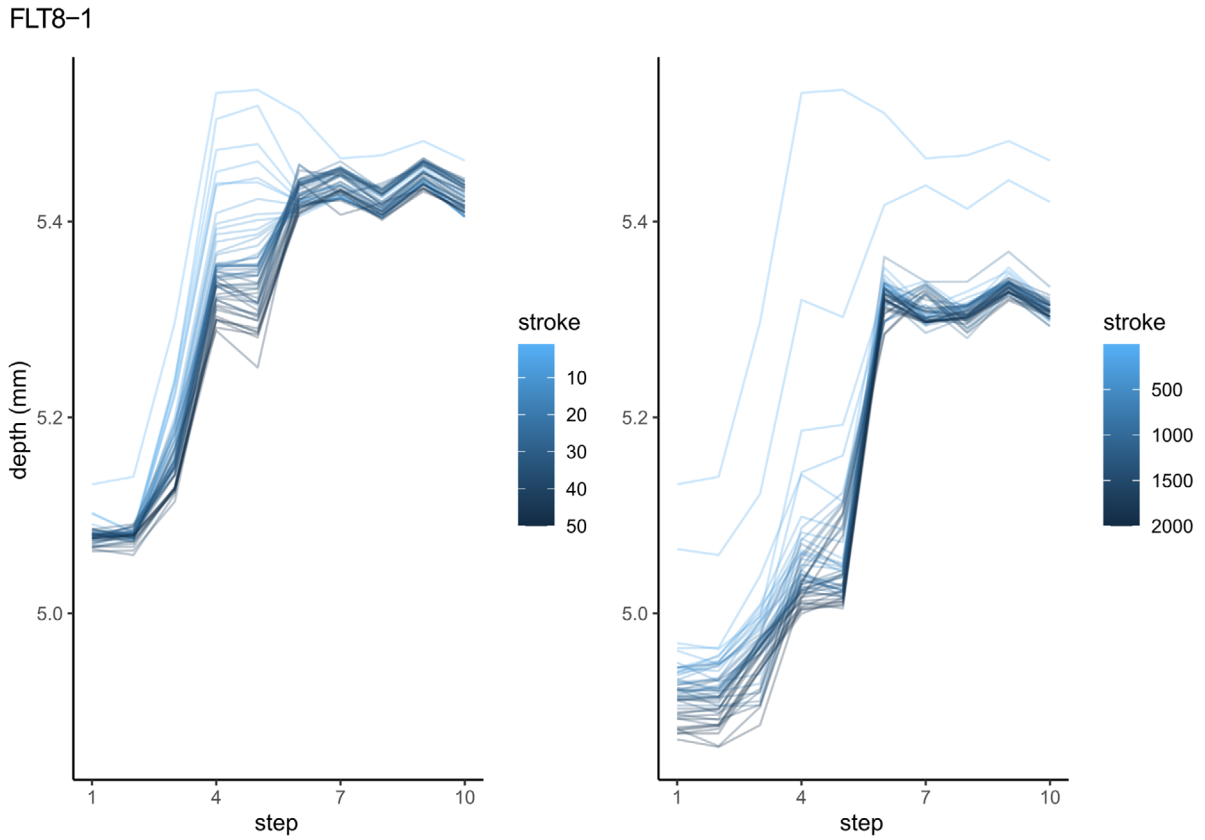

Fig. 145 Sensor recorded penetration depth achieved with a cutting movement performed with the SMARTTESTER® during the tool function experiment. Exemplarily presented here the recording of sample FLT8-1. The left graph shows each cutting stroke within the first cycle (0 to 50 strokes). The right graph shows each 40th cutting stoke within all cycles (0 to 2000 strokes). The darker the colour, the more increased is the penetration depth.

Data analysis – tool function experiment

The final experiment was the tool function experiment (**fig. 38**). Raw material, edge angle and movement served as independent variables. Tool efficiency, durability and performance were tested on artificial bone plates. In total 24 unifacially cut standard samples were used. The samples can be separated in the following groups: twelve flint and twelve lydite standard samples with six times 35° and 45° edge angle each. Three samples per category were used for cutting, three samples per category for carving.

In a first step analogous to the experiment before, the sensor data from the SMARTTESTER® will be presented. In the focus of this analysis stands again the data recorded with the depth sensor. The individual results per sample are accessible as plots showing the first 50 strokes and additionally each 40th stroke combined (**fig. 145**). The plots illustrate a continuous increase in penetration depth throughout the experiment with an especially rapid increase during the first strokes. In order to put the efficiency, here only measured as penetration depth, in relation to all 24 samples, the absolute depth achieved per sample was calculated. As reported for the previous experiment, sometimes software issues with the SMARTTESTER® appeared, leading to wrong recordings. These wrong recordings are identifiable in the plots. Within the recorded data, recorded data for single strokes reaches values beyond the possible moving radius of the mechanical device. Thus, some outliers are included in the data. The outliers are not only visible when checking the individual penetration depth per stroke and sample (**fig. 146**), but also in the plots showing the absolute penetration

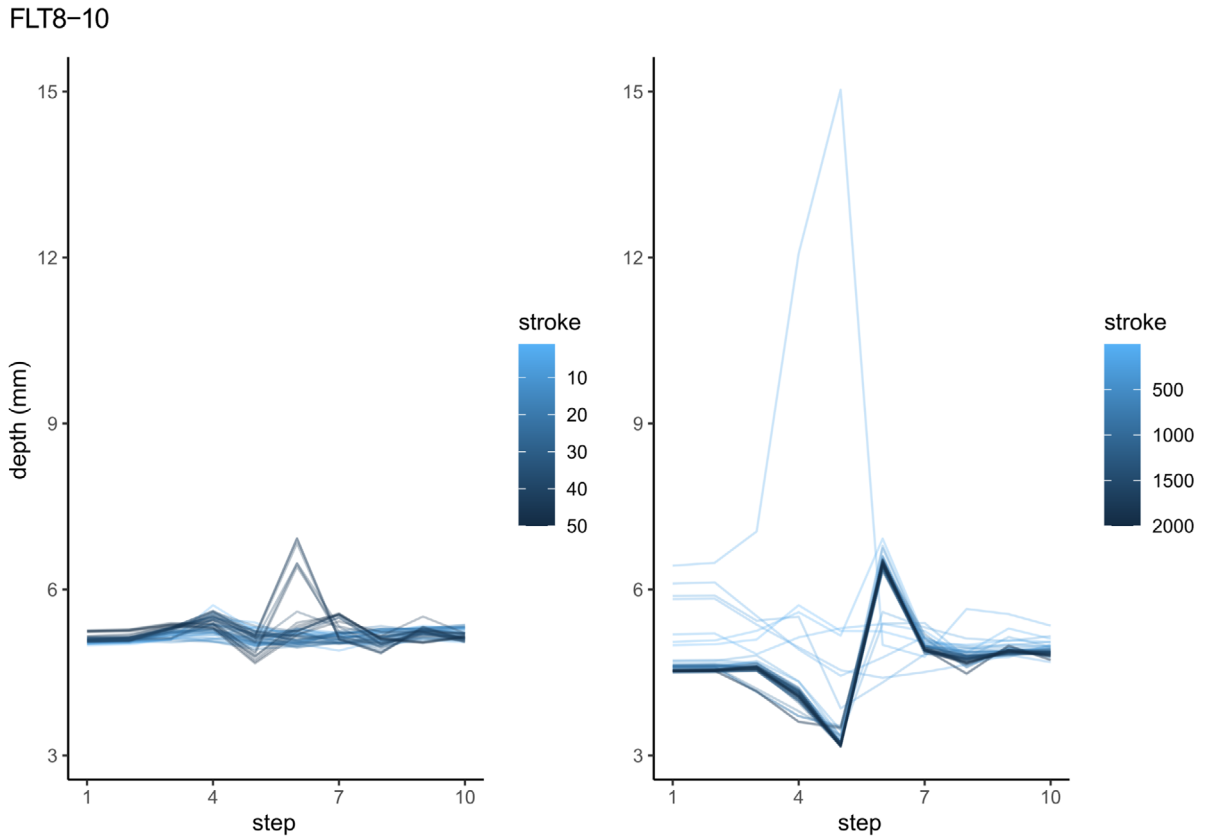

Fig. 146 Sensor recorded penetration depth achieved with a carving movement performed with the SMARTTESTER® during the tool function experiment. Exemplarily presented here the recording of sample FLT8-1. The left graph shows each cutting stroke within the first cycle (0 to 50 strokes). The right graph shows each 40th cutting stoke within all cycles (0 to 2000 strokes). The recording includes outliers as displayed with the light blue line reaching up to 15 mm depth. The darker the colour, the more increased is the penetration depth.

depth. This specific plot (**fig. 147**) includes next to the penetration depth also the information about the sample, the raw material, the edge angle and the movement. Three samples, FLT8-3, FLT8-4 and FLT8-10 differ from the other samples. These are the three identified outliers. In order to get a better resolution of the correctly displayed data, the outliers have been removed (**fig. 148**). The biggest penetration depth was reached with a lydite sample (LYDIT5-7). With the exception of this sample, the penetration depth reached during cutting is comparable between the 35° and the 45° samples. Concerning the carving, the 45° samples achieved a comparable higher penetration depth than the 35° samples. A general tendency is that the lydite samples penetrated deeper into the contact materials than the flint samples. While this observation is not so clear for carving, it is undoubtedly seen for cutting.

In regard of tool efficiency, the edge angle measurements need to be mentioned. As for the other two experiments, the edge angles of the n = 24 samples were measured before and after each cycle (**fig. 149**). Before explaining the data, one outlier has to be reported. The first edge angle calculation (before) for sample FLT8-3 is not reflecting the accurate value. This sample was produced with 45° edge angle, but displays a 55° edge angle. An examination of the raw data revealed small holes in the 3D data along the edge. Apparently, also in this case, filling the holes changed the edge angle. However, this is the only data point, which needs to be excluded for interpretation.

The results for cutting differ depending on the edge angle. While the shift in the edge angle is only minimal for the three flint and lydite standard samples with 45°, the results are different for the 35° samples. For one flint sample (FLT8-6), only minimal changes could be observed, but the two other samples (FLT8-4 and

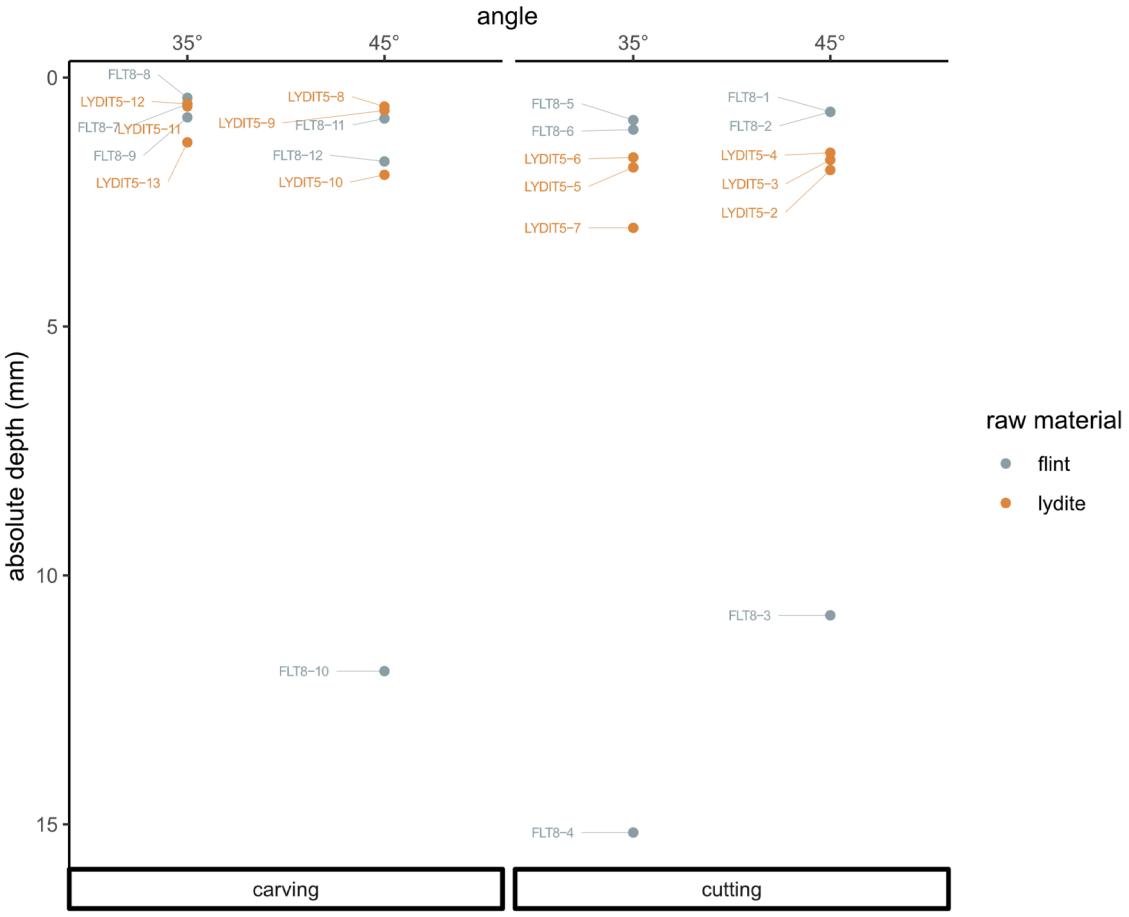

Fig. 147 Absolute cutting depth of all samples used during the tool function experiment. The samples are organised according to the performed task and the edge angle of the standard sample.

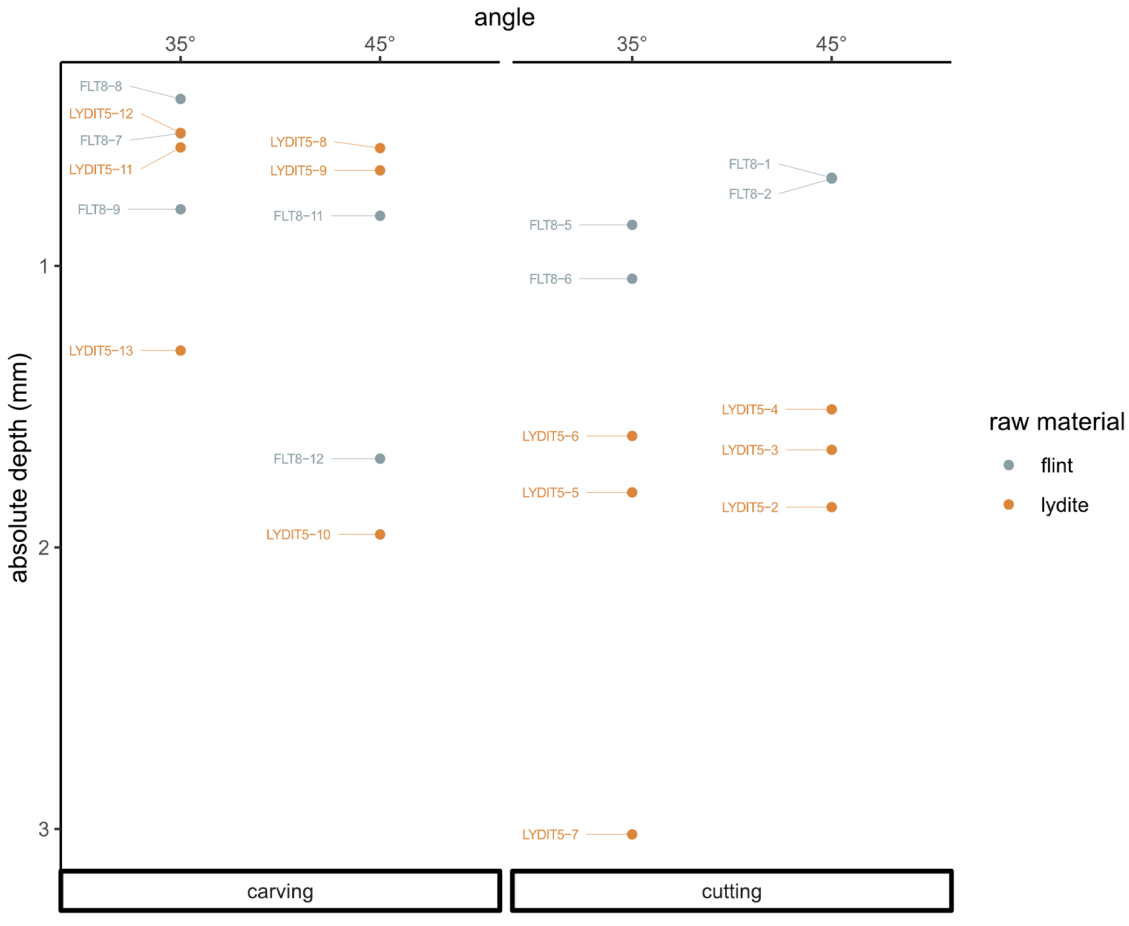

Fig. 148 Absolute cutting depth of all samples used during the tool function experiment. The samples are organised according to the performed task and the edge angle of the standard sample. Outliers removed.

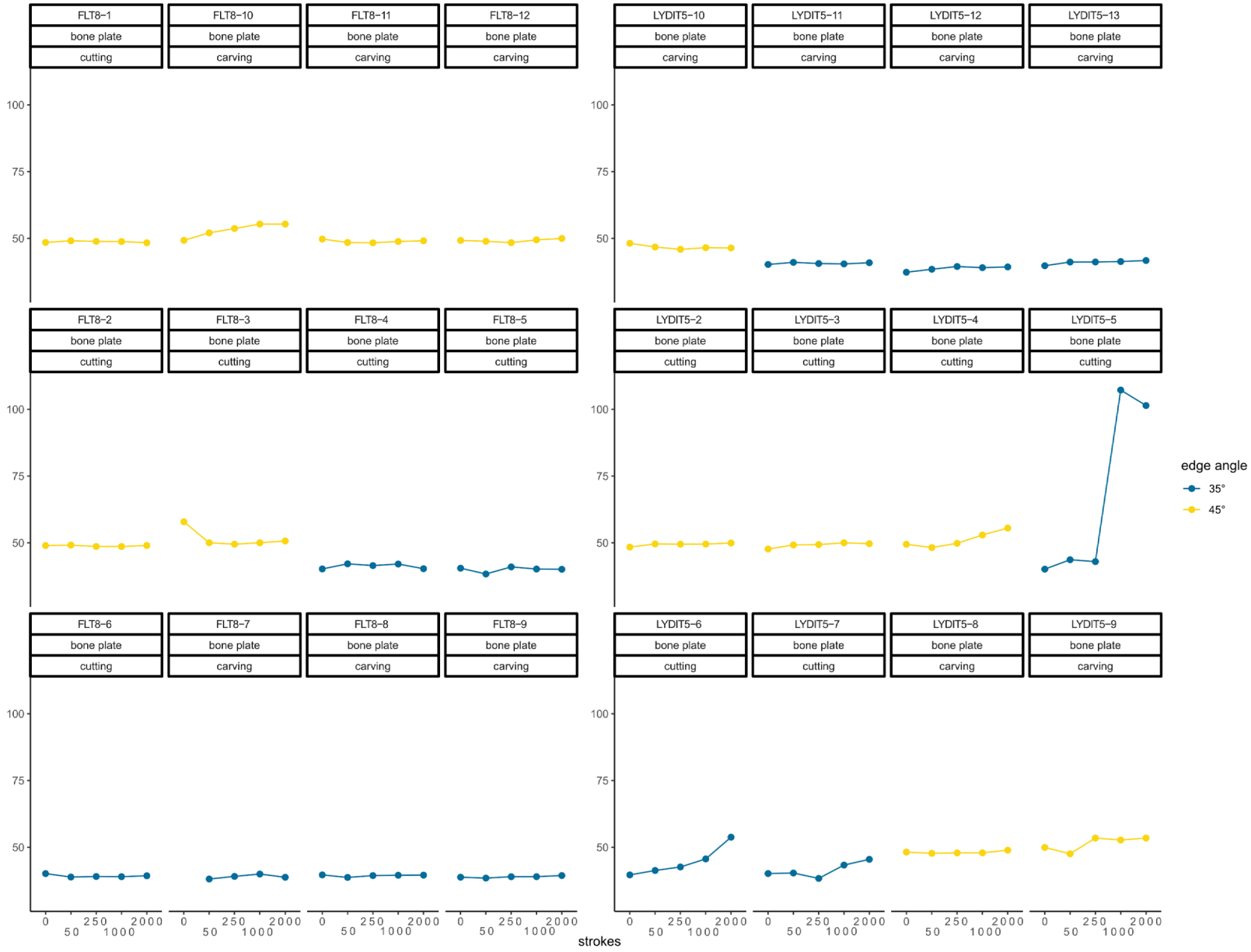

Fig. 149 Edge angle values calculated per sample used during the tool function experiment (calculated with the »3-point« procedure; mean value of section 2 to 8 and distance 3 to 6). The data points per sample represent the values after the performance of each cycle (0, 50, 250, 1000 and 2000 cutting strokes).

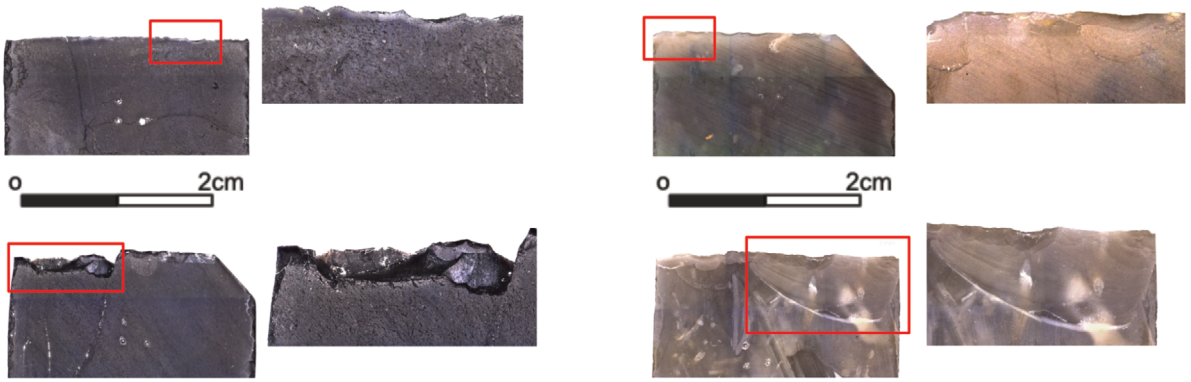

Fig. 150 Tool alteration on standard samples made of lydite (left) and flint (right) after 2000 strokes used during the tool function experiment. – Not to scale.

FLT8-5) display material loss and thus, a slight shift in edge angle values towards increased bluntness. For the three lydite samples with a 35° edge angle, a decrease in acuteness is clearly visible and illustrated by continuous material loss throughout the experiment. One sample changed from 35° to approximated 75° due to a fracture. Surprisingly the six samples with a 35° used for carving did not change significantly. The same counts for a majority of the 45° samples used for carving. Nevertheless, two samples, one flint and one lydite sample, experienced some alternation after 50 strokes, leading in both cases to a continuous but small increase in the edge angle.

In general, the 10° difference between the two sets of standard samples (35° and 45°) seems to make a difference in durability when used to perform cutting strokes. Although, none of the samples were altered or damaged in a way that it could not function anymore. All 24 samples completed the 2000 strokes. However, the 35° samples exhibit more damage in the sense of small fractures and material loss. This observation cannot be transferred to the results from the carving movement. Irrespective of the raw material, more alteration could be documented for the 45° samples.

The edge angle measurements can be correlated with the volume loss of the standard samples. The volume of each sample was calculated based on the 3D models. Thus, the measurements can only be as precise as the quality of the 3D model allows. On average, lydite samples experience a volume loss of 0.21 % (~ 0.37 mm³). Flint samples display a slightly higher volume loss of 0.36 % (~ 0.52 mm³). These values could be verified with the weight measurements. Although the lydite samples fracture more and thus also experience more frequent and significant damage, on average, the material loss is only minor. However, the lydite samples appear more fragile and tiny particles break away, which is reflected in the edge angle measurements (**fig. 150**). By contrast, the flint samples more often display material loss comparable to retouch and not fractures. The retouch-like material loss might go further on the surface and could explain the bigger loss in volume and weight. Moreover, this type of material loss might not change the edge angle in a way that the breaking particles do on the lydite.

Another aspect is the quality of the cuts or scratches produced on the bone plates (**fig. 151**). Quality can be defined by the regularity, the uniformity and the width of the cuts or scratches. In this sense, quality is one relevant aspect in order to evaluate tool performance. As already mentioned for the initial experiment, the cuts produced with flint samples optically differ slightly from the ones produced with the lydite samples. This observation is only based on a visual assessment. The flint cuts appear as thin lines, whereas the lydite cuts seem thicker and less precise. In particular the cuts produced with the 35° lydite samples seem broader. For the majority of the traces left on the bone plates during carving, no significant difference between the

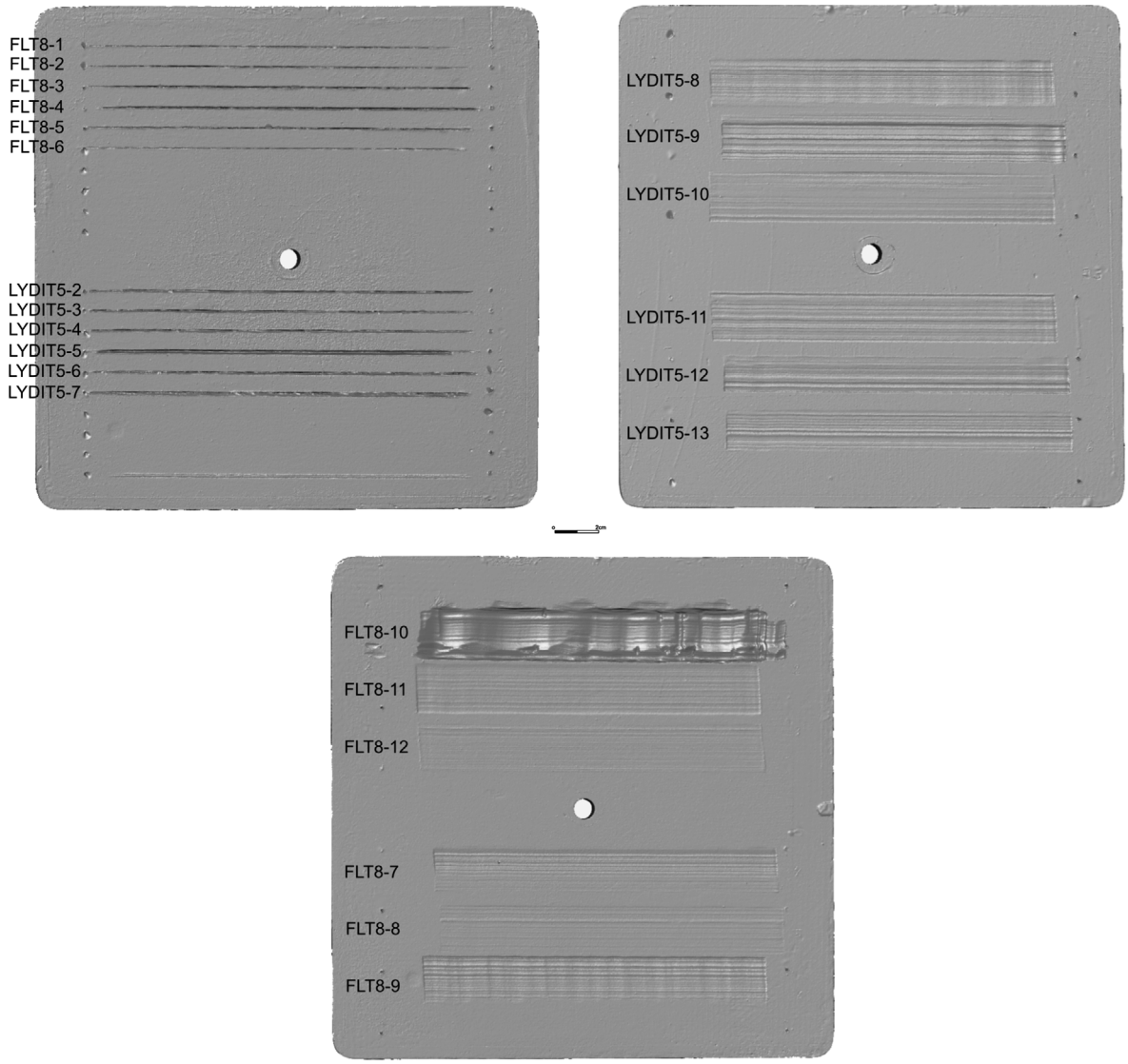

Fig. 151 3D scans of the artificial bone plates used during the tool experiment after 2000 strokes. The upper left scan shows the plate used for cutting, the upper right scan the plate used for carving with lydite samples. The lower scan illustrates the scan of the bone plate used for carving with flint samples.

traces caused by the flint samples and the ones caused by the lydite samples is noticeable. One exception is the trace left by the flint sample FLT8-10. This sample achieved a comparable high penetration depth. During the first cycle, the sample was not perfectly fixed in the sample holder and was able to move a little. Thus, the contact between the sample and the bone plate did not happen exactly parallel to each other. During the second cycle, this problem was solved, and the samples could not move anymore in the sample holder. As a result of the first cycle, the surface of the bone plate (the trace) was a bit uneven causing more resistance and friction which in turn caused more alteration on the tool.

A qualitative and quantitative use-wear analysis was conducted for eight samples from the tool function experiment (see **appendix II**). These eight samples always include one sample *per* raw material, edge angle and movement. For the qualitative use-wear analysis, only the samples from before and after 2000 strokes were analysed. All images of the use-wear analysis can be found as figures in the supplementary material. All four samples used for cutting developed use-wear throughout the four cycles of the experiment (**fig. 152**). The use-wear traces are visible on the »dorsal« as well as the »ventral« surface of the standard

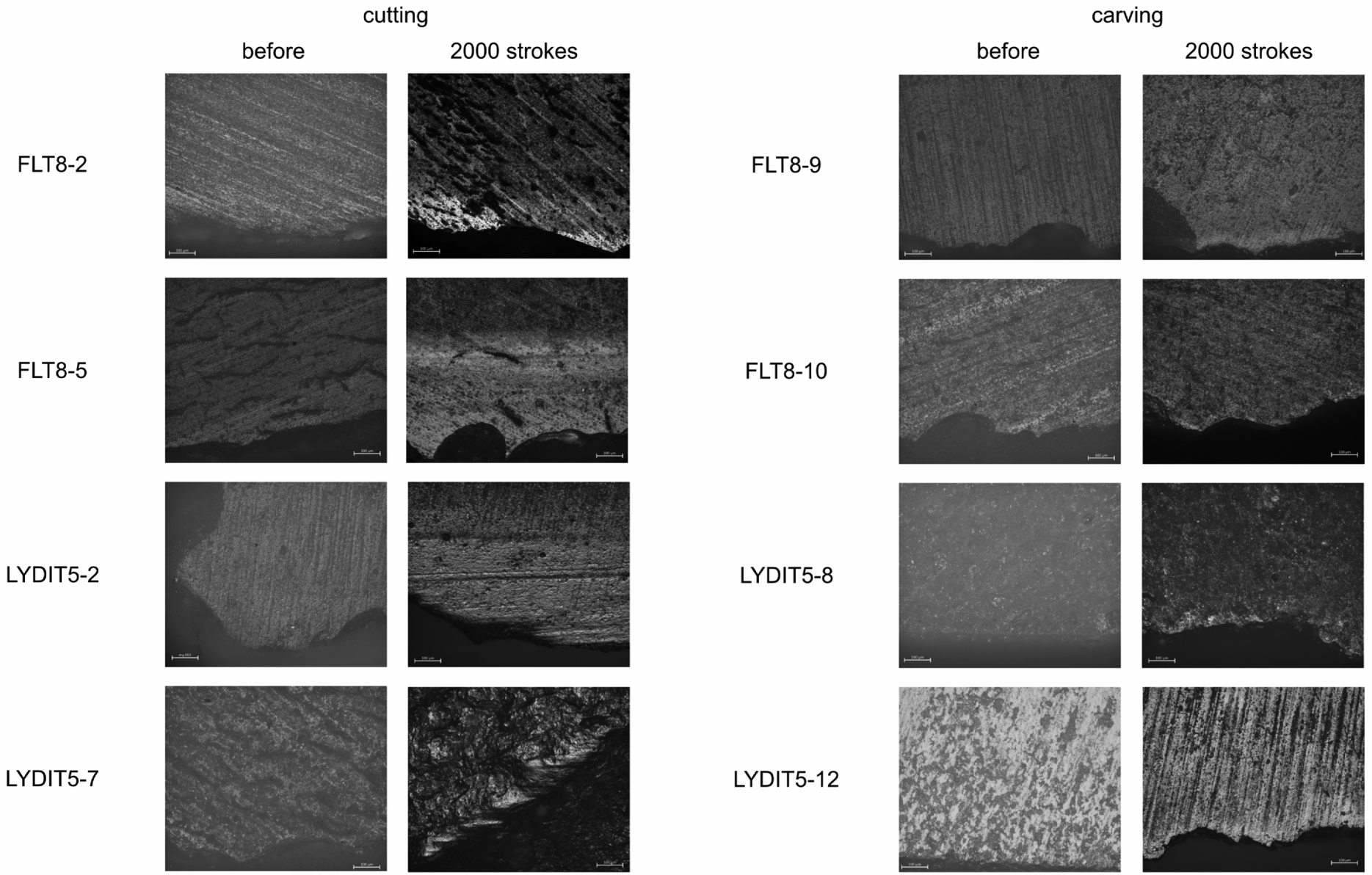

Fig. 152 Use-wear formation on the analysed flint and lydite standard samples before and after (2000 strokes) performing the tool function experiment. The left side shows the samples used for cutting, the right side the samples used for carving (all images are taken with a 10× optical objective).

samples. One exception is the flint sample FLT8-2, which did only develop use-wear on the »ventral« surface (D). The samples used for the carving movement also developed use-wear within the 2000 strokes. However, the use-wear traces are often marginal. The reason for that can likely be seen in the low penetration depth into the contact material. Thus, there was less possibility of friction between the samples and the contact material. While the flint sample FLT8-9 displays use-wear traces on both surfaces, the other three samples developed use-wear traces only either on the dorsal or ventral surface.

The same eight samples were selected for the quantitative use-wear analysis, whereas the data was only acquired on the samples after 2000 strokes. Well-developed use-wear traces were selected for the analysis. The eight traces were measured three times each, as done similarly for the other performed qualitative use-wear analyses. Again, the data was calculated based on the identical 34 parameters (see **tab. 10**). Scatterplots from each parameter combined with information about the sample, the raw material, the task and the edge angle display the results (**fig. 153**). Prominent within these scatterplots are two data points. Both of the data points belong to the categories flint and carving. One of the samples has a 35° edge angle (FLT8-9-B1-01-a), the other one a 45° edge angle (FLT8-10-C1-01-b). These tow samples clearly differ from the corresponding tow measurements per use-wear trace. A review of the raw data made an identification of these two data points as possible outliers. In one case, the acquired data included some data from next to the use-wear trace, in the other case the scan went beyond the edge. In both cases, the results are misleading and should be thus excluded as outliers. Although the data analysis leads to no significant results, differences between the categories are visible. The data acquired on the flint samples used for carving shows a variance between the 35° edge angle results and the 45° edge angle results. Moreover, the results from the sample with the 35° edge angle tend to be more homogeneous. The lydite samples also display differences between the 35° and 45° edge angles, whereas the results are homogeneous in both cases. A significant variance between the two groups of raw material, flint and lydite, are not noticeable.

The data was explored further with a principal component analysis. The PCA was applied on the identical seven components used for the previously described PCAs, the parameters *Sq, Ssk, Vmc, Mean density of furrows, Isotropy, Asfc* and *HAsfc9*. The variance in *Sq, Vmc* and *Mean density of furrows* is explained by Principal component 1 (PC1), reflecting 53.06 % of the variance. Principal component 2 (PC2) accounts for 19.47 % of the variance with *Ssk, Isotropy, Asfc* and *HAsfc9*. The first PCA reflects this variance combined with the movement, cutting and carving (**fig. 154**). The data scatters mainly on the right part of the PC1 axis and clearly overlaps.

A second PCA visualises the variance of the raw material of the standard samples based on the same seven components (**fig. 155**). Although the data overlaps again in the right part of the PC1 axis, the data scatters in different directions.

The only PCA that results in distinct clusters is the third applied PCA (**fig. 156**). This PCA reflects the variance combined with the edge angles, 35° and 45°. The results are consistent with the results mentioned from the scatterplots mentioned before. The cluster from the 35° edge angle is narrow, while the cluster from the 45° is scattered more, likely due to the less homogeneous data.

The data from the quantitative use-wear analysis acquired on the samples from the tool function experiment leads to unexpected results. Neither the raw material of the standard samples nor the performed movement seems to affect the measured features of the use-wear traces. However, the edge angles of the standard samples seem to have an effect.

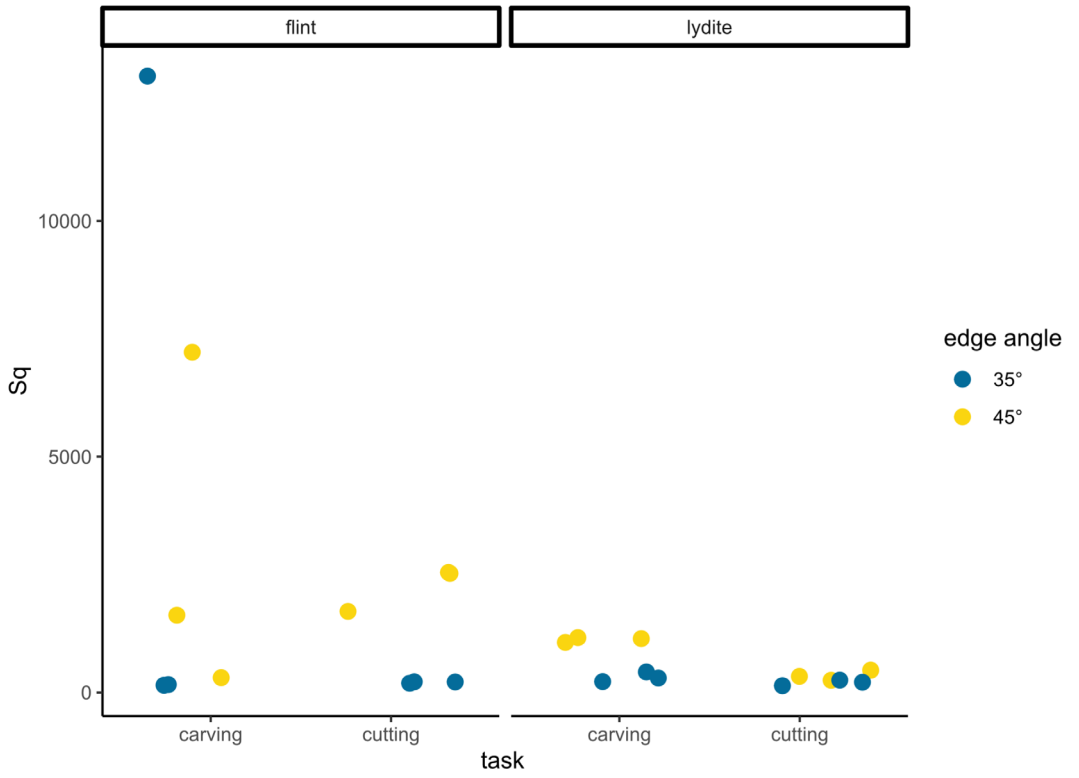

Fig. 153 *Sq* values measured on the flint and lydite samples after 2000 strokes used during the tool function experiment. Three data points are shown per sample, reflecting the three measurements taken per use-wear trace (spot a, b and c). The data is categorised according to the performed task. The colour indicates the edge angle of the standard samples.

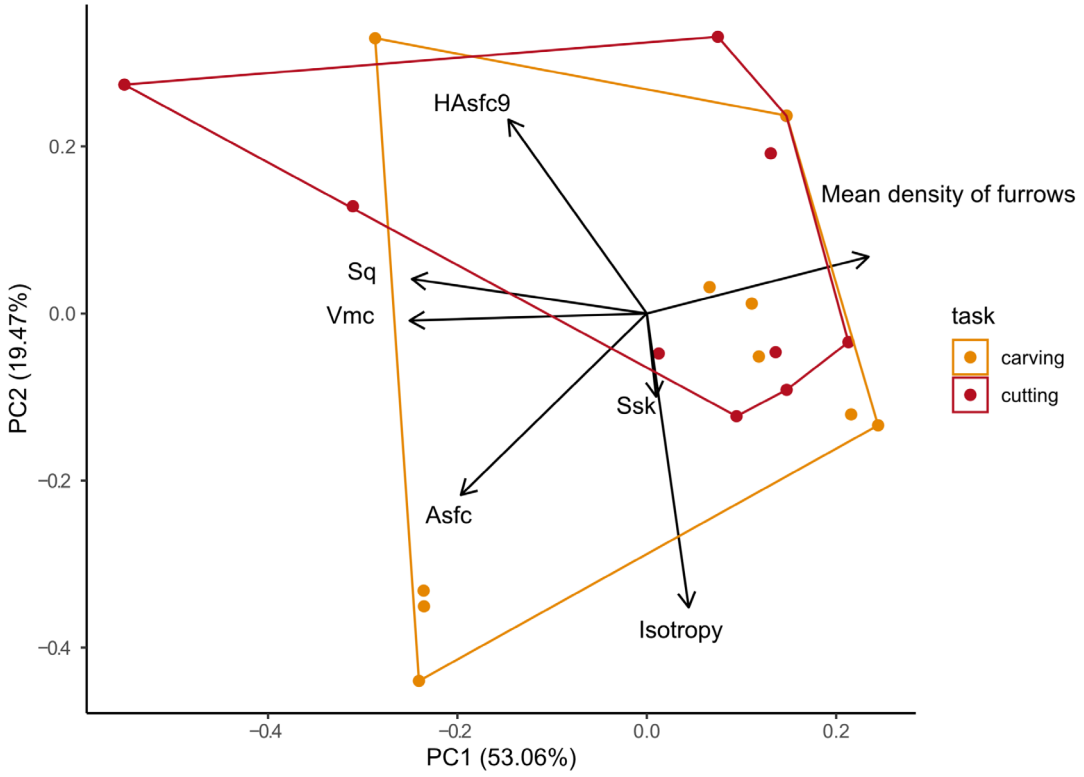

Fig. 154 Principal component analysis applied on the measured use-wear traces of the analysed standard samples from the tool function experiment, reflecting variation regarding the performed task.

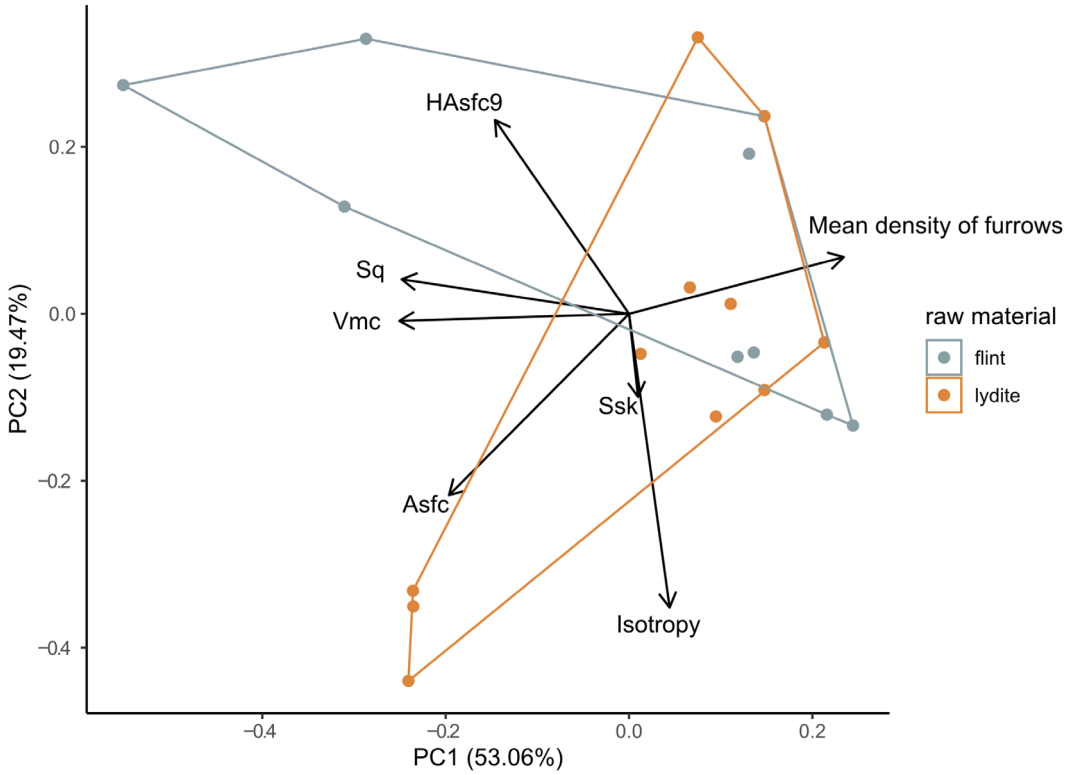

Fig. 155 Principal component analysis applied on the measured use-wear traces of the analysed standard samples from the tool function experiment, reflecting variation regarding the raw material of the standard samples.

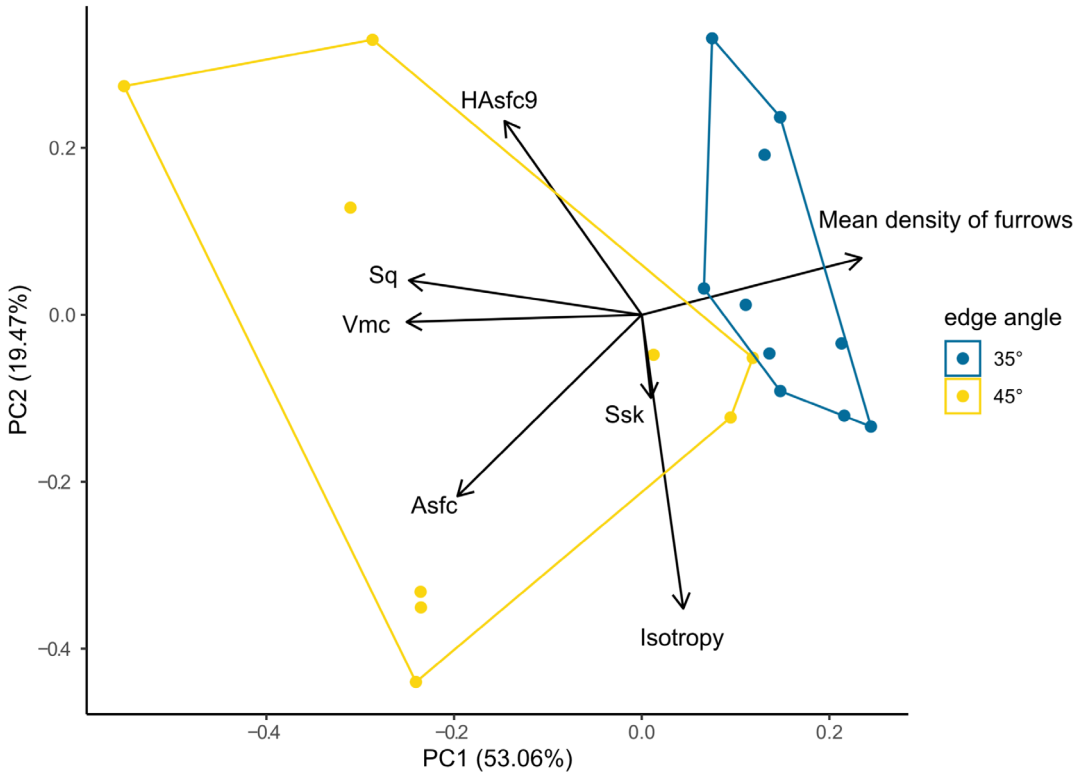

Fig. 156 Principal component analysis applied on the measured use-wear traces of the analysed standard samples from the tool function experiment, reflecting variation regarding the edge angle of the standard samples.

Combined data of the experiments

It was possible to combine the data from the three experiments in several ways. First, the alteration of the tool and thus the change of the edge angle will be addressed. Throughout the three experiments, a reproducible trend could be noticed: The lower the edge angle, the more alteration occurs on the tool's edge. This trend gets strengthened through two additional impacts, the raw material of the standard samples and the characteristics of the contact material. Concerning the raw material, flint seems to be more durable than lydite, which is likely due to the raw material properties of the tool. The hardness of the contact material seems also to be of influence. However, the hardness of the contact material might not be the only relevant aspect concerning the material properties. The artificial bone plates do have a comparable shore hardness to the fresh cow scapula used during the »artificial VS. natural« experiment. Still, the cow scapula had a stronger effect on the tool alteration than the artificial bone plate. The mentioned trend could be observed for cutting movements, not for carving. The standard samples with the lower 35° edge angle used for carving display only minimal alteration compared to the samples with the 45° edge angles.
The results from the qualitative use-wear analysis of the »artificial VS. natural« experiment and the tool function experiment can be compared. The comparison is possible for all samples used for cutting on artificial bone plates. All samples belonging to this category developed use-wear traces within the 2000 strokes. Interestingly, visible use-wear traces on flint samples only formed after 2000 strokes. By contrast, lydite samples displayed use-wear traces already after 50 strokes.
Moreover, some results from the quantitative use-wear analysis of the »artificial VS. natural« and the tool function experiment have been combined. While all the data from the tool function experiment could be used for a comparison, only the data acquired on the 60° samples used for cutting on bone plates from the »artificial VS. natural« experiment was included. To do so, data was combined in one plot per parameter (fig. 157). The results from the samples with the 35° edge angle are, compared to the 45° and 60° samples, more homogenous. This observation was already mentioned beforehand, but in combination with 60° samples, it becomes more obvious. The data obtained on the samples with the 60° edge angle clearly differs from the other data points.
To summarise, the standard samples made of lydite turned out to be more fragile and more easily affected by alteration (e. g. due to hardness, schistosity). Furthermore, the raw material promotes the formation and development of use-wear traces. At the same time, the lydite samples are more efficient in cutting when judged by the penetration depth solely. However, efficiency defines the ratio between cost and benefits. Benefits, in this case, can be measured based on the achieved penetration depth. Costs are the loss of material and volume. In this sense, lydite exhibits a greater loss when judged by single artefacts. In one case (initial experiment, LYDIT1-4), the loss was so severe, that it affected the durability. In the course of the experiment, the sample fractured so much, that the functionality could not be retained. Thus, the sample was not able to achieve the goal (2000 strokes). However, the lydite sample described above is an exception. Although the other lydite samples used for cutting or carving experienced material loss, the loss was not enough to lose the functionality. Measured on the change in volume and weight (tool function experiment), the loss of raw material is slightly higher on flint samples. Nevertheless, likely due to the raw material properties, the flint samples alter in a different way than the lydite samples. While material loss on flint samples appears more as retouch-like, material loss on lydite samples displays fractures and breakages. This observed difference is also expressed in the shift of the edge angle values.

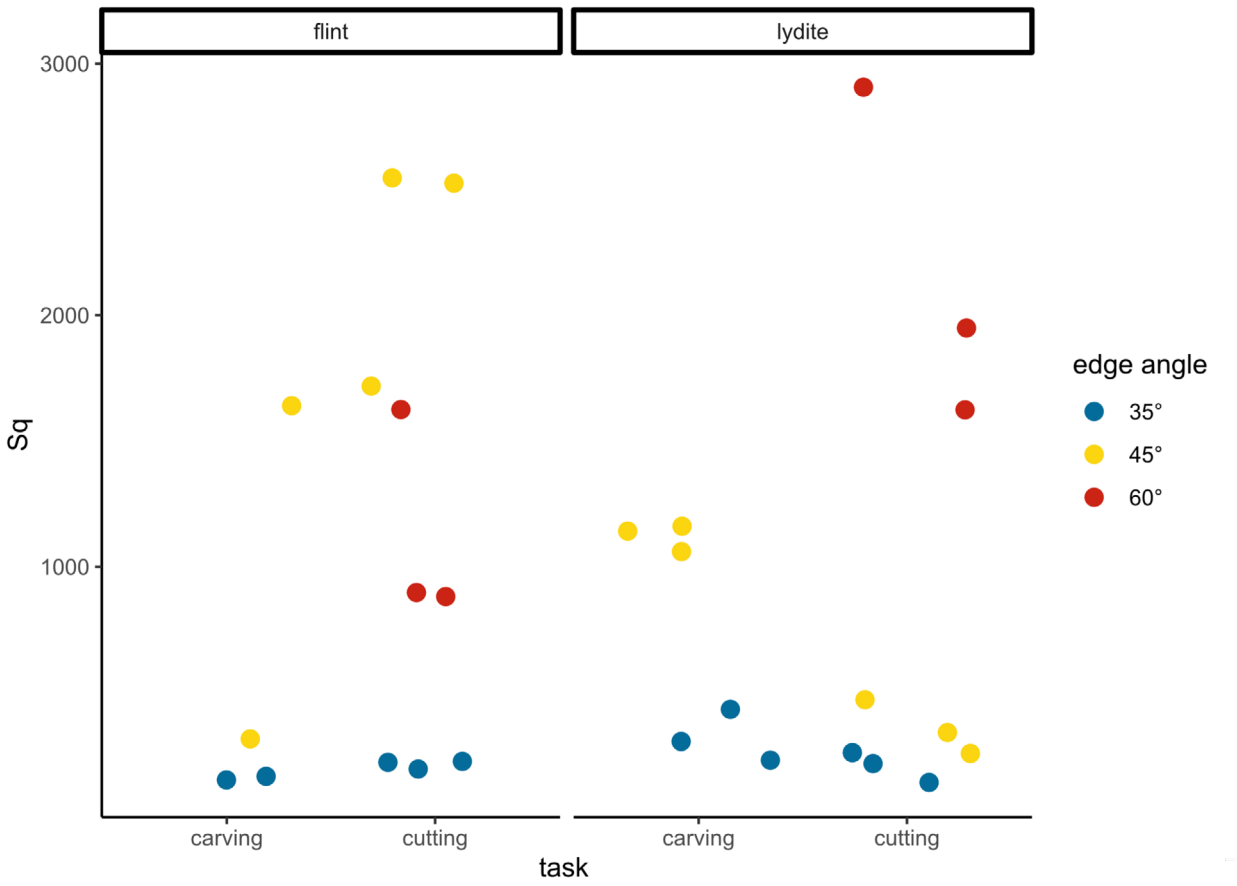

Fig. 157 *Sq* values measured on the flint and lydite samples after 2000 strokes used during the tool function experiment and the »artificial VS. natural« experiment. Three data points are shown per sample, reflecting the three measurements taken per use-wear trace (spot a, b and c). The data is categorised according to the performed task. The colour indicates the edge angle of the standard samples. The 35° and 45° samples have been used during the tool function experiment, the 60° samples during the »artificial VS. natural« experiment.